UNIVERSIDADE FEDERAL DO PARANÁ

ISABELLA GIZZI JIACOMINI

DESENVOLVIMENTO E CARACTERIZAÇÃO DE ANTICORPOS RECOMBINANTES COM POTENCIAL TERAPÊUTICO

CURITIBA

2022

ISABELLA GIZZI JIACOMINI

DESENVOLVIMENTO E CARACTERIZAÇÃO DE ANTICORPOS RECOMBINANTES COM POTENCIAL TERAPÊUTICO

Tese apresentada como requisito parcial à obtenção do título de doutora em Microbiologia, Parasitologia e Patologia ao Programa de Pós-graduação em Microbiologia, Parasitologia e Patologia, Setor de Ciências Biológicas, da Universidade Federal do Paraná.

Orientadora: Profª. Drª. Larissa Magalhães Alvarenga

CURITIBA

2022

DADOS INTERNACIONAIS DE CATALOGAÇÃO NA PUBLICAÇÃO (CIP)
UNIVERSIDADE FEDERAL DO PARANÁ
SISTEMA DE BIBLIOTECAS – BIBLIOTECA DE CIÊNCIAS BIOLÓGICAS

Jiacomini, Isabella Gizzi.
Desenvolvimento e caracterização de anticorpos recombinantes com potencial terapêutico. / Isabella Gizzi Jiacomini. – Curitiba, 2022.
1 recurso on-line : PDF.

Orientadora: Larissa Magalhães Alvarenga.

Tese (Doutorado) – Universidade Federal do Paraná, Setor de Ciências Biológicas. Programa de Pós-Graduação em Microbiologia, Parasitologia e Patologia.

1. Anticorpos monoclonais. 2. DNA recombinante. 3. Imunoterapia. I. Título. II. Alvarenga, Larissa Magalhães. III. Universidade Federal do Paraná. Setor de Ciências Biológicas. Programa de Pós-Graduação em Microbiologia, Parasitologia e Patologia.

Bibliotecária: Rosilei Vilas Boas- CRB-9/939

MINISTÉRIO DA EDUCAÇÃO
SETOR DE CIÊNCIAS BIOLÓGICAS
UNIVERSIDADE FEDERAL DO PARANÁ
PRÓ-REITORIA DE PESQUISA E PÓS-GRADUAÇÃO
PROGRAMA DE PÓS-GRADUAÇÃO MICROBIOLOGIA,
PARASITOLOGIA E PATOLOGIA - 40001016044P0

TERMO DE APROVAÇÃO

Os membros da Banca Examinadora designada pelo Colegiado do Programa de Pós-Graduação MICROBIOLOGIA, PARASITOLOGIA E PATOLOGIA da Universidade Federal do Paraná foram convocados para realizar a arguição da tese de Doutorado de **ISABELLA GIZZI JIACOMINI** intitulada: **Desenvolvimento e caracterização de anticorpos recombinantes com potencial terapêutico**, sob orientação da Profa. Dra. LARISSA MAGALHÃES ALVARENGA, que após terem inquirido a aluna e realizada a avaliação do trabalho, são de parecer pela sua APROVAÇÃO no rito de defesa.

A outorga do título de doutora está sujeita à homologação pelo colegiado, ao atendimento de todas as indicações e correções solicitadas pela banca e ao pleno atendimento das demandas regimentais do Programa de Pós-Graduação.

CURITIBA, 27 de Abril de 2022.

Assinatura Eletrônica
29/04/2022 13:24:23.0
LARISSA MAGALHÃES ALVARENGA
Presidente da Banca Examinadora

Assinatura Eletrônica
29/04/2022 21:47:02.0
BRENO CASTELLO BRANCO BEIRÃO
Avaliador Interno (UNIVERSIDADE FEDERAL DO PARANÁ)

Assinatura Eletrônica
29/04/2022 14:48:26.0
MARCELO MÜLLER DOS SANTOS
Avaliador Externo (UNIVERSIDADE FEDERAL DO PARANÁ)

Assinatura Eletrônica
02/05/2022 17:16:27.0
GISELI KLASSEN
Avaliador Interno (UNIVERSIDADE FEDERAL DO PARANÁ)

Assinatura Eletrônica
29/04/2022 19:13:49.0
LEONARDO FOTI
Avaliador Externo (INSTITUTO CARLOS CHAGAS)

In memoriam de Victor Maltese Stocco

‘’Àquele que é capaz de fazer infinitamente mais do que tudo o que pedimos ou pensamos, de acordo com o Seu poder que atua em nós.’’
Efésios 3:20

AGRADECIMENTOS

Agradeço a Deus: Pai, Filho e Espírito, por mais do que sequer poderia expressar. Agradeço por ter sido criada exatamente assim, apaixonada por ciência e pela sua Criação. Lhe agradeço por tanto abençoar aquela garotinha brincando de cientista com tudo que encontrava no quintal, que não tinha nem ideia de que um dia seria uma cientista de verdade. Agradeço por me guiar, capacitar, me dar uma Esperança que vai além de todas as coisas.

Sou grata aos meus pais, Josias e Helen, meus maiores incentivadores, e os que mais me amam nesse vasto mundo. Vocês são minha definição de tudo que é bom e virtuoso e me inspiram diariamente. Obrigada por me propiciarem uma educação maravilhosa, por terem me colocado como prioridade, mesmo os recursos sendo muitas vezes escassos e eu não merecendo. Obrigada por rirem e chorarem comigo, por tanto intercederem por mim. Agradeço também a minha irmã Isadora, minha melhor amiga e fiel companheira, que me ama e amou incondicionalmente até aqui. Obrigada por sentir tão profundamente, por me cuidar, torcer e sofrer comigo em toda essa jornada, mesmo que há alguns muitos milhares de quilômetros de distância.

Agradeço à Profa. Larissa Magalhães Alvarenga por esses oito anos de parceria. Pela quantidade imensurável de coisas que me ensinou durante toda minha formação. Por ter acreditado no meu potencial, me confiado responsabilidades, me animado e me erguido nos momentos em que forças me faltavam. Por ter sido mais do que Professora e Orientadora (que já são papéis notáveis), mas também uma amiga verdadeira. Deixo aqui minha inefável gratidão.

Agradeço ao Prof. Phillipe Billiald, que cruzou meus caminhos tem algum tempo e foi gradativamente se tornando um grande mentor, encorajador e propiciador de muitas das minhas conquistas. Obrigada por tanto cuidado, apoio, confiança no meu trabalho e ajuda, tudo isso tem sido tem valor inestimável. Agradeço também a sua esposa, Stéphanie Billiald, por toda a hospitalidade, carinho e cuidado.

Agradeço à Profa. Juliana de Moura, que tem me acompanhado por tantos anos ao lado da Profa. Larissa. Obrigada por todo o ensino, ajuda, carinho e genuinidade. Obrigada pela orientação e acompanhamento até aqui.

Agradeço ao Dr. Nicolas, que me recebeu prontamente na França durante o período do doutorado sanduíche. Obrigada pelo tanto que me ensinou, pela mentoria,

paciência e cuidado. Agradeço também a Fanny e Catherine, integrantes da equipe do Dr. Nicolas, cujo apoio e treinamento foram imprescindíveis. Agradeço por livremente compartilharem seu conhecimento comigo.

Agradeço a todos que foram fundamentais no meu processo de formação. Desde meus professores que me inspiraram a seguir carreira em ciência já no ensino fundamental, até meus professores do curso de Biomedicina na UFPR e do PPG. Os admiro muito e divido essa conquista com cada um de vocês.

Agradeço aos membros da banca, Prof. Breno Beirão, Profa. Giseli Klassen e Prof. Marcelo Muller e Dr. Leonardo Foti, por aceitarem tão prontamente avaliar meu trabalho e pelas considerações tão cuidadosas e fundamentais.

Aos amigos e companheiros de laboratório de Imunoquímica que tanto me ensinaram. Obrigada Dra. Alessandra Becker Finco, por tanta paciência, bondade e disposição, muito do que eu sei, você que me ensinou. Agradeço à Dra. Sabrina Karim-Silva, a quem admiro imensamente e muito contribuiu para minha formação. Ao Prof. Luís Felipe Minozzo, que além de sempre cuidar da minha postura (que ainda precisa de muito trabalho) e me lembrar da importância da positividade, me ensinou os princípios por trás de muita coisa que acontecia no laboratório. A Bianca Costa (pela paciência em me escutar, pelas suas lindas aquarelas e sua sabedoria compartilhada comigo), Mariana Fernandes (por todo o apoio, admiração, gestos de carinho, chás, bolos, cookies, caminhadas, conversas e desabafos), Martina Beltramino (pelos alfajores argentinos, delícias da Dona Consuelo, desabafos, ensaios de hemólise compartilhados e pela literal força para tirar os nalgenes da centrífuga refrigerada), Bruno Araújo (pelas risadas, amizade e solidariedade), foi um prazer dividir tantos anos de trabalho com vocês, obrigada por tudo que me ensinaram e tudo que compartilhamos, obrigada pela amizade valiosa de cada um. Por fim, agradeço a Izadora Rossi e Tamara Costa, amigas muito queridas e cientistas brilhantes que apareceram durante esse período.

Agradeço a uma pessoa fantástica que infelizmente nos deixou muito cedo. Meu primeiro aluno de Iniciação Científica e caro amigo, Victor Maltese Stocco. A você, que tanto acreditou em mim, me animou e aconselhou, sempre uma fonte de luz e alegria, dedico esse trabalho.

A Pedro Osis, que chegou por aqui quase na reta final, mas que teve um impacto maior do que eu poderia mensurar e descrever em palavras. Obrigada por me enxergar de uma maneira tão bonita, encorajar e amar genuinamente. Agradeço também a seus pais, Glaucia e Acir e seu irmão, Elias, fundamentais nesses últimos meses e muito especiais. Obrigada por todo o carinho e orações.

Agradeço aos meu avós Adão e Maria, que já não estão mais conosco nesse plano, mas que foram partes fundamentais na formação do meu caráter. Suas vozes ecoam na eternidade do meu coração.

Sou grata a minha avó Sônia, que sempre esteve ao meu lado durante esse período. Obrigada pelo cuidado, apoio, ligações e cafés da tarde.

Sou grata por tantos amigos maravilhosos com os quais tive o privilégio de conviver durante esses anos todos, verdadeiros presentes de Deus em minha vida. Em muitos momentos, eles me ofereceram palavras de ânimo, intercederam por mim, sofreram comigo, foram sinceros e genuínos. Sobretudo, chegaram comigo até aqui. Divido com todos vocês esta conquista. Obrigada Adam Sugi, Adner Franco, Débora Spisla, Vivian Kern, Lucas Farias, Tatiana Badotti, Marina Saade, Larissa Silva, Helena Spisla, Natasha Polato, Náthali Giacomini, Lucas Ikenaga, Bernardo Abreu, Henrique Grando, Tomas Mantelato, Vinícius Alves, Gabriel Brustolim, Raissa Camargo e Raquel Refatti.

Agradeço também ao Programa de Pós-graduação em Microbiologia, Parasitologia e Patologia e a UFPR por terem possibilitado a realização desse trabalho. Às agências de fomento: CAPES (Coordenação de Aperfeiçoamento de Pessoal de Nível Superior), CNPq (Conselho Nacional de Desenvolvimento Científico e Tecnológico) pelo apoio à pesquisa.

RESUMO

Com o advento da tecnologia de hibridoma para produção de anticorpos monoclonais e da tecnologia do DNA recombinante, surge a engenharia de anticorpos recombinantes. Essas proteínas têm ganhado espaço na pesquisa biomédica ao longo dos últimos anos e passaram a ser amplamente empregadas na clínica, hoje compondo o principal pilar da terapêutica baseada em proteínas. Em um levantamento realizado em 2021, o órgão regulatório norte-americano FDA (*Federal Drug Administration*) já havia aprovado mais de 120 moléculas de anticorpos monoclonais (mAbs) para uso terapêutico, enquanto cerca de 870 moléculas estão em processo de desenvolvimento clínico. Considerando a relevância da imunoterapia e visando o desenvolvimento de insumos terapêuticos mais específicos, seguros e efetivos, estudos no sentido do desenvolvimento e melhoramento dessas moléculas são de suma importância. Objetivando reduzir o seu potencial imunogênico, surgem estratégias para humanização de mAbs de origem heteróloga, consequentemente permitindo um aumento de sua biossegurança. Adicionalmente, considerando-se a íntima relação entre estrutura/função de anticorpos, estudos para investigação da influência da estrutura bi/tridimensional de imunoglobulinas em parâmetros biofísicos e sua funcionalidade são bastante relevantes. Para isso, os mAbs LimAb7, S1A0 e glenzocimab, que apresentam diferentes aplicações farmacológicas, foram utilizados como *templates* para o estudo de sua humanização, regiões estruturais e mecanismo de inibição, respectivamente. Variantes humanizadas do anticorpo LimAb7 (e de diferentes formatos) foram produzidas com sucesso, segundo diferentes critérios de humanização. Suas propriedades biofísicas foram avaliadas e puderam ser otimizadas, bem como sua reatividade frente ao alvo, que permaneceu inalterada. Adicionalmente, as regiões estruturais do mAb S1A0 (scFv) foram mutadas e diversas variantes produzidas. Observou-se que essas mutações geraram ganhos significativos nas propriedades físico-químicas dessas moléculas. Por fim, o co-cristal do mAb Glenzocimab e seu alvo, a proteína GPVI, foi realizado e analisado *in silico* e os mecanismos de inibição do mAb foram sugeridos como impedimento estérico e indução de mudança conformacional do alvo. De maneira geral, os dados aqui compilados oferecem norteamento importante para a produção de mAbs terapêuticos.

Palavras-chave: anticorpos monoclonais; recombinantes; humanização; estrutura; imunoterapia.

ABSTRACT

With the dawn of hybridoma technology for the production of monoclonal antibodies and of recombinant DNA technology, recombinant antibodies engineering arises. These proteins have gained space in biomedical research over the last few years and have come to be widely used in the clinic, today making up the main pillar of protein-based therapy. In a survey carried out in 2021, the US FDA (Federal Drug Administration) had already approved more than 120 molecules of monoclonal antibodies (mAbs) for therapeutic use, while about 870 molecules are in the clinical development process. Considering the relevance of immunotherapy and aiming to develop more specific, safe, and effective therapeutic mAbs, studies focused on the development and improvement of these molecules are of paramount importance. Given the immunogenic potential of heterologous mAbs, strategies have emerged for their humanization, consequently allowing an increase in their biosecurity. Additionally, considering the close relationship between structure/function of antibodies and protein in general, studies investigating the influence of the two/three-dimensional structure of immunoglobulins on biophysical parameters and their functionality are quite relevant. Bearing that in mind, mAbs LimAb7, S1A0 and Glenzocimab, which have different therapeutic applications, were used as templates for the study of their humanization, framework regions, and mechanism of inhibition, respectively. Humanized variants of the LimAb7 antibody were successfully produced in various formats, according to different humanization criteria. Its biophysical properties were evaluated and optimized, as well as its reactivity, which remained unchanged. Additionally, the framework regions of mAb S1A0 (scFv) were mutated, and several variants produced. It was observed that these mutations generated significant gains in the physicochemical properties of these molecules. Finally, the co-crystal of mAb Glenzocimab and its target, the GPVI protein, was performed and analyzed in silico and the mechanisms of inhibition of the mAb were suggested as steric hindrance and induction of conformational change of the target. In general, the data compiled here provide important guidance to the production of therapeutic mAbs.

Keywords: monoclonal antibodies; recombinant; humanization; structure; immunotherapy.

SUMÁRIO

1. INTRODUÇÃO:

Anticorpos são glicoproteínas globulares produzidas por plasmócitos e que reagem especificamente com os antígenos que estimularam sua produção. São as principais moléculas efetoras da resposta imune adaptativa e possuem uma série de funções associadas com o reconhecimento e neutralização de patógenos e toxinas, participação em efeitos celulares associados a eliminação dos mesmos e imunomodulação.

Considerando a especificidade, bem como as funções efetoras dos anticorpos, a aplicabilidade dessas moléculas tem revolucionado a terapêutica e diagnóstico de diversas doenças. O surgimento das tecnologias de hibridoma e *phage display,* permitiu a produção de anticorpos monoclonais (mAbs) contra uma vasta gama de antígenos e essas proteínas têm sido amplamente produzidas e caracterizadas. Adicionalmente, o advento da tecnologia do DNA recombinante contribuiu para o desenvolvimento de anticorpos recombinantes escalonáveis, formatados das mais diferentes maneiras e produzidos em diferentes sistemas de expressão procarióticos e eucarióticos.

Atualmente, mais de 100 anticorpos monoclonais recombinantes já foram aprovados pelo FDA para o tratamento de cânceres, doenças autoimunes, distúrbios de coagulação, doenças neurodegenerativas, dentre outras. A terapia de anticorpos para o tratamento de câncer tem mais de 15 anos de história e é hoje a mais importante estratégia para tratar pacientes com câncer hematológico e tumores sólidos (SCOTT et al. 2012).

Considerando-se variáveis como a biossegurança, eficácia e escalonabilidade (do inglês *developabilty*) de anticorpos monoclonais, surgem diversas estratégias para sua otimização e uso farmacológico. Uma delas consiste na humanização de anticorpos heterólogos, através da substituição das regiões estruturais dos seus domínios variáveis, por regiões estruturais de imunoglobulinas humanas, através da estratégia cunhada como enxerto de CDRs, diminuindo-se assim sua imunogenicidade. Adicionalmente, esforços têm sido realizados no sentido da otimização das propriedades físico-químicos de anticorpos recombinantes, que determinam o quão passíveis de desenvolvimento e farmacologicamente viáveis são essas moléculas. Parâmetros como a estabilidade térmica e química, tolerância à

baixos pHs, agregação, afinidade ao alvo, rendimento de produção e funcionalidade são avaliados cuidadosamente e tem sido associados diretamente com a estrutura desses anticorpos.

Tendo isso em vista, o presente estudo objetiva a concepção, desenvolvimento e produção de anticorpos recombinantes com potencial terapêutico, no escopo da: (i) humanização dessas moléculas, visando uma melhora da sua biossegurança e redução da sua imunogenicidade, (ii) estudo e otimização dos seus parâmetros físico-químicos através de alterações na sua estrutura e (iii) compreensão dos seus mecanismos de inibição a proteínas bioativas. Esses tópicos foram abordados em alguns estudos aqui apresentados que estão compilados e apresentados sobre a forma de capítulos.

O primeiro capítulo descreve a humanização de anticorpos através de dois trabalhos produzidos visando a aplicação terapêutica dessas moléculas e sua otimização estrutural e funcional. Para isso, o mAb LimAb7 (ALVARENGA et al., 2003), que reconhece e neutraliza a principal família de toxinas do veneno da aranha marrom *Loxosceles intermedia*, as Fosfolipases D, foi utilizado como *template.* Seus domínios variáveis humanizado segundo diferentes critérios desenvolvidos nos dois trabalhos neste capítulo. O LimAb7 pode ser humanizado com sucesso e diversas variantes foram produzidas segundo diferentes critérios de humanização, formatos e sistema de expressão. Em seguida, suas propriedades biofísicas, como estabilidade térmica, rendimento, agregação, afinidade ao antígeno e funcionalidade foram avaliadas e observou-se uma otimização desses parâmetros dependente da estratégia de humanização aplicada, formato do anticorpo e sistema de expressão escolhido.

No segundo capítulo, o estudo das regiões estruturais de domínios variáveis de anticorpos e seu envolvimento nas propriedades biofísicas dessas moléculas foi explorado.Para isso, diversas mutações foram realizadas nas regiões de *framework* do mAb 4F11E12, produzido no formato de scFv (denominado S1A0), que reconhece a principal proteína de superfície do protozoário *Toxoplasma gondii* (GRAILLE et al., 2005). Essas mutações foram agrupadas em diferentes *clusters* e diversas variantes mutadas foram produzidas. Observou-se que todas as mutações acarretaram ganhos expressivos no rendimento, estabilidade térmica e química, tolerância a pH e reatividade ao alvo. Os dados obtidos mostram que moléculas com grande identidade

de sequência podem apresentar parâmetros biofísicos totalmente distintos, sugerindo assim um envolvimento complexo das regiões de *framework* e mais especificamente, de alguns resíduos específicos de aminoácidos nesse processo.

Por fim, um estudo acerca do mecanismo de inibição do anticorpo Glenzocimab (LEBOZEC et al., 2017), em fase final de desenvolvimento para o tratamento de distúrbios de coagulação, foi realizado, visando o entendimento da relação entre a estrutura e função de anticorpos. Através da cristalografia de raio-X do complexo antígeno/anticorpo, essa interação pode ser modelada tridimensionalmente e visualizada com o auxílio de softwares de bioinformática. As análises *in sílico* desses modelos permitiriam o estudo dos mecanismos pelos quais o Glenzocimab inibe seu alvo, sendo sugeridos o impedimento estérico e as induções de mudanças conformacionais na estrutura do antígeno.

De maneira geral, os resultados aqui descritos possuem relevância no contexto do desenvolvimento de anticorpos recombinantes, na sua humanização e entendimento dos seus mecanismos de inibição, permitindo norteamento no sentido da produção de mAbs mais adaptados para suas finalidades.

2. REVISÃO BIBLIOGRÁFICA:

2.1. Estrutura de Anticorpos

Anticorpos, ou imunoglobulinas, são moléculas glicoproteicas produzidas pelos plasmócitos (linfócitos B maduros) e que pertencem a um grupo de proteínas globulares encontrados no soro/plasma. Reagem diretamente contra antígenos aos quais são complementares, sendo estes antígenos responsáveis pela indução da sua produção. Os anticorpos estão divididos em 5 classes (isotipos) estruturalmente e funcionalmente distintas, que por sua vez podem ser ainda subclassificadas (subtipos). Essa classificação define-se pelo tipo de cadeia pesada que foram essas moléculas, de maneira que as cadeias α, δ, ε, γ e μ compõe os anticorpos IgA, IgD, IgE, IgG e IgM, respectivamente (GOULET et al., 2021).

. As imunoglobulinas G, isotipo mais abundante e caracterizado, possuem uma estrutura no formato de Y (por isso também denominados de gama globulinas) e massa de aproximadamente 150 kDa (Figura 1). São compostas por duas cadeias pesadas idênticas (55 kDa) e duas cadeias leves idênticas (23 kDa), ambas com um domínio variável um domínio constante. Na cadeia leve está o domínio variável de cadeia leve (VL) e um domínio constante (CL). Na cadeia pesada, um domínio variável (VH), e três domínios constantes (CH1, CH2, CH3), dois deles (CH2-CH3) responsáveis por compor a região Fc (fragmento cristalizável), porção efetora das IgGs. Nos domínios variáveis (V-domains) de cadeia leve (VL) e pesada (VH), encontram-se regiões hipervariáveis, denominadas CDRs (cluster differentiating regions), regiões determinantes na complementariedade ao antígeno e que interagem diretamente com ele. Cada cadeia é composta por três CDRs, intercalados por quatro regiões estruturais (ou de framework) (SCHROEDER et al., 2010, CHIU et al., 2018).

Os anticorpos são as proteínas mais diversas conhecidas até hoje. Possuem uma identidade de sequência de amino ácidos entre si de aproximadamente 90-95% e os 5-10% de variação restantes correspondem às regiões hipervariáveis (CDRs – cluster differentiating regions), onde como o nome já sugere, há uma grande variação nos resíduos de amino ácidos. A alta variabilidade de sequencias polipeptídicas encontradas nos CDRs de diferentes imunoglobulinas é responsável por possibilitar a existência de anticorpos com as mais diversas especificidades (SINGH et al., 2014).

Considerando isto, as regiões de CDRs são imprescindíveis para a função e especificidade dos anticorpos. O loop H3 (CDR3 da cadeia pesada) possui uma

variabilidade aumentada em relação aos demais *loops* de CDR (XU et al., 2000) e foi apontado como mediador da potente neutralização viral do anticorpo anti-HIV-1 PG16 através da formação de um subdomínio estrutural único e estável (PEJCHAL et al., 2010). Contudo, diversos estudos têm também explorado e demonstrado a relevância das regiões estruturais na manutenção da funcionalidade e orientação tridimensional de anticorpos (ZHOU et al., 2020), ou até mesmo no melhoramento das propriedades biofísicas dessas moléculas (HONEGGER et al., 2009), tendo em vista que aproximadamente 20% das regiões responsáveis pela ligação anticorpo-antígeno se encontram fora dos CDRs (DONDELINGER et al., 2018).

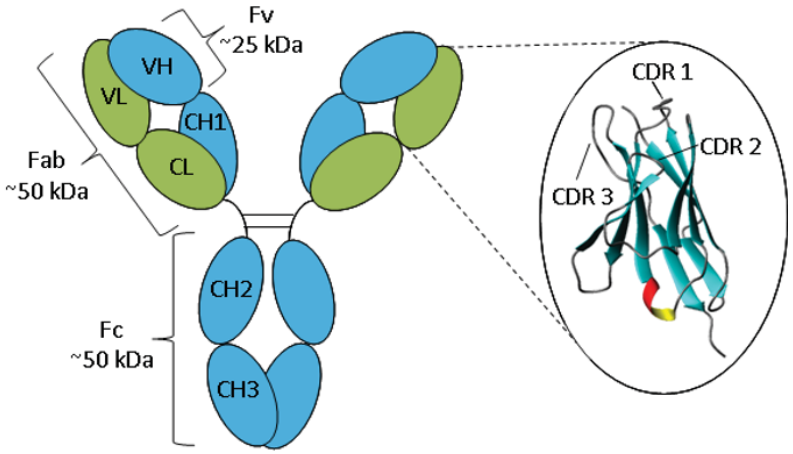

Figura 1. Estrutura de uma Imunoglobulina G. IgGs são glicoproteínas tetraméricas compostas por duas cadeias leves e duas cadeias pesadas idênticas. Sua estrutura pode ser dividida em porção Fab, onde estão as regiões variáveis (Fv) e os CDRs (três CDRs nas cadeias leves e três nas cadeias pesadas), responsáveis pela interação com antígeno e porção Fc, associada com suas funções efetoras.
Fonte: https://absoluteantibody.com/antibody-resources/antibody-overview/antibody-structure/

2.2. Funções de Anticorpos:

Devido a seu potencial de ligação específico a diferentes alvos, bem como suas funções imunes (JIANG et al., 2011), os anticorpos têm sido amplamente utilizados na biomedicina, para o tratamento e diagnóstico de uma série de enfermidades, bem como na pesquisa básica.

As principais funções efetoras de anticorpos (Figura 2) podem ser divididas em i. Independentes de células ou moléculas efetoras; ii. Dependentes do sistema de complemento; iii. Dependentes da interação da porção Fc com receptores para Fc e iv. Imunomoduladoras. Dentre as funções compreendidas em (i), encontram-se a neutralização da infectividade de microrganismos, principalmente de vírus e bactérias, podendo atuar no impedimento de diversos estágios do ciclo de vida deste patógenos, seja inibindo sua adesão, entrada, sequestro da maquinaria celular e saída das células dos hospedeiros. Anticorpos também possuem a capacidade de inibição da atividade de proteínas com atividade catalítica, como toxinas e demais enzimas não-tóxicas. (LASTRA et al., 2021)

Em relação aos mecanismos efetores dependentes do sistema de complemento, mencionados em (ii), anticorpos possuem a capacidade de se ligar a proteínas ativadoras da cascata de complemento (e.g. C1q), resultando na lise de células infectadas por patógenos ou desses organismos *per se.* Adicionalmente, uma série de eventos celulares podem ser estimulados a partir de anticorpos, mais especificamente da interação da sua porção Fc com receptores complementares (iii). Esses efeitos variam de acordo com a natureza da célula com a qual o anticorpo interage, as citocinas presentes no meio, a natureza do imunocomplexo anticorpo-antígeno e a presença do sistema de complemento. Dentre estes mecanismos encontram-se a citotoxicidade celular dependente de anticorpos (ADCC), mediada por linfócitos NK (*Natural Killer*) e a fagocitose ou opsonização. Por fim, no tocante as funções imunomoduladoras (iv) de anticorpos, é descrita a interação entre imunocomplexos com receptores do tipo FcγR como importantes para geração, secreção e supressão de diversas substâncias pro-inflamatórias. Adicionalmente, a ativação do sistema complemento por anticorpos pode influenciar na produção de proteínas dessa cascata, como a C5a, que atuam como importantes agente quimiotáticos. (FORTHAL et al., 2014)

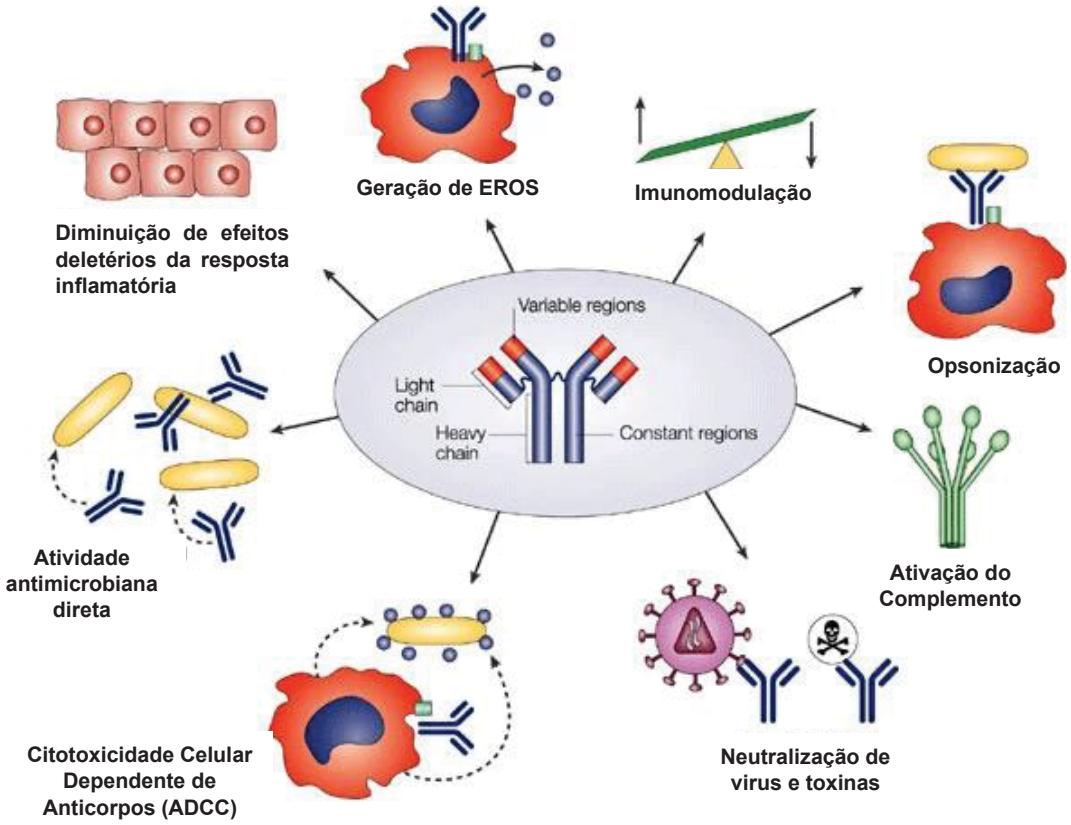

Figura 2. Funções Efetoras associadas às regiões Fab e Fc de Anticorpos.

EROS – espécies reativas de oxigênio.

Fonte: Adaptado de Casadevall et al., 2004.

2.2.1. Mecanismos de Neutralização/Inibição da Atividade de Enzimas por Anticorpos

Dentre as funções associadas diretamente aos anticorpos e independentes tanto do sistema de complemento, quando da porção Fc, está a sua capacidade de neutralizar proteínas bioativas (sejam elas tóxicas ou não) de maneira direta.

A interação de anticorpos, enzimas e seus substratos e os mecanismos de inibição enzimática por anticorpos foram descritos em detalhe por CINADER, 1957. Na maioria dos casos, a interação de enzimas com anticorpos específicos resulta na queda da atividade enzimática *in vitro*. Os atividade inibitória dos anticorpos é atribuída a sua ligação à enzima, o que impediria a catálise do seu substrato. Essa interação pode provocar a alteração da posição estrutural de amino ácidos dessa enzima, bem como das suas cadeias laterais, modificando-se sua conformação. Adicionalmente, anticorpos podem alterar a estrutura de enzimas promovendo sua

agregação e afuncionalidade. Por fim, anticorpos podem ser reativos a epítopos localizados em sítios reguladores (alostéricos) e catalíticos de enzimas, e assim, afetar diretamente sua atividade por impedimento estérico e alostérico (LASTRA et al., 2021). A Figura 3 ilustra, de maneira esquemática, os mecanismos de inibição enzimática promovido por anticorpos

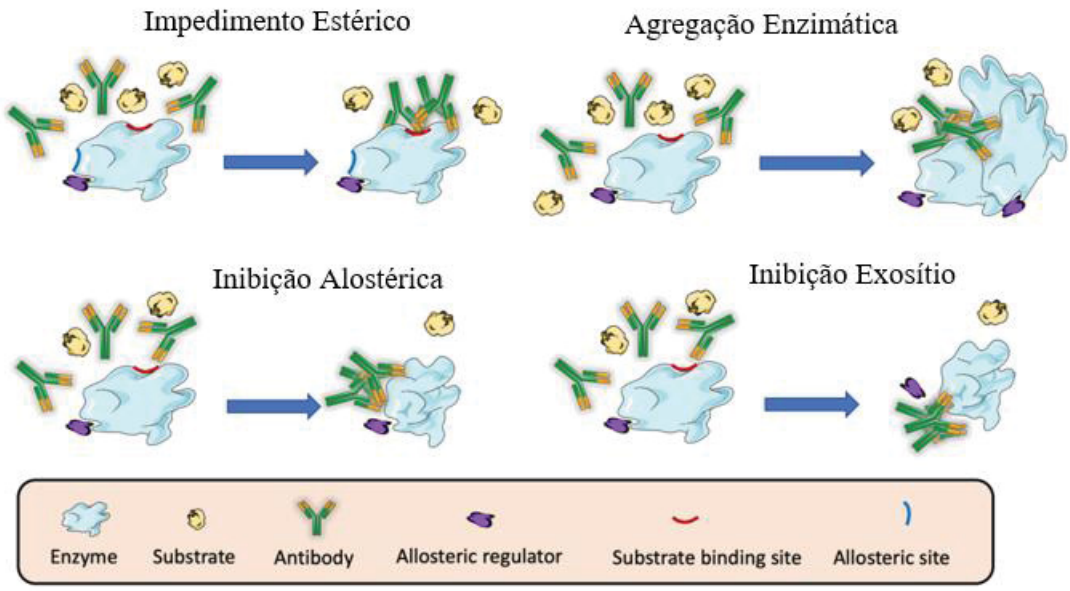

Figura 3. Principais mecanismos de inibição enzimática utilizados por anticorpos. Em vermelho está indicado o sítio catalítico das enzimas, que se liga ao seu substrato (representado em amarelão) e em azul, seu sítio alostérico, onde os reguladores alostéricos se ligam (coloridos em roxo). Fonte: Adaptado de Lastra et al., 2021.

O conhecimento dos mecanismos de neutralização/inibição de diferentes anticorpos e como estes estão reciprocamente implicados com sua estrutura pode ser útil para a engenharia de anticorpos e na geração de moléculas com alta afinidade à uma série de alvos terapêuticos, tendo em vista que inibidores enzimáticos tem se mostrado relevantes para diversas aplicações terapêuticas (SELLEGREN, 2010). Uma vez elucidados esses mecanismos, o desenvolvimento de inibidores farmacológicos, ou mesmo a produção de anticorpos com características similares para neutralização/inibição de outras proteínas biologicamente ativas, se torna viável. Além de permitir, de maneira generalista, um aprofundamento do conhecimento de

quais interações estruturais e moleculares são fundamentais para a funcionalidade e capacidade de neutralização de anticorpos.

Para isso, algumas estratégias *in sílico* foram desenvolvidas*,* como a modelagem estrutural de proteínas através da homologia com estruturas cristalizadas e, portanto, já resolvidas (GROMIHA et al., 2019), bem como o *docking* molecular, baseado em algoritmos para geração de milhares de possíveis modelos de interação entre anticorpo/antígeno, ranqueados de acordo com critérios específicos para a predição de quais modelos mais se aproximam da real conformação (AMBROSETTI et al., 2019). Contudo, o padrão ouro para o mapeamento de epítopos permanece o método estrutural de cristalografia acoplada a raios-X do complexo de ligação, dado que ela possibilita a obtenção de modelos de resoluções quase atômicas da interação entre anticorpos e antígenos (TORIDE KING & BROOKS, 2018), permitindo inclusive, o mapeamento de epítopos conformacionais de alta complexidade.

Desse modo, através dessas técnicas e metodologias, os mecanismos de interação de anticorpos e proteínas bioativas pode ser estudado a fundo, o que permite não só conhecimento do anticorpo e seu alvo em si, mas futura otimização para o desenvolvimento farmacêutico dessas moléculas e aplicabilidade para a produção de outras moléculas de anticorpos inibitórias.

2.3. Anticorpos Monoclonais

O advento da produção de anticorpos monoclonais (mAbs) de origem principalmente murina (KOHLER & MILSTEIN, 1975) através da tecnologia de hibridoma, e posteriormente, de origem humana, por *phage display* (WINTER & MILSTEIN, 1991), foi um dos grandes impulsionadores deste processo. Por definição, anticorpos monoclonais possuem especificidade a um único epítopo de um determinado antígeno, ou seja, são oriundos de um único plasmócito. Este plasmócito pode ser imortalizado através da sua fusão com células de mieloma e então individualizado durante o processo de clonagem, como na tecnologia de hibridoma (Figura 4). Alternativamente, mRNA dessas células pode ser isolado e utilizado para construção de bibliotecas em células procarióticas e eucarióticas que expressam fragmentos de anticorpos na sua superfície, como no *phage display.* Consequentemente, essas tecnologias criaram a possibilidade de produzir-se

anticorpos de diferentes organismos, com potencial especificidade a qualquer antígeno proteico, de maneira uniforme e reprodutível (SINGH et al., 2018).

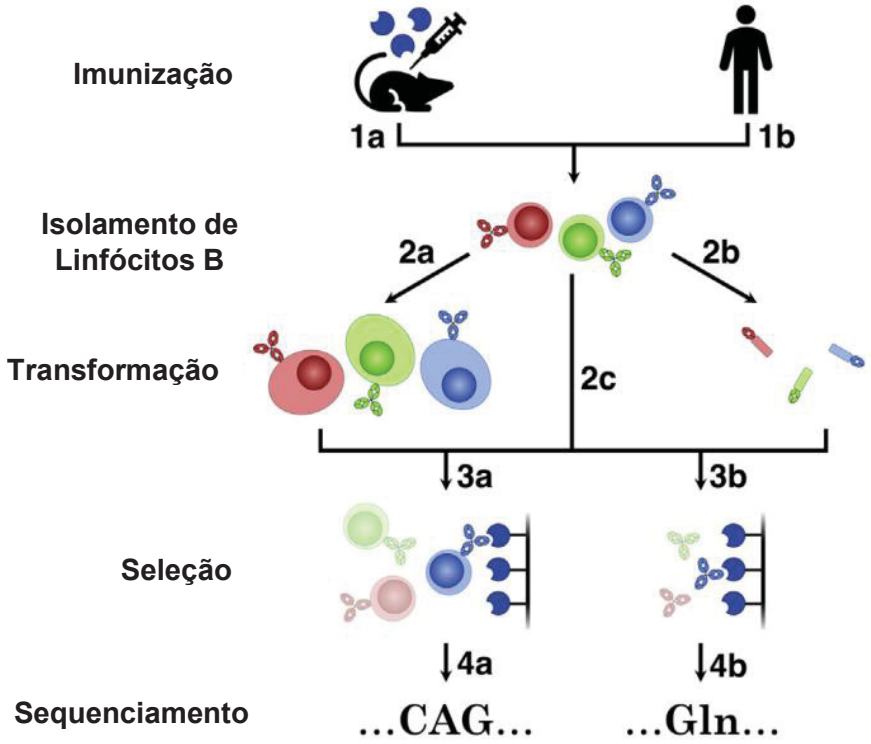

Figura 4. Estratégias para identificação das regiões variáveis de anticorpos. Genes V(D)J rearranjados podem ser obtidos a partir do baço de animais imunizados (1a) ou de pacientes doentes crônicos (1b). Após o isolamento das células B, as regiões variáveis dos receptores de células B (os anticorpos) são utilizadas para a geração de domínios variáveis de anticorpos expressos que podem ser utilizados em *screenings* funcionais. Uma estratégia consiste na imortalização das células B através da sua fusão com células de mieloma, gerando hibridomas produtores de anticorpos altamente proliferativos (tecnologia de hibridoma) – 2a. Alternativamente, o mRNA dessas células pode ser isolado e utilizado para construção de bibliotecas em células procarióticas e eucarióticas que expressam fragmentos de anticorpos na sua superfície (2b). Independente da estratégia utilizada, experimentos são realizados para seleção das moléculas de anticorpos funcionais, que se ligam ao antígeno de interesse. Essa seleção pode ser realizada no nível celular, através de citometria de fluxo (3a), ou através da detecção do antígeno por parte dos anticorpos secretados nos sobrenadantes celulares, em ensaios de ELISA (3b). Após essas análises,

candidatos ótimos podem ser identificados e sequenciados (4a/4b). Fonte: Adaptado de Goulet et al., 2019.

2.3.1. Anticorpos Recombinantes

A engenharia de anticorpos recombinantes, por sua vez, foi uma consequência direta da produção de anticorpos monoclonais por tecnologia de hibridoma e revolucionária na imunoterapia e na pesquisa biomédica. Dados os inconvenientes acerca da produção e emprego da soroterapia clássica, a utilização de anticorpos monoclonais e agora recombinantes surge como uma solução viável para muitos problemas, já que sua construção em sistemas procarióticos e eucarióticos é capaz de sintetizar e expressar grandes quantidades de anticorpos contra vários antígenos, o que diminui o custo da produção e de acordo com sua construção, bem como de uma diversidade de parâmetros físico-quimicos e imunogênicos, poderia evitar o desencadeamento de respostas imunológicas indesejadas(SAAED et al, 2017). Essas moléculas podem ser formatadas de diversas maneiras, segundo o seu objetivo de emprego e com implicâncias na sua farmacocinética e farmacodinâmica. A carga, solubilidade e estabilidade do anticorpo recombinante também podem ser alteradas de acordo com seu delineamento e construção, assim como sua especificidade e reconhecimento do antígeno alvo (AHMAD *et al*, 2012).

2.3.2. Formatação de Anticorpos Recombinantes

Os formatos nos quais anticorpos recombinantes podem ser produzidos são os mais variáveis (Figura 5). Monômeros (scFv – *single chain variable fragments*) ou dímeros (*diabodys*) apenas dos domínios variáveis, Fabs ou (Fab',)2 com algumas das porções constantes ou até mesmo no formato de imunoglobulina inteira (BATES et al., 2019).

Em alguns estudos, os scFvs (fragmentos variáveis de cadeia única) foram associados à uma alta penetração em tumores in vivo e uma alta capacidade de ligação a proteínas, receptores, antígenos tumorais ou outros anticorpos, sendo assim ótimos vetores para marcação celular e estudos de imagem (OLAFSEN e WU, 2010). Tendo em vista seu baixo peso molecular e rápida difusão nos tecidos, acredita-se que sejam candidatos ideais para a neutralização de substâncias tóxicas provenientes

de envenenamento, já que a ligação de um scFv específico ao sítio de ligação de uma molécula tóxica inativaria seu sítio ativo, e consequentemente inibiria seu efeito prejudicial. No entanto, algumas de suas propriedades farmacocinéticas podem ser indesejadas no contexto de tratamento. Devido a seu tamanho pequeno (na ordem de 25 kDa), sua excreção é majoritariamente renal e seu tempo de meia vida é bastante curto (0.5-30 horas). Adicionalmente, não apresentam porção Fc, portanto não são reciclados através da interação com os receptores FcRn, como as IgGs (LAUSTSEN et al., 2018).

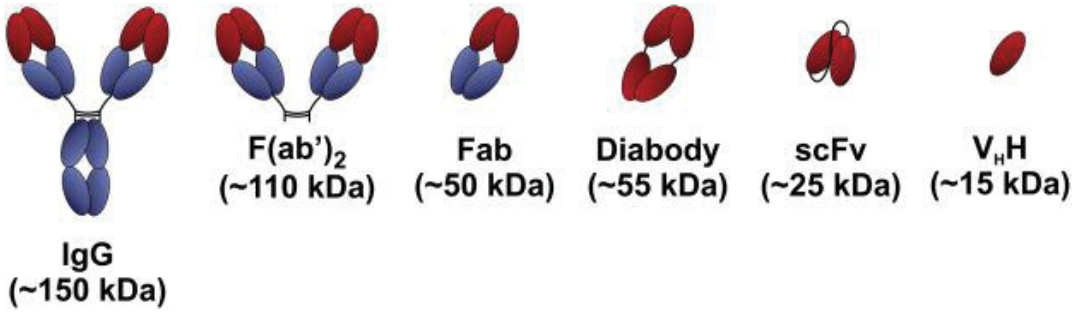

Figura 5. Representação esquemática dos diferentes formatos de anticorpos utilizados na clínica e experimentalmente. IgG: imunoglobulina tipo G inteira. F(ab')2: região específica de interação com antígeno de IgG. Fab: monômero da região específica de interação com antígeno de IgG. Diabody: dímeros não covalentes de fragmentos de anticorpos de cadeia única (scFVs). scFv: fragmentos variáveis de cadeia única. VHH: fragmentos de anticorpos de domínio único. Fonte: Adaptado de Laustsen et al, 2018.

Nesse sentido exploram-se adicionalmente outros formatos de fragmentos de anticorpos, como os diabodys (ligação de duas moléculas de scFv idênticas ou não), as porções Fab e (Fab',)2, os VHHs (domínio variável de anticorpos de cadeia pesada única), produzidos em camelídeos (FERNANDES et al., 2017), desprovidos de cadeia-leve, mas ainda sim, funcionais, e até mesmo o formato de IgG inteira, que de uma perspectiva farmacocinética apresentam um maior tempo de meia vida, diversas funções efetoras ligadas à porção Fv e a possibilidade de reciclagem por receptores FcRn, possibilitando assim um prolongamento do tratamento e administração em intervalos de tempo maiores. No entanto, sua difusão tecidual não é ótima como a de

um scFv ou diabody e sua natureza heteróloga implica em uma maior chance de ocorrerem reações adversas bem como um tempo de meia vida menor, quando comparam-se à IgGs e Fabs autólogas (LAUSTSEN et al., 2018, TANG et al., 2021)

Por fim, o tamanho da molécula e o formato a ser escolhido, assim como outras características devem ser avaliadas durante a concepção e produção de anticorpos recombinantes, de acordo com suas finalidades de emprego.

2.4. Imunoterapia:

A soroterapia, introduzida no final do século XIX pelos cientistas Emil Von Behring e Kitasato Shibasaburo (para toxina tetânica e diftérica), Albert Calmette, Césaire Phisalix e Gabriel Bertrand (para venenos de serpentes), marca o início da terapia baseada em anticorpos (DOS SANTOS et al., 2018; SQUAIELLA-BAPTISTÃO et al; 2018). A administração de soros policlonais de origem heteróloga, provenientes de animais imunizados com diversas toxinas, permitiam a imunização passiva de humanos (e outros animais) e a remediação de diversas condições. Contudo, a descoberta dos antibióticos, iniciada com a Penicilina em, por Albert Fleming (FLEMING, 1944), combinada com a toxicidade (devido a origem heteróloga) e alto custo de produção dos soros policlonais levaram a uma redução drástica na sua utilização. No entanto, a soroterapia continua sendo válida para o tratamento de enfermidades para as quais não existem fármacos disponíveis e sobretudo, ainda representam o padrão de ouro para a neutralização de misturas complexas de veneno e o tratamento de envenenamentos (SQUAIELLA-BAPTISTÃO et al; 2018).

A partir da década de 40, avanços na pesquisa básica de anticorpos como a descoberta da sua estrutura, diversidade, da recombinação V(D)J e da teoria de seleção clonal de Brunet, que afirmava que cada célula B produzia um anticorpo único e específico, conduziram o desenvolvimento da tecnologia do hibridoma, em 1975 (KOHLER & MILSTEIN, 1975). Torna-se então possível a geração de células híbridas que secretam anticorpos monoclonais, contra qualquer antígeno de escolha e em quantidades ilimitadas. Isso abre novamente os caminhos para a terapia baseada em anticorpos, entretanto, com um foco terapêutico distinto do inicial, não restrito apenas a doenças infecciosas e envenenamentos. O primeiro mAb a ser aprovado pelo FDA (U.S. *Food and Drug Administration*) para uso clínico é o muromonab, em 1986, visando tratamento da rejeição de transplantes. Assim, mAbs passam a ser considerados ‘’balas mágicas’’, dirigidos contra uma variedade de alvos terapêuticos,

pouco a pouco se estabelecendo de maneira importante na clínica e atualmente representando um dos maiores pilares da terapêutica baseada em proteínas (CHIU et al., 2019).

Essas moléculas têm sido empregadas como agonistas e antagonistas de proteínas circulantes e de receptores celulares, em processos de sinalização celular, no delivery de fármacos a alvos específicos, na neutralização de toxinas bacterianas e animais, e como mediadores de citoxicidade dependentes, ou não (ADCC – antibody dependent cell citotoxicity), do sistema de complemento (CDC – complement dependent citotoxicity) (CARTER et al., 2001; BECK et al., 2010; WEINER et al., 2015; LAUSTSEN et al., 2018). Diversos anticorpos monoclonais já foram aprovados como ferramentas terapêuticas para humanos pelo órgão FDA nos Estados Unidos, respeitando os critérios de segurança e imunogenicidade. Adicionalmente, segundo um levantamento realizado em 2021, cerca de 870 mAbs se encontram em processo de desenvolvimento terapêutico (MULLARD et al., 2021). Estas moléculas poderão ser usadas como marcadores moleculares ou no tratamento de importantes s como doenças cardiovasculares, autoimunes, infecciosas, inflamatórias, para envenenamentos, distúrbios de circulação e no câncer (GRAILLE et al., 2005; LEAVY, 2010; LEBOZEC et al., 2017, LAUSTSEN et al., 2018).

Considerando isto, alguns desafios surgem no momento da concepção, produção e otimização de mAbs para terapia. Na tentativa de diminuir-se a imunogenicidade dessas moléculas, através principalmente da quimerização e humanização, existe a possibilidade de perda ou diminuição de seu potencial terapêutico, estabilidade, afinidade e especificidade (PAVLINKOVA et al., 2001; MAKABE et al., 2008; GETTS et al., 2010; SAFDARI et al., 2013; FERNANDEZ-QUINTERO et al., 2019). Visando contornar esses problemas, estratégias como mutagênese randômica ou direcionada de domínios constantes e variáveis tem sido descritas e empregadas, visando (1) mimetizar uma maturação da afinidade in vitro dessas moléculas e assim otimizar a ligação com o alvo; (2) para manutenção de sua especificidade ao alvo, a despeito de ganhos ou perdas na afinidade; (3) para melhora de suas propriedades biofísicas (como estabilidade, solubilidade, agregação) e (4) para diminuição de sua imunogenicidade após a predição de peptídeos nessas sequencias que tem ligação favorável à MHC I/II. (RABIA et al., 2018 ; DOS SANTOS et al., 2018 ; GOULET et al., 2022).

2.4.1. Humanização de Anticorpos

A ampla utilização de anticorpos como insumos terapêuticos para diversas doenças está condicionada a diminuição ou eliminação de respostas imunes adversas, que possam prejudicar ou mesmo inviabilizar o tratamento com tais moléculas. A administração de anticorpos de origem heteróloga a humanos pode muitas vezes implicar em reações adversas precoces do tipo anafiláticas IgE-mediadas e não IgE-mediadas (ativação do sistema complemente) ou tardias, como a doença do soro, justamente porque essas moléculas apresentam uma origem considerada estranha pelo sistema imune e são passiveis de serem interpretadas como corpos estranhos (SANTOS et al., 2018).

Tendo isso em vista, surgiu a estratégia de humanização de anticorpos, descrita pela primeira vez em 1984, propunha a construção de anticorpos quiméricos compostos de regiões variáveis murinas e regiões constantes humanas (MORRISON et al., 1984). Menos de uma década depois, em 1997, o FDA aprova a utilização do Daclizumab (ZENAPAX™, Biogen), primeiro anticorpo humanizado empregado no tratamento de pacientes em processo de rejeição de transplantes renais (PRZEPIORKA et al., 2000).

Em linhas gerais, a humanização de anticorpos se dá a partir da sequência de aminoácidos de um anticorpo não-humano e, consiste no ‘’transplante’’ (do inglês, *grafting*) dos seus CDRs (*cluster differentiating regions*) contidos nas regiões hipervariáveis de cadeia leve e pesada, responsáveis pela interação direta de um anticorpo com um antígeno, em uma região de *framework* de um anticorpo humano, visando-se se manter sua especificidade e afinidade (Figura 6) (AHMADZADEH et al., 2014).

Hoje, dentre os 127 mAbs aprovados pelo FDA, encontram-se majoritariamente moléculas humanizadas (48%), seguidas de humanas (33%), quiméricas (14%) e então inteiramente murinas (4%) (Base de Dados Drugs@FDA). As estratégias para humanização de moléculas de anticorpos são diversas e estão em constante desenvolvimento e refinamento visando a produção de moléculas pouco imunogênicas, com maior ou inalterada afinidade, e com manutenção da especificidade pelo antígeno em relação ao anticorpo cognato não-humano (SAFDARI et al., 2013).

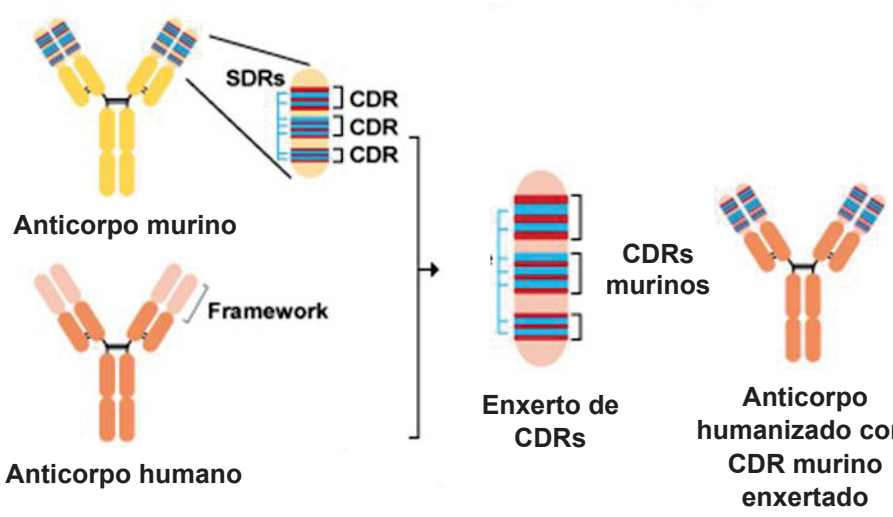

Figura 6. Humanização de Anticorpos. Estratégia de *Grafting* (transplante ou enxerto) das sequências codificantes dos CDRs murinos em sequências que codificam regiões estruturais (de framework) de anticorpos humanos para o design e produção de anticorpos humanizados. Fonte: Adaptado de http://www.abnova.com/HumanizedAb.

Dentre as principais estratégias de humanização de anticorpos estão (1) o transplante (do inglês, *grafting*) dos CDRs não-humanos em frameworks de IgGs humanas baseando-se na homologia entre essas regiões de framework; (2) a humanização através do transplante dos CDRs não-humanos em frameworks oriundos de genes codificantes de anticorpos de linhagens germinativas humanas e não de IgGs já secretadas, e por fim, (3) a humanização baseando-se na homologia apenas das regiões de CDR não-humanas e putativas humanas. (AUBREY et al., 2018).

É importante ressaltar a diferença entre anticorpos quiméricos e humanizados. Os primeiros consistem em sequências de regiões variáveis inteiramente murinas combinadas com regiões estruturais e constantes humanas. Por sua vez, a proposta de humanização consiste estritamente na inserção apenas das regiões hipervariáveis murinas (CDRs), ainda passivas de mutações pontuais, em regiões estruturais (ou de *framework*) humanas, presentes ainda nos domínios variáveis. Para cada molécula de anticorpo quimérica ou humanizada há uma nomenclatura farmacológica determinada. Por exemplo, para anticorpos monoclonais quiméricos utiliza-se o sufixo –xi (e.g. Abci**xi**mab). Já para anticorpos humanizados os sufixos –zu (e.g.

Alemtu**zu**mab) e –xizu (e.g. Oteli**xizu**mab) podem ser empregados, o primeiro em casos em que apenas as regiões de CDR murinas são mantidas e o último quando apenas uma das regiões variáveis é considerada humanizada, sendo a outra inteiramente murina, processo que se denomina humanização via intermediário quimérico. Por fim, para anticorpos inteiramente humanos, o sufixo –u é utilizado (e.g. Adalim**u**mab) (WHO, 2009, FDA), (MAYRHOFER et al., 2019).

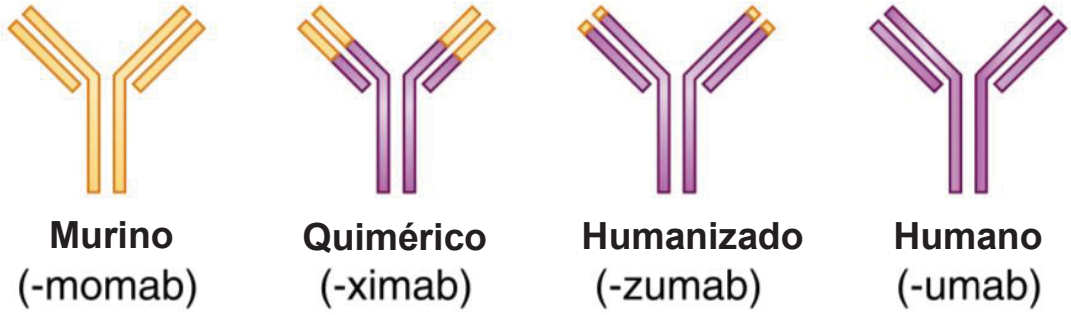

Figura 7. Nomenclatura de anticorpos terapêuticos. Representação esquemática das estruturas de imunoglobulinas murinas, quiméricas, humanizadas e humanas (da esquerda para a direita) e os sufixos utilizados para sua nomenclatura na clínica. As regiões de origem murina estão representadas pela cor amarela e as regiões de origem humana em roxo. Fonte: Adaptado de Wiseman et al, 2016.

Dentre as vantagens em se humanizar anticorpos monoclonais está a possibilidade de utilizar-se sequências de anticorpos gerados a partir de organismos imunizados com o antígeno de interesse (E.g. camundongos imunizados com toxinas) e, portanto, com maior afinidade ao alvo em questão, pois a resposta imune do animal utilizado foi devidamente direcionada a este antígeno e as imunoglobulinas por ele produzidas otimizadas através dos mecanismos fisiológicos imunes de maturação de afinidade e *switch* de classe de anticorpos específicos (ADLER et al. 2017).

Contudo, o processo de humanização requer bastante atenção e estudo no momento de sua execução. A escolha das mutações a serem realizadas nas regiões variáveis deve ser planejada cuidadosamente para que a molécula humanizada não perca ou reduza drasticamente sua funcionalidade. A mutação de resíduos únicos de aminoácidos pode provocar perda de afinidade, especificidade e até mesmo de funcionalidade (SAFDARI et al., 2013). Dentre alguns parâmetros importantes a serem considerados durante o processo de humanização estão as características de

developability, segurança e eficácia da molécula a ser humanizada e produzida. Critérios como manutenção ou melhoramento da estabilidade, ausência de agregação e dimerização, rendimento de produção, funcionalidade e baixa imunogenicidade são desejáveis e devem ser cuidadosamente avaliados. Adicionalmente, a elegibilidade dessas moléculas para processamento *downstream* também deve ser estudada e considerada (GRONEMEYER et al., 2015; BAILLY et al., 2020).

2.4.2. Bibliotecas de Anticorpos Humanos

Outra estratégia amplamente utilizada na indústria farmacêutica no desenvolvimento de insumos terapêuticos é a obtenção de anticorpos humanos específicos a diferentes ligantes através da tecnologia de *phage display*, utilizando-se bibliotecas de fagos expressando em suas superfícies as regiões variáveis de anticorpos humanos. Em linhas gerais, essas bibliotecas são construídas a partir da extração do RNA de um pool de células B humanas, amplificação apenas das regiões gênicas codificantes de anticorpos e sua posterior inserção em fagemídeos (KUMAR et al., 2019). A partir deste *approach* é possível selecionar os fagos expressando regiões VH/VL reativas a qualquer alvo de escolha.

Atualmente, estão liberados pelo FDA para tratamento de enfermidades 10 anticorpos humanos produzidos através de *phage display* e bibliotecas humanas. O pioneiro, Adalimumab (Humira), aprovado em 2002, tem como alvo o receptor da citocina TNF-α e é útil no tratamento de condições de inflamação crônica, dentre estas muitas desencadeadas por auto-imunidades como a Doença de Crohn e Espondilite Anquilosante (LAUSTSEN et al., 2018a). Apenas em 2016, este anticorpo foi utilizado no tratamento de 1 milhão de pessoas, gerando um faturamento de 16 bilhões de dólares para a farmacêutica AbbVie Inc.

De fato, a produção de anticorpos para tratamento a partir de bibliotecas humanas é bastante vantajosa quando se consideram fatores como tempo de produção, custo, não-necessidade da utilização/manipulação de animais, obtenção rápida da sequência gênica codificante do anticorpo em questão e possibilidade da produção de anticorpos contra alvos não necessariamente imunogênicos. No entanto, essa metodologia só pode ser realizada através de uma biblioteca de anticorpos humanos, pré-existente, ou que deve ser construída em um processo relativamente laborioso (LEDSGAARD et al., 2018).

Adicionalmente, anticorpos humanos provenientes de bibliotecas não-imunes

podem apresentar baixa afinidade e/ou avidez aos alvos contra os quais foram selecionados (RICHARD et al., 2013; STEWART et al., 2007), quando comparados a anticorpos murinos provenientes de camundongos imunizados com o antígeno de interesse e, portanto, que desenvolvem toda uma resposta imune de maturação de afinidade, hipermutações somáticas e *switch* de classe desses anticorpos (LEDSGAARD et al., 2018). Anticorpos provenientes de bibliotecas não imunes são compostos pelo repertório de imunoglobulinas dos doadores, pré-formado e provavelmente não "primados" contra antígenos de interesse (ADLER et al., 2017). No entanto, essa questão pode ser contornada através da realização de ciclos adicionais de seleção (do inglês *biopanning*) de scFvs com maior afinidade ao alvo e também através de mutações pontuais na sequência codificante visando aumento de afinidade (LEDSGAARD et al., 2018b; ADLER et al., 2017;).

Também deve ser considerado o fato de que nas bibliotecas de phage apenas são produzidos anticorpos nos formatos de scFvs ou Fabs, sem a porção Fc, que é a responsável por diversos mecanismos imunes efetores como opsonização, ativação do sistema do complemento e mesmo, reciclagem dessas moléculas, com consequente prolongamento de seu tempo de meio vida (KUMAR et al., 2019). Contudo, de uma perspectiva que preconiza anticorpos neutralizantes (nAbs), como por exemplo, no tratamento de envenenamentos (STOYANOVA et al., 2012; RONCOLATO et al., 2013;), ou mesmo, na busca de potentes antivirais (KUMAR et al., 2018), não existe um consenso no papel da porção Fc como determinante do potencial neutralizante de um fragmento de anticorpo (KRISHNA et al., 2016; LAUSTSEN et al., 2018), justamente pois muitas vezes o objetivo maior ser a obtenção de anticorpos com afinidade elevada por determinado antígeno tóxico, que ao se ligarem a este alvo, o neutralizam e possibilitam sua rápida excreção, característica principalmente dos scFvs. (ALEWIN et al., 2015).

Tendo isso em vista, fica evidente o interesse na utilização da tecnologia de *phage display* para obtenção de fragmentos de anticorpos humanos na perspectiva de tratamento para diferentes doenças com menor probabilidade de suscitar reações adversas às vítimas e potencialmente, com melhores resultados. No entanto, é importante ressaltar que ainda existe possibilidade (por mais que bastante reduzida) de ocorrer uma resposta adversa quando anticorpos de origem autóloga são administrados a humanos (HARDING et al., 2010).

2.5. Critérios para Produção de Anticorpos Terapêuticos – Da *Developability* ao *Downstream*

Avanços importantes na engenharia de anticorpos durante a última década permitiram melhorias na sua produção, bem como o aumento da eficácia e segurança no emprego. A melhor compreensão sobre a estrutura e funções dos anticorpos, abrem caminho para a geração de novos (e otimizados) insumos terapêuticos baseados em anticorpos para o tratamento de doenças humanas (LU et al., 2020).

Nesse sentido, diversos critérios de *developability,* (viabilidade de moléculas progredirem com sucesso desde sua descoberta até o seu desenvolvimento através da avaliação de suas propriedades físico-químicas), biossegurança e eficácia são considerados e trabalhados no contexto da indústria farmacêutica (XU et al., 2019). Estes em conjunto, visam a produção de anticorpos terapêuticos funcionais, com bom rendimento de produção, livres de contaminantes, termoestáveis, tolerantes à grandes variações de pH, de baixa imunogenicidade e de custo/benefício rentável, incluindo-se também as etapas de processamento *downstream* desses insumos (como a filtração, esterilização por altas temperaturas e baixos pHs para inativação viral, remoção de agregados etc.) (SHUKLA et al., 2007; JARASCH et al., 2015).

Vários fatores devem ser considerados no *design* de anticorpos terapêuticos, dado que cada um deles tem um impacto direto na estrutura proteica e consequentemente na sua atividade biológica e potencial terapêutico. A escolha do alvo para o qual o anticorpo será desenvolvido e da estratégia para o tal tem um efeito direto na estrutura primária e terciárias dos domínios variáveis desse anticorpo. Diferenças ao nível dos domínios variáveis influenciam diretamente a natureza da interação anticorpo/antígeno, incluindo afinidade, especificidade e funcionalidade, caso o anticorpo tenha um efeito inibitório. Em conjunto, essas propriedades biológicas determinam a potência dessas moléculas, bem como seu índice terapêutico – razão entre a dose tóxica e a dose capaz de produzir a resposta clinicamente desejada.

Nesse sentido, fatores com a subclasse, isotipo e alótipo dos anticorpos afetam a estrutura e função das regiões constantes, o que por sua vez demanda a necessidade da escolha de um sistema de expressão adequado para sua produção e determina como essas moléculas se ligam os receptores de Fc (FcRs), relevantes para as funções efetoras destes e para o aumento do seu tempo de meia vida, através

da reciclagem por receptores Fc-Rn. Dessa forma, vários determinantes devem ser considerados ao nível da estrutura e função de anticorpos terapêuticos no momento do seu *design* e concepção (Figura 7). Embora características estruturais distintas tenham consequências funcionais muitas vezes sobrepostas, anticorpos podem ser projetados de forma a combinar todas as características desejadas em uma única molécula otimizada (GOULET et al., 2019).

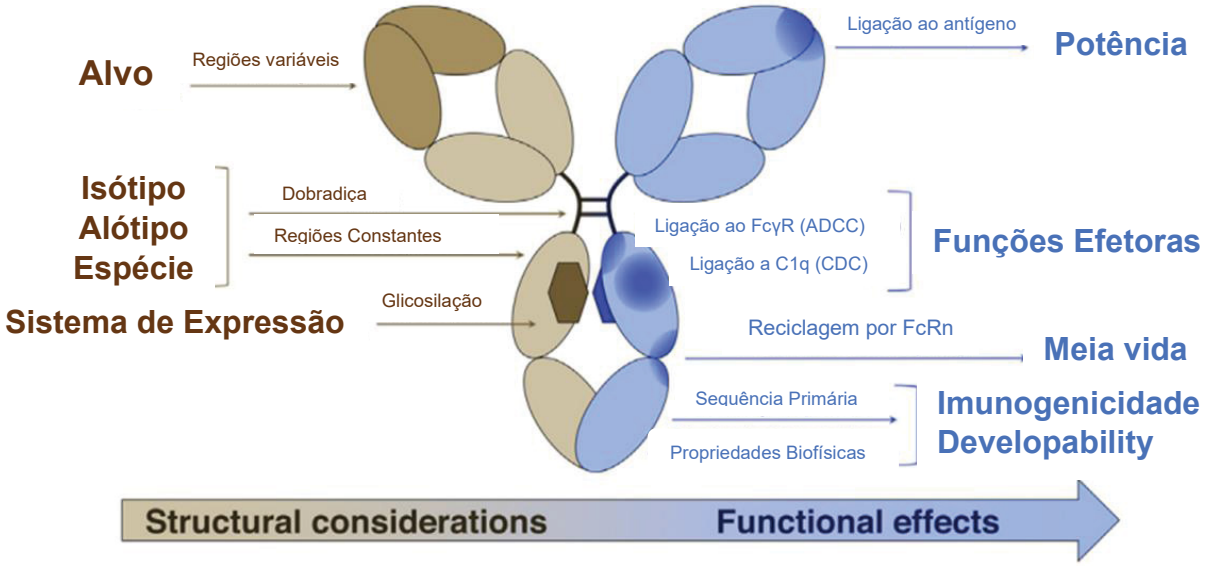

Figura 7. Considerações acerca da produção de anticorpos terapêuticos.

Fonte: Adaptado de Goulet et al., 2019.

Tendo isso em vista, ao ponderar-se a concepção, produção, caracterização e emprego biotecnológico de anticorpos, sobretudo na terapêutica, algumas questões são levantadas: (1) a importância da biossegurança destes insumos e de estudos no sentido da redução da imunogenicidade destas moléculas; (2) a manutenção da sua funcionalidade, principalmente mediante sua humanização, produção recombinante e os diferentes sistemas de expressão usados para o tal; (3) ao considerar a produção em larga escala dessas moléculas, quais parâmetros de qualidade devem ser avaliados e quais variáveis são relevantes para seu melhoramento; (4) a capacidade do inibição de seu alvo, caso este tenha atividade biológica, bem como o estudo dos mecanismos moleculares envolvidos neste processo.

2.6. Justificativa do Estudo:

Dada a relevância dos anticorpos monoclonais na terapêutica de diversas patologias, estudos da sua estrutura e função pode promover avanços e aperfeiçoamentos significativos no seu processo de concepção, produção, otimização e aplicação terapêutica. Para isso, parâmetros acerca da segurança, eficácia e *developability* (propriedades biofísicas) dessas moléculas necessitam ser explorados e caracterizados.

Logo, no presente estudo, a humanização de anticorpos foi estudada por Karim Silva et al., 2020 e explorada mais amplamente por Jiacomini et al., 2022 (em processo de submissão). Como modelo para ambos os estudos, o anticorpo LimAb7 (ALVARENGA et al., 2003), uma IgG_1 murina com potencial neutralizante *in vivo* e *in vitro* frente toxinas dermonecróticas do veneno da aranha marrom *Loxosceles intermedia*, foi empregado. Esse anticorpo foi produzido anteriormente com sucesso em diversos formatos recombinantes murinos (KARIM SILVA et al., 2016, JIACOMINI et al., 2016), contudo, visando sua evolução para diminuição da sua imunogenicidade e futura administração terapêutica, a humanização do LimAb7 foi considerada.

Inicialmente, os formatos de scFv e diabody foram produzidos e duas variantes humanizadas foram geradas e estudadas segundo sua estabilidade, afinidade e potencial de neutralização (KARIM SILVA et al., 2020). Subsequentemente, um segundo estudo (JIACOMINI et al., 2022) visando melhorar parâmetros biofísicos e estudar mais profundamente os diferentes critérios para humanização de sequências de anticorpos, produziu dezesseis Fabs derivados do LimAb7, combinando quatro diferentes critérios de humanização distintos, e analisados quanto à diferentes parâmetros físico-químicos e funcionais. Deste modo, os estudos supracitados e detalhados na íntegra a seguir, possibilitam um aprofundamento no conhecimento geral e aplicado da humanização de anticorpos monoclonais com fins terapêuticos.

Levando em conta essa relação intrínseca entre estrutura e função de anticorpos e sua relevância no entendimento dos mecanismos de interação anticorpo/antígeno, o estudo de Aubrey et al., 2020, explorou detalhadamente a participação das regiões estruturais (ou de *framework)* na promoção de fragmentos recombinantes de anticorpos com propriedades biofísicas evoluídas através da mutação pontual de resíduos de amino ácidos nessas regiões. Certas mutações promoveram aumentos significativos no rendimento de produção, tolerância à baixo pH e estabilidade térmica

dos fragmentos estudos, demonstrando assim, que as regiões estruturais (como o nome já sugere) são um importante arcabouço para o sustentamento estrutural, e consequentemente funcional, dos CDRs.

Por fim, o conhecimento de quais os parâmetros mais influentes para a concepção de moléculas ótimas, bem como de seu mecanismo de inibição é muito importante, considerando que análises *in silico* devem sempre ser validadas em análises in vitro/in vivo. Tais elementos foram avaliados no estudo de Billiald et al., 2022 (em processo de submissão), que buscou entender através da estrutura cristalizada de um Fab humanizado (LEBOZEC et al, 2017) ligado a seu alvo trombolítico (Glicoproteína 6 – GPIV), o mecanismo pelo qual a inibição do alvo ocorre. Para o tal, análises cuidadosas ao nível da estrutura tridimensional do anticorpo e do antígeno, em sua forma ligada e não ligada, foram realizadas através de ensaios *in sílico* e *in vitro*. Combinados, esses dados permitiram a elucidação do mecanismo de inibição do Fab, por impedimento estérico e indução de mudança conformacional, e como no estudo de Aubrey et al., 2022, conduziu a um avanço significativo no entendimento da relação estrutural e funcional de anticorpos.

Tendo isso em vista, os dados apresentados nos estudos aqui compilados, oferecem norteamento importante no sentido da produção, desenvolvimento e otimização de moléculas de anticorpos recombinantes mais adaptadas e otimizadas para aplicação terapêutica.

3. OBJETIVOS

Objetivo Geral

- Estudos sobre a humanização, a produção melhorada e os mecanismos de ação de anticorpos recombinantes com potencial terapêutico.

Objetivos Específicos

- Humanização do anticorpo monoclonal LimAb7 segundo diferentes critérios para a escolha dos *frameworks* aceptores.
- Produção de diversas variantes humanizadas (scFv, diabody e Fab) do LimAb7 em diferentes formatos e sistemas de expressão.
- Caracterização dos fragmentos humanizados produzidos segundo diversos parâmetros biofísicos
- Avaliação da manutenção da reatividade das moléculas humanizadas ao alvo e da sua especificidade às Fosfolipases D de *L. intermedia*.
- Avaliar a capacidade de diferentes mutações na região de *framework* do anticorpo SA01 influenciarem na melhora ou piora de suas propriedades biofísicas, com consequente ganho de produção.
- Após a obtenção do co-cristal do anticorpo Glenzocimab ligado a proteína GpVI, estudar através de análises de bioinformática de modelos estruturais o mecanismo de inibição pelo qual o anticorpo impede seu alvo de se ligar ao colágeno.

4. CAPÍTULO I: HUMANIZAÇÃO DE ANTICORPOS MONOCLONAIS

4.1. Produção de gerações preliminares de fragmentos de anticorpos humanizados a partir do anticorpo monoclonal LimAb7

Loxoscelism: Advances and challenges in the design of antibody fragments with therapeutic potential

Abstract: Envenoming due to *Loxosceles* spider bites still remains a neglected disease with particular medical concern in the Americas. To date, there is no consensus for the treatment of envenomed patients, yet horse polyclonal antivenoms are usually infused to patients with identified severe medical condition. It is widely known that venom proteins in the 30-35 kDa range with sphingomyelinase D (SMasesD) activity, reproduce most toxic effects observed in loxoscelism. Hence, we believe that monoclonal antibody fragments targeting such toxins might pose an alternative safe and effective treatment. In the present study, starting from the monoclonal antibody LimAb7, previously shown to target SMasesD from the venom of *L. intermedia* and neutralize its dermonecrotic activity, we designed humanized antibody V-domains, then produced and purified as recombinant single-chain antibody fragments (scFvs). These molecules were characterized in terms of humanness, structural stability, antigen-binding activity, and venom-neutralizing potential. Throughout this process, we identified some blocking points that can impact the Abs antigen-binding activity and neutralizing capacity. *In silico* analysis of the antigen/antibody amino acid interactions also contributed to a better understanding of the antibody's neutralization mechanism and led to reformatting the humanized antibody fragment which, ultimately, recovered the functional characteristics for efficient *in vitro* venom neutralization.

Keywords: venom; antivenom; neutralization; loxosceles; sphingomyelinase D; humanization; scFv

1. INTRODUCTION

To date the *Loxosceles* genus is comprised of 139 described spider species, differentially distributed and found in all five continents where different species have been reported [1]. In Brazil, *L. intermedia, L. gaucho*, and *L. laeta* are of particular medical concern, as in 2019 the number of envenomings was 8,490, in which 11 were fatal for humans [2,3]. The diagnosis for loxoscelism is often impaired and belated given bites are usually painless and often unnoticed including clinical manifestations that appear only several hours afterwards. Symptoms start two to eight hours post-event and are marked by an intense inflammatory reaction at the bite site, and followed by local necrosis that can lead to ulcers of variable sizes. Such lesions often heal within 6 to 8 weeks, and can leave lasting scars which may even require surgical excision [4]. Viscerocutaneous, also designated as systemic loxoscelism, is the most serious clinical manifestation and accounts for up to 27% of cases [5]. It is characterized by fever, nausea, hematuria, hemoglobinuria, and disseminated intravascular coagulation. Occasionally, extensive hemolysis may lead to acute kidney injury and renal failure, the primary cause of loxoscelism associated death.

Usually, bites result in the intradermal injection of few microliters of venom corresponding to around 50 micrograms of protein. As indicated by 2D electrophoresis, the protein content of the venom has great interspecies similarity with proteins ranging from 2 to 94 kDa. This includes serine proteases, serine protease inhibitors, hyaluronidases, inhibitor cystine knot (ICK) peptides and phospholipases D (PLD), the latter being the most studied and well-characterized venom components due to their ability to induce dermonecrotic lesions and hemolysis [6]. More than 25 spots immunologically related to PLD toxins have been identified in the *L. intermedia* venom, most of them being SMase D related [7]. A great number of studies has been carried out on these toxins. Nine isoforms of PLDs have been recombinantly produced and expressed as soluble and active enzymes that reproduce most of the toxic effects observed in loxoscelism [8–12]. X-ray crystallography analysis of recombinant LiRecDT1 SMase D (SMase D LiRecDT1) from *L. intermedia*, both wild-type and H12A-mutant forms, are available and the catalytic pocket of the enzyme is well-identified [13]. This and other reports reveal important insights into the enzymatic properties of each one of the isoforms, but also underline clear differences in the hydrolytic ability of PLD isoforms within the *Loxosceles* genus.

To date, there is no consensus treatment for the management of patients who are admitted to the hospital 12 to 24 h after the bite [14,15]. Symptomatic and non-specific treatments have been implemented in most countries for the treatment of the less critical cases. In South America, horse polyclonal antivenoms are available and usually infused intravenously to all patients showing viscerocutaneous loxoscelism. These preparations are mostly comprised of $F(ab)'_2$, but also whole IgGs (Peru) [14–16]. They target all the components of the venom and may neutralize toxins by various mechanisms, including direct inhibition of the toxin's catalytic site, steric hindrance, and allosteric inhibition. However, these *Loxosceles* antivenoms have often been less successful than those produced for the treatment of snake envenomings, in light of their effectiveness [15]. There is no direct relationship between toxicity of the venom's molecules and their immunogenicity, and antibodies raised against *Loxosceles* dermonecrotic toxins often show low interspecies cross-reactivity [17,18]. In addition, such conventional antivenoms based on animal immunization belong to the category of blood-based products as defined by the regulatory authorities, with safety concerns, not chemically well-defined components, and high batch to batch variability. Polyclonal

antibodies present limited specific activity, thus they might bind to toxin components, but not necessarily neutralize them and could be effectively substituted with specific anti-SMase D antibodies [19]. In this context, recombinant binding-proteins with toxin neutralization potential could be an interesting alternative.

One promising and suitable strategy for whole venom neutralization consists in using monoclonal or polyclonal antibody fragments. Several antibodies discovered against *Loxosceles* venom components have been previously generated [17,20,21]. However, only one (LimAb7) satisfies all the criteria required in terms of specificity, affinity, and neutralizing capacity [20]. LimAb7 specifically binds to 32-35 kDa components of *L. intermedia* venom and is reactive to the SMase D LiRecDT1 toxin. This antibody was also shown to neutralize the venom's dermonecrotic activity in rabbits, while recombinant antibody fragments preserved antigen-binding affinity and the ability to neutralize the venom *in vitro* [22]. Nonetheless, the potential immunogenicity of antibodies from mouse origin is a major barrier to infusion in humans. This drawback can be overcome by modifications on the framework regions of the antibody's V-domains, through a process termed antibody humanization, which reduces its immunogenic potential while maintaining the bioactivity of the antibody molecule [23,24]. All things considered, we hereby designed and evaluated a recombinant humanized antibody fragment constructed from LimAb7 complementarity determining regions (CDRs). During this process, we clearly identified some blocking points that could impact in the antibody's antigen-binding activity, neutralizing capacity, and pharmaceutical development. *In silico* mapping of the antigen/antibody interaction also contributed to a better understanding of its intrinsic neutralization mechanism and has led us to reformat the humanized antibody fragment which, ultimately, recovered the functional characteristics required for efficient *in vitro* neutralization of the venom.

2. RESULTS

2.1. Design of a humanized scFv anti- L. intermedia venom

Structural analysis of LimAb7 allowed us to identify all three CDRs of each V-domain (Fig. 1). Length-independent canonical class and sub-class for the non-H3 CDRs were identified as L1–similar to 3/17A; L2–1/7A; L3–similar to 5/11A; H1– similar to 1/10A; H2–2/10A. The packing angle of VH and VL domains, influential to the topography of the antigen-combining site, was predicted to be -42.8 [30]. The humanness score of the V-domain sequences (-1.132 and -1.164 for VH and VL, respectively) clearly indicated a high risk of immunogenicity, all parameters being accounted for further humanization [43] .

Sequence database searches allowed us to identify human germline genes closely related to LimAb7 V-domains (IGHV and IGKV) and perform an alignment of the deduced AA residues sequences. We also aligned the LimAb 7 sequences with NEWM (PDB : 7FAB) and REI (PDB : 1REI) myeloma antibody sequences for VH and VL, respectively. These sequences are often used in a "fixed framework" strategy for antibody humanization [24]. However, NEWM was dropped of this study due to its substantial sequence dissimilarity with IGHV-LimAb7 (<50% identity), whilst the human germline IGKV sequence (IGKV1-27*01) was identified as one of the most similar human template for the kappa chain (60.0 % identity).

For each of the LimAb7 V-domains, 29 AA residues differed from the human acceptor frameworks (FR). We paid close attention to maintaining cohesion between most residues at positions in VL and VH buried in the interface between the domains. In order to create and secure a PpL binding site that is highly dependent on several

residues belonging to IGKV FR1 and residues L90 and L127 as well, the whole FR1 of REI protein was introduced while maintaining residues T (L90) and K (L127) [32]. All throughout the process, the modifications were approved after detailed analysis in order to confirm the ongoing improvement of the humanness Z-score and the decrease of the residual immunogenicity (Fig. 2). Canonical class and sub-class CDRs were preserved for L1, L2, L3 and H1 while high similarity with canonical class 2/10A was maintained for H2 (residue H80: preferentially Arg, but also Val). The expected VH/VL packing angle was slightly modified upon the process (-42.8 for LimAb7 and -45.4 for the humanized version) but this change was considered acceptable. Lastly, 23 and 26 residues were mutated for IGHV and IGKV, respectively. A 3D structural model of the humanized V-domains of LimAb7 is shown in Fig. 2C.

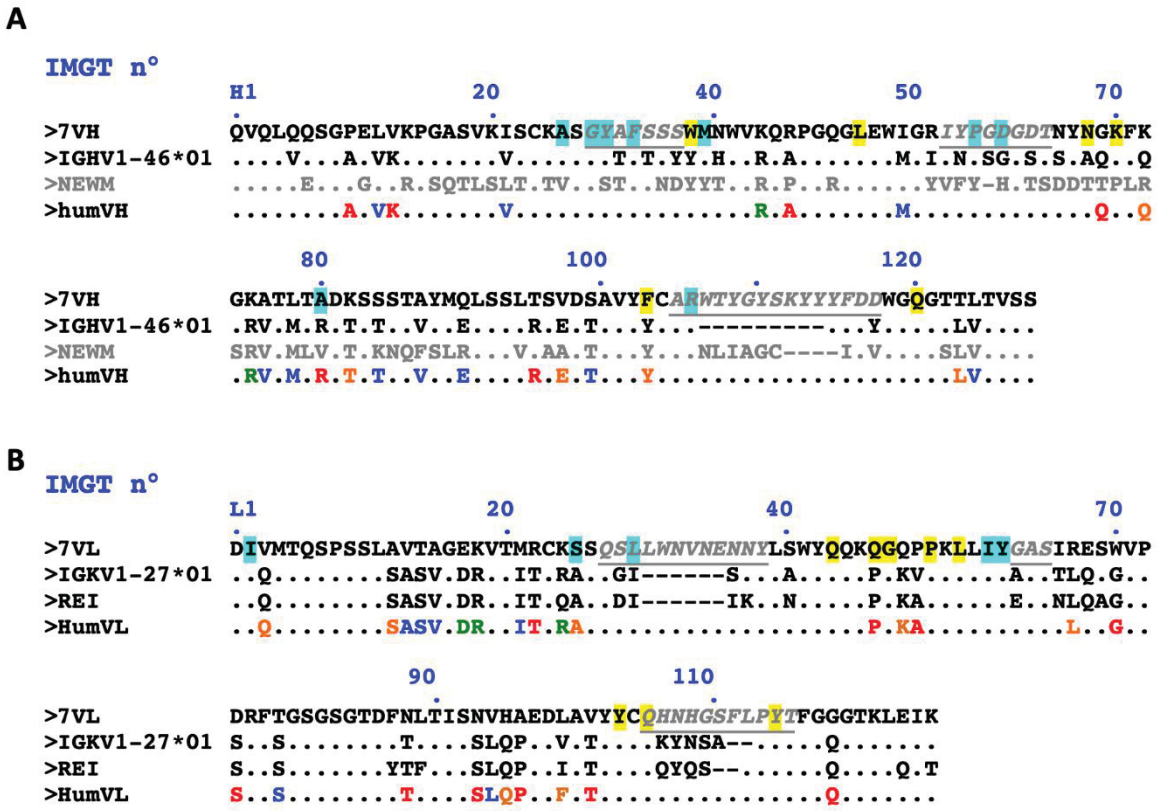

Figure 1. Design of humanized LimAb7 V-domains. A- Sequence alignment of the mouse LimAb7 IGHV (7VH) with human germline sequence IGHV1-46*01, the NEWM protein sequence ("fixed framework" strategy) and the humanized LimAb7 IGHV (humVH) that retains antigen-binding activity. B- Sequence alignment of the mouse LimAb7 IGKV (7VL) with human germline sequence IGKV1-27*01, the REI protein sequence ("fixed framework" strategy) and the humanized LimAb7 IGKV (humVL) that retains antigen-binding activity. CDRs according to IMGT are in italic, underlined, grey. Residues at key sites for canonical structures are highlighted in blue. Residues buried in VH/VL interfaces are underlined in yellow. Based on the physico-chemical classes of the amino acids (AA), differences in the framework regions of mouse LimAb7 and its humanized variants are classified into very similar AA (green), similar AA (blue), dissimilar AA (orange) and very dissimilar AA (red).

A

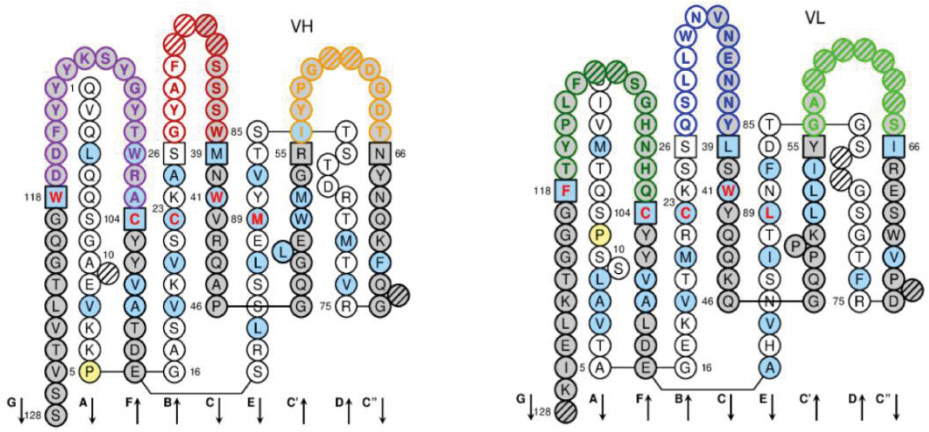

B

Sequence identity (%) with closest human germline and the humanness Z-score [--]

	V-domain		Individual humanized FR region		
	Mouse	Humanized	FR1	FR2	FR3
IGHV	67.3 [-1.132]	86.7 [-0.080]	96	100	95
IGkV	71 [-1.644]	84.2 [0.232]	100	100	100

C

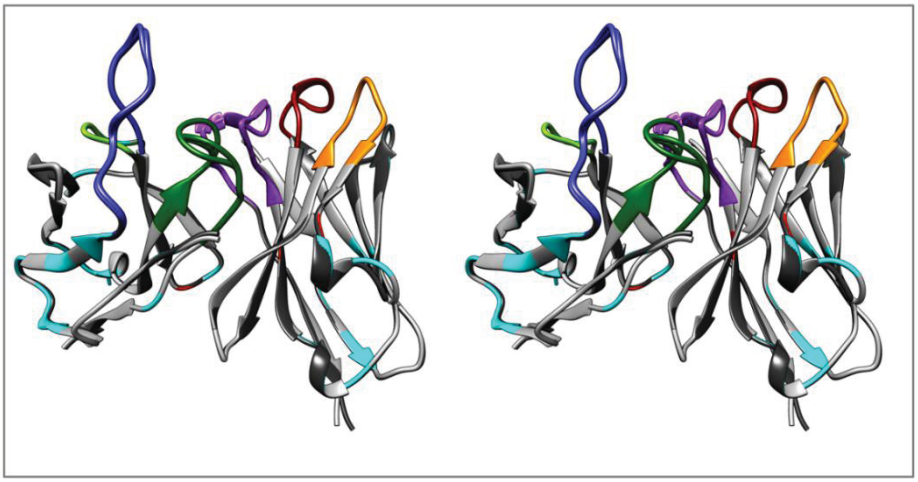

Figure 2. LimAb7 humanized V-domains. A- Secondary structure representation of the variable region sequences in the "*collier de perles*" format. B- Comparative analysis between the LimAb7 antibody mouse variable region sequences and the modified sequences after humanization with human germline sequences. Percentage of sequence identity with the closest human germline considering the whole V-domain sequence or each individual humanized FR. The humanness Z-score of each domain is also indicated into brackets. C- Stereo view of scFv$_{15}$hLi7 with coloured CDRs (H1: red, H2: orange; H3: purple; L1: blue; L2: light blue; L3: forest green). Mutated residues exposed at the surface are in cyan. Residues buried in VH/VL interfaces and mutated upon humanization are in red.

2.2. Primary screening of scFv$_{15}$hLi7

A synthetic codon-optimized bacterial gene encoding the monomeric single-chain antibody fragment scFv$_{15}$hLi7 made up from the humanized VH domain of LimAb7 fused to the humanized VL domain via a flexible 15 residues linker was designed (Fig.

3A). Pilot expression was carried in the periplasm of bacteria and the recombinant antibody fragment was isolated from other periplasmic proteins by affinity chromatography using PpL-affinity resin (Fig. 3B). No precipitation was observed in the elution peak after neutralization and buffer exchange to PBS pH 7.2. A samples' electrophoretic profile analysis confirmed the identity of the purified protein which appeared as a unique 29 kDa protein after Coomassie Blue staining, as well as after Western blotting using the PpL-peroxidase conjugate under non-reducing conditions. Dot blot allowed a rapid screening to validate the ability of scFv$_{15}$hLi7 to bind *L. intermedia* venom in a specific manner with no detectable cross-reactivity with *L. laeta* and *L. gaucho venoms* (Fig. 3C).

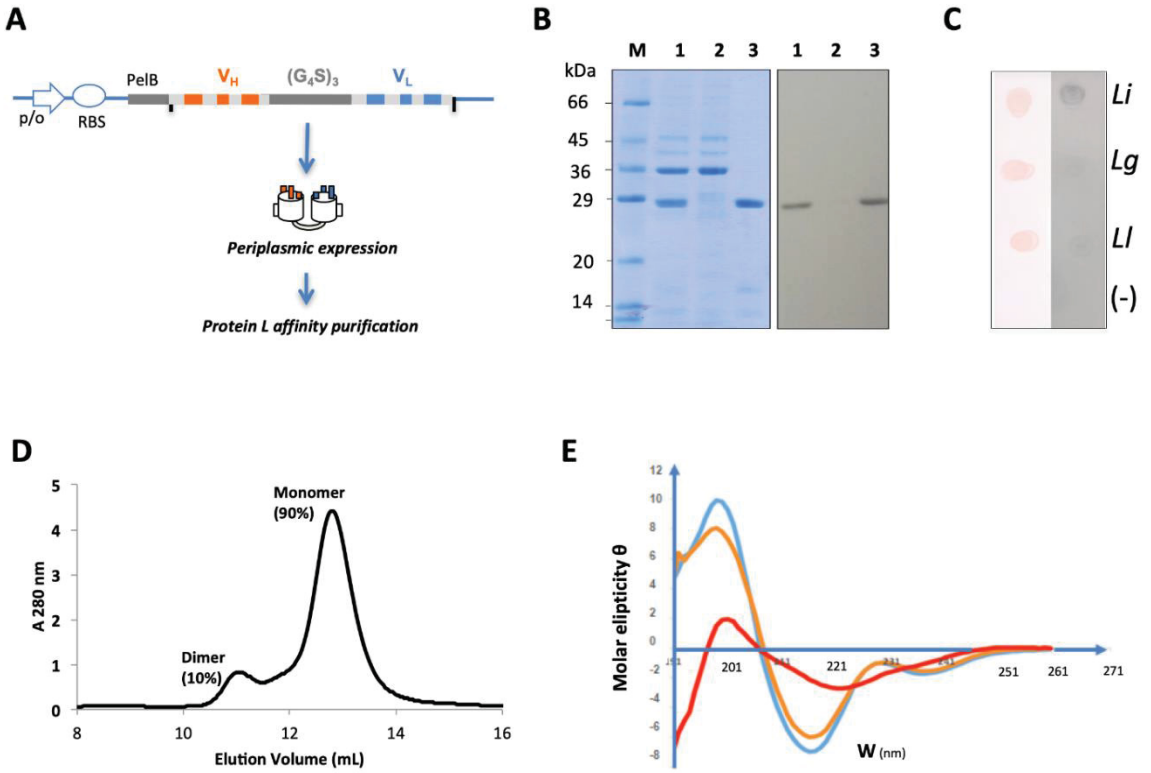

Figure 3. Design, expression and purification of scFv$_{15}$hLi7. A- Schematic representation of the design and expression cassette. The open reading frame is under the control of a T7 promoter and contains a PelB signal sequence for periplasmic expression followed by a cDNA encoding humanized VH and VL fused together via a (Gly$_4$Ser)$_3$ linker. This allows expression of monomeric untagged scFv$_{15}$hLi7. B- Protein expression scFv$_{15}$hLi7 analysis in periplasmic extract by polyacrylamide gel electrophoresis (SDS-PAGE) and Western blot, before and after affinity purification. Left: 12.5% SDS-PAGE gel under non reducing conditions stained with Coomassie blue. The numbers correspond to PpL affinity chromatography column fractions (1) crude periplasmic extract; (2) column flow-through fraction, containing many of the bacterial proteins observed in the crude periplasmic extract; (3) proteins eluted by an acid solution pH 2.8. (M) Molecular weight marker (Sigma M3913). Right: nitrocellulose membrane for Western blot analysis developed with PpL-peroxidase conjugate. C- Dot blot analysis of the periplasmic extract containing recombinant scFv$_{15}$hLi7. *L. intermedia (Li), L. gaucho (Lg)*, and *L. laeta (Ll)* venoms (2.5 µg) spotted onto nitrocellulose membrane. Left panel:

Confirmation of venom's presence in the membrane by Ponceau reversible staining. Right panel: nitrocellulose membrane incubated with periplasmic extract containing recombinant scFv15hLi7, developed with PpL-peroxidase. D- Size-exclusion chromatography of the PpL-purified scFv15hLi7 using a calibrated Superdex 75 10/300GL column. E- Far UV-CD analysis of the PpL-purified scFv15hLi7 at 20 °C (blue), 40 °C (orange) and 50 °C (red).

2.3. Physico-chemical characterization and stability analysis of scFv$_{15}$hLi7

Based on the observations stated above, PpL-purified scFv$_{15}$hLi7 was produced at a larger scale at Genscript (Piscataway, NJ) and used for further characterization. SDS-PAGE and Western blotting confirmed correct production and PpL-purification of the recombinant protein. The UV-Vis spectra of the PpL-purified scFv$_{15}$hLi7 was monitored to detect the presence of submicron-aggregates. The shape of the spectra was in conformity with that of a soluble protein and confirmed that no significant aggregation / precipitation phenomenon occurred. The value recorded at 320 nm which reflects the scattering of light by large aggregates present in the sample was very low as compared to the value recorded at 280 nm, the ratio A_{320nm}/A_{280nm} being 2.5 %.

PpL-purified scFv$_{15}$hLi7 was analysed after SE-HPLC in order to confirm purity and for the detection of nanoaggregates and/or degradation products of the scFv in solution (Fig.3 D). Two peaks of elution were observed. The smaller peak eluted at a volume ~11 mL corresponded to proteins exhibiting an apparent Mr of 40-50 kDa whereas the major peak, accounting for 90% of the total protein amount, eluted at ~13 mL, corresponding to proteins with an apparent Mr of 25-30 kDa. Based on that apparent Mr, the first peak was expected to be a dimeric form of the scFv related to either a misfolding occurring during the expression or an aggregation phenomenon during the purification process, such as elution in acidic condition. The second peak was likely to be the monomeric form of scFv$_{15}$hLi7.

We also used circular dichroism spectroscopy as a tool to monitor structural stability of scFv$_{15}$hLi7 (Fig. 3E). We did not observe any major changes at temperatures beneath 35 °C. At 40 °C, a decrease of the ellipticity at 200 nm was observed and the ellipticity continued to decrease at 50 °C and 60 °C with a concomitant increase of the ellipticity at 218 nm, in the same range of temperature. The shape of the CD spectrum of scFv$_{15}$hLi7 solutions at temperature under 35 °C showed features of a β-sheet-enriched structure, with a minimum at 218 nm and a maximum at ~ 201nm, typical of antibody-like structures. As temperature increases above 35 °C, the CD spectra of scFv$_{15}$hLi7 displayed no isodichroic point. As a result, the folding of scFv$_{15}$hLi7 cannot be described by a two-state equilibrium, revealing the multidomain nature of the scFv$_{15}$hLi7 fragment. At temperatures above 35 °C, the protein structure of scFv$_{15}$hLi7 is unstable and likely unfolded. Other than CD spectroscopy, we carried out a nano-differential scanning fluorimetry (nano-DSF) analysis. In using a 10μM solution of PpL-purified scFv$_{15}$hLi7, we observed a melting temperature (T_M) of 42.2 °C with an onset temperature of denaturation of 37.0 °C and an onset temperature of aggregation of 41.8 °C.

2.4. scFv$_{15}$hLi7 antigen-binding characterization

The recognition profile and specificity of the scFv$_{15}$hLi7 against *Loxosceles* venoms and recombinant SMase D LiD1 toxin was identified after the electrophoretic migration of the venom components followed by a nitrocellulose membrane transfer of these proteins and evaluation of the antibody-fragment binding capacity as compared

to the parental mouse IgG. When scFv$_{15}$hLi7 was assessed against the venom of different *Loxosceles* species, only the *L. intermedia* venom led to a recognition profile of two bands in the 32–35 kDa molar range, suggesting that the epitope recognized by this fragment is shared by several SMase D isoforms only pertaining to *L. intermedia* (Fig. 4A).

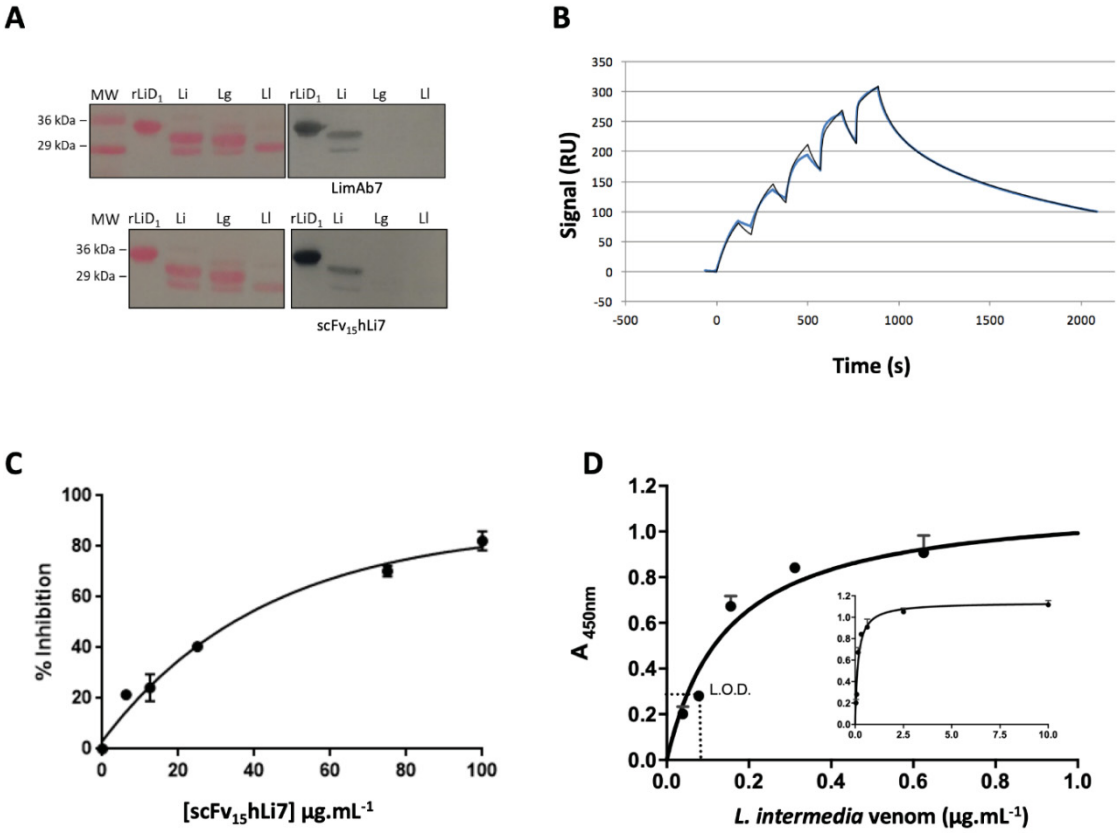

Figure 4. Functional characterization of PpL-purified scFv$_{15}$hLi7. A- Western blot analysis of the LimAb7 and periplasmic extract containing recombinant scFv$_{15}$hLi7. *L. intermedia (Li), L. laeta (Ll) and L. gaucho* (Lg) (10 µg of each venom) or SMase D LiD1 (rLiD1) (10 µg) were resolved in a 15% polyacrylamide gel by SDS-PAGE under non-reducing conditions and transferred to a nitrocellulose membrane. Left panel: Confirmation of venom's presence in the membrane by Ponceau reversible staining. Upper right panel: membrane incubated with LimAb7 (20 µg.mL^{-1}) and developed with peroxidase-conjugated rabbit anti-mouse IgG. Lower right panel: membrane incubated with periplasmic extract containing recombinant scFvLi$_{15}$hLi7 and developed with peroxidase-conjugated PpL. B- Interaction of immobilized rLiD1 with increasing concentration of PpL-purified scFv$_{15}$hLi7 (0.125; 0.25; 0.5; 1.0; 2.0 µM) analyzed by surface plasmon resonance (SPR) (Biacore 100 and fitting with heterogeneous analyte model, monomer 90%, dimer 10%). C- Competitive ELISA: immobilized *L. intermedia* (10 µg.mL^{-1}) and added 1 µg.mL^{-1} of LimAb7 with increasing amounts of scFv$_{15}$hLi7. Immunocomplexes were revealed using peroxidase-conjugated anti-mouse Fc antibodies. D- Sandwich ELISA: immobilized horse anti-*L. intermedia* venom F(ab)'$_2$ (10 µg.mL^{-1}) and captured *L. intermedia* venom gradient. 20 µg.mL^{-1} of scFv$_{15}$hLi7

were added. Immunocomplexes were revealed using peroxidase-conjugated PpL. The inserted graph is the same graph with smaller x-axis scale.

Binding affinity of PpL-purified $scFv_{15}hLi7$ and kinetics for binding to immobilized LiD1 were analyzed in real time (Fig. 4B). According to SE-HPLC analysis, the heterogeneous analyte model, which consists of two populations of molecules capable to bind to the immobilized target independently, was used. The kinetic constants measured for the monomeric $scFv_{15}hLi7$ representing 90% of the antibody population were $k_a = 18.2 \times 10^4\ M^{-1}\ s^{-1}$, $k_d = 103 \times 10^{-4}\ s^{-1}$ resulting in a dissociation constant K_D = 56.6 nM. Under similar experimental conditions, mouse dimeric $scFv_5Li7$ and IgG LimAb7 were previously shown to have significant better kinetic characteristics with a K_D of 0.98 nM and 0.085 nM, respectively [22].

The competitive ELISA assay also allowed us to evidence the ability of $scFv_{15}hLi7$ to compete with the parental IgG LimAb7 in a dose-dependent fashion. Fig. 4C shows the inhibition profile in the presence of the recombinant antibody fragment. Higher concentrations of the fragment have shown to inhibit the binding of the parental IgG to the venom components and thereby result in a decrease in reactivity. It was estimated that about 38 $\mu g.mL^{-1}$ of $scFv_{15}hLi7$ is required to inhibit 50% of LimAb7 binding. A sandwich ELISA confirmed the ability of $scFv_{15}hLi7$ to bind to toxins of the *L. intermedia* venom in a dose-dependent and saturable manner with a lower limit of detection of up to 78 $ng.mL^{-1}$ of soluble toxin (Fig. 4D). Following this functional characterization, we moved to the evaluation of $scFv_{15}hLi7$'s ability to neutralize the hemolytic activity of *L. intermedia* venom. Unfortunately, we couldn't observe any neutralization, whatever the experimental conditions were (data not shown). This result led us to reconsider the design of the humanized antibody fragment.

2.5. Modeling and docking of LimAb7, $scFv_{15}hLi7$ with LiRecDT1

In order to better understand LimAb7's neutralization mechanism, we proceeded to the modeling of LimAb7 and $scFv_{15}hLi7$ V-domains' structures, prior to *in silico* docking prediction with putative target SMase D LiRecDT1 (PDB: 3RLH). The molecular docking between LimAb7, $scFv_{15}hLi7$ and their molecular target was then performed and the lowest energy score interactions between the antibodies' VH/VL and LiRecDT1 are represented in Fig. 5. The docking analysis shows LimAb7 VH and VL CDR interactions in accordance with (D233, K234, R235, Y253). Contacts between LimAb7, $scFv_{15}hLi7$ and regions of SMase D LiRecDT1 (K58, K59) (D21, E22, D25), respectively, that have been indicated as highly immunogenic and targets of neutralizing anti-LiRecDT1 antibodies, residues 58-72 (CYGSKKYENFNDFLKGLR) and residues 25-51 (NLGANSIETDVSFDDNANPEYTYHGIP) were also identified. Moreover, contacts between LimAb7 and amino acids G54 and R55 were detected, some of the residues that have been previously indicated as being important for the stabilization of the catalytic loop and substrate interaction are conserved between SMase D LiRecDT1 and SMase LiDI [44,45]. The docking analysis for the $scFv_{15}hLi7$/SMase D LiRecDT1 still shows contacts in the same regions as the murine antibody (LimAb7), however some contacts with substrate-binding relevant amino acids are lost (D233, G54). Furthermore, new contacts have been observed including residues D21, E22, N25, D255 suggesting a displacement in the site of interaction when compared to LimAb7 (Table supplement 2).

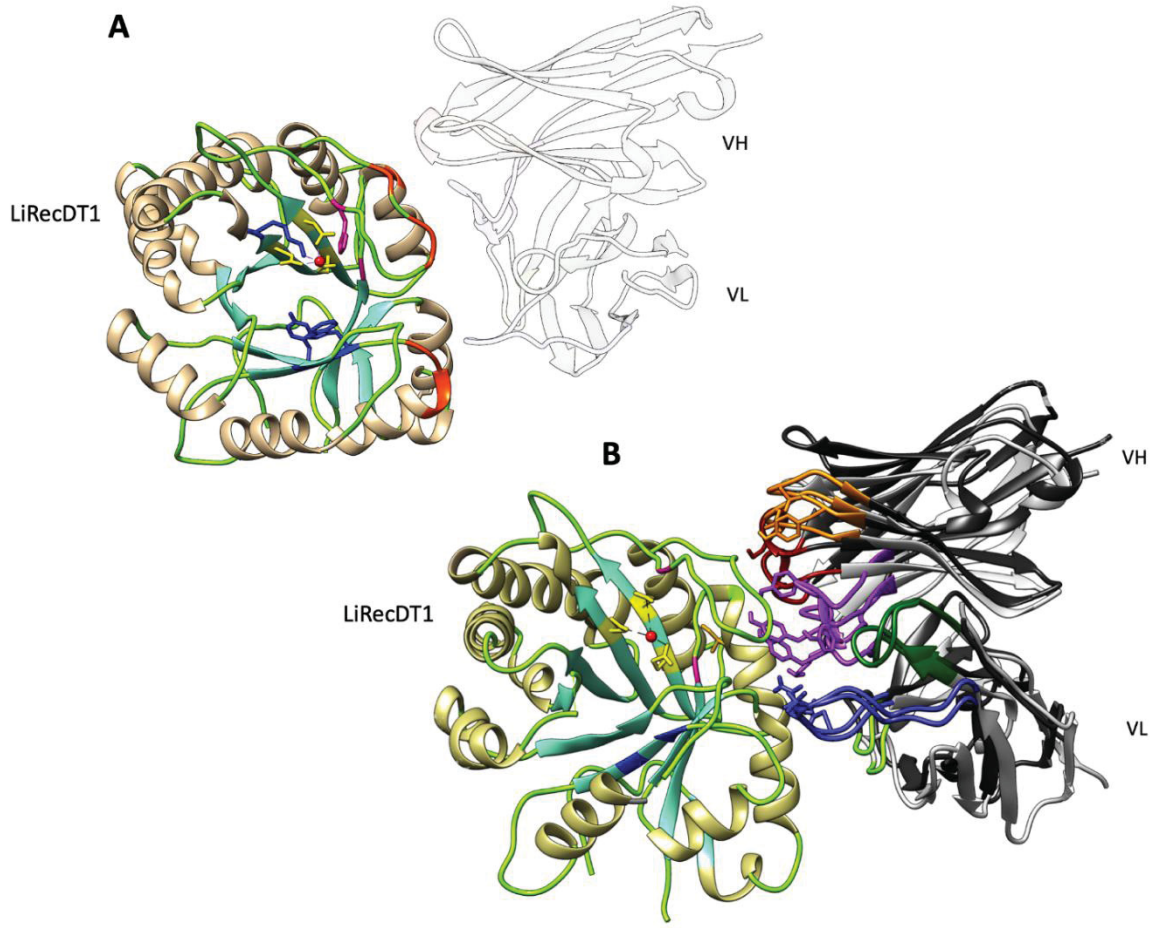

Figure 5. - Docking of LimAb7, scFv$_{15}$hLi7 with LidRecDT1. A- Docking results showing antibodies binding sites on the surface of SMase D (LiRecDT1, PDB: 3RLH). Ribbon representations of antibody-Lid1 interactions where the residues proposed to be involved in catalysis (H12A, H47A) are coloured in magenta, magnesium-ion binding (E32A, D34A, D91A) in yellow and substrate recognition (K93A, Y228A, and W230A) are coloured in blue; the amino acid compounds in the predicted epitope for Limab7 are represented in orange. B- Superimposition of the best scoring docking models for LimAb7 and scFv$_{15}$hLi7. The VL and VH CDRs are coloured according to the IMGT colour scheme and the framework regions in black for LimAb7 and grey for scFv$_{15}$hLi7.

2.6. Re-Design of humanized scFv anti- L. intermedia venom

Considering that the catalytic pocket of SMase D LiRecDT1 and LimAb7 epitope do not overlap according to docking analysis, and also that the humanization process slightly altered the antigen-antibody interaction, we decided to re-design the humanized antibody fragment as follows. First, we introduced two back mutations (F 103>Y in IGHV and P 46>Q in IGKV according to IMGT numbering) in the sequence of the humanized antibody fragment. We anticipated that these back mutations should restore the original VH/VL packing angle (-42.8), the original topography of the antigen-binding site and possibly the structural stability of the paratope. Secondly, we produced this new version of humanized antibody in two formats: a monomeric scFv also designated scFv$_{15}$hLi7m (25kDa) and a larger dimeric scFv$_5$hLi7m (50kDa) (Fig. 6).

For both recombinant proteins, the yield of production after PpL capture from the periplasm of induced HB2151 bacteria was higher than 1mg.L^{-1} of culture under standard conditions of culture and induction (2.4 mg.L^{-1} and 1.2 mg.L^{-1} for $scFv_{15}$hLi7m and $scFv_5$hLi7m, respectively). In both cases, we did not observe any tendency to aggregation, precipitation or proteolyis as indicated by the low A_{320nm}/A_{280nm} ratio (<2.5%) and SDS-PAGE analysis (Fig. 6B). Size-exclusion chromatography elution profile indicated that 100 per cent of the $scFv_5$hLi7m was produced as a dimer. The $scFv_{15}$hLi7m was mainly produced as a monomeric molecule but we also observed an additional peak corresponding to misfolded proteins or dimeric structures. The nano-DSF analysis performed with both recombinant proteins in comparison with the first generation molecule did not show any improvement of the thermal stability upon the double mutation and dimerization into a diabody molecule (Fig. 6C).

The preservation of the recognition profile and specificity of the $scFv_{15}$hLi7m and $scFv_5$hLi7m fragments against venom components was confirmed after Western blotting. When both fragments were assessed against the venom of different *Loxosceles* species, only the *L. intermedia* venom led to a recognition profile of proteins in the 32–35 kDa molar range, suggesting that the epitope recognized by this fragment is shared by SMaseD isoforms only pertaining to *L. intermedia* (Fig. 7A). The ELISA test was used to compare the affinity of the purified $scFv_{15}$hLi7, $scFv_{15}$hLi7m and $scFv_5$hLi7m against a recombinant SMase D and the *L. intermedia* whole venom. No improvement in affinity was observed for the mutated version when tested against recombinant LiD1, one of the phospholipases present in the Loxtox family (Fig. 7B). However, $scFv_5$hLi7m was able to recognize the *L. intermedia* whole venom with greater apparent affinity, thus being expected to produce steric hindrance within the different targets present in the venom (Fig. 7C).

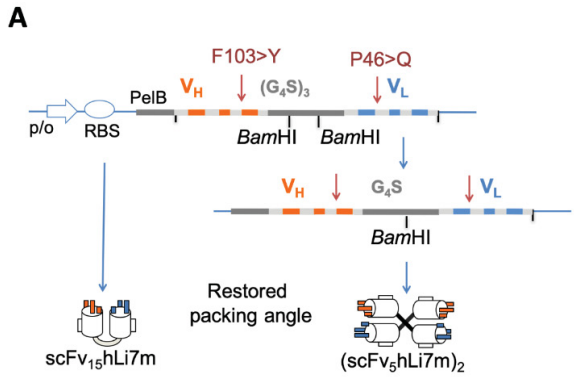

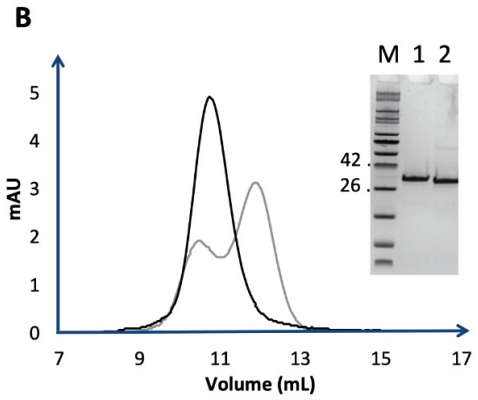

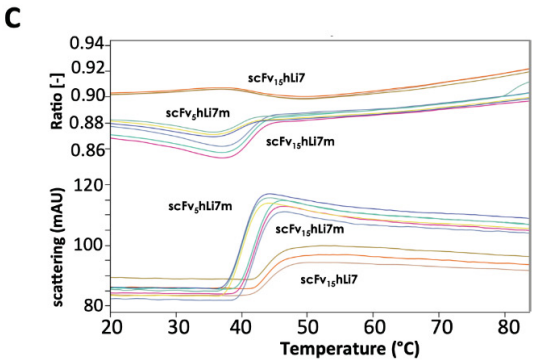

	$T_{denaturation}$ (°C)	T_M (°C)	$T_{aggregation}$ (°C)
$scFv_{15}$hLi7	37.00±0.10	42.23±0.28	41.79±0.14
$scFv_{15}$hLi7m	37.07±0.06	41.32±0.04	38.66±0.17
$scFv_5$hLi7m	35.63±0.06	39.73±0.07	38.66±0.15

Figure 6. Expression, purification and physico-chemical characterization of scFvhLi7m. A- Schematic representation of the design and expression cassette. The open reading frame contains a PelB signal sequence for periplasmic expression. cDNA encoding humanized VH and VL are fused together via a sequence encoding a $(Gly_4Ser)_3$ linker and cloned in frame with the PelB sequence. For expression of $(scFv_5hLi7m)_2$, the plasmid was double digested with *Bam*HI and then self ligated. B- Size-exclusion chromatography of the PpL-purified $scFv_{15}hLi7m$ (grey) and $scFv_5hLi7m$ (black) using a calibrated Superdex 75 10/300GL column. The insert shows SDS-PAGE analysis of PpL purified $scFv_{15}hLi7m$ (1) and $scFv_5hLi7m$ (2) under reducing conditions. M: Molecular weight marker (kDa). C- Nano-DSF and thermal stability analysis of PpL purified $scFv_{15}hLi7m$, $scFv_5hLi7m$ in comparison to the first generation $scFv_{15}hLi7$. On set temperature of denaturation, T_M and onset temperature of aggregation are indicated in the table.

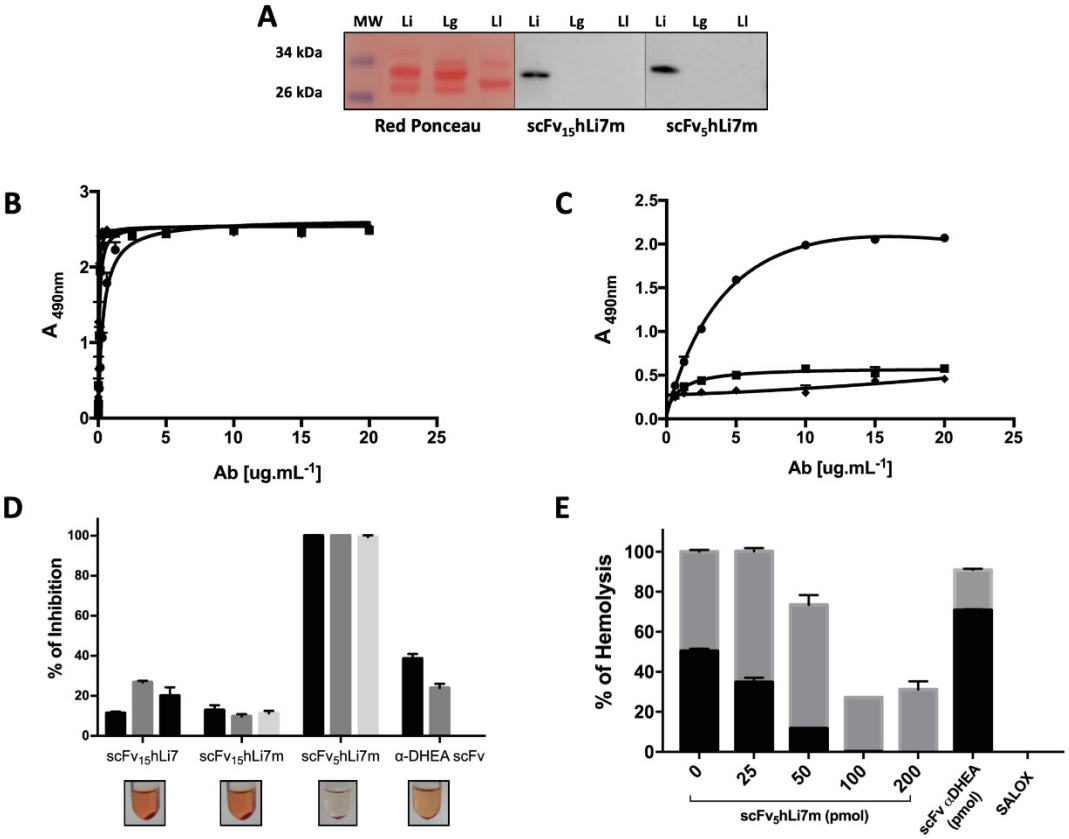

Figure 7. - Functional characterization of scFvhLi7m. A- Western blotting after SDS-PAGE 15% of 10µg *Loxosceles* venoms under non-reducing conditions stained with Red Ponceau (left) or incubated with periplasmic extracts of the $scFv_{15}hLi7m$ (middle) and $scFv_5hLi7m$ (right), and then developed with peroxidase-conjugated PpL. Li: *L. intermedia*; Lg: *L. gaucho*; Ll: *L. laeta*. (MW) Molecular weight marker (ThermoScientific 26634). B- Indirect ELISA: immobilized SmaseD LiD1 and added increasing amounts of $scFv_{15}hLi7$(■), $scFv_{15}hLi7m$ (w) or $scFv_5hLi7m$ (●). Immunocomplexes were revealed using peroxidase-conjugated PpL. C- Indirect ELISA: immobilized *L. intermedia* venom and added increasing amounts of $scFv_{15}hLi7$ (■),

scFv$_{15}$hLi7m (w) or scFv$_5$hLi7m (●). Immunocomplexes were revealed using peroxidase-conjugated PpL. D- Inhibition of hemolytic activity. Human erythrocytes were incubated with *L. intermedia* venom (0.75µg) in the presence of different amounts of antibody: 50pmol (black), 25pmol (dark grey) and 12.5pmol (light grey) for 24 h under gentle agitation at 37°C. Ringer buffer was used as a negative control. The results are expressed in percentage of hemolysis inhibition and the venom alone in the absence of antibody was considered as 100% of hemolysis. Visual inspection of samples is represented in relation to respective antibody fragments. E- *in vitro* hemolytic assay. Human erythrocytes were incubated with *L. intermedia* venom (10 µg) in the presence of different concentrations of antibody, with (grey) or without (black) normal human serum. Irrelevant scFv αDHEA (200pmol) and horse hyperimmune serum (SALOX, 1:500) were used as controls. The results are expressed in percentage of hemolysis and the venom alone, in the absence of antibody, was considered as 100% of hemolysis.

2.7. L. intermedia venom neutralization

In order to assess the humanized antibody fragments capacity to inhibit the hemolytic effects of the *L. intermedia* venom we performed a hemolysis assay, in presence or absence of the complement system. Different amounts of humanized antibody fragments were incubated with human erythrocytes in the presence of *L. intermedia* venom (0.75 and 10 µg.mL^{-1}). scFv$_5$hLi7m (in all molarities) was able to inhibit 100% of the venom's (0.75 µg.mL^{-1}) hemolytic activity, when compared to the humanized variants scFv$_{15}$hLi7, the scFv$_{15}$hLi7m or the irrelevant scFv (Fig. 7D).

The hemolysis of red blood cells challenged with the venom (10 µg) was strongly inhibited (> 90%) in the presence of 50-200 pmol scFv$_5$hLi7m, when the complement system was absent (Fig. 7E). When normal human serum was added to erythrocytes previously incubated with venom and scFv$_5$hLi7m, an inhibition of up to 68% of complement-dependent hemolysis was observed (Fig. 7E). Horse polyclonal sera anti-*L. intermedia* venom (SALOX, 1:500) was used as a positive control for hemolysis inhibition under these assay conditions. Additionally, when tested in the presence of 0.75 µg.mL^{-1} and 10 µg.mL^{-1} of *L. intermedia* venom, Limab7 (50pmol) was able to neutralize 100 and 80% of the hemolysis, respectively (data not shown). An irrelevant scFv anti-DHEA was also employed as a negative control [46].

3. DISCUSSION

Today, there is no consensus concerning the efficacy of any reported therapy for the treatment of loxoscelism. It is well-established that SMases D play a key role in dermonecrosis and hemolysis, and a number of studies are focusing on the selection of chemical compounds capable of interfering with SMases activity [47]. In this context, the development of neutralizing therapeutic antibodies directed against SMases may also provide an efficient alternative to conventional serum therapy as currently implemented in Brazil. It has been widely reported that many *Loxosceles* spp. venom proteins induce the production of non-neutralizing antibodies, later present in the total IgG pool of anti-venoms [48,49]. This brings upon the need for the employment of SMases D or their immunorelevant domains as major immunogens in the immunization process, given the significance of these toxins in the course of envenomation [48,50–53]. In addition to this, over the last years, there has been a rising demand for advancements in the conception of anti-venom production. Despite intensive research

to develop alternatives for conventional anti-loxoscelism serum therapy, to date, the LimAb7 still remains the only monoclonal antibody able to neutralize the dermonecrotic activity of the *L. intermedia* venom, as reported by studies in animal models [20]. Recently, we have shown that recombinant LimAb7 antibody fragments (diabodies) preserved *in vitro* neutralizing capacity of inhibiting SMase D activity, as well as hemolysis induced by *L. intermedia* venom [22]. However, clinical trials of these molecules in humans is not feasible for safety reasons, unless the antibody's V-domains are humanized. Hence, we designed humanized V-domains and produced them in the scFv format, which is the minimal antibody building block that preserves antigen-binding activity while being well tolerated when administered to humans. We also successfully engineered a PpL binding motif in order to make the purification of antibody fragments using affinity chromatography possible, without requiring the insertion of an epitope tag. This strategy is essential considering future pharmaceutical developments [54–56]. The monomeric scFv was produced in bacteria and characterized from a physico-chemical point of view. Our functional studies indicated that the humanized scFv preserved its specificity and antigen-binding activity but did not conserve its capacity of neutralizing SMase D activity *in vitro*. A slight shift in the interaction surface between the targeted toxin and the antibody upon humanization was suspected by antigen/antibody docking analysis. Overall, these apparently disappointing observations underlined the need to fully understand the mechanism of toxin neutralization prior to the design of an antibody fragment with appropriate format for neutralization.

Antibody humanization demands careful study of a molecule's structural and conformational features. The most commonly employed method for humanization consists in grafting murine CDRs into whole human framework regions. Still, it has been demonstrated that some murine framework residues, denoted as vernier zone residues, are able to interfere in the CDR loops conformation thus affecting antibody binding affinity [54,57]. Although many methods have been reported for humanization, the immunogenicity of therapeutic antibodies is still a discussed matter [58,59]. The generated antibody fragment must maintain, not only target specificity and high affinity, but also structural and thermal stability as well as preserving or acquiring the capacity to bind to PpL. Considering this, we have produced a minimal size antigen-binding molecule ($scFv_{15}$hLi7) in order to test the intrinsic properties of its humanized V-domains without the influence of additional constant domains. The humanization process did not lead to molecules producing aggregates and no precipitation or degradation phenomena were detected after SEC-HPLC. This is a positive point, taken that the presence of aggregates in drugs of protein nature can cause adverse effects such as reduced drug efficacy, infusion reactions and potentially hypersensitivity reactions [60–62].

The $scFv_{15}$hLi7 exhibited a significantly improved humanness with a Z-score in the range of 0. It preserved the recognition specificity of the parental antibody LimAb7, even though its affinity significantly decreased when compared to its murine counterpart according to SPR analysis which were carried out under non-optimal conditions. Indeed, the density of LiD1 protein immobilized on the sensorchip was higher than the optimal value for affinity assessment either because of partial misfolding of LiD1 or random covalent immobilization hiding the epitope surface. We anticipate to better evaluate these parameters as additional data is generated using alternative methods which allow the determination of affinity in free solution [63]. Finally, the recombinant antibody showed a limit of detection of 78 $\mu g.mL^{-1}$ in ELISA and was able to compete with the parental mouse IgG. Still, the humanized LimAb7 V-

domains were not able to neutralize the biological activity of the venom or the recombinant sphingomyelinase when expressed in the scFv format. Aiming to better understand this, we have focused on the SMaseD toxins, which play a key role in loxoscelism. These enzymes have been widely studied and characterized regarding their preferential substrates [64,65], structural basis [1,2,47,68,69], toxicity [5,68], immunogenicity [69,70] and representativeness in the whole venom [71]. SMases D are also designated dermonecrotic toxins as their recombinant forms have shown to reproduce most of the toxic effects observed in loxoscelism, including dermonecrotic lesions and antigenic properties of the venom[5]. Our SmaseD/LimAb7 and SmaseD/scFv$_{15}$hLi7 docking data clearly support the hypothesis that the interaction between the toxin and the antibody fragments does not occur at the catalytic site of the enzyme. This observation is in agreement with previous overlapping peptide scanning analysis, and also screening of peptide phage-display libraries which identified a putative epitope region located far from the catalytic and Mg^{2+}-binding sites of the enzyme [25,44,45]. This is not entirely surprising given that, unlike small neurotoxins which are usually recognized by antibodies at their pharmacological site, larger enzymatic toxins such as PLD are neutralized via other effects such as steric hindrance, making this the first ever reported antibody to neutralize animal toxins via this mechanism [72–74]. With its typical minimal size, the monovalent scFv$_{15}$hLi7 could not meet this requirement. The lack of neutralizing ability observed with the scFv fragments (first scFv$_{15}$hLi7 and later with scFv$_{15}$hLi7m) supports the hypothesis of a steric hindrance mechanism for neutralization. Even more important, the results obtained with the murine IgG or its diabody fragment illustrate the difficulty of choosing the most suitable format in terms of size and valence.

The slight shift in the interaction region with the Smase D observed upon the humanization of LimAb7 V-domains may also have significant consequences regarding the affinity of the antibody fragment for the targeted toxin and also its stability. The decrease in the affinity for the toxin and potentially the non-optimal thermal stability we observed for scFv$_{15}$hLi7 could be related to some of the mutations that also altered the VH/VL packing angle. Recent studies have shown that a high degree of cooperation between the VH/VL is required for mutual stabilization and also that a limited number of residues buried inside the antibody domain are critical to maintain the topography of the antigen-binding site [30,55,75]. The mutation H80 A>R slightly impacts the canonical H2 conformation. A charged residue at this position, close to H58 P (CDR H2) and H30 F (CDR H1), could have led to the disruption of an optimal packing of the CDRs and alter the interaction with the target. Hence, residues H103 F>Y; L46 Q>P were back mutated in the revised sequences scFv$_{15}$hLi7m and scFv$_{5}$hLi7m, in an attempt to restore some of the parental antibody's binding features. As expected, we observed an increased apparent affinity of the second generation scFv$_{5}$hLi7m for the immobilized whole venom (ELISA) as compared with scFv$_{15}$hLi7. However, this was not the case for the recombinant Smase D LiD1 given that this specific toxin may not be the best representative of the *Loxosceles* (Loxtox) phospholipase D family targeted by LimAb7. Indeed, the Loxtox family has been extensively characterized and is comprised of a great amount of Smase D isoforms [24, 64], with distinct biological activities (e.g. hemolytic and sphingomyelinase activities were not significant for LiD1, despite producing dermonecrosis *in vivo*) [40]. We also observed that the thermal stability of the molecule was not optimal and this may be a consequence of some of the mutations introduced. However the back mutation of residues H103 and L46, expected to restore the packing angle, did not

have any positive impact on the thermal stability. This makes unclear how important it is to preserve the packing angle at least in this particular case study.

The experimental validation of our *in silico* docking analysis and humanized fragment re-design was carried out through *in vitro* hemolysis assays in the presence of the venom and the humanized variants. This approach was selected as a primary screening because it is elucidative and also easier to implement rather than measuring the inhibition of SMase activity *in vitro* which requires indirect methods with several enzymatic steps sensitive to pH and other potential irrelevant enzyme inhibitors. The crucial role of hemolysis in the context of Loxosceles spp. envenoming has been thoroughly described, both via direct and complement dependent activation [68,76–78]. The fact that only the diabody neutralizes the hemolysis validates the docking predictions and confirms that neutralization occurs via a steric hindrance mechanism and corroborates well with previous experiments carried out independently using other experimental strategies [25].

Our findings report for the first time the successful production of a humanized antibody fragment able to neutralize *L. intermedia* venom hemolytic activity *in vitro*, in a complement dependent (68% of neutralization) and independent manner (100% of neutralization). Therefore, the humanized diabody ($scFv_5Li7m$) paves the way for the development of therapeutic recombinant antibodies in loxoscelism. Major advantages of this approach can be foreseen. Immunization of big warm blood animals would no longer be required for production of antivenoms. Additionally, antibody fragments would be prepared without requiring any enzymatic fragmentation that is often deleterious in terms of antigen-binding activity. The specific activity would be higher than the one of polyclonal antivenoms that contain many irrelevant antibodies. Finally, the cDNA encoding the recombinant antibody fragment would be available indefinitely while polyclonal antibodies are never rigorously defined and vary from batch to batch. Of course, diabodies may not be appropriate for human injection due to short half-life and potentially low thermal stability [79]. However, these molecules can be re-designed into Fab fragments which format has yet been proven to be more stable, suitable for human infusion and efficient for the treatment of several diseases [80]. In a Fab, both VH/VL and CH/CL interactions contribute to the functional stability of the antibody fragment and potentially to the *in vivo* toxin neutralization capacity as suggested previously [81]. In addition, one can consider site-specific PEGylation of scFvs for enhancing the pharmacokinetic properties, the conformational stability, protection from proteolysis and immunogenicity [82]. Altogether, these findings represent a proof of concept on humanized mouse antibodies specific to animal toxins, encouraging the optimized production of molecules for *in vivo* assessment.

4. MATERIALS AND METHODS

4.1. Venoms and toxins

Vacuum dried venoms from *L. laeta, L. gaucho*, and *L. intermedia* spiders were provided by *Centro de produção e pesquisa de imunobiológicos* (CPPI), Piraquara, PR, Brazil and resuspended in a 10mM Na_2HPO_4 buffer containing 137mM NaCl and 2.7 mM KCl (PBS), pH 7.4 at a concentration of 0.8-1 $mg.mL^{-1}$.

The recombinant SMase D LiD1 from *L. intermedia* (Uniprot: P0CE81), presenting 99.67% of identity with LiRecDT1 (PDB: 3RLH) was a gift from Dr. Felicori Figueredo (UFMG, Belo Horizonte, MG, Brazil) (Genbank accession number: AY340702).

4.2. Monoclonal and polyclonal antibodies

The LimAb7 hybridoma was produced after the immunization of adult female BALB/c mice with *L. intermedia* venom. It has been previously shown to secrete a well-characterized monoclonal IgG_{1k} that neutralizes the democratic activity of *L. intermedia* spider venom, and binds to the SMase D LiD1 as well as several other 32-35kD related proteins of the *L. intermedia* venom, interestingly, not cross-reacting with any components of *L. laeta* and *L. gaucho* venoms, given their considerable interspecies homology [20,25].

Horse hyperimune sera (SALOX) reactive to *L. intermedia*, *L. laeta*, and *L. gaucho* venoms was produced by CPPI. Horse IgG $F(ab)'_2$ anti-*L. intermedia* venom was prepared as previously reported [20].

4.3. Bacteria

The *Escherichia coli* AD494 (DE3) pLysS strain (Novae, Nottingham, UK) and HB2151 (Stratagene, La Jolla, CA) were selected for protein expression. Bacteria culture media was purchased from AthenaES (Baltimore, MD, USA) and all chemicals were of standard grade and acquired from Sigma Aldrich (Saint-Louis, MO, USA) or equivalent.

4.4. Protein quantification

Protein concentration was determined by the Bradford reagent (Bio-Rad Laboratories, Hercules, CA, USA). Alternatively, purified protein concentration was measured by the absorbance at 280nm using, for each purified protein, the molar extinction coefficients (ε) determined by the ProtParam tool [26].

4.5. Humanization of antibody V-domains

The structure of mouse LimAb7 Fv (Genbank accession number KT381972) was previously modeled [27]. Amino acid numbering and sequence analysis were carried out using the Web interface IMGT tools and database (IMGT/DomainGapAlign).

Humanized versions of LimAb7 V-domains were generated by grafting all six CDRs onto human IGKV and IGHV domains having high sequence identity and closely related canonical classes with LimAb7 V-domains. The protocol was adapted from a previous one [24]. After grafting the CDRs to human FR regions, each amino acid (AA) substitution was inspected individually, based on the physico-chemical classes of the AA differences [28]. We considered the humanness score (Z-score), which compares the sequences with a set of known human sequences assigned to germline derived families, aiming to achieve a score close or above 0 [29]. VH/VL packing angle and residues that might play an important role in maintaining the correct binding-site topography were identified [30]. Additional refinements were carried out in IGKV-FR1 in order to generate a PpL-binding site without altering predicted humanization and residual immunogenicity as previously suggested [31,32]. Finally, the designed sequences were compared with human germline genes in order to calculate a human germinality [33].

4.6. Generation and purification of humanized $scFv_{15}$hLi7 and $scFv_5$hLi7m

Codon optimized DNA encoding humanized V-domains fused together in the VH - VL orientation via a sequence encoding the $(G_4S)_3$ linker were synthesized at Genscript (Piscataway, NJ, USA) and cloned into the prokaryotic expression vectors pET-22b (+) or pSW1, in frame with the PelB signal sequence [34].

Production and PpL-purification of $scFv_{15}hLi7$ (first generation of the humanized scFv) were carried out under generic conditions at Genscript (Piscataway, NJ, USA). Purified $scFv_{15}hLi7$ concentration was adjusted to 0.57 mg. mL^{-1} in PBS pH 7.2. Aliquoted samples were stored at - 80 °C.

For the $scFv_{15}hLi7m$'s (second generation of the humanized scFv) construction, two *Bam*HI restriction sites were introduced in the nucleotide sequence encoding the $(G_4S)_3$ linker. Therefore, double digestion with *Bam*HI followed by self-ligation of the plasmid allowed the generation of a vector encoding diabody $scFv_5hLi7m$ which differs from $scFv_{15}hLi7m$ by the size of its linker peptide (G_4S). Both scFvs were produced by *E. coli* AD494 (DE3) pLysS bacteria transformed with vector pET-22b (+) containing the insert of interest as previously described [22]. Alternatively, we used HB2151 strains transformed with pSW1 vector for scFv production under generic conditions and PpL capture [35]. The scFv-containing fractions were pooled and subjected to dialysis in PBS, pH 7.4 overnight at 4 °C.

4.7. SDS-PAGE, Western blot and Dot blot

To assess bacterial periplasmic extracts for scFv expression, samples were resolved by SDS-PAGE under non-reducing conditions on 12.5% polyacrylamide gel. Proteins migrated at 150 V for 2 h at room temperature. Subsequently, gels were either stained with Coomassie Brilliant Blue for protein identification or transferred onto a 0.45 mm nitrocellulose membrane, for 2 h, 100 V at 4 °C. The quality of the transfer was checked by transitional staining with Red Ponceau. In order to verify the expression of the scFvs, the membrane's non-specific binding sites were first blocked for 1 h in PBS containing 5% (w/v) non-fat dry milk and 0.3% (v/v) Tween 20. Next, membranes were incubated with peroxidase-conjugated PpL (ThermoFisher, Waltham, MA, USA) in PBS, pH 7.4, containing 0.05% Tween 20, for 1h at 37 °C and stained with DAB/Chloronaphtol.

Aiming to confirm the fragments specificity against the *L. intermedia* venom, the periplasmic extracts were analysed by dot blot. Firstly, *L. laeta*, *L. gaucho*, and *L. intermedia* venom (2.5 µg each) were immobilized on to nitrocellulose membrane, then the non-specific binding sites were blocked with non-fat milk as described above. Next, membranes were incubated with the scFv periplasmic extracts (for 1 h at 37 °C) and after with peroxidase-conjugated PpL (ThermoFisher, Waltham, MA, USA) for scFv detection. Lastly, membranes were stained with DAB/Chloronaphtol.

Additionally, *L. laeta*, *L. gaucho*, *L. intermedia* venoms, and recombinant Smase D LiD1 were subjected to an SDS-PAGE on a 15% acrylamide gel and transferred onto a 0.45 mm nitrocellulose membrane in order to verify the scFv's binding to the dermonecrotic toxins. The immunocomplexes were detected with peroxidase-conjugated PpL (ThermoFisher, Waltham, MA, USA) or peroxidase-conjugated rabbit anti-mouse IgG (Sigma, 1:4000). Between all intermediate steps, three washings with PBS (pH 7.4) containing 0.05% Tween 20 were performed.

4.8. UV-Vis analysis

UV-Vis spectra (from 220 to 350 nm) were carried out in triplicate after dilution of samples at the 0.5 AU_{280nm} in PBS pH 7.2.

4.9. Size-exclusion chromatography

100 µL of PpL-purified scFv (2 or 10µM) were analysed by size-exclusion high pressure liquid chromatography (SEC-HPLC) using a prepacked Superdex 75

10/300GL column calibrated with standards from GE Healthcare. Proteins were eluted with PBS pH 7.2 at a rate of 0.5 ml.min^{-1} and detected with a UV recorder at 280 nm.

4.10. Circular Dichroism

CD spectra were obtained on a Model CD6 spectrometer (Jobin-Yvon-Spex, Longjumeau, France) at different temperatures from 15 to 60 °C using a thermoregulated bath using a quartz sample cell with a 1 mm path length. The ellipticity was scanned from 200 to 250 nm with an increment of 1 nm, an integration time of 2 s, and a constant band-pass of 2 nm. The concentration of the scFv$_{15}$hLi7 protein was adjusted to 0.114 mg.mL^{-1} in PBS, pH 7.4.

4.11. Nano-DSF

The samples (10μM) were loaded in standard nano-DSF capillaries and measured using the Prometheus NT.48 instrument (NanoTemper, Munchen, DE) containing aggregation optics. The LED intensity was set to 10%, whereas the temperature ramp was set from 20 to 95 °C with 1 °C per min. As negative control one duplicate was integrated containing heat denatured protein.

4.12. Enzyme-linked immunosorbent assay

Sandwich ELISA: Plates (Nunc MaxiSorp™, ThermoFisher, Waltham, MA, USA) were coated with 100 µL of a 10 µg.ml^{-1} solution of IgG F(ab)'$_2$ horse anti- *L. intermedia* venom in carbonate buffer pH 9.6 at 4 °C overnight. After blocking (2% casein in PBS), 100 µl of *L. intermedia* venom (0.039 – 10 µg.mL^{-1}) were added and incubated for 1 h at 37 °C. The plates were washed and incubated with solution of scFv$_{15}$hLi7 (20 µg.mL^{-1}). Lastly, 100 µL of peroxidase-conjugated PpL (ThermoFisher Scientific, Waltham, MA, USA) were added for 1 hour at room temperature.

Competitive ELISA: Plates were coated with *L. intermedia* venom (100 µL, 10 µg.mL^{-1}) for 16 h at 4 °C and then saturated with 2% casein diluted in PBS for 60 min, at 37 °C. Next, solutions containing LimAb7 (1 µg.mL $^{-1}$) and scFv$_{15}$hLi7 (6.25 – 100 µg.mL^{-1}) were incubated for 1 h, at 37 °C. Immunocomplexes formed with the IgG were detected by adding peroxidase-conjugated anti-mouse IgG (1:4.000, Sigma).

Indirect ELISA: Plates were coated with *L. intermedia* venom or SMase D Lid1 (100 µL, 2.5 µg.mL^{-1}) for 16 h at 4 °C, and then saturated with 2% casein diluted in PBS for 60 min. Further, different concentrations of scFv (0.156 – 20 µg.mL^{-1}) were added at 37 ° C for 1 h. Immunocomplexes were detected by adding peroxidase-conjugated PpL (ThermoFisher, Waltham, MA, USA).

In both ELISA formats, immunocomplexes were revealed by the addition of substrate (0.2% 2,2/-6azino-bis (2-ethylbenzthiazoline-6-sulphonic acid) to a 0.05 M citric acid buffer, pH 4.0 containing 0.015% hydrogen peroxide (Sigma, UK), for 15 min. Absorbance at 405 nm was measured using an ELISA plate reader. All incubation steps were carried out at 37 °C. All assays were conducted in triplicates. ELISA standard curves were fitted by non-linear regression, using the Saturation Binding - One site -Specific binding function. Statistical analyses and graphics were performed in GraphPad Prism v7.0 for MacOSX (GraphPad Software, San Diego, CA, USA).

4.13. SPR analysis

The BIAcore T100 instrument and all reagents were obtained from GE Healthcare Life Sciences, Europe. SMase D LiD1 was covalently attached to a CM5-sensor chip

using standard amine coupling through EDC/NHS chemistry (approximately 3500 RU). The purified IgG and scFv diluted in PBS, pH 7.4, were passed over the immobilized target (LiD1) at a flow rate of 30 μL.min^{-1} for 1 min at 25°C. The binding kinetics were analyzed using the single-cycle kinetic method with no regeneration between sample injections. Experimental Rmax were 8750 RU and 2900 RU for the IgG and the scFv, respectively. Kinetic constants (k_a, k_d) were deduced from the analysis of association and dissociation rates of at least four different antibody concentrations (0.125 μM - 2.0 μM). The dissociation constant K_D was calculated as $K_D = k_a/k_d$. Sensorgrams were analysed using the BIA evaluation version 2.0.2 software. All experiments were carried out in duplicate.

4.14. Modeling and molecular docking

In order to investigate which amino acid residues might participate in the antigen–antibody interaction, we performed homology modeling of murine monoclonal antibody LimAb7 and scFv$_{15}$hLi7 using the MODELLER tool [36]. In this step, antibody sequences were aligned through a BLAST [37] search and their templates were identified based on sequence identity, query coverage and E-value criteria (Table supplement 1). Utilizing the template choices, for each antibody, 1000 models were generated with the MODELLER tool (9.2v) and then selected according to their ZDOPE score values [38]. Subsequently, model quality was evaluated by comparing the predicted structures with their respective templates via superimposition and atomic RMSD (root mean square deviation) assessment. The chosen cut-off RMSD values of Cα trace between all homology structures and templates was <2.00 Å. Moreover, model energy minimization and loop refinement were carried out in attempt to increase the model's quality using the Chimera software [39] and MODELLER tool, , ensuring >90% of models' AA residues were in favored Ramachandran Plot regions. After modeling the three structures, the ClusPro2.0 server [40] was used to predict the interactions between the modelled antibodies and the Smase D LiRecDT1 (PDB: 3RLH). The LiRecDT1 SMase was selected instead of SMase LiD1 given its X-ray data is available and it only differs from LiD1 by two AA residues. The antibody mode was selected with the non-CDR regions masked automatically [41]. The antibody structures were submitted as the receptor and SMase D LiRecDT1 as the ligand. ClusPro selected the 1000 best scoring solutions, clustered them according to RMSD criteria, and the lowest ClusPro energy score, representing the greatest probability of antigen-antibody interaction, was selected [40]. Amino acid contacts and interaction parameters between the antibodies and their targets were assessed through the PDBSum online platform [42].

4.15. Neutralization of the hemolytic activity

Blood from human healthy donors was collected in tubes containing sodium citrate buffer (BD Plastipak, Franklin Lakes, NJ USA). The platelet-rich plasma and buffy coat were removed by aspiration after centrifugation at 200 x g for 15 min. Packed erythrocytes were washed three times with Ringer Solution (125 mM NaCl, 5 mM KCl, 1 mM $MgSO_4$, 32 mM HEPES, 5 mM glucose, 1 mM $CaCl_2$, pH 7.4, 300 mOsm/kg H_2O) and redissolved at a final concentration of 10^8 cells.mL^{-1}. In order to evaluate the neutralization potential of the antibodies, 0.75 μg of venom were incubated with the following antibody molarities (12.5 - 50 pmol). After 24 h of gentle agitation and incubation at 37 °C, samples were centrifuged (5 min, 200 x g) and the absorbance at 570 nm of the supernatants was read. Samples were analyzed in triplicates along with

negative (Ringer solution) and positive (distilled water containing 0.1% (v/v) Triton X-100) controls. Absorbance values were converted to percentage of hemolysis considering the absorbance at 570 nm of 0.75 µg of venom as 100% lysis.

Subsequently, the inhibition of hemolysis was evaluated in the presence of the components of the complement system. In order to do this, a 1mL solution containing 10^8 erythrocytes was treated with *L. intermedia* venom (10 µg) in the presence of different antibody quantities (25 – 200 pmol) for 24 h under gentle agitation and incubation at 37 °C. Samples were centrifuged (5 min, 200 x g) and the absorbance at 570 nm of the supernatants was read. Next, erythrocytes were washed three times with Ringer solution and incubated with 500 µl of a solution of normal human serum, diluted 1:2, for one hour at 37 °C. Unlysed cells were centrifuged and the absorbance of the supernatant was measured at 570 nm and expressed as percentage of hemolysis. After subtracting all samples absorbance from the absorbance at 570 nm obtained from Ringer treated erytrocytes, before and after complement incubation, the lysis percentage was calculated (absorbance $_{\text{sample}}$ / (absorbance $_{\text{venom without / complement}}$ + absorbance $_{\text{venom with / complement}}$) x 100 considering the sum of the absorbance at 570 nm of the venom before complement incubation and absorbance at 570 nm of venom after complement incubation as 100% of hemolysis. Mean and standard deviation were determined from duplicate samples.

This study has been approved by the human research ethics committee from *Setor de Ciências da Saúde do Universidade Federal do Paraná* (Curitiba, PR, Brazil) under the certificate number CEP/SD2911004.

Supplementary Materials: The following are available online at www.mdpi.com/xxx/s1, Table S1: In silico modeling data., Table S2: Hydrogen Bonds between the amino acid residues of the antibodies and Lid1.

Conflicts of Interest: The authors declare that the research was conducted in the absence of any commercial or financial relationships that could be considered as a potential conflict of interest.

REFERENCES

[1] Chaves-Moreira D, Senff-Ribeiro A, Wille ACM, Gremski LH, Chaim OM, Veiga SS. Highlights in the knowledge of brown spider toxins. J Venom Anim Toxins Trop Dis 2017; 23:6.

[2] Cordeiro FA, Amorim FG, Anjolette FAP, Arantes EC. Arachnids of medical importance in Brazil: main active compounds present in scorpion and spider venoms and tick saliva. J Venom Anim Toxins Trop Dis 2015; 21:24.

[3] Ministério da Saúde. Brasília: Brasil. Sistema de Informação de Agravos de Notificação SINAN; [updated 2020 March, cited 2020 March]. Available from: http://tabnet.datasus.gov.br/cgi/deftohtm.exe?sinannet/cnv/animaisbr.def .

[4] Swanson DL, Vetter RS. Loxoscelism. Clin Dermatol 2006; 24:213–21.

[5] Gremski LH, Trevisan-Silva D, Ferrer VP, Matsubara FH, Meissner GO, Wille ACM, Vuitika L, Dias-Lopes C, Ullah A, de Moraes FR, et al. Recent advances in the understanding of brown spider venoms: From the biology of spiders to the molecular mechanisms of toxins. Toxicon Off J Int Soc Toxinology 2014; 83:91–120.

[6] Gremski LH, da Justa HC, da Silva TP, Polli NLC, Antunes BC, Minozzo JC,

Wille ACM, Senff-Ribeiro A, Arni RK, Veiga SS. Forty Years of the Description of Brown Spider Venom Phospholipases-D. Toxins 2020; 12:164.
[7] Wille ACM, Chaves-Moreira D, Trevisan-Silva D, Magnoni MG, Boia-Ferreira M, Gremski LH, Gremski W, Chaim OM, Senff-Ribeiro A, Veiga SS. Modulation of membrane phospholipids, the cytosolic calcium influx and cell proliferation following treatment of B16-F10 cells with recombinant phospholipase-D from Loxosceles intermedia (brown spider) venom. Toxicon Off J Int Soc Toxinology 2013; 67:17–30.
[8] Kalapothakis E, Araujo SC, de Castro CS, Mendes TM, Gomez MV, Mangili OC, Gubert IC, Chávez-Olórtegui C. Molecular cloning, expression and immunological properties of LiD1, a protein from the dermonecrotic family of Loxosceles intermedia spider venom. Toxicon Off J Int Soc Toxinology 2002; 40:1691–9.
[9] Fernandes Pedrosa M de F, Junqueira de Azevedo I de LM, Gonçalves-de-Andrade RM, van den Berg CW, Ramos CRR, Ho PL, Tambourgi DV. Molecular cloning and expression of a functional dermonecrotic and haemolytic factor from Loxosceles laeta venom. Biochem Biophys Res Commun 2002; 298:638–45.
[10] da Silveira RB, Pigozzo RB, Chaim OM, Appel MH, Dreyfuss JL, Toma L, Mangili OC, Gremski W, Dietrich CP, Nader HB, et al. Molecular cloning and functional characterization of two isoforms of dermonecrotic toxin from Loxosceles intermedia (brown spider) venom gland. Biochimie 2006; 88:1241–53.
[11] da Silveira RB, Pigozzo RB, Chaim OM, Appel MH, Silva DT, Dreyfuss JL, Toma L, Dietrich CP, Nader HB, Veiga SS, et al. Two novel dermonecrotic toxins LiRecDT4 and LiRecDT5 from brown spider (Loxosceles intermedia) venom: from cloning to functional characterization. Biochimie 2007; 89:289–300.
[12] Appel MH, da Silveira RB, Chaim OM, Paludo KS, Silva DT, Chaves DM, da Silva PH, Mangili OC, Senff-Ribeiro A, Gremski W, et al. Identification, cloning and functional characterization of a novel dermonecrotic toxin (phospholipase D) from brown spider (Loxosceles intermedia) venom. Biochim Biophys Acta 2008; 1780:167–78.
[13] Ullah A, de Giuseppe PO, Murakami MT, Trevisan-Silva D, Wille ACM, Chaves-Moreira D, Gremski LH, da Silveira RB, Sennf-Ribeiro A, Chaim OM, et al. Crystallization and preliminary X-ray diffraction analysis of a class II phospholipase D from Loxosceles intermedia venom. Acta Crystallograph Sect F Struct Biol Cryst Commun 2011; 67:234–6.
[14] Hogan CJ, Barbaro KC, Winkel K. Loxoscelism: old obstacles, new directions. Ann Emerg Med 2004; 44:608–24.
[15] Isbister GK, Fan HW. Spider bite. Lancet Lond Engl 2011; 378:2039–47.
[16] Pauli I, Minozzo JC, da Silva PH, Chaim OM, Veiga SS. Analysis of therapeutic benefits of antivenin at different time intervals after experimental envenomation in rabbits by venom of the brown spider (Loxosceles intermedia). Toxicon Off J Int Soc Toxinology 2009; 53:660–71.
[17] Guilherme P, Fernandes I, Barbaro KC. Neutralization of dermonecrotic and lethal activities and differences among 32-35 kDa toxins of medically important Loxosceles spider venoms in Brazil revealed by monoclonal antibodies. Toxicon Off J Int Soc Toxinology 2001; 39:1333–42.
[18] Ramada JS, Becker-Finco A, Minozzo JC, Felicori LF, Machado de Avila RA, Molina F, Nguyen C, de Moura J, Chávez-Olórtegui C, Alvarenga LM. Synthetic

peptides for in vitro evaluation of the neutralizing potency of *Loxosceles* antivenoms. Toxicon 2013; 73:47–55.
[19] Laustsen AH, Solà M, Jappe EC, Oscoz S, Lauridsen LP, Engmark M. Biotechnological Trends in Spider and Scorpion Antivenom Development. Toxins 2016; 8: 226.
[20] Alvarenga LM, Martins MS, Moura JF, Kalapothakis E, Oliveira JC, Mangili OC, Granier C, Chávez-Olórtegui C. Production of monoclonal antibodies capable of neutralizing dermonecrotic activity of Loxosceles intermedia spider venom and their use in a specific immunometric assay. Toxicon Off J Int Soc Toxinology 2003; 42:725–31.
[21] Dias-Lopes C, Felicori L, Rubrecht L, Cobo S, Molina L, Nguyen C, Galéa P, Granier C, Molina F, Chávez-Olortegui C. Generation and molecular characterization of a monoclonal antibody reactive with conserved epitope in sphingomyelinases D from Loxosceles spider venoms. Vaccine 2014; 32:2086–92.
[22] Karim-Silva S, Moura J de, Noiray M, Minozzo JC, Aubrey N, Alvarenga LM, Billiald P. Generation of recombinant antibody fragments with toxin-neutralizing potential in loxoscelism. Immunol Lett 2016; 176:90–6.
[23] Harding FA, Stickler MM, Razo J, DuBridge RB. The immunogenicity of humanized and fully human antibodies. mAbs 2010; 2:256–65.
[24] Aubrey N, Billiald P. Antibody Fragments Humanization: Beginning with the End in Mind. Methods Mol Biol Clifton NJ 2019; 1904:231–52.
[25] de Moura J, Felicori L, Moreau V, Guimarães G, Dias-Lopes C, Molina L, Alvarenga LM, Fernandes P, Frézard F, Ribeiro RR, et al. Protection against the toxic effects of Loxosceles intermedia spider venom elicited by mimotope peptides. Vaccine 2011; 29:7992–8001.
[26] Appel RD, Bairoch A, Hochstrasser DF. A new generation of information retrieval tools for biologists: the example of the ExPASy WWW server. Trends Biochem Sci 1994; 19:258–60.
[27] Jiacomini I, Silva SK, Aubrey N, Muzard J, Chavez-Olortegui C, De Moura J, Billiald P, Alvarenga LM. Immunodetection of the “brown” spider (Loxosceles intermedia) dermonecrotoxin with an scFv-alkaline phosphatase fusion protein. Immunol Lett 2016; 173:1–6.
[28] Honegger A, Plückthun A. Yet another numbering scheme for immunoglobulin variable domains: an automatic modeling and analysis tool. J Mol Biol 2001; 309:657–70.
[29] Abhinandan KR, Martin ACR. Analyzing the “degree of humanness” of antibody sequences. J Mol Biol 2007; 369:852–62.
[30] Abhinandan KR, Martin ACR. Analysis and prediction of VH/VL packing in antibodies. Protein Eng Des Sel PEDS 2010; 23:689–97.
[31] Muzard J, Adi-Bessalem S, Juste M, Laraba-Djebari F, Aubrey N, Billiald P. Grafting of protein L-binding activity onto recombinant antibody fragments. Anal Biochem 2009; 388:331–8.
[32] Lakhrif Z, Pugnière M, Henriquet C, di Tommaso A, Dimier-Poisson I, Billiald P, Juste MO, Aubrey N. A method to confer Protein L binding ability to any antibody fragment. mAbs 2016; 8:379–88.
[33] Ehrenmann F, Lefranc M-P. IMGT/DomainGapAlign: IMGT standardized analysis of amino acid sequences of variable, constant, and groove domains (IG, TR, MH, IgSF, MhSF). Cold Spring Harb Protoc 2011; 2011:737–49.
[34] Ward ES, Güssow D, Griffiths AD, Jones PT, Winter G. Binding activities of

a repertoire of single immunoglobulin variable domains secreted from Escherichia coli. Nature 1989; 341:544–6.
[35] Devaux C, Moreau E, Goyffon M, Rochat H, Billiald P. Construction and functional evaluation of a single-chain antibody fragment that neutralizes toxin AahI from the venom of the scorpion Androctonus australis hector. Eur J Biochem FEBS 2001; 268:694–702.
[36] Sali A, Overington JP. Derivation of rules for comparative protein modeling from a database of protein structure alignments. Protein Sci Publ Protein Soc 1994; 3:1582–96.
[37] Altschul SF, Lipman DJ. Protein database searches for multiple alignments. Proc Natl Acad Sci U S A 1990; 87:5509–13.
[38] Luiz M, Pereira S, Prado N, Gonçalves N, Kayano A, Moreira-Dill L, Sobrinho J, Zanchi F, Fuly A, Fernandes C, et al. Camelid Single-Domain Antibodies (VHHs) against Crotoxin: A Basis for Developing Modular Building Blocks for the Enhancement of Treatment or Diagnosis of Crotalic Envenoming. Toxins 2018; 10:142.
[39] Pettersen EF, Goddard TD, Huang CC, Couch GS, Greenblatt DM, Meng EC, Ferrin TE. UCSF Chimera--a visualization system for exploratory research and analysis. J Comput Chem 2004; 25:1605–12.
[40] Kozakov D, Hall DR, Xia B, Porter KA, Padhorny D, Yueh C, Beglov D, Vajda S. The ClusPro web server for protein-protein docking. Nat Protoc 2017; 12:255–78.
[41] Brenke R, Hall DR, Chuang G-Y, Comeau SR, Bohnuud T, Beglov D, Schueler-Furman O, Vajda S, Kozakov D. Application of asymmetric statistical potentials to antibody-protein docking. Bioinforma Oxf Engl 2012; 28:2608–14.
[42] Laskowski RA, Watson JD, Thornton JM. Protein function prediction using local 3D templates. J Mol Biol 2005; 351:614–26.
[43] Gao SH, Huang K, Tu H, Adler AS. Monoclonal antibody humanness score and its applications. BMC Biotechnol 2013; 13:55.
[44] Murakami MT, Fernandes-Pedrosa MF, Tambourgi DV, Arni RK. Structural basis for metal ion coordination and the catalytic mechanism of sphingomyelinases D. J Biol Chem 2005; 280:13658–64.
[45] Vuitika L, Chaves-Moreira D, Caruso I, Lima MA, Matsubara FH, Murakami MT, Takahashi HK, Toledo MS, Coronado MA, Nader HB, et al. Active site mapping of Loxosceles phospholipases D: Biochemical and biological features. Biochim Biophys Acta 2016; 1861:970–9.
[46] Fogaça RL, Alvarenga LM, Woiski TD, Becker-Finco A, Teixeira KN, Silva SK, de Moraes RN, Noronha L de, Noiray M, de Figueiredo BC, et al. Biomolecular engineering of antidehydroepiandrosterone antibodies: a new perspective in cancer diagnosis and treatment using single-chain antibody variable fragment. Nanomed 2019; 14:689–705.
[47] Lopes PH, Murakami MT, Portaro FCV, Mesquita Pasqualoto KF, van den Berg C, Tambourgi DV. Targeting *Loxosceles* spider Sphingomyelinase D with small-molecule inhibitors as a potential therapeutic approach for loxoscelism. J Enzyme Inhib Med Chem 2019; 34:310–21.
[48] de Almeida DM, Fernandes-Pedrosa M de F, de Andrade RMG, Marcelino JR, Gondo-Higashi H, de Azevedo I de LMJ, Ho PL, van den Berg C, Tambourgi DV. A new anti-loxoscelic serum produced against recombinant sphingomyelinase D: results of preclinical trials. Am J Trop Med Hyg 2008; 79:463–70.

[49] Duarte CG, Bonilla C, Guimarães G, Machado de Avila RA, Mendes TM, Silva W, Tintaya B, Yarleque A, Chávez-Olórtegui C. Anti-loxoscelic horse serum produced against a recombinant dermonecrotic protein of Brazilian Loxosceles intermedia spider neutralize lethal effects of Loxosceles laeta venom from Peru. Toxicon Off J Int Soc Toxinology 2015; 93:37–40.
[50] Felicori L, Fernandes PB, Giusta MS, Duarte CG, Kalapothakis E, Nguyen C, Molina F, Granier C, Chávez-Olórtegui C. An in vivo protective response against toxic effects of the dermonecrotic protein from Loxosceles intermedia spider venom elicited by synthetic epitopes. Vaccine 2009; 27:4201–8.
[51] Dias-Lopes C, Guimarães G, Felicori L, Fernandes P, Emery L, Kalapothakis E, Nguyen C, Molina F, Granier C, Chávez-Olórtegui C. A protective immune response against lethal, dermonecrotic and hemorrhagic effects of Loxosceles intermedia venom elicited by a 27-residue peptide. Toxicon Off J Int Soc Toxinology 2010; 55:481–7.
[52] Figueiredo LFM, Dias-Lopes C, Alvarenga LM, Mendes TM, Machado-de-Ávila RA, McCormack J, Minozzo JC, Kalapothakis E, Chávez-Olórtegui C. Innovative immunization protocols using chimeric recombinant protein for the production of polyspecific loxoscelic antivenom in horses. Toxicon Off J Int Soc Toxinology 2014; 86:59–67.
[53] Lima S de A, Guerra-Duarte C, Costal-Oliveira F, Mendes TM, Figueiredo LFM, Oliveira D, Machado de Avila RA, Ferrer VP, Trevisan-Silva D, Veiga SS, et al. Recombinant Protein Containing B-Cell Epitopes of Different Loxosceles Spider Toxins Generates Neutralizing Antibodies in Immunized Rabbits. Front Immunol 2018; 9:653.
[54] Safdari Y, Farajnia S, Asgharzadeh M, Khalili M. Antibody humanization methods - a review and update. Biotechnol Genet Eng Rev 2013; 29:175–86.
[55] Lebozec K, Jandrot-Perrus M, Avenard G, Favre-Bulle O, Billiald P. Design, development and characterization of ACT017, a humanized Fab that blocks platelet's glycoprotein VI function without causing bleeding risks. mAbs 2017; 9:945–58.
[56] Lebozec K, Jandrot-Perrus M, Avenard G, Favre-Bulle O, Billiald P. Quality and cost assessment of a recombinant antibody fragment produced from mammalian, yeast and prokaryotic host cells: A case study prior to pharmaceutical development. New Biotechnol 2018; 44:31–40.
[57] Dondelinger M, Filée P, Sauvage E, Quinting B, Muyldermans S, Galleni M, Vandevenne MS. Understanding the Significance and Implications of Antibody Numbering and Antigen-Binding Surface/Residue Definition. Front Immunol 2018; 9:2278.
[58] Waldmann H. Human Monoclonal Antibodies: The Benefits of Humanization. Methods Mol Biol Clifton NJ 2019; 1904:1–10.
[59] Doevendans E, Schellekens H. Immunogenicity of Innovative and Biosimilar Monoclonal Antibodies. Antibodies 2019; 8:21.
[60] Moussa EM, Panchal JP, Moorthy BS, Blum JS, Joubert MK, Narhi LO, Topp EM. Immunogenicity of Therapeutic Protein Aggregates. J Pharm Sci 2016; 105:417–30.
[61] van der Kant R, Karow-Zwick AR, Van Durme J, Blech M, Gallardo R, Seeliger D, Aßfalg K, Baatsen P, Compernolle G, Gils A, et al. Prediction and Reduction of the Aggregation of Monoclonal Antibodies. J Mol Biol 2017; 429:1244–61.
[62] Morgan H, Tseng S-Y, Gallais Y, Leineweber M, Buchmann P, Riccardi S,

Nabhan M, Lo J, Gani Z, Szely N, et al. Evaluation of in vitro Assays to Assess the Modulation of Dendritic Cells Functions by Therapeutic Antibodies and Aggregates. Front Immunol 2019; 10:601.
[63] Jerabek-Willemsen M, Wienken CJ, Braun D, Baaske P, Duhr S. Molecular interaction studies using microscale thermophoresis. Assay Drug Dev Technol 2011; 9:342–53.
[64] Coronado MA, Ullah A, da Silva LS, Chaves-Moreira D, Vuitika L, Chaim OM, Veiga SS, Chahine J, Murakami MT, Arni RK. Structural Insights into Substrate Binding of Brown Spider Venom Class II Phospholipases D. Curr Protein Pept Sci 2015; 16:768–74.
[65] Lajoie DM, Roberts SA, Zobel-Thropp PA, Delahaye JL, Bandarian V, Binford GJ, Cordes MHJ. Variable Substrate Preference among Phospholipase D Toxins from Sicariid Spiders. J Biol Chem 2015; 290:10994–1007.
[66] Dias-Lopes C, Neshich IAP, Neshich G, Ortega JM, Granier C, Chávez-Olortegui C, Molina F, Felicori L. Identification of new sphingomyelinases D in pathogenic fungi and other pathogenic organisms. PloS One 2013; 8:e79240.
[67] de Giuseppe PO, Ullah A, Silva DT, Gremski LH, Wille ACM, Chaves Moreira D, Ribeiro AS, Chaim OM, Murakami MT, Veiga SS, et al. Structure of a novel class II phospholipase D: catalytic cleft is modified by a disulphide bridge. Biochem Biophys Res Commun 2011; 409:622–7.
[68] Tambourgi DV, Gonçalves-de-Andrade RM, van den Berg CW. Loxoscelism: From basic research to the proposal of new therapies. Toxicon Off J Int Soc Toxinology 2010; 56:1113–9.
[69] Felicori L, Araujo SC, de Avila RAM, Sanchez EF, Granier C, Kalapothakis E, Chávez-Olórtegui C. Functional characterization and epitope analysis of a recombinant dermonecrotic protein from Loxosceles intermedia spider. Toxicon Off J Int Soc Toxinology 2006; 48:509–19.
[70] Mendes TM, Oliveira D, Figueiredo LFM, Machado-de-Avila RA, Duarte CG, Dias-Lopes C, Guimarães G, Felicori L, Minozzo JC, Chávez-Olortegui C. Generation and characterization of a recombinant chimeric protein (rCpLi) consisting of B-cell epitopes of a dermonecrotic protein from Loxosceles intermedia spider venom. Vaccine 2013; 31:2749–55.
[71] Gremski LH, da Silveira RB, Chaim OM, Probst CM, Ferrer VP, Nowatzki J, Weinschutz HC, Madeira HM, Gremski W, Nader HB, et al. A novel expression profile of the Loxosceles intermedia spider venomous gland revealed by transcriptome analysis. Mol Biosyst 2010; 6:2403–16.
[72] Laustsen AH, María Gutiérrez J, Knudsen C, Johansen KH, Bermúdez-Méndez E, Cerni FA, Jürgensen JA, Ledsgaard L, Martos-Esteban A, Øhlenschlæger M, et al. Pros and cons of different therapeutic antibody formats for recombinant antivenom development. Toxicon Off J Int Soc Toxinology 2018; 146:151–75.
[73] Engmark M, Andersen MR, Laustsen AH, Patel J, Sullivan E, de Masi F, Hansen CS, Kringelum JV, Lomonte B, Gutiérrez JM, et al. High-throughput immuno-profiling of mamba (Dendroaspis) venom toxin epitopes using high-density peptide microarrays. Sci Rep 2016; 6:36629.
[74] Engmark M, Lomonte B, Gutiérrez JM, Laustsen AH, De Masi F, Andersen MR, Lund O. Cross-recognition of a pit viper (Crotalinae) polyspecific antivenom explored through high-density peptide microarray epitope mapping. PLoS Negl Trop Dis 2017; 11:e0005768.
[75] Röthlisberger D, Honegger A, Plückthun A. Domain interactions in the Fab

fragment: a comparative evaluation of the single-chain Fv and Fab format engineered with variable domains of different stability. J Mol Biol 2005; 347:773–89.
[76] Chaves-Moreira D, Chaim OM, Sade YB, Paludo KS, Gremski LH, Donatti L, de Moura J, Mangili OC, Gremski W, da Silveira RB, et al. Identification of a direct hemolytic effect dependent on the catalytic activity induced by phospholipase-D (dermonecrotic toxin) from brown spider venom. J Cell Biochem 2009; 107:655–66.
[77] Tambourgi DV, Paixão-Cavalcante D, Gonçalves de Andrade RM, Fernandes-Pedrosa M de F, Magnoli FC, Paul Morgan B, van den Berg CW. Loxosceles Sphingomyelinase Induces Complement-Dependent Dermonecrosis, Neutrophil Infiltration, and Endogenous Gelatinase Expression. J Invest Dermatol 2005; 124:725–31.
[78] Manzoni-de-Almeida D, Squaiella-Baptistão CC, Lopes PH, van den Berg CW, Tambourgi DV. Loxosceles venom Sphingomyelinase D activates human blood leukocytes: Role of the complement system. Mol Immunol 2018; 94:45–53.
[79] Quintero-Hernández V, Del Pozo-Yauner L, Pedraza-Escalona M, Juárez-González VR, Alcántara-Recillas I, Possani LD, Becerril B. Evaluation of three different formats of a neutralizing single chain human antibody against toxin Cn2: neutralization capacity versus thermodynamic stability. Immunol Lett 2012; 143:152–60.
[80] Voors-Pette C, Lebozec K, Dogterom P, Jullien L, Billiald P, Ferlan P, Renaud L, Favre-Bulle O, Avenard G, Machacek M, et al. Safety and Tolerability, Pharmacokinetics, and Pharmacodynamics of ACT017, an Antiplatelet GPVI (Glycoprotein VI) Fab: First-in-Human Healthy Volunteer Trial. Arterioscler Thromb Vasc Biol 2019; 39:956–64.
[81] Quintero-Hernández V, Juárez-González VR, Ortíz-León M, Sánchez R, Possani LD, Becerril B. The change of the scFv into the Fab format improves the stability and in vivo toxin neutralization capacity of recombinant antibodies. Mol Immunol 2007; 44:1307–15.
[82] Lawrence PB, Price JL. How PEGylation influences protein conformational stability. Curr Opin Chem Biol 2016; 34:88–94.

4.2. Otimização da produção de fragmentos de anticorpo humanizados derivados do LimAb7 (em processo de submissão):

Multiparameter optimization of a humanized antibody fragment: Strategies and pitfalls

Isabella Gizzi Jiacomini [1,2], Martina Beltramino[1], Fanny Boursin[2], João Carlos Minozzo[3], Juliana Ferreira de Moura[1], Luíza Helena Gremski[4], Sílvio Sanches Veiga[4], Philippe Billiald[4], Larissa Magalhães Alvarenga[1], Nicolas Aubrey[2]

[1] Programa de Pós-Graduação em Microbiologia, Parasitologia e Patologia – Departamento de Patologia Básica, Universidade Federal do Paraná, CEP 81531-980 Curitiba, PR, Brazil.
[2] ISP UMR 1282, INRA, Université de Tours, Team BioMAP, 31 avenue Monge, 37200 Tours, France.
[3] Centro de Produção e Pesquisa de Imunobiológicos – Piraquara, PR, Brazil
[4] Departamento de Biologia Celular, Universidade Federal do Paraná, CEP 81531-980 Curitiba, PR, Brazil.
[5] IPSIT, School of Pharmacy, University Paris-Saclay, 92296, Châtenay-Malabry, France.

Corresponding author:

Larissa M. Alvarenga: lmalvarenga@gmail.com,

Highlights:

- The production of humanized Fab fragments against animal toxins is reported for the first time.
- Host cell expression system can be a determinant factor in the improvement of physio-chemical features, such as production yield and stability of recombinant antibodies.
- The screening of humanized antibodies based on *in silico* sequence motif studies and physio-chemical parameters could provide guidance towards the development of optimal antibody molecules.

Abstract:

The use of monoclonal antibodies in therapy has been growing by the day and many discussions entail its safety, rentability, viability and effectiveness. To this date, around 130 antibody molecules have been approved by FDA for the treatment of various maladies. Aiming for the large-scale production of these molecules, the recombinant DNA technology is largely employed, and antibodies are expressed in various systems, prokaryotic and eukaryotic. So much so, that all commercial

monoclonal IgGs are recombinantly produced. Moreover, considering the organism of origin of these antibody fragments and its immunogenicity, antibody humanization and the use of human antibody libraries have been vastly proposed. Around 50% of commercial mAbs are humanized and 35% of human origin. In this context, we introduce LimAb7, a mouse monoclonal antibody capable of binding and completely neutralizing brown spider's *Loxosceles intermedia* dermonecrotic toxins *in vivo* and *in vitro*. This antibody has been produced in both mouse and humanized scFv and diabody formats, however our results indicated losses in fragment affinity, stability and neutralizing capacity leading us to infer that molecule size and format might be of importance to the maintenance of parental antibody features. Aiming to develop evolved, more structurally stable, and neutralizing antibody fragments, we report for the first time the design of humanized antibody light and heavy V-domains produced and purified as Fab fragments (Fab') against spider venom toxins. Improvements in the constructs were observed with respect to physiochemical stability, target binding and maintenance of binding pattern. As their venom neutralizing features remain to be characterized in vivo/in vitro, we believe this data sheds new light on antibody humanization and increase of fragment stability by producing a parental molecule in different recombinant formats.

Key words: antibody humanization, developability, physio-chemical features.

1. Introduction

Recombinant proteins have been broadly produced and possess a great spectre of applications, ranging from basic research to pharmaceutical development, paving the way and being responsible for great breakthroughs in biotechnology and therapy. Their clinical use is comprised of recombinant hormones, cytokines, growth factors, thrombolytic drugs and blood clotting factors, enzymes allowing the treatment of various diseases, and notably, antibodies, the protagonists of the emerging and promising immunotherapy. [1].

To date, around 130 monoclonal antibodies (mAbs) and 40 human/non-human polyclonal antibody mixtures have been approved by the U.S. Food and Drug Administration (FDA) for the treatment of numerous pathologies [2]. Many variables entail the monoclonal antibody therapy discussions such as molecule origin (human, humanized, chimeric, murine), format (sdAbs, scFvs, Fabs, whole IgGs), safety, immunogenicity, route of administration and pharmacokinetics/pharmacodynamics [3; 4]. The majority of the mAbs are humanized whole IgGs, followed by human whole IgGs, produced mainly in eukaryote expression systems and by phage display in human antibody libraries, respectively (e.g., PER.C6® human cells, NS0 murine myeloma cells, CHO (Chinese Hamster Ovary) cells) [5].

There are many important criteria to be considered when developing therapeutical antibodies. Target binding is the major such as score of humanization, best expression system, different antibody formats more adapted to the distinct applications and biophysical features, to produce stable, functional, and non-aggregating molecules should be considered. [6]. Target binding may be the

greatest concern, yet once a lead molecule is humanized and its immunogenicity is significantly lowered, a series of features regarded as “developability” assume certain importance. For monoclonal antibodies, these properties include the expression system, purification strategy, yield of production, conformation and colloidal stability, low immunogenicity, low to no aggregation, and maintenance of functionality [7, 8, 9]. Risking failure in any of the above-mentioned criteria has a high cost, specially at the latest stages of production. This instigates efforts in the sense of predicting molecules’ developability based on not only the amino acid sequences, but also through experimentally determined physio-chemical features [10].

Concerning a template that would be fitting for the study of the abovementioned criteria, we introduce LimAb7, a murine monoclonal antibody capable of binding and completely neutralizing, both *in vivo* and in *vitro*, a myriad of dermonecrotic toxins present in brown spider venom, termed Phospholipases D (*Loxosceles intermedia*) [11]. Recombinant molecules derived from LimAb7 were previously produced [12, 13, 14], but challenges such as improving production yield, lowering molecule immunogenicity, and maintaining target recognition weren’t thoroughly established. The murine origin of monoclonal antibodies is barrier to administration to humans, given their potential immunogenicity [12]. That could be overcome by modifying LimAb7s framework regions through a process known as humanization, that consists in the grafting of human framework regions to the murine CDRs, thus allowing a reduction of the molecule’s immunogenicity while maintaining its features [15, 9].

All in all, the present study aimed to produce novel humanized LimAb7 derived constructs in the Fab format, thus attempting to improve fragments’ structural features and stability and target recognition. V-domains were once again humanized and 16 Fab variants were designed, produced, and analysed. Additionally, a protein L binding site was also inserted in the light chain of all humanized sequences, to enable Fab purification [16]. In terms of their structural, physio-chemical, and immunochemical features, we were able to observe that LimAb7 derived Fab fragments have their physio-chemical highly improved in comparison to other previously developed formats and out of the 16 variants produced, one was chosen for further immunochemical characterizations in terms of functionality and binding site maintenance. In addition to the enhancement of fragments physio-chemical properties, we have observed that the selected humanized Fab construct shows to retain the same binding features as the parental molecule, LimAb7. Hence, the evaluation of all physio-chemical criteria present in this study could be carefully considered when choosing a lead therapeutical antibody molecule and aiming its batch production.

2. Materials and Methods

2.1. Design of humanized V-domains

Amino acid residues were identified according IMGT numbering scheme and the human germline genes most alike LimAb7's V-domains was identified by the IMGT/DomainGapAlign tool from the International ImmunoGeneTics information system (IMGT). Humanized versions of LimAb7 V-domains were generated by grafting all six CDRs onto human IGKV and IGHV domains, as described by Aubrey et al., 2018 [9], and following different criteria for the choice of human framework template, described in detail in Table 1.

Briefly, various humanization strategies were considered aiming to generate a high number of different possibilities. The criteria that stood out were (a) similarity of germline, (b) utilization of fixed FR templates, (c) templates with high sequence identity to LimAb7, (d) a commercial mAb (Obinutuzumab) FR sequences. Next, each amino acid (AA) substitution was inspected individually, based on the physio-chemical classes of the AA differences. The humanness score (Z-score), a parameter that compares the sequences with a set of known human sequences assigned to germline derived families, was evaluated and a score close or above 0 was desired. Following *in silico* analysis, some humanized sequences were discarded and 4 different VH and VL humanized sequences were chosen.

Additional refinements were carried out in IGKV-FR1 for the inclusion of a PpL-binding site without altering predicted humanization and residual immunogenicity. Finally, the 4 humanized VH and VL domains were paired together to generate 16 LimAb7 Fab variants (B1 to F8). In addition, a chimeric Fab (A1) containing the mouse LimAb7's V-domains and the human Fab CH1 and CL (IGHG1*01 and IGKC*01, respectively) domains were also designed, to be used as a control. All VH and VL sequences were also alignment through the Clustal Omega tool [17] to observe the sequences' identity in relation to the murine parental sequences.

2.2. Generation and production of humanized Fab variants

Humanized VH and VL designed sequences were chemically synthesized (Genscript), amplified and purified. These sequences were each individually inserted in pcDNA 3.4 expression vectors, generating 4 VH and 4 VL vectors. These VH and VL vectors were ligated to CH1 and CL domains (IGHG1*01 and IGKC*01, respectively) domains respectively through the Golden Gate Assembly technology (NEB – New England Biosciences). For confirmation of successful assembled plasmids, vectors were digested with XhoI and XbaI (Promega) endonucleases and resolved in a 1% agarose gel. Band fragmentation patterns were then evaluated with the help of the Serial Cloner 2.6 software.

CHO (Chinese Hamster Ovary) [18] cells were thawed and harvested in Erlenmeyer's until they reached $3x10^5$ cells.mL^{-1}. Cells were then co-transfected with the plasmids containing the correspondent constructs in a proportion of 1/3 VH-CH1 to 2/3 VL-CL for the Fabs. Transient expression was performed under standard conditions (FreeStyleTM Max Reagent, Life Technology, 12651–014). Cell viability was evaluated daily by trypan blue 0.4% (Thermo Fisher), and

supernatants were collected 6 days post-transfection when cell viability fell below 80%. Next, supernatants were spun and filtered to eliminate debris and Fab expression and functionality were evaluated in ELISA and Western Blot assays in the presence of peroxidase conjugated Protein L.

2.3. Fab purification

Fab variants were purified from transiently transfected CHO-S cells pool supernatants using Capto L affinity chromatography (GE Healthcare, 17–5478–01) according to the manufacturer instructions. Elution was done through gradually decreasing the pH in a 0.1 M Glycine solution until a pH of 2.3 was reached. Excess salt was removed from the samples through a molecular filtration column (Sephadex G 25 Superfin – G&E Life Sciences). All procedures were carried out on a bidimensional HPLC system ÄKTA Pure 150 (G&E Life 36 Sciences) instrument. Protein concentration was determined after A280nm measurements (ThermoFisher, 23235). Purity and expression were evaluated through an SDS-PAGE in which 2μM of Fab fragments were resolved in a 12% polyacrylamide gel under reducing and non-reducing conditions and evidenced through Coomassie Blue Staining.

2.4. Physio-chemical Analysis –Thermal and pH stability

The UV-Vis spectra (from 220 to 350 nm) analysis were carried out in triplicate after dilution of Fab samples in PBS, pH 7.2. The pH stability of was also measured for Fabs A1 and E4. Each molecule was diluted in either PBS, pH 7.2 or Glycine 1M at pH ranging from 2 to 6. Then, samples (10μM) were loaded in standard nanoDSF (Differential Scanning Fluorimetry) capillaries and analysed using the Prometheus NT.48 instrument. The LED intensity was set to 10%, whereas the temperature ramp was set from 20 to 95 °C with 1 °C per min. As negative control one duplicate was integrated containing heat denatured protein. The onset temperatures were determined according to Menzen and Fries [19].

2.5. Physio-chemical Analysis – SEC-HPLC

Fabs (5 μM) (in 100 μL) were analysed by size-exclusion high pressure liquid chromatography (SEC-HPLC) using a prepacked Superdex 75 10/300GL column calibrated with standards from GE Healthcare. Proteins were eluted with PBS, pH 7.2 at a rate of 0.5 ml.min-1 and detected with a UV recorder at 280 nm.

2.6. Immunochemical characterization of purified Fab fragments

Vacuum dried venoms from *L. laeta, L. gaucho*, and *L. intermedia* spiders as well as horse hyperimune sera (SALOX) reactive to *L. intermedia, L. laeta, and L. gaucho* venoms were provided by *Centro de produção e pesquisa de imunobiológicos* (CPPI), Piraquara, PR, Brazil. The recombinant PLD (Phospholipase D) LiRecDT1 (PDB: 3RLH) was a gift from Dr. Silvio Sanches Veiga (UFPR, Curitiba, PR, Brazil). **Indirect ELISA – Enzyme-linked Immunosorbent Assay**: For the assessment of the Fabs binding to the whole

venom and PLD LiRecDT1, polystyrene plates were either coated with *Loxosceles intermedia* venom or LiRecDT1 (5 $\mu g.mL^{-1}$ and 1 $\mu g.mL^{-1}$ diluted in coating buffer, respectively). After blocking with BSA 3%, Fab preparations diluted in PBS in a range of protein quantity from 1µM - 0.01 µM, were incubated on the plates with the coated antigen for 1 hour, at 37°C. Bound Fab detection was done by adding peroxidase conjugated Protein L (PpL) diluted 1:800 (Pierce, 32420) and evidenced by the addition of TMB (3,3',5,5'-Tetramethylbenzidine – Sigma Aldrich). The reaction was stopped with H_2SO_4 2M (50 mL/well). Absorbance was read at 450 nm. Three washings with 200 µL/well of the dilution buffer were performed between each intermediate step. Each point was measured in duplicate.
Western Blotting: L. intermedia whole venom (5 µg/lane) was resolved in a 12.5 % polyacrylamide gel under reducing conditions and transferred onto a nitrocellulose membrane. The membrane was blocked with casein 5% and tween 0.02% diluted in PBS, each venom lane cut into strips and then each incubated with either 5 $\mu g.mL^{-1}$ of Fabs or 2.5 $\mu g.mL^{-1}$ of the parental molecule LimAb7 (positive control) or an irrelevant monoclonal antibody (negative control). Peroxidase conjugated Anti-human Fab (Sigma A0293) was added (diluted 1:40000) for the detection of Fabs and peroxidase conjugated anti-mouse (Sigma A9044) (diluted 1:5000) for the detection of controls. Immunocomplexes were revealed by the addition of ECL and DAB/Chloronaftol. Between each incubation step, membranes were washed three times with PBS-Tween 0.05%.

2.7. In silico Analysis of VH Variant C

The murine LimAb7 heavy chain sequence was aligned with VH **C** humanized variant sequence using the Mutalin [20] interface, under the *Difference* output style mode. Next, VHs E, C and of LimAb7 were individually modelled using the online MODELLER tool [21]. Antibody sequences were aligned through a BLAST [22] search and their templates identified based on sequence identity, query coverage and E-value criteria. Subsequently, model quality was evaluated by comparing the predicted structures with their respective templates via superimposition and atomic RMSD (root mean square deviation) assessment. The chosen cut-off RMSD values of Cα trace between modelled structures and templates was <2.00 Å. Structural homology models were visualized using UCSF Chimera v1.15 (developed by the Resource for Biocomputing, Visualization, and Informatics at the University of California, San Francisco) and superimpositions between models were carried out using the Matchmaker tool (Structure Comparison > Matchmaker tool).

2.8. Immunogenicity MHC II Studies

Here, the NetMHCIIpan-4.0 algorithm was used to predict epitopes presented by class II human leukocyte antigen molecules (HLA-II) within the antibody sequences [23].

Core peptides were calculated and tabulated for both, VH and VL domains. Scoring was performed across multiple alleles, allowing sequences to be evaluated for the presence of strong binders, weak binders, and no binders to any allele of MHCII. Only strong binders have been retained for this study. Seventeen

HLA-DR molecules DRB1 alleles covering a wide range of the population were selected. Taken collectively, DRB1 eight alleles 0101, 0301, 0401, 0701, 0801, 1101, 1301, 1501, along with their respective family members, “cover” well over 95% of the human population [24]. DRB1 alleles 0402, 0803, 0901, 1202, 1402 are common alleles within the Central Western Europe. DRB1 1001 and 1103 are risk alleles for anti-drug antibodies (ADA). The length of tested peptides was set to 15-mers. Threshold for strong binders (% rank) and for weak binder (%rank) were set by default to 2 and 10, respectively. In addition, regions of the sequence that contained putative T cell epitopes were also screened for homology with the non-redundant human proteome databases and sequences of published epitopes that have been catalogued in the immune epitope database (IEDB) at the La Jolla Institute for Allergy and Immunology (https://www.iedb.org/).

2.9. Immunochemical Characterization of Fab E4:

2.9.1. Competition ELISA – Enzyme Linked Immunosorbent Assay

For the assessment of the ability of Fab to bind to the LiRecDT1 in the presence of the parental molecule, LimAb7 a competition ELISA was carried out. Briefly, polystyrene plates were coated with LiRecDT1 (7 nM) diluted in coating buffer). After blocking with casein, Fab preparations (700 - 0.007 nM nM) were diluted in a solution containing PBS and 1 nM of mouse LimAb7 and incubated on the plates with the coated antigen for 1 hour, at 37°C. Bound LimAb7 detection was done by adding peroxidase conjugated anti-mouse IgG diluted 1:4,000 (Merck, A9044) and evidenced by the addition of OPD (o-phenylenediamine dihydrochloride – Sigma Aldrich). The reaction was stopped with H_2SO_4 2M (50 mL/well). Absorbance was read at 490 nm. Three washings with 300 µL/well of the PBS-Tween 0.05% were performed between each intermediate step. Each point was measured in duplicate.

2.9.2. Sandwich ELISA - Enzyme Linked Immunosorbent Assay

For evaluating whether the Fab E4 binding site to the target, LiRecDT1, remained the same as the parental molecule, plates were coated with LimAb7 (6.6 nM, diluted in coating buffer). After blocking with casein, LiRecDT1 (14 nM) was added to all plate wells and incubated for 1 hour at 37 °C. Next, Fab preparations diluted in PBS in a range of protein quantity from 36 - 0.00036 nM, diluted by a factor of 10, were incubated on the plates with the captured LiRecDT1 for 1 hour, at 37°C. Bound Fab detection was done by adding peroxidase conjugated anti-human Fab IgG diluted 1:40,000 (Sigma, I5260) and evidenced by the addition of OPD (o-phenylenediamine dihydrochloride – Sigma Aldrich). The reaction was stopped with H_2SO_4 2M (50 mL/well). Absorbance was read at 490 nm. Three washings with 300 µL/well of the PBS-Tween 0.05% were performed between each intermediate step. Each point was measured in duplicate. The assay’s positive control consisted in anti-*Loxosceles* HRP horse pAb diluted at 1:300 and the negative control, of 6.6 nM of human pAb irrelevant antibodies.

3. Results

3.1. Design of humanized LimAb7 Fabs

LimAb7V-domains were successfully humanized following 4 different criteria, according to Aubrey & Billiald, 2019 [9] and sequences containing FR modifications are depicted in Figure 1 A and B. Four humanized VH/VL sequences were designed and chemically synthesized. The percent humanization of each of the designed sequences, as well as their Z-score, was determined and data shows that constructs that receive the VH **C** possess a higher Z-score. However, for the VH **B**, a better percent humanization and a more balanced Z-score were achieved. Regarding the VL sequences, VLs **4** and **8** show greater percentage of humanization. Nonetheless, the best Z-score pertains to the VL **8** sequence (Figure 2A).

V-domain humanized sequences were successfully ligated to their Fv correspondents, though golden gate DNA Assembly and once the individual VH/VL constructs were generated and ligated to vectors. Once the accuracy of the DNA constructions was verified through enzymatic digestion and sequencing, the CHO cells were co-transfected with VH-CH1 and VL-CL vectors, making up for 16 different VH/VL combinations.

3.2. Transient expression of Fabs, structural and analytical characterization

CHO-cells supernatant was collected 10 days post-transfection for preliminary protein expression analysis and further fragment purification. The purification yield of all constructs is depicted in Figure 3 and expressed as $mg.L^{-1}$ of culture media. Constructions yielding the highest protein levels were as follows: Fab B8 > F8 > E4 > E2 > B2 > E8 > F4 > E2, evidencing a probable relationship between VL sequences **8, 4** and **2** and VH sequences **B, F** and **E** and intensity of protein expression. Interestingly, as constructs generated from the VH **C** sequence were not well produced, independently from the combined VL. All yield values are detailed in Supplementary Table 1.

Initial purity of produced proteins was evaluated through an SDS-PAGE. The apparent molecular mass of the bands observed for the Fabs was 26 kDa (under reducing conditions) and 55 kDa (non-reducing conditions), except for all four VH **C** Fabs, where a 26 kDa band was observed instead. Fragments B8, F8 and F2 also indicate the presence of a discrete 26 kDa band (Supplementary Figure 1).

Fabs were assessed in terms of their aggregation, dimerization, and thermal stability. No significant aggregation was detected, and a slight dimerization was detected through SEC-HPLC limited to VH **C** and VL **8** Fabs (Figure 2B). In

general, fragments are stable until 60-65 °C, except for VH **C** fragments, in which the T_m drops significantly (42-48 °C). The VL **2** and VH **B** sequences seem to positively influence in the thermal stability, as the fragments build up from these sequences show a higher T_m (Figure 2C). All T_m values are depicted in detail in Supplementary Table 2.

3.3. Preliminary Characterization of Recombinant Humanized Molecules:

ELISA assays in the presence of humanized Fab fragments were carried out for whole *Loxosceles intermedia* venom (data not shown) and PLD antigen LiRecDT1 reactivity and specificity analysis. Most fragments retained binding to both the whole venom and the PLD, however in different intensities. Binding curves of Fabs to LiRecDT1 that are more dislocated to the left suggest higher reactivity for the antigen (F8, B8, E4, B4 in Figure 3A). Antigen binding intensity seems to be associated to the VL following a VL **4** > VL **8** > VL **5** hierarchy. Western Blot evaluation for Fab binding to whole *L. intermedia* venom shows that all tested Fabs maintain the same pattern of antigen recognition, observed around 29-34 kDa region, characteristic of the venom PLDs (Figure 3B).

Moreover, VH **C** structure was modelled and aligned with the parental heavy chain amino acid sequence and 3D structure, given it was not accurately expressed (Supplementary Figure 1). Mutations exclusive of VH **C** were highlighted and amino acid (AA) side chains were exposed. Some non-conservative AA substitutions are observed where side chain orientation and AA functional nature are remarkably different (A16E, R45M, Q49K, G69P, K70S, K75Q and T95Q) (Supplementary Figure 2).

All things considered, after the production, physio-chemical and functional evaluation of all 16 produced Fab fragments criteria such as (i) humanization percent and Z-score, (ii) production yield, (iii) thermal stability, (iv) dimerization and aggregation, (v) LiRecDT1 binding ability, were all weighted in (Figure 3D).

3.4. Further Characterization of Fab E4

3.4.1. pH Stability Analysis:

The pH stability of FabE4 was evaluated in comparison to the chimeric Fab molecule, A1. We observed that when diluted in glycine buffer solution pH 2 and 3, the melting temperature of both molecules drops significantly and at the same proportion for both. However, once a pH of 4 is reached the T_m for both molecules is re-established and similar to when they are diluted in PBS. Both Fabs A1 and E4 have shown a similar behaviour in their thermal stability and the differences between their T_m under the different conditions testes is not significant (Figure 3C).

3.4.2. Immunogenicity Analysis:

The NetMHCIIpan-4.0 algorithm was used to predict epitopes presented by HLA-II molecules within the antibody sequences. Four “strong” binder spots were found in the VL-domain (VL **4**). Two of them **FTFTISSLQ** and **YTFGQGTKL** are fully human (i.e., present in the human germline) and conserved among known isolates of human antibodies. These sequences represent a minimal risk for immunogenicity.

For humanized antibody Limab7 VH domain (VH **E**), only two hot spots are reported of which one is common to the closest human germline and should not be relevant (**FKGRVTITA; YMELSSLRS**). The remaining hot spot (**FKGRVTITA**) partially overlaps with contact residues of CDR-H2 in the broad sense of the definition. This spot is reported in only 3 out of the 17 alleles tested, including DRB1-080.

The remaining hot peptides (**YYCQHNHGS** and **LLIYGASIL**) whose sequences do not occur within the human germline are derived from or partially overlap with CDR-L2 and CDR-L3. They may be the only ones that embody some potential for immunogenicity. However, each of them occurs within one of the alleles tested: DRB1-0301 for **YYCQHNHGS** and DRB1-1501 for **LLIYGASIL**, thus in a low frequency.

3.4.3. Functional Characterization of Fab E4

Next, aiming to further evaluate the binding functionality of the selected molecules, a series of different ELISA assays were carried out. First, Fab E4 binding to different *Loxosceles* venoms was evaluated in an indirect ELISA. Both fragments retain the ability to exclusively bind *Loxosceles intermedia,* just like LimAb7, the parental molecule (data not shown). Moreover, these fragments were assessed in their ability to compete with LimAb7 for the binding of RecDT1, their target. An excess of 700 times more Fab E4 was used in relation to LimAb7, and fragment amounts were serially decreased until a ratio of 0.07 fragment molecules to 1 LimAb7 molecule was reached. Competition providing total LimAb7 inhibition was achieved for the ratio of 700:1, however, in a ratio of 0.7:1, LimAb7 exhibits higher binding ability, inhibiting around 80% of Fab E4 binding to RecDT1 (Figure 4A). Percent inhibition was calculated by considering LimAb7 reactivity when no Fabs were present as 100% reactivity/no inhibition. Lastly, to initially investigate whether Fab E4 retained the same binding site as the parental molecule, a sandwich ELISA was done. LimAb7 was used as the capture antibody for RecDT1. Subsequently, Fab E4 and A1 (chimeric LimAb7 Fab) was added in a series of different concentrations and their binding to captured DT1 was evaluated. Both assayed antibodies show no significant binding to captured RecDT1 and in terms of positive and negative controls, suggesting their RecDT1 binding site had already been occupied by LimAb7, given it’s probably preserved (Figure 4B). Percent inhibition of Fab binding to captured LiRecDT1 was calculated by considering the positive control’s reactivity as 100% reactivity/no inhibition.

4. Discussion

The employment of antibodies in the clinic has been revolutionary for the diagnosis and treatment of numerous pathologies. In the scope of their development, many efforts focused on the production of human and humanized antibody molecules have been made, aiming to reduce their immunogenicity, thus offering a bigger guarantee on their safety for human therapeutic administration. Considering the real viability of recombinant serotherapy [25], stablishing a pathway for the conception of humanized monoclonal antibody molecules, eligible for batch production, poses an interesting alternative.

The monoclonal antibody LimAb7 was one of the pioneers in the production of molecules for the treatment and study of Loxoscelism [11] and considering its promise we humanized this molecule. The Fab format was initially pondered for the construction of novel LimAb7 derived humanized molecules, mainly due to its bigger size (around 54 kDa) that is shown to increase stability in some cases [26, 27] and its wide and traditional clinical use [28]. In the present study, designing 16 Fab variants allowed for a thorough screening of these molecules once they were produced and thus augmented the chances of producing a lead molecule fit for large-scale production and *in vivo/in vitro* validation studies following the same criteria considered in the production of therapeutic antibody ACT17 [8].

During the study, production, and characterization of the candidates, different parameters were carefully considered. Regarding the influence of different VH and VL sequences on the production yield, we concluded that both domains seem important, more evident in VHs **B** and **F** and VLs **2** and **8** that are present on highest yield products. Interestingly, all molecules made up from the VH **C**, independently from their VL, show significantly lower production yield. The participation of the heavy domain regions (VH) has been previously described as key and even main determinant in the production of humanized recombinant antibodies specially in terms of antigen binding properties [29, 30, 31]. Given VH **B** sequences were closest in identity to the parental VH and the VH C being the most dissimilar or mutated in relation to VH **A**, the results observed corroborate the literature [32].

SDS-PAGE under non-reducing conditions of the Fab constructs show bands of unexpected masses for all Fabs made up from VH **C** (Supplementary Figure 1). On top of that, these 4 Fabs also presented low production yield as aforementioned, poor thermal stability and low target reactivity. VH **C** possesses the best humanization score amongst all 4 VHs and the biggest sequence dissimilarity from the parental mouse VH. The excessive sequence modification and/or the point mutation of key structural residues (especially on FR3) on this VH may have altogether accounted for the design of an afunctional VH or even a highly unstable domain uncapable of accurately dimerizing with the VL after its secretion thus hampering the production of functional Fabs [33]. Moreover, *in silico* sequence and structure analysis of VH **C** in terms of LimAb7 VH and humanized Fab E4, show some non-conservative point amino acid mutations, and different charge and 3D orientation of amino acid side-chains, which could've compromised molecule stability and folding [34, 35] This suggests that the humanization score, even if relevant for predicting molecule immunogenicity [36], is not a definitive

parameter for antibody functionality, and should be considered alongside other parameters [37].

At the time of co-transfection for Fab expression, ratios between VH and VL vectors must be carefully established for the generation of functional Fab molecules, given that the VL is naturally more produced [38]. Due to the possible single chain excess observed in our SDS-PAGE results, FvH/FvL ratios should be studied further, aiming at a more balanced expression [39]. This could probably explain the presence of additional bands for some Fabs in nonreducing SDS-PAGE, possibly indicating and production excess of either one of the chains, which would have been only possible to distinguish in doing and immunoblot revealed by anti-Fd and anti-VL antibodies, as in the study of Lebozec et al. [8]. Nonetheless, the applied VH/VL ration in the present study was able to generate viable and functional Fabs.

Thermal stability is also an important criterion, rigorously considered in the immunotherapy industry, given molecule storage, sterilization, and downstream procedures [40, 41]. This was also taken into account in the present study, where we observed a noteworthy improvement in the melting temperature (T_m °C) (+-20°C) of all Fab constructs (except for VH **C**, whose T_m is no higher than 48°C) in comparison to the humanized fragments published by Karim-Silva et al., 2020 [14], which might be partly related to the higher Fab fragment size as compared to scFvs and diabodies, as well as changing the expression system from prokaryotic to eukaryotic cells [26, 42].

Molecule structural integrity, purity and stability can directly affect its safety and efficacy. These parameters can be evaluated by Size-Exclusion Chromatography (SEC-HPLC) [43]. Our SEC-HPLC data shows the presence of dimers and/or possible aggregates in molecules with the VL **8**. Despite having the best antigen reactivities and production yields – especially for VHs **B** and **F** (Fabs B8 and F8), VL **8** presents some exclusive point mutations in relation to the mice VL sequence and other humanized VLs, especially at the FR3 region. This region has been previously described as paramount in the antigen/antibody complex interaction, through stabilizing the antibody structure, as well as for *Streptococci* protein L binding, even though its binding site is located on VL FR1. [31]. This amino acid substitutions might have favoured its binding to the latter, thus justifying the high antigen reactivity observed for VL **8** in ELISA, given the assay is revealed by peroxidase conjugated Protein L. Nonetheless, the mismatches with the murine sequence may have accounted for its loss of structural stability [44] as observed for **VL 8**, where the formation of aggregates and or/ dimers and lowest T_m values were obtained, thus disqualifying this VL candidate.

Construct's reactivity to their expected target, LiRecDT1, was confirmed through an indirect ELISA assay. Amongst all tested fragments, we noticed constructs made up from the VH E showed promising results. These constructs also indicated great structural stability and balanced humanization/Z scores. VH **E** possesses some residue mismatches in the FR2 regions to the parental sequence and the other humanized VHs, however it did not present any functional impairments and poor physio-chemical parameters whatsoever. All in all, VH **E** seems to have maintained functionality and stability in relation to the parental molecule and a

better reactivity in antigen-binding assays. Amongst all 4 humanized VLs, **VL 5** was cast-off because it was not as well produced as other VLs. Hence, **VL 4** was considered most promising variable light chain sequence and was selected. Considering this, variant **E4** was chosen as a lead for further characterization. This decision was based on various biochemical and physio-chemical criteria and the fact that E4 presented the most balanced score amongst all these considered parameters.

Intending to characterize Fab E4 more in depth, immunogenicity MHC II studies were carried out. The regional analysis of the E4 light and heavy chain V-sequences identified a very limited number of epitope clusters of which several are shared with the most closely related human germline. Non-germline amino acid sequences mainly found in the CDRs are usually considered to be the main driver of immunogenicity, provided they can be presented by HLA class II molecules. [45]. Considering this *in silico* predictive analysis, we did not identify any sequence homolog to epitopes from *Mus musculus* (mouse).

Subsequently, our analysis of E4 stability when diluted in glycine buffer with different acidic pHs, shows that both the chimeric and humanized Fabs have a good and similar maintenance of their T_m under acidic pH. However, a steep loss of stability is observed under a pH of 2.0, which should be considered, given therapeutic antibody molecules should ideally be tolerant to pH variations, specially aiming their increased bioavailability, and viral inactivation during pharmaceutical development at low pH [46, 47, 48].

Moreover, different format ELISAs were carried out to investigate whether humanization had affected their binding pattern. First, the molecules were assessed as to their ability to bind other *Loxosceles* species venoms apart from *L. intermedia* venom (data not shown). Humanized Fab molecules have shown to retain an exclusive binding reactivity towards *L. intermedia* venom's PLDs, identical to the parental molecule, LimAb7 and additional recombinant constructs [11, 13, 14]. The antibody's functionality in terms of paratope was preserved, as shown in the sandwich ELISA in which no signal is detected when humanized Fabs are incubated, given the antibody molecule used to capture their target shares their CDR sequences, thus binding epitope. The contrary has been observed when anti-*Loxosceles* polyclonal antibodies are employed in the same sandwich ELISA format [11, 13]. Additionally, Fab E4 was allowed to compete with the parental molecule LimAb7, for RecDT1 in various concentrations. Total inhibition of LimAb7 binding to the target was achieved by E4 and control Fab A1, however only in the presence of Fab excess. The competition between humanized Fab E4 and LimAb7 was reduced in a dose-dependent fashion, thus indicating the parental molecule retains higher binding than its derived recombinant humanized constructs, corroborating the literature [49, 50, 51].

In the context of envenomation therapy, heterologous polyclonal antibodies are traditionally employed, however, some groups have been entertaining the use of recombinant antibodies given their great biotechnological potential [25, 52]. All things considered, the screening of humanized antibodies based on *in silico* analysis and biochemical/physio-chemical parameters could provide considerable guidance towards the development of optimal molecules. However, knowing which

predictions are paramount for the conception of humanized lead molecules and its large-scale production remains an important object of study considering that *in silico* analysis should always be supported by *in vitro* data.

5. Conflict of Interest

The authors declare that the research was conducted in the absence of any commercial or financial relationships that could be considered as a potential conflict of interest.

6. Acknowledgements

LMA, NA and PB contributed to the outline and design of the study. IGJ performed the functional analysis with the help of MB and training from FB and Catherine Horiot. JCM gently provided the *Loxosceles* venoms and anti-loxoscelic horse sera (SALOX). LHG and SSV provided the recombinant toxin, LiRecDT1. LMA, IGJ and PB wrote the first version of the manuscript. All authors read and approved the submitted version.

7. Funding

This study was supported by Conselho Nacional de Desenvolvimento Científico e Tecnológico, CNPq, Brazil (No.401355/2014-4, No. 472460/2013-7, No. 308314/2020-4), Fundação Araucária No. 04/2013, Coordenação de Aperfeiçoamento de Pessoal de Nível Superior – Brasil (CAPES) – Finance Code 001, and the french higher education and research ministry under the program “Investissements d’avenir” (LabEx MabImprove ANR- 10-LABX-53–01). CAPES also granted IGJ with a special visiting researcher fellowship under the Brazilian Scientific Mobility Program CAPES-PRINT.

8. References

[1] P.V. Pham, Chapter 19 – Medical Biotechnology: Techniques and Applications, in: D. Barh, V. Azevedo (Eds.), Omics Technologies and Bio Engineering, Academic Press, 2018: pp. 449–469. https://doi.org/10.1016/B978-0-12-804659-3.00019-1.

[2] Center For Drug Evaluation And Research (U.S.). (2021). Drugs@FDA. Washington D.C: U.S. Food and Drug Administration, Center for Drug and Evaluation Research.

[3] S. Singh, N.K. Tank, P. Dwiwedi, J. Charan, R. Kaur, P. Sidhu, V.K. Chugh, Monoclonal Antibodies: A Review, Current Clinical Pharmacology. 13 (n.d.) 85–99. https://www.eurekaselect.net/article/85198 (accessed December 30, 2021).

[4] R.-M. Lu, Y.-C. Hwang, I.-J. Liu, C.-C. Lee, H.-Z. Tsai, H.-J. Li, H.-C. Wu, Development of therapeutic antibodies for the treatment of diseases,

Journal of Biomedical Science. 27 (2020) 1. https://doi.org/10.1186/s12929-019-0592-z.
[5] J. Li, Z. Zhu, Research and development of next generation of antibody-based therapeutics, Acta Pharmacol Sin. 31 (2010) 1198–1207. https://doi.org/10.1038/aps.2010.120
[6] S.H. Tam, S.G. McCarthy, A.A. Armstrong, S. Somani, S.-J. Wu, X. Liu, A. Gervais, R. Ernst, D. Saro, R. Decker, J. Luo, G.L. Gilliland, M.L. Chiu, B.J. Scallon, Functional, Biophysical, and Structural Characterization of Human IgG1 and IgG4 Fc Variants with Ablated Immune Functionality, Antibodies. 6 (2017) 12. https://doi.org/10.3390/antib6030012.
[7] G. Rodrigo, M. Gruvegård, J.M. Van Alstine, Antibody Fragments and Their Purification by Protein L Affinity Chromatography, Antibodies. 4 (2015) 259–277. https://doi.org/10.3390/antib4030259.
[8] K. Lebozec, M. Jandrot-Perrus, G. Avenard, O. Favre-Bulle, P. Billiald, Design, development and characterization of ACT017, a humanized Fab that blocks platelet's glycoprotein VI function without causing bleeding risks, Mabs. 9 (2017) 945–958. https://doi.org/10.1080/19420862.2017.1336592.
[9] N. Aubrey, P. Billiald, Antibody Fragments Humanization: Beginning with the End in Mind., Methods in Molecular Biology. (2019). https://doi.org/10.1007/978-1-4939-8958-4_10.
[10] T. Jain, T. Sun, S. Durand, A. Hall, N.R. Houston, J.H. Nett, B. Sharkey, B. Bobrowicz, I. Caffry, Y. Yu, Y. Cao, H. Lynaugh, M. Brown, H. Baruah, L.T. Gray, E.M. Krauland, Y. Xu, M. Vásquez, K.D. Wittrup, Biophysical properties of the clinical-stage antibody landscape, PNAS. 114 (2017) 944–949. https://doi.org/10.1073/pnas.1616408114
[11] L.M. Alvarenga, M.S. Martins, J.F. Moura, E. Kalapothakis, J.C. Oliveira, O.C. Mangili, C. Granier, C. Chávez-Olórtegui, Production of monoclonal antibodies capable of neutralizing dermonecrotic activity of Loxosceles intermedia spider venom and their use in a specific immunometric assay, Toxicon. 42 (2003) 725–731. https://doi.org/10.1016/j.toxicon.2003.09.006.
[12] S. Karim-Silva, J. de Moura, M. Noiray, J.C. Minozzo, N. Aubrey, L.M. Alvarenga, P. Billiald, Generation of recombinant antibody fragments with toxin-neutralizing potential in loxoscelism, Immunology Letters. 176 (2016) 90–96. https://doi.org/10.1016/j.imlet.2016.05.019
[13] I. Jiacomini, S.K. Silva, N. Aubrey, J. Muzard, C. Chavez-Olortegui, J. De Moura, P. Billiald, L.M. Alvarenga, Immunodetection of the "brown" spider (Loxosceles intermedia) dermonecrotoxin with an scFv-alkaline phosphatase fusion protein, Immunology Letters. 173 (2016) 1–6. https://doi.org/10.1016/j.imlet.2016.03.001
[14] S. Karim-Silva, A. Becker-Finco, I.G. Jiacomini, F. Boursin, A. Leroy, M. Noiray, J. de Moura, N. Aubrey, P. Billiald, L.M. Alvarenga, Loxoscelism: Advances and Challenges in the Design of Antibody Fragments with Therapeutic Potential, Toxins. 12 (2020) 256. https://doi.org/10.3390/toxins12040256.

[15] Y. Safdari, S. Farajnia, M. Asgharzadeh, M. Khalili, Antibody humanization methods – a review and update, Biotechnol Genet Eng Rev. 29 (2013) 175–186. https://doi.org/10.1080/02648725.2013.801235
[16] Z. Lakhrif, M. Pugnière, C. Henriquet, A. di Tommaso, I. Dimier-Poisson, P. Billiald, M.O. Juste, N. Aubrey, A method to confer Protein L binding ability to any antibody fragment, Mabs. 8 (2015) 379–388. https://doi.org/10.1080/19420862.2015.1116657
[17] F. Sievers, A. Wilm, D. Dineen, T.J. Gibson, K. Karplus, W. Li, R. Lopez, H. McWilliam, M. Remmert, J. Söding, J.D. Thompson, D.G. Higgins, Fast, scalable generation of high-quality protein multiple sequence alignments using Clustal Omega, Mol Syst Biol. 7 (2011) 539. https://doi.org/10.1038/msb.2011.75.
[18] G. Urlaub, L.A. Chasin, Isolation of Chinese hamster cell mutants deficient in dihydrofolate reductase activity, Proc Natl Acad Sci U S A. 77 (1980) 4216–4220. https://doi.org/10.1073/pnas.77.7.4216.
[19] T. Menzen, W. Friess, High-Throughput Melting-Temperature Analysis of a Monoclonal Antibody by Differential Scanning Fluorimetry in the Presence of Surfactants, Journal of Pharmaceutical Sciences. 102 (2013) 415–428. https://doi.org/10.1002/jps.23405.
[20] F. Corpet, J. Gouzy, D. Kahn, Browsing protein families via the “Rich Family Description” format, Bioinformatics. 15 (1999) 1020–1027. https://doi.org/10.1093/bioinformatics/15.12.1020.
[21] B. Webb, A. Sali. Comparative Protein Structure Modeling Using Modeller. Current Protocols in Bioinformatics 54, John Wiley & Sons, Inc., 5.6.1-5.6.37, 2016. https://doi.org/10.1002/cpbi.3
[22] Madden T. The BLAST Sequence Analysis Tool. 2002 Oct 9 [Updated 2003 Aug 13]. In: McEntyre J, Ostell J, editors. The NCBI Handbook [Internet]. Bethesda (MD): National Center for Biotechnology Information (US); 2002-. Chapter 16. Available from: http://www.ncbi.nlm.nih.gov/books/NBK21097/
[23] B. Reynisson, B. Alvarez, S. Paul, B. Peters, M. Nielsen, NetMHCpan-4.1 and NetMHCIIpan-4.0: improved predictions of MHC antigen presentation by concurrent motif deconvolution and integration of MS MHC eluted ligand data, Nucleic Acids Res. 48 (2020) W449–W454. https://doi.org/10.1093/nar/gkaa379.
[24] A. Sanchez-Mazas, J.M. Nunes, D. Middleton, J. Sauter, S. Buhler, A. McCabe, J. Hofmann, D.M. Baier, A.H. Schmidt, G. Nicoloso, M. Andreani, Z. Grubic, J.-M. Tiercy, K. Fleischhauer, Common and well-documented HLA alleles over all of Europe and within European sub-regions: A catalogue from the European Federation for Immunogenetics, HLA. 89 (2017) 104–113. https://doi.org/10.1111/tan.12956.
[25] T.P. Jenkins, A.H. Laustsen, Cost of Manufacturing for Recombinant Snakebite Antivenoms, Frontiers in Bioengineering and Biotechnology. 8 (2020). https://www.frontiersin.org/article/10.3389/fbioe.2020.00703 (accessed March 21, 2022).

[26] V. Quintero-Hernández, V.R. Juárez-González, M. Ortíz-León, R. Sánchez, L.D. Possani, B. Becerril, The change of the scFv into the Fab format improves the stability and in vivo toxin neutralization capacity of recombinant antibodies, Molecular Immunology. 44 (2007) 1307–1315. https://doi.org/10.1016/j.molimm.2006.05.009
[27] H. Ma, C. Ó'Fágáin, R. O'Kennedy, Unravelling enhancement of antibody fragment stability – Role of format structure and cysteine modification, J Immunol Methods. 464 (2019) 57–63. https://doi.org/10.1016/j.jim.2018.10.012.
[28] R. Kunert, D. Reinhart, Advances in recombinant antibody manufacturing, Appl Microbiol Biotechnol. 100 (2016) 3451–3461. https://doi.org/10.1007/s00253-016-7388-9
[29] K.T. Xenaki, S. Oliveira, P.M.P. van Bergen en Henegouwen, Antibody or Antibody Fragments: Implications for Molecular Imaging and Targeted Therapy of Solid Tumors, Frontiers in Immunology. 8 (2017) 1287. https://doi.org/10.3389/fimmu.2017.01287
[30] K. Masuda, K. Sakamoto, M. Kojima, T. Aburatani, T. Ueda, H. Ueda, The role of interface framework residues in determining antibody VH/VL interaction strength and antigen-binding affinity, The FEBS Journal. 273 (2006) 2184–2194. https://doi.org/10.1111/j.1742-4658.2006.05232.x
[31] C.T.-T. Su, W.-L. Ling, W.-H. Lua, J.-J. Poh, S.K.-E. Gan, The role of Antibody Vκ Framework 3 region towards Antigen binding: Effects on recombinant production and Protein L binding, Sci Rep. 7 (2017) 3766. https://doi.org/10.1038/s41598-017-02756-3
[32] M.L. Fernández-Quintero, K.B. Kroell, F. Hofer, J.R. Riccabona, K.R. Liedl, Mutation of Framework Residue H71 Results in Different Antibody Paratope States in Solution, Front Immunol. 12 (2021) 630034. https://doi.org/10.3389/fimmu.2021.630034.
[33] T. Cnudde, Z. Lakhrif, J. Bourgoin, F. Boursin, C. Horiot, C. Henriquet, A. di Tommaso, M.O. Juste, I.G. Jiacomini, I. Dimier-Poisson, M. Pugnière, M.-N. Mévélec, N. Aubrey, Exploration and Modulation of Antibody Fragment Biophysical Properties by Replacing the Framework Region Sequences, Antibodies. 9 (2020) 9. https://doi.org/10.3390/antib9020009.
[34] K. Winkler, A. Kramer, G. Küttner, M. Seifert, C. Scholz, H. Wessner, J. Schneider-Mergener, W. Höhne, Changing the antigen binding specificity by single point mutations of an anti-p24 (HIV-1) antibody, J Immunol. 165 (2000) 4505–4514. https://doi.org/10.4049/jimmunol.165.8.4505
[35] Y. Myung, D.E.V. Pires, D.B. Ascher, mmCSM-AB: guiding rational antibody engineering through multiple point mutations, Nucleic Acids Research. 48 (2020) W125–W131. https://doi.org/10.1093/nar/gkaa389.
[36] S.H. Gao, K. Huang, H. Tu, A.S. Adler, Monoclonal antibody humanness score and its applications, BMC Biotechnol. 13 (2013) 55. https://doi.org/10.1186/1472-6750-13-55.
[37] P. Chames, M. Van Regenmortel, E. Weiss, D. Baty, Therapeutic antibodies: successes, limitations and hopes for the future, Br J Pharmacol. 157 (2009) 220–233. https://doi.org/10.1111/j.1476-5381.2009.00190.x.

[38] P. Bhoskar, B. Belongia, R. Smith, S. Yoon, T. Carter, J. Xu, Free light chain content in culture media reflects recombinant monoclonal antibody productivity and quality, Biotechnol Prog. 29 (2013) 1131–1139. https://doi.org/10.1002/btpr.1767.
[39] S. Schlatter, S.H. Stansfield, D.M. Dinnis, A.J. Racher, J.R. Birch, D.C. James, On the optimal ratio of heavy to light chain genes for efficient recombinant antibody production by CHO cells, Biotechnol Prog. 21 (2005) 122–133. https://doi.org/10.1021/bp049780w
[40] A.D. McConnell, X. Zhang, J.L. Macomber, B. Chau, J.C. Sheffer, S. Rahmanian, E. Hare, V. Spasojevic, R.A. Horlick, D.J. King, P.M. Bowers, A general approach to antibody thermostabilization, Mabs. 6 (2014) 1274–1282. https://doi.org/10.4161/mabs.29680.
[41] H. Ma, C. Ó'Fágáin, R. O'Kennedy, Antibody stability: A key to performance – Analysis, influences and improvement, Biochimie. 177 (2020) 213–225. https://doi.org/10.1016/j.biochi.2020.08.019.
[42] A. Frenzel, M. Hust, T. Schirrmann, Expression of Recombinant Antibodies, Frontiers in Immunology. 4 (2013). https://www.frontiersin.org/article/10.3389/fimmu.2013.00217 (accessed March 21, 2022).
[43] H.E. Mohamed, A.A. Mohamed, M.A. Al-Ghobashy, F.A. Fathalla, S.S. Abbas, Stability assessment of antibody-drug conjugate Trastuzumab emtansine in comparison to parent monoclonal antibody using orthogonal testing protocol, Journal of Pharmaceutical and Biomedical Analysis. 150 (2018) 268–277. https://doi.org/10.1016/j.jpba.2017.12.022.
[44] F. Courtois, N.J. Agrawal, T.M. Lauer, B.L. Trout, Rational design of therapeutic mAbs against aggregation through protein engineering and incorporation of glycosylation motifs applied to bevacizumab, Mabs. 8 (2016) 99–112. https://doi.org/10.1080/19420862.2015.1112477.
[45] F.A. Harding, M.M. Stickler, J. Razo, R.B. DuBridge, The immunogenicity of humanized and fully human antibodies: residual immunogenicity resides in the CDR regions, Mabs. 2 (2010) 256–265. https://doi.org/10.4161/mabs.2.3.11641.
[46] T. Igawa, F. Mimoto, K. Hattori, pH-dependent antigen-binding antibodies as a novel therapeutic modality, Biochimica et Biophysica Acta (BBA) – Proteins and Proteomics. 1844 (2014) 1943–1950. https://doi.org/10.1016/j.bbapap.2014.08.003.
[47] M. Hebditch, R. Kean, J. Warwicker, Modelling of pH-dependence to develop a strategy for 81abelling8181 mAbs at acidic steps in production, Computational and Structural Biotechnology Journal. 18 (2020) 897–905. https://doi.org/10.1016/j.csbj.2020.03.002.
[48] R. Wälchli, M. Ressurreição, S. Vogg, F. Feidl, J. Angelo, X. Xu, S. Ghose, Z. Jian Li, X. Le Saoût, J. Souquet, H. Broly, M. Morbidelli, Understanding mAb aggregation during low pH viral inactivation and subsequent neutralization, Biotechnol Bioeng. 117 (2020) 687–700. https://doi.org/10.1002/bit.27237.

[49] T. Nakanishi, K. Tsumoto, A. Yokota, H. Kondo, I. Kumagai, Critical contribution of VH–VL interaction to reshaping of an antibody: The case of humanization of anti-lysozyme antibody, HyHEL-10, Protein Sci. 17 (2008) 261–270. https://doi.org/10.1110/ps.073156708.

[50] Y. Fernández-Marrero, L. Roque-Navarro, T. Hernández, D. Dorvignit, M. Molina-Pérez, A. González, K. Sosa, A. López-Requena, R. Pérez, C. Mateo de Acosta, A cytotoxic humanized anti-ganglioside antibody produced in a murine cell line defective of N-glycolylated-glycoconjugates, Immunobiology. 216 (2011) 1239–1247. https://doi.org/10.1016/j.imbio.2011.07.004.

[51] M.L. Fernández-Quintero, M.C. Heiss, K.R. Liedl, Antibody humanization—the Influence of the antibody framework on the CDR-H3 loop ensemble in solution, Protein Engineering, Design and Selection. 32 (2019) 411–422. https://doi.org/10.1093/protein/gzaa0

[52] A. Nazari, M. Samianifard, H. Rabie, A.Z. Mirakabadi, Recombinant antibodies against Iranian cobra venom as a new emerging therapy by phage display technology, J. Venom. Anim. Toxins Incl. Trop. Dis. 26 (2020). https://doi.org/10.1590/1678-9199-JVATITD-2019-0099.

FIGURES:

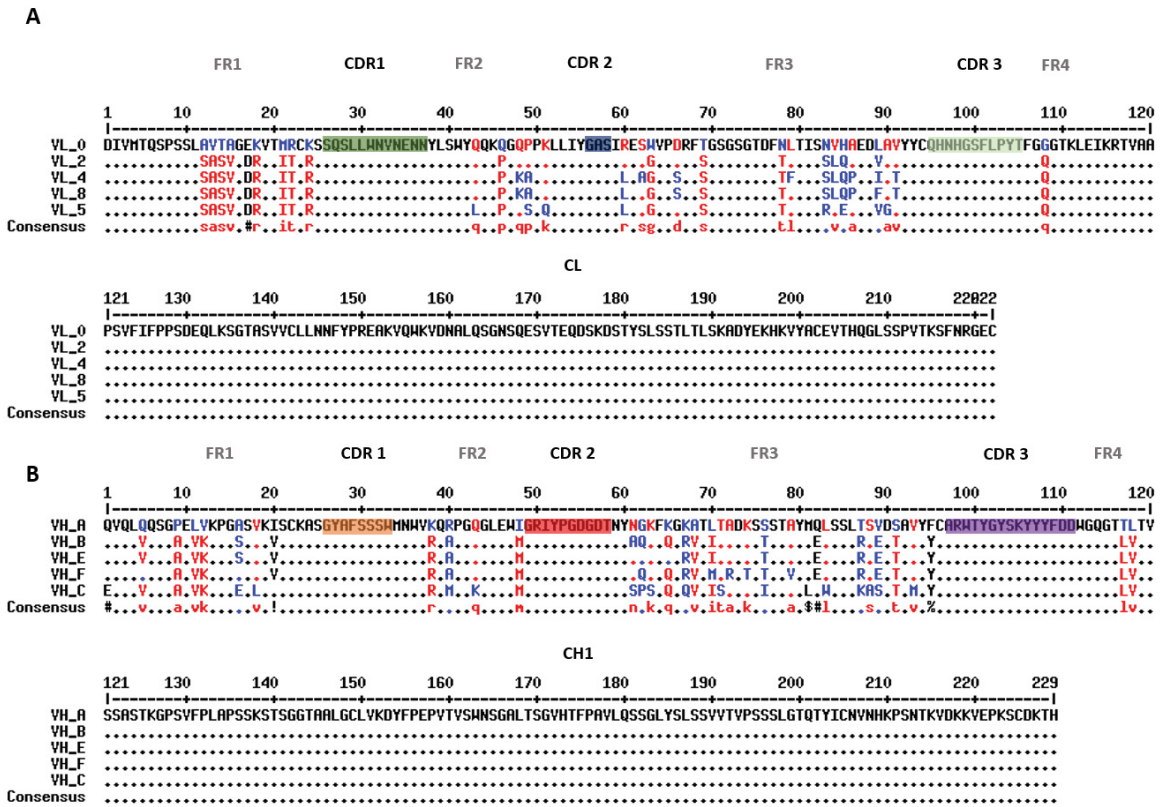

Figure 1. Design of humanized LimAb7 V-domains. A) Sequence alignment of the mouse LimAb7 IGHL (VL_0) with 4 humanized IGKappaV templates (VL_2, VL_4,

VL_8 and VL_5) and the framework regions of their most similar human germline genes. B) Sequence alignment of the mouse LimAb7 IGHV (VH_A) with 4 humanized IGHV templates (VH_B, VH_E, VH_F and VH_C) and the framework regions of their most similar human germline genes CDRs are highlighted according to the IMGT colouring scheme. Amino acid residues are coloured according to the conservation in mismatch AA functional groups (black – high consensus; red – low consensus; blue – neutral).

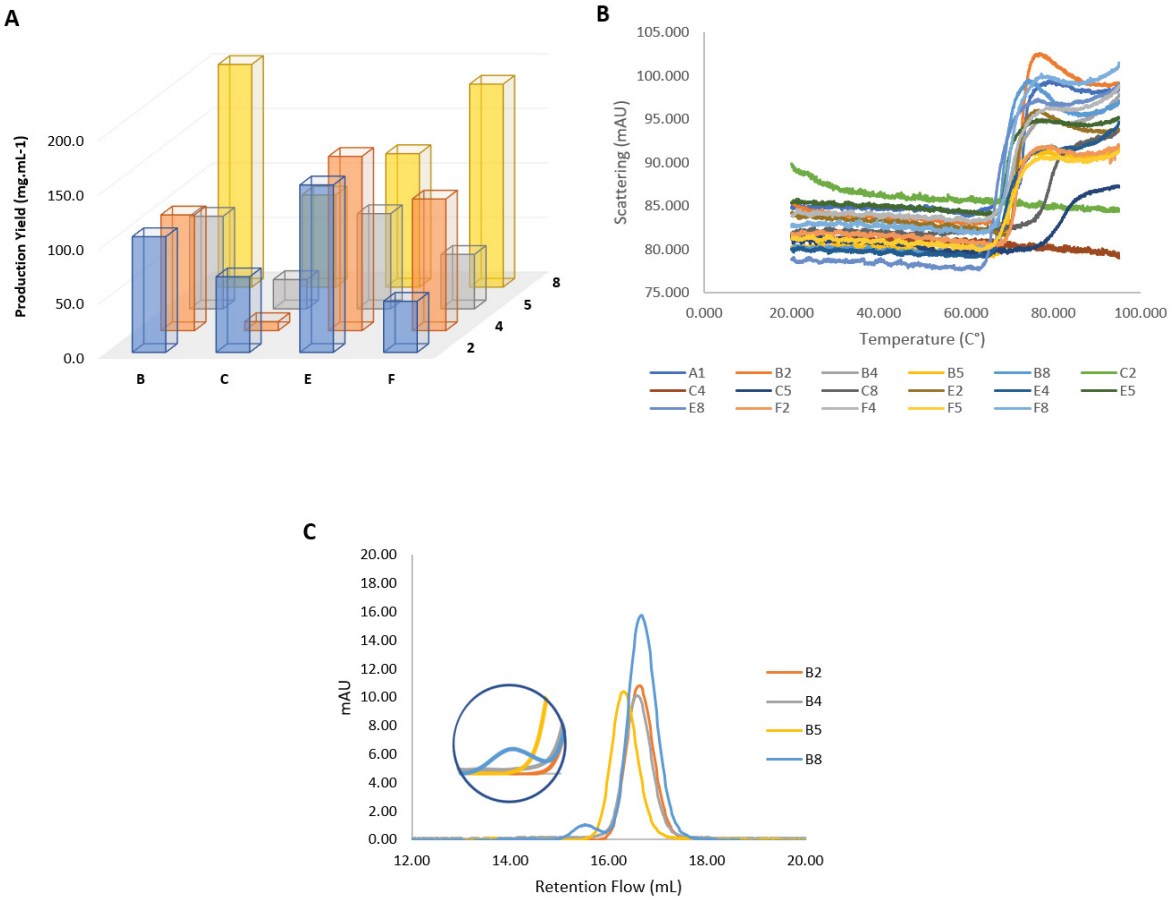

Figure 2. Physio-chemical Humanized Fab Screening Assays. A) Purification Yield – 3D depiction of the production yield of each one of the 16 constructs, produced in CHO cells and expressed in mg. L^{-1}. Units. B) Thermal-stability – Melting temperatures for all constructs were determined by nano differential scanning fluorimetry (nanoDSF) analysis, in which samples were loaded in standard nanoDSF capillaries and measured using the Prometheus NT.48 instrument. C) SEC-HPLC – Size Exclusion Chromatography/High Performance Liquid Chromatography – chromatograms for all the 16 constructs allow the evaluation of physio-chemical parameters such as the presence of dimers and/or aggregates in the purified fractions. Dimerization/aggregation peaks are zoomed in and represented on the circles on the left of chromatograms.

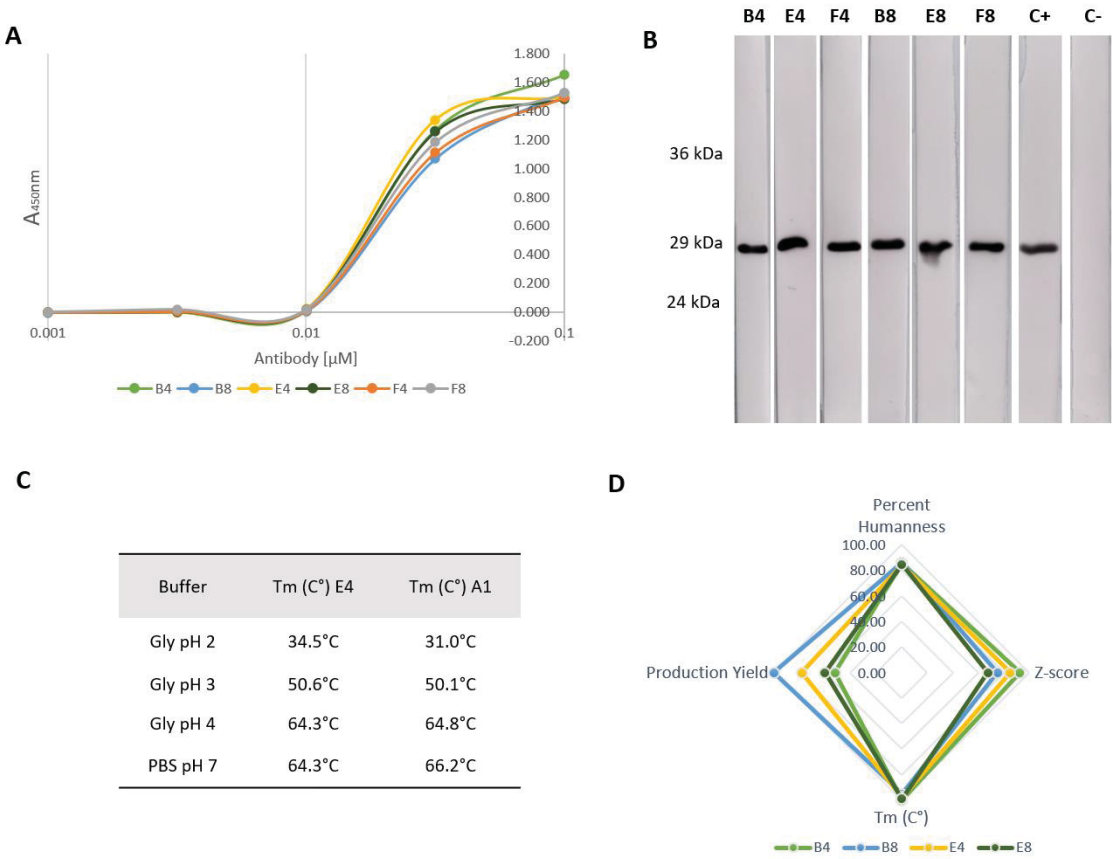

Buffer	Tm (C°) E4	Tm (C°) A1
Gly pH 2	34.5°C	31.0°C
Gly pH 3	50.6°C	50.1°C
Gly pH 4	64.3°C	64.8°C
PBS pH 7	64.3°C	66.2°C

Figure 3. Humanized Fab Immunochemical characterization assays. A) Indirect ELISA – Enzyme-Linked Immunoassay: produced constructs were assessed as to their ability to bind one of LimAb7's targets, LiRecDT1 (PDB: 3RLH). Fab preparations were incubated and immunocomplexes were revealed through the addition of Protein-L Peroxidase. B) Western Blot – *Loxosceles intermedia* whole venom immobilized on a nitrocellulose membrane and incubated with different Fabs. The maintenance of their reactivity's to the venom was compared to the parental murine IgG molecule LimAb7 (positive control) and an irrelevant mAb was used as the negative control. C) pH Stability Analysis – Fabs E4 and A1 were diluted in varying pH solutions and their thermal stability was measured with nanoDSF instrument. D) Comparison between best binding affinity Fabs according to different physio-chemical criteria – spider web representation of the score attained by each one of the four Fabs that had the most reactivity in the ELISA assays and maintained the same pattern of reactivity when compared to the parental molecule in western blot assays. Score ranges from 0 to 100, the latter being the maximum score. The closest the colored lines representing the different Fabs are to each tip of the pentagon, the highest their score in that criterion. The most balanced molecule is the one whose most edges are closest to the pentagon's borders.

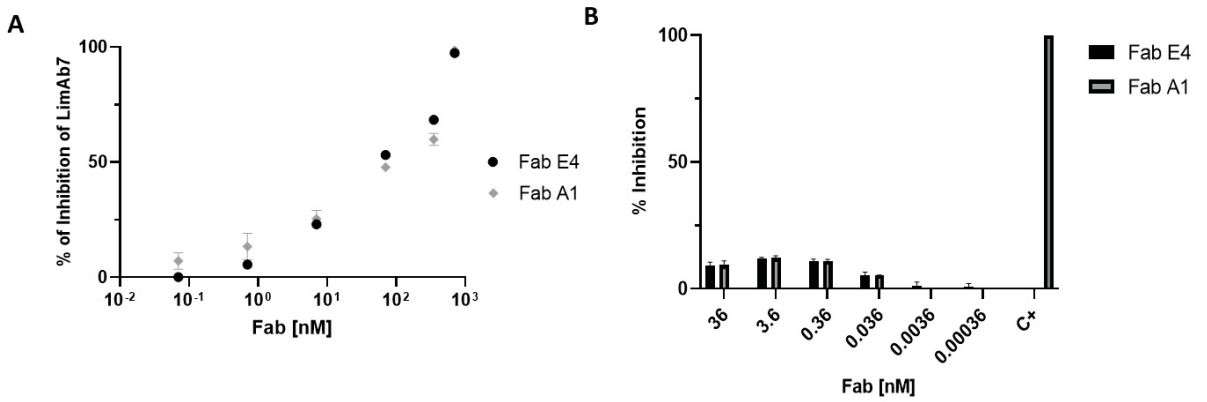

Figure 4. Functional Characterization of Fab E4. A) Competition ELISA between mAb7 and humanized LimAb7 variant: LiRecDT1 was immobilized on the plate and incubated with various dilutions of Fabs in a solution with a fixed amount of LimAb7. Data are plotted in percent inhibition of LimAb7 binding to the target, LiRecDT1, by humanized Fabs assayed. Inhibition was calculated considering the points with LimAb7 alone as a 100% of reactivity. B) Sandwich ELISA between mAb7 and humanized LimAb7 variants, Fab E4 and A1: LimAb7 was immobilized on the plate and incubated with RecDT1 and the Fabs were added in varying molarities. The assay's positive control consisted in anti-*Loxosceles* HRP horse pAb and the negative control, human pAb irrelevant antibodies. Data are plotted in percent inhibition of Fabs binding to the target, LiRecDT1.

Antibody V-domain	Template & Criteria	% Identity to Parental Sequence	Z-score	Packing Angle	Canonical Class	Closest human germline gene and % identity
VH 0	IGHV1-82*01 Mus musculus	100		A/0 – 42.8		
VH B (TH1)*	IGHV1-69*08 (a)	81.3	0.085	B/2 – -43.3 B/4 – -43.3 B/5 – -43.3 B/8 – -43.3	H1/H1-7-A H2/H2-6-A	IGHV1-69*08 88.8% - 98 overlap
VH C (TH2)*	HV551_HUMAN ©	75.4	0.173	C/2 – -45.5 C/4 – - 45.4 C/5 – -45.5 C/8 – -45.4	H1/H1-7-A H2/H2-6-A	IGHV5-51*01 90.8% - 98 overlap
VH E (TH4)*	Obinutuzumab (d)	83.6	0.060	E/2 – -45.4 E/4 – -45.5 E/5 – -45.4 E/8 – -45.4	H1/H1-7-A H2/H2-6-A	IGHV1-69*08 85.7% - 98 overlap
VH F (TH3)*	ACT_17* (e)	82.1	-0.074	F/2 – -45.4 F/4 – -45.4 F/5 – -45.4 F/8 – -45.4	H1/H1-7-A H2/H2-6-A	IGHV1-46*01 86.7% - 98 overlap
VL 0	IGHKV-8-28*01 Mus musculus	100				
VL 2 (TL1)*	IGKV4-1*01 (a)	84.3	0.408		L1/ L1- 16,17-A L2/ L2-7-A	IGKV4-1*01 78% - 100 overlap
VL 4 (TL4)*	REI (prost) <<(b)	77.39	-0.325		L1/ L1- 16,17-A L2/ L2-7-A	IGKV1-33*01 82.3% - 96 overlap
VL 8 (TL5)*	ACT_17* (e)	80	0,046		L1/ L1- 16,17-A L2/ L2-7-A	IGKV1-27*01 82.1% -95 overlap
VL 5 (TL6)*	Obinutuzumab (d)	79.1	-0.710		L1/ L1- 16,17-A L2/ L2-7-A	IGKV2-28*01 75% - 96 overlap

Table 1. Antibody Humanization. Main features of the LimAb7 V-domains and the humanized V-domains designed for the development of humanized Fabs. Humanization criteria: (a*) human germline most similar to LimAb7; (b*) fixed human framework sequences; (c*) high sequence identity; (d) framework templates from Obinutuzumab; e) framework template from Glenzocimab (Lebozec et al., 2017). Packing angle was predicted after pairing VL and VH humanized variants. Z-score: a value in the [-1.0; +1.0] is preferable and indicating of a high humanness degree. *: Following the protocols described by Aubrey & Billiald, 2019.

SUPPLEMENTARY MATERIALS:

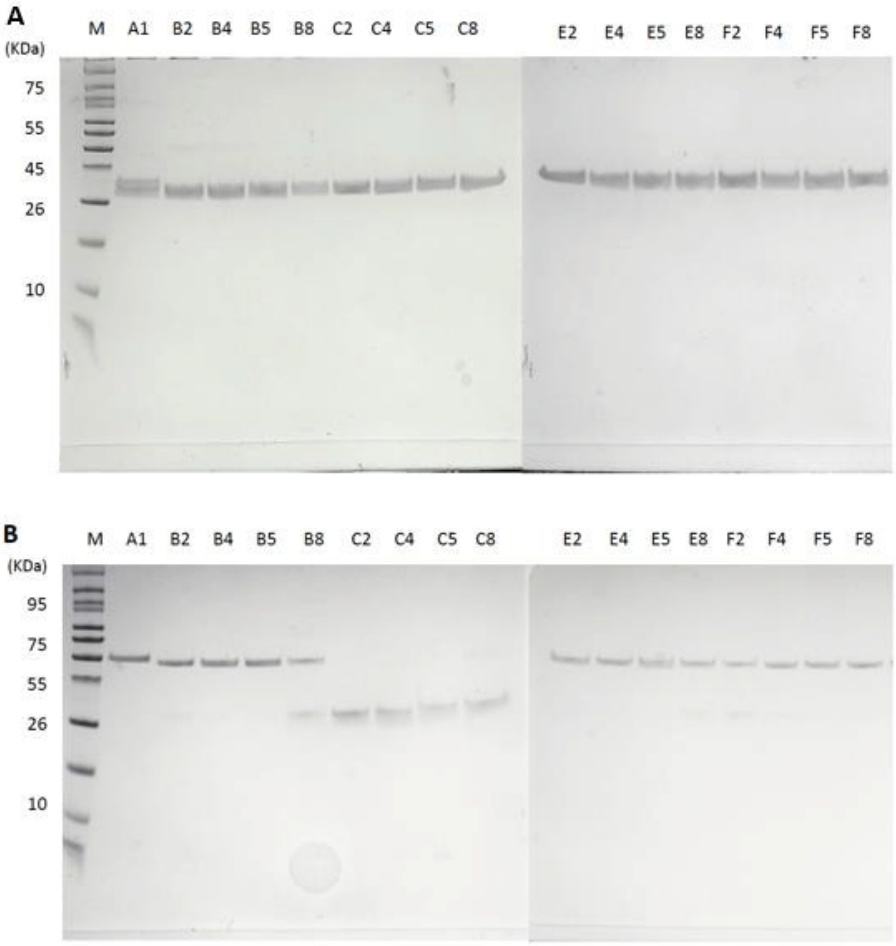

Supplementary Figure 1. SDS-PAGE of protein-L purified Fab fragments – purified humanized (B2-B8, C2-C8, E2-E8 and F2-F8) and chimeric (A1) Fabs were loaded onto a 10% and 12% polyacrylamide gel and resolved under reducing (A) and non-reducing (B) conditions, respectively. Protein bands were later evidenced through Coomassie Blue staining.

A

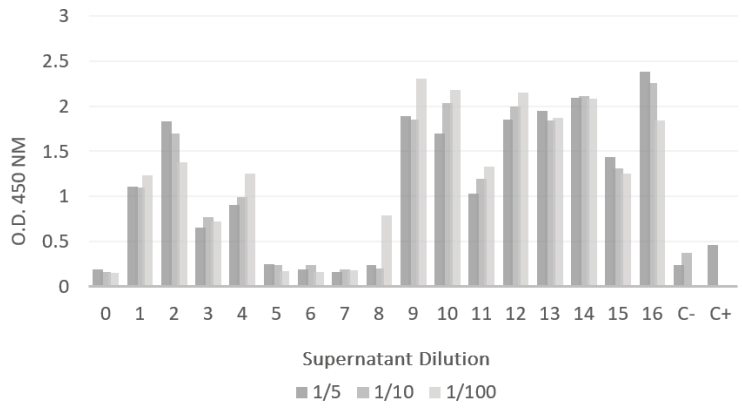

Nom	Variant
A1	0
B2	1
B4	2
B5	3
B8	4
C2	5
C4	6
C5	7
C8	8
E2	9
E4	10
E5	11
E8	12
F2	13
F4	14
F5	15
F8	16

Supplementary Figure 2. Evaluation of Fab construct culture supernatants prior to purification: Cell culture supernatants for each Fab construct were collected, spun and filtered, in order to remove cellular debris – A) ELISA – Enzyme-linked immunosorbent assay: an ELISA plate was coated with *L. intermedia* venom. Next, the plate was incubated with the supernatant of different transfected CHO-cells flasks (each corresponding to a different construct) diluted 1/5, 1/10 and 1/100. The binding of the constructs in the cell supernatants to the venom was detected by the addition of Protein L – HRP.

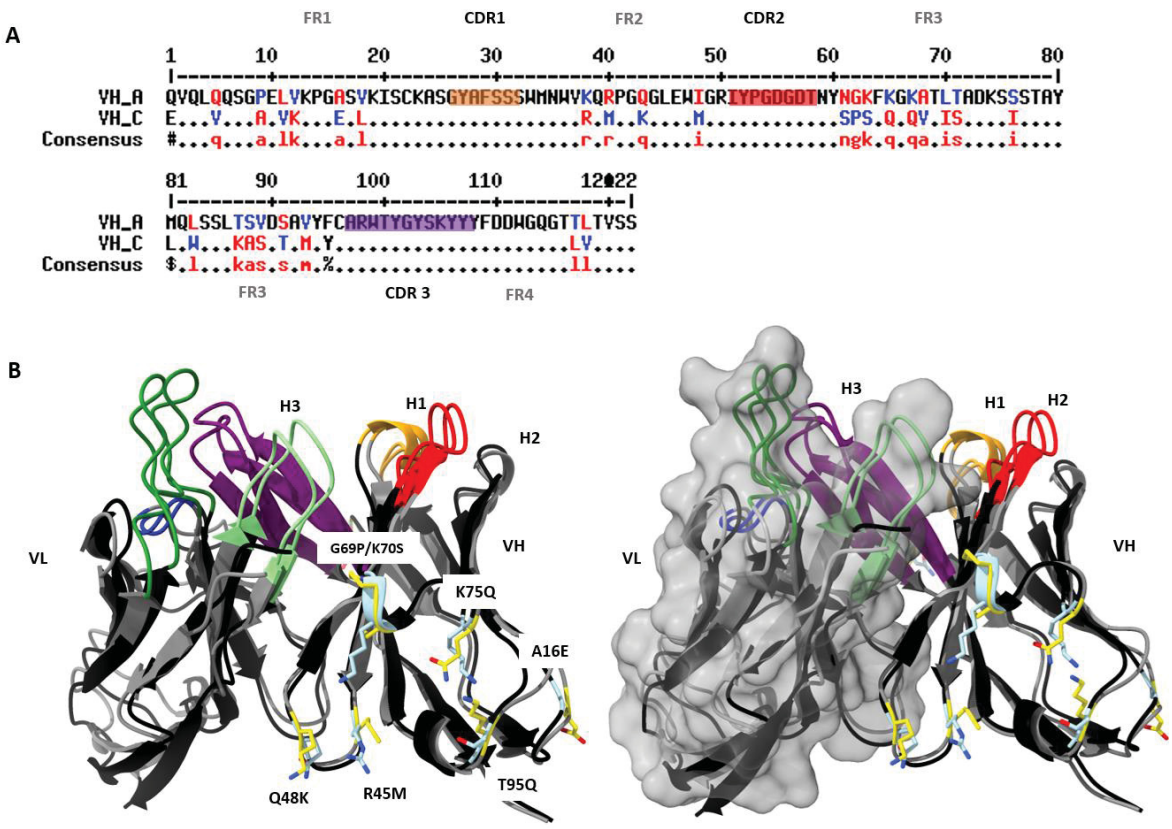

Supplementary Figure 3. Sequence And Structure Alignment Analysis of VH C. A) VH **C** and LimAb7 sequences were aligned using the Mutalin interface. CDRs are coloured according to the IMGT scheme. Mutations are coloured in (black – high consensus; red – low consensus; blue – neutral). Black dots represent amino acid conservation. B) Superimposed 3D structures of LimAb7 and VH **C**. Heavy and light chain CDRs are coloured according to the IMGT scheme and amino-acid mutations exclusive of VH **C** are highlighted in yellow (in VH **C**) and blue (in LimAb7) and amino acid side chains coloured in heteroatom scheme. Light chain surface representation is depicted on the right panel.

Name	Variant	Yield ($mg.L^{-1}$)
A1	0	92.3
C4	6	10.2
C5	7	33.4
F5	15	50.0
F2	13	54.5
C2	5	74.3
C8	8	87.6
B5	3	88.4
E5	11	90.9
B4	2	109.2
F4	14	122.8
E8	12	124.0
B2	1	150.7
E2	9	153.5
E4	10	159.8
F8	16	186.1
B8	4	205.2

Supplementary Table 1. Purification Yield – 3D depiction of the production yield of each one of the 16 constructs, produced in CHO cells and expressed in mg. L-1. Units. Absolute values for each construct are expressed in the table.

Name	Variant	T_m (C°)
A1	0	64.5
B2	1	68.9
C8	8	42.8
C5	7	45.6
C4	6	48.3
C2	5	48.7
F8	16	62
E8	12	62.9
B8	4	63.2
E5	11	63.3
E4	10	63.5
F5	15	63.6
F4	14	64.1
B4	2	65.2
B5	3	66.3
F2	13	66.5
E2	9	67.3

Supplementary Table 2. Thermal-stability – Melting temperatures for all constructs were determined by nano differential scanning fluorimetry (nanoDSF) analysis, in

which samples (10μM/construct) were loaded in standard nanoDSF capillaries and measured using the Prometheus NT.48 instrument. Absolute values for the T_m (°C) of each construct are expressed in the table.

5. SEGUNDO CAPÍTULO: ESTUDOS ESTRUTURAIS DE ANTICORPOS

5.1. Exploração e Modulação das Propriedades Biofísicas de Fragmentos de Anticorpos associados a regiões estruturais ou de *framework*.

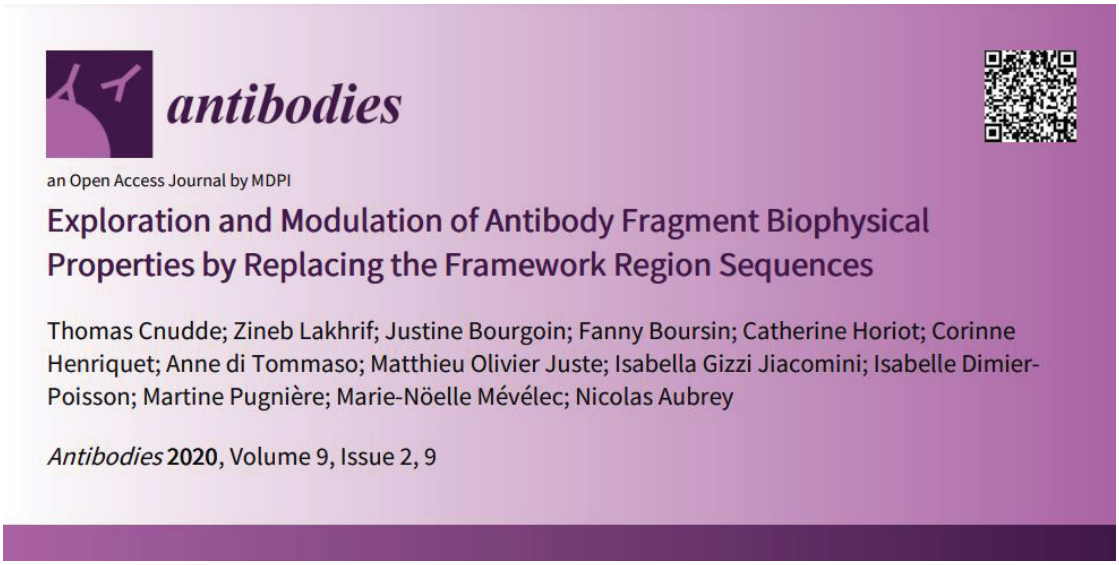

Exploration and Modulation of Antibody Fragment Biophysical Properties by Replacing the Framework Region Sequences

Abstract: In order to increase the successful development of recombinant antibodies and fragments, it seems fundamental to enhance their expression and/or biophysical properties, such as the thermal, chemical, and pH stabilities. In this study, we employed a method bases on replacing the antibody framework region sequences, in order to promote more particularly single-chain Fragment variable (scFv) product quality. We provide evidence that mutations of the VH- C-C^0 loop might significantly improve the prokaryote production of well-folded and functional fragments with a production yield multiplied by 27 times. Additional mutations are accountable for an increase in the thermal (+19.6 C) and chemical (+1.9 M) stabilities have also been identified. Furthermore, the hereby-produced fragments have shown to remain stable at a pH of 2.0, which avoids molecule functional and structural impairments during the purification process. Lastly, this study provides relevant information to the understanding of the relationship between the antibody's amino acid sequences and their respective biophysical properties.

Keywords: engineering; framework regions; Protein L (PpL); single-chain Fragment variable (scFv); stabilities; production

1. Introduction

Over recent years, various alternative antibody formats have been designed [**1**]. Converting these molecules into therapeutic drugs remains a challenge since therapeutic antibodies must satisfy several developability criteria [**2**,**3**]. Antigen recognition activity is carried by antibody fragments mainly represented by monovalent Fabs or single-chain variable fragments (scFv) [**4**]. A scFv is an artificial protein composed of heavy (VH) and light (VL) variable domains joined together via a flexible short peptide linker that might also contain a C-terminal flag peptide for affinity purification or 93abelling. On the other hand, the Fab format allows VH/VL interface stabilization and better preservation of the molecule's antigen-binding properties [**5**]. Regardless, heterogeneous biophysical properties have been reported and greatly vary from one molecule to another [**6**,**7**,**8**,**9**]. Up to date, predicting the qualities of a conventional antibody format, and even more so, of complex engineered antibody structures, remains an arduous task [**10**].

When re-engineering variable domains, affinity maturation and antibody humanization are carefully considered and worked on [**11**,**12**,**13**,**14**,**15**,**16**]. In some cases, mutations in the antibody complementarity determining regions (CDRs) have shown to improve molecule stability [**17**,**18**] thus being able to repair intrinsic flaws in the packing between two V-domains [**19**]. More precisely, additional work has been carried out on the structural role of framework regions (FRs). Several random mutation strategies have been undertaken to improve variable domains' stability [**20**,**21**] and/or the VH/VL interactions [**22**], stability, and activity [**23**,**24**]. Stability improvements and decrease in molecule aggregation were obtained by stabilizing the VH-βC″-βD loop using the VH-K64R substitution [**25**,**26**] or charged mutations [**27**,**28**,**29**,**30**]. These studies provide interesting findings; however, the suggested mutations remain localized and punctual. Few approaches have provided information on the role of the overall structure. Indeed, it is not yet fully understood how protein sequences translate into molecule biophysical properties [**31**].

In order to assess this, we developed a general methodology to replace the FR sequences, aiming to locate and identify amino acid (AA) residues or clusters responsible for the maintenance of different biophysical properties. This approach is comprised of the following steps: (i) identifying high sequence identity FRs for the VH and VL in order to limit the number of AA substitutions, (ii) grouping the different AA substitutions in clusters based on a structural three-dimensional model, and finally, (iii) producing and characterizing a set of fragments ranging from the more mutated to intermediate variants. The main advantage of this methodology is the use of natural sequences to generate mutations with predictable impact or not.

In the present study, a method allowing the replacing of the FR sequences was performed using the scFv format, given it is expected to be more sensitive to such changes when compared to a Fab. A scFv derived from the antibody 4F11E12 was chosen as a model [**32**]. This antibody specifically recognizes the major surface antigen 1 (SAG1) of *Toxoplasma gondii*, a protozoan parasite responsible for toxoplasmosis infection, which has recently been used to enhance parasite detection via an scFv-alkaline phosphatase immunoconjugate [**33**]. The main purpose of this

study is to improve our knowledge on the origins of the biophysical properties of antibody fragments as well as the development of an original optimization strategy.

2. Results

2.1. Biophysical Properties of Wild-Type scFv

ScFv S1A0 was built from the association of the heavy (VH A) and light (VL 0) variable wild-type domains of murine 4F11E12 monoclonal IgG2a antibody (**Figure 1**A). Given that in the scFv format, the VL domain is not recognized by the protein L (PpL) [**8**], a His-Tag has been used so that scFv S1A0 could be purified by affinity chromatography with a HisTrap™ HP column in a pure and homogeneous approach (**Figure 1**B). Purified S1A0 exhibited a 100% monomeric structure, a midpoint temperature I of 60.9 °C, and a midpoint chemical denaturation of 2.6 M (DC_{50}) with aqueous guanidinium (GdnHCl). It has been shown to recognize the target antigen with good affinity. However, it also has poor biophysical properties (**Figure 1**C). Firstly, the production yield calculated from the quantities obtained after elution was considered somewhat low (around 0.3 mg/L). Secondly, it demonstrated a weak "pH stability" as it was sensitive to pH 2.0 as illustrated by the precipitation of at least 30% of the overall protein amount after centrifugation and overnight dialysis against phosphate-buffered saline (PBS). Nevertheless, the purified scFv S1A0 routinely exhibited aggregation even at low concentrations (200 µg/mL).

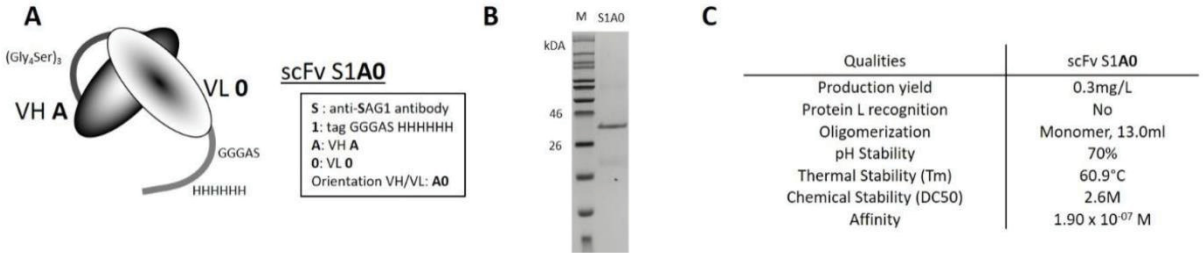

Figure 1. Structural and functional characterization of original wild-type single-chain Fragment variable (scFv). (**A**) Schematic representation of recombinant scFv S1A0 with structural features and nomenclature. ScFv S1A0 was constructed from the association of the heavy (VH A) and light (VL 0) variable wild-type domains of anti-SAG1 ("S") antibody and the inclusion of peptide flag $Gly_3AlaSerHis_6$ in C-terminal ("1"). (**B**) Coomassie-stained sodium dodecyl sulfate-polyacrylamide gel electrophoresis (SDS-PAGE) for analysis of purified scFv S1A0 under reducing conditions. M: Molecular marker. (**C**) Production yield and biophysical properties of scFv S1A0.

2.2. Methodology for Replacing the Framework (FR) Sequences

Step no. 1: Replacing the FR sequences

In order to identify a set of key residues responsible for the poor biophysical properties of S1A0, the FR shifting method was applied (**Figure 2**). The first step was the design of a scFv with a sequence identity of about 90% in FR regions.

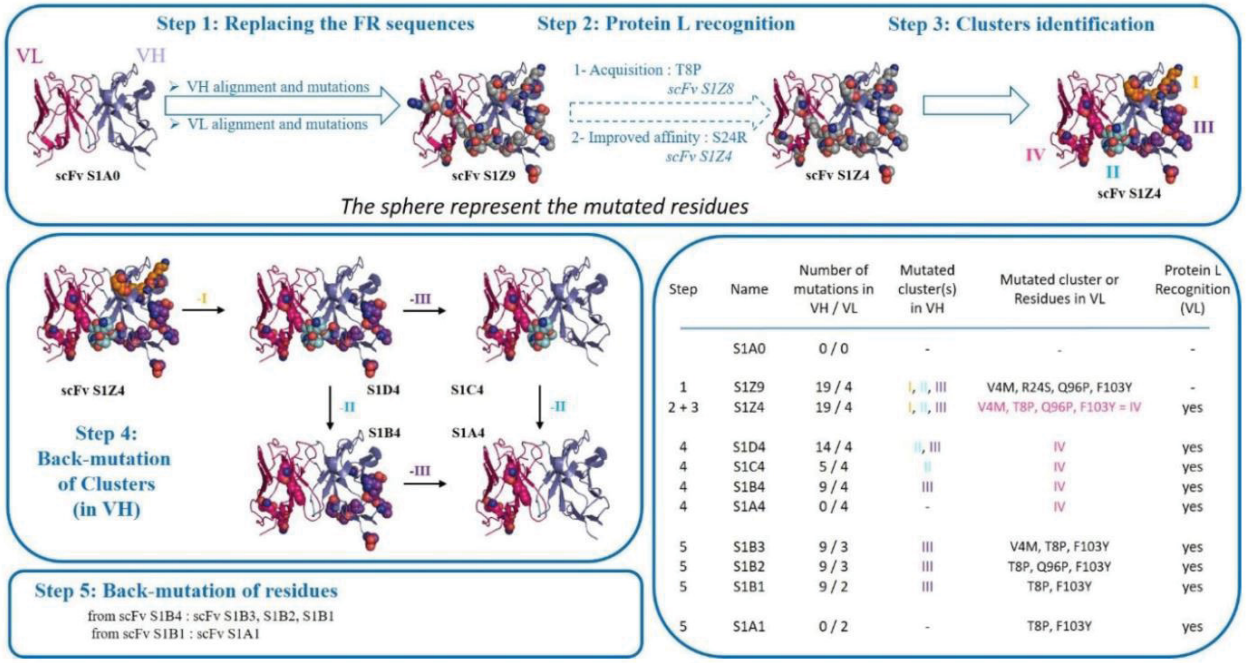

Step	Name	Number of mutations in VH / VL	Mutated cluster(s) in VH	Mutated cluster or Residues in VL	Protein L Recognition (VL)
	S1A0	0 / 0	-	-	-
1	S1Z9	19 / 4	I, II, III	V4M, R24S, Q96P, F103Y	-
2 + 3	S1Z4	19 / 4	I, II, III	V4M, T8P, Q96P, F103Y = IV	yes
4	S1D4	14 / 4	II, III	IV	yes
4	S1C4	5 / 4	II	IV	yes
4	S1B4	9 / 4	III	IV	yes
4	S1A4	0 / 4	-	IV	yes
5	S1B3	9 / 3	III	V4M, T8P, F103Y	yes
5	S1B2	9 / 3	III	T8P, Q96P, F103Y	yes
5	S1B1	9 / 2	III	T8P, F103Y	yes
5	S1A1	0 / 2	-	T8P, F103Y	yes

Figure 2. Design of scFvs for the exploration of biophysical properties. Flowchart depicting the stepwise process leading from scFv S1A0 to the creation of all scFvs needed for the exploration of biophysical properties. Ribbon representations of 1YNT structure showing amino acid residue mutations in spheres according mutations of different scFvs. Grey spheres represent mutations after the replacement of FR sequences (step 1) and the method employed to confer Protein L binding ability (step2). Mutations are depicted as divided into four clusters: cluster I, AA close to CDRs (orange)—cluster II, AA connecting C-C' strands (blue)—cluster III, all other AA on the VH domain (purple) and cluster IV, AA on the VL domain (pink). Additional information regarding each one of the scFv constructs was indicated in the table, at the lower right.

Firstly, in order to design scFvs with new framework regions, it was necessary to compare the amino acid sequence of heavy and light domains on a V- or J-REGION domain directory. For this, defining the antibody's paratope was also imperative. In accordance with the 1YNT structure [32], the paratope was considered to correspond to the CDRs described by IMGT, but slightly extended (Figure 3). According to the IMGT®/DomainGapAlign tool [34], the variable domains with the highest similarity were IGHV1S137*01/IGHJ2*01 and IGKV10-96*01/IGKJ2*01, with a percent identity of 95.9% and 98.9%, respectively (Figure 3). Secondly, an alignment of 100 murine sequences (Mus musculus) were chosen for the VH domain. Indeed, the percentage of identity indicated skews the research taking into account the residues of the FRs and the CDRs belonging to the V or J gene. The results and the order were different when only the FRs residues were used (% of FR identity, Figure 3). The primary search criteria were the low distribution of the FRs modifications throughout the variable sequence. Thus, all the sequences with a FR1 carrying more than four modifications

distributed on the strands A and B were ignored. The choices were furthermore restrained since (i) only 8 sequences out of 100 met this criteria: IGH1-15*01, IGHV1-62-1*01, IGHV1-54*01, IGHV1-63*01, IGHV1-63*02, IGHV1-54*02, IGHV1-54*03, IGHV1S52*01, (ii) the differences were localized especially on FR2 and FR3 with little modifications of the N-terminal extremity and (iii) five residue mismatches were located on the C-C′ loop (Figure 3). The influence of this loop on the biophysical properties of a scFv was rather intriguing since it was very exposed to the solvent and it seemed to interact little with AA residues of other strands. Nevertheless, it could have an influence on the fragment's affinity, since C and C' strands structurally support CDR2 and CDR3, respectively. Moreover, some VH domains were then privileged in order to (i) avoid reducing the stability of the scFv with the presence of Y103 and (ii) not to modify the stability of the VH-VL interaction in the absence of V42A. Thus, the two templates, IGHV1-15*01 and IGHV1-63*02, were interesting and very similar. A variant of the IGHV1-63*02 gene with 73.5% identity, containing 16 mutations in the FRs, was chosen, given it only had two modifications in the FR1, and a fragment with a VH domain belonging to the same gene had been previously produced with a production yield of the order of 1 mg/L (unpublished data). Additionally, for the FR4 sequence alignment, four murine IGHJ genes were indicated by IMGT®. The sequence of the IGHJ3 gene exhibited the biggest sequence identity, even when compared to the IGHJ2 gene, especially in regards to the AA functional group and length. Hence, in order to also generate sequence variability in the FR4, the three close AA mutations were made in accordance to the IGHJ3 gene. Lastly, the VH Z (118 AA) was created by combining the framework sequences of variant IGHV1-63*02 and IGHJ3*01. It showed an identity of 83.9% compared with the VH A with 19 substitutions distributed as follows: 2 in FR1, 6 in FR2, 8 in FR3, and 3 in FR4 (Figure 3).

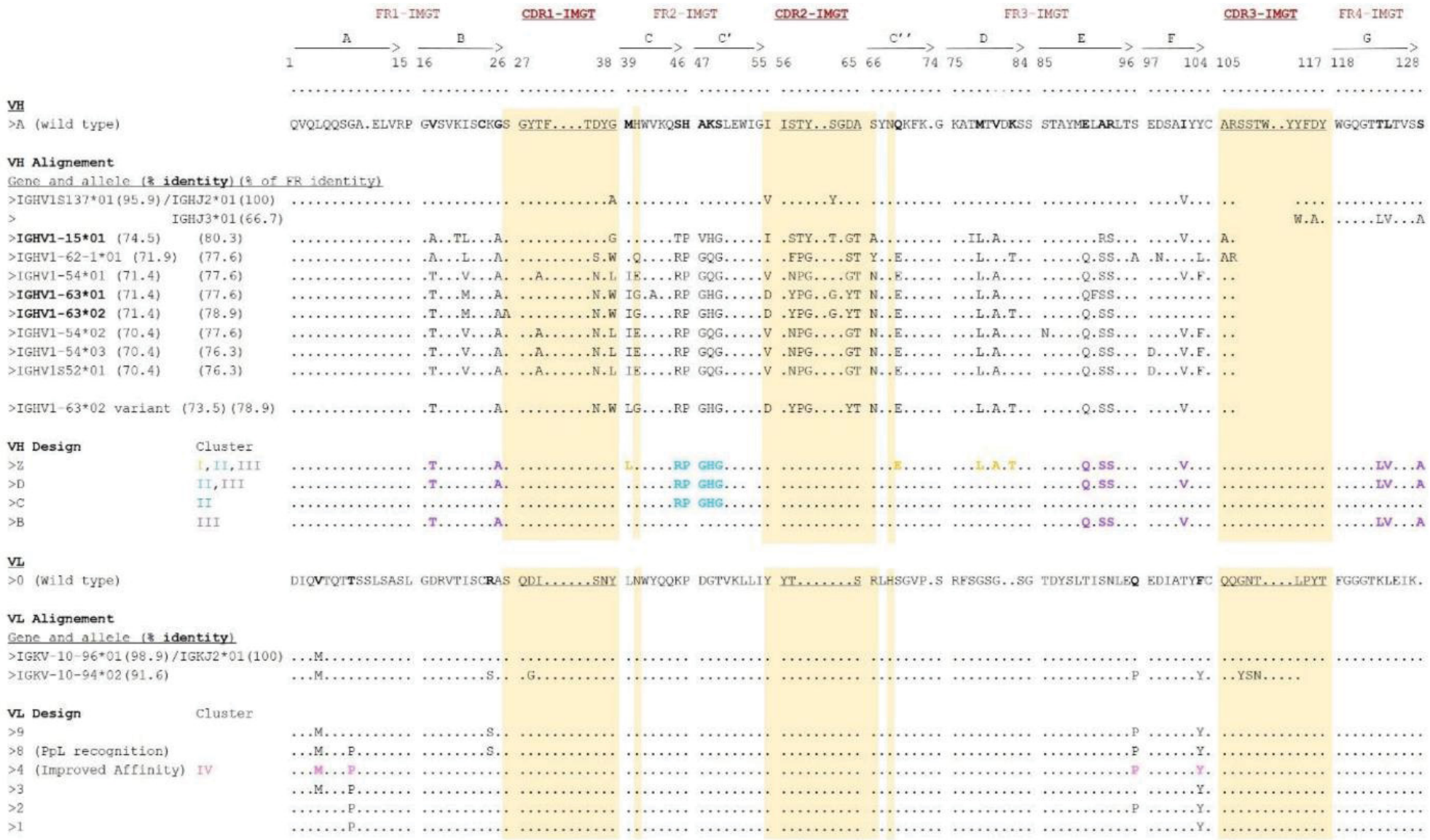
FR1-IMGT
CDR1-IMGT
FR2-IMGT
CDR2-IMGT
FR3-IMGT
CDR3-IMGT
FR4-IMGT
A
B
C
C'
C''
D
E
F
G
1 15 16 26 27 38 39 46 47 55 56 65 66 74 75 84 85 96 97 104 105 117 118 128
VH
>A (wild type) QVQLQQSGA.ELVRP GVSVKISCKGS GYTF....TDYG MHWVKQSH AKSLEWIGI ISTY..SGDA SYNQKFK.G KATMTVDKSS STAYMELARLTS EDSAIYYC ARSSTW..YYFDY WGQGTTLTVSS
VH Alignement
Gene and allele (% identity) (% of FR identity)
>IGHV1S137*01(95.9)/IGHJ2*01(100)
> IGHJ3*01(66.7)
>IGHV1-15*01 (74.5) (80.3)
>IGHV1-62-1*01 (71.9) (77.6)
>IGHV1-54*01 (71.4) (77.6)
>IGHV1-63*01 (71.4) (77.6)
>IGHV1-63*02 (71.4) (78.9)
>IGHV1-54*02 (70.4) (77.6)
>IGHV1-54*03 (70.4) (76.3)
>IGHV1S52*01 (70.4) (76.3)
>IGHV1-63*02 variant (73.5)(78.9)
VH Design Cluster
>Z I,II,III
>D II,III
>C II
>B III
VL
>0 (Wild type) DIQVTQTTSSLSASL GDRVTISCRAS QDI.....SNY LNWYQQKP DGTVKLLIY YT.....S RLHSGVP.S RFSGSG..SG TDYSLTISNLEQ EDIATYFC QQGNT....LPYT FGGGTKLEIK.
VL Alignement
Gene and allele (% identity)
>IGKV-10-96*01(98.9)/IGKJ2*01(100)
>IGKV-10-94*02(91.6)
VL Design Cluster
>9
>8 (PpL recognition)
>4 (Improved Affinity) IV
>3
>2
>1

Figure 3. Amino acid sequence of heavy-chain variable (VH) and light-chain variable (VL) domains according to the IMGT® numbering. The wild-type sequences of the VH and VL domains were aligned according to the IMGT®/DomainGapAlign feature. Only sequences with the highest percentage of identity and sequences of interest were shown. The different sequences of the VH and VL domains were designed without taking into account the amino acid residues present in extended CDRs (depicted in yellow). Only mutations performed on both domains were shown. For the VH and VL domains, mutated residues are stained according to the clusters they belong to (cluster I: orange; cluster II: blue; cluster III: purple and cluster IV: pink).

Many Aas have been mutated in the VH domain, hence further VL domain mutations have been limited. Using the DomainGapAlign tool, and compared to IGKV10-96, IGKV10-94 was preferentially selected according to the presence of Y103 amino acid residue that improves scFv stability. All alleles make up for at least three AA modifications: V4M, Q96P, and F103Y. IGKV10-94*02 was particularly chosen because it also had a key amino acid in the interaction with the protein L: R24S. So, for the VL 9 (108 AA), the IGKV10-94*02 was only used for the introduction of four residue substitutions, two on the FR1 (V4M, R24S) and two on the FR3 (Q96P, F103Y), thus leading to 96.3% of identity (**Figure 3**). Therefore, the scFv S1Z9 displayed 23 substitutions compared with scFv S1A0 (89.8% identity in variable domains).

Step no. 2 (optional): Protein L recognition

In this method, conferring the fragment a “protein L recognition” feature (step 2) is optional (**Figure 2** and **Figure 3**). Nevertheless, it is advisable to introduce it, given the fact that it facilitates the purification process of all other variants. In a previous report, it was demonstrated that the VL-T8P substitution on IGKV-10-94 allows recognition by Protein L (scFv S1Z8) and that the VL-S24R substitution directly influences a fragment’s affinity for Protein L (scFv S1Z4), resulting in changes in elution profiles during purification (7). Thus, both scFvs were successively designed and produced. They were purified by affinity chromatography with a HiScreen™ Capto™ L column, both yielding molecule’s concentrations in the range of 5 mg/L. As expected, the presence of an Arginine at L-24 position allowed capture of scFv S1Z4 by PpL, leading to an elution within a limited volume (2 mL) and at a rather high concentration when compared with scFv S1Z8 (L-S24), which displayed a larger elution volume, of about 8 mL (**Figure 4**A). Therefore, this arginine was conserved in all other scFv variants due to its ability to enhance purification of concentrated protein fractions.

A

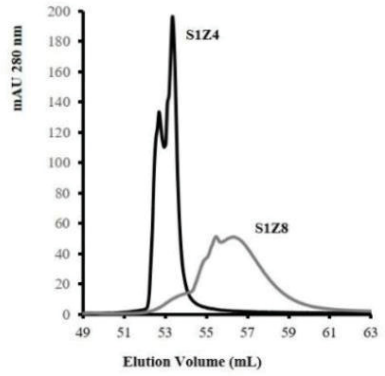

B

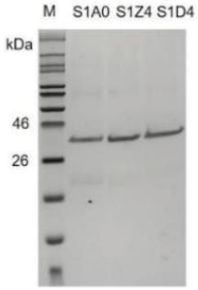

C

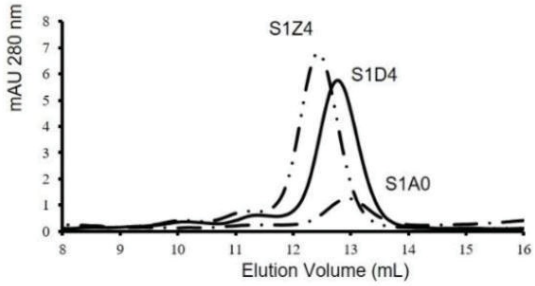

D

Qualities	scFv S1**A0**	scFv S1**Z4**	scFv S1**D4**
Production yield	0.3mg/L	4.6mg/L	8.2mg/L
Protein L recognition	No	Yes	Yes
Oligomerization	Monomer, 13.0mL	Monomer, 12.4mL	Monomer, 12.8mL
pH Stability	70%	95%	91%
Thermal Stability (Tm)	60.9°C	79.9°C	80.5°C
Chemical Stability (DC50)	2.6M	nd	3.8M
Affinity	1.90 x 10^{-07} M	nd	4.00 x 10^{-07} M

Figure 4. Structural and functional characterization of the scFvs S1Z8, S1Z4, and S1D4. (**A**) Affinity chromatography in a HiScreen™ Capto™ L column. The chromatogram shows the elution profiles of S1Z4 (black line) and S1Z8 (grey line), demonstrating a faster and more concentrated elution for S1Z4. (**B**) SDS-PAGE analysis on purified scFv variants under reducing conditions. M: Molecular marker. (**C**) Analytical Size-exclusion chromatography (SEC) chromatogram on a calibrated Superdex 75 10/300 GL column of the following purified scFv variants: wild-type S1A0 (one dot-dashed line), S1Z4 (two dot-dashed line) and S1D4 (solid line). (**D**) Production yield and biophysical properties of the three analyzed scFvs.

Previously diluted scFv S1Z4 (400 µg/mL) was recovered without any signs of aggregation after dialysis, exhibiting better pH stability than scFv S1A0 (**Figure 4**B). Size exclusion chromatography (SEC) performed on scFv S1Z4 indicated that this variant remained as monomers as scFv S1A0 (**Figure 4**C). Nevertheless, the fragment showed a smaller elution volume of 12.4 mL. The thermal stability of scFv S1Z4 was significantly high with a Tm of 79.9 °C. Unexpectedly, the biophysical properties observed for the scFv S1Z4 were very different from those obtained for S1A0, showing improved pH and thermal stabilities (+19 °C) and production yield (+4.3 mg/L) (**Figure 4**D).

Steps no. 3 and 4: Cluster identification and Back-mutation of residues

A third step 3 was then performed, in which various clusters on the VH domain were identified based on three-dimensional structural analysis. Clusters were defined as following: (i) cluster I: amino acids (AA) close to CDRs, (ii) cluster II: AA connecting C-C' strands and (iii) cluster III: all other AA (**Figure 2** and **Figure 3**). Cluster IV was designed with the mutations on VL domain.

In a fourth step, different fragment variants were constructed aiming to better understand the relationship between AA clusters and the improvement of scFv qualities. ScFv S1D4, which is the equivalent of scFv S1Z4 without cluster I

substitutions, had the highest production yield (8.2 mg/L) and was recovered pure and without any molecule aggregation after dialysis (**Figure 4**). Moreover, the thermal stability showed a slight increase from 79.9 °C to 80.5 °C. ScFv S1D4 and scFv S1A0 were also in their monomeric forms, with elution volumes of 12.8 and 13 mL, respectively, unlike scFv S1Z4 (12.4 mL). Thus, cluster I mutations had a slightly negative impact on the qualities of scFv S1Z4 (production, thermal stability, and conformation).

As means to better analyze the impact of clusters II and III mutations on the VH domain, three new fragment variants were generated from scFv S1D4: (i) scFv S1B4 with only cluster III substitutions, (ii) scFv S1C4 with only cluster II substitutions, (iii) scFv S1A4 without any substitutions (**Figure 2**, **Figure 3**, and **Figure 5**).

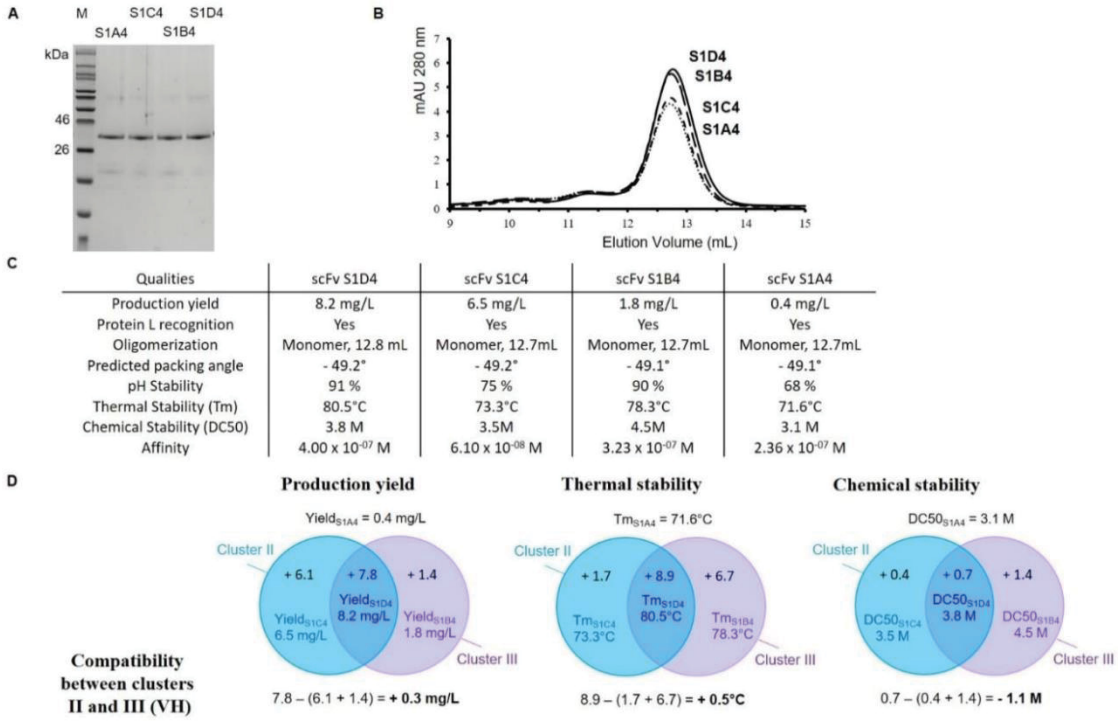

Figure 5. Structural and functional characterization of the scFvs S1D4, S1C4, S1B4 and S1A4. (**A**) SDS-PAGE analysis of purified scFv variants under reducing conditions. M: Molecular marker. (**B**) Analytical Size-exclusion chromatography (SEC) chromatogram on a calibrated Superdex 75 10/300 GL column of the purified scFv variants: scFv S1D4 (solid line), scFv S1B4 (long dashed line), scFv S1C4 (short dashed line) and scFv S1A4 (dotted line). (**C**) Production yield and biophysical properties of the three analyzed scFvs. (**D**) Venn diagram for analysis of production yield, thermal stability and chemical stability following the presence of clusters II and III mutations. Compatibility has been calculated below the diagrams.

After Protein L purification, all three variants were also obtained without any contaminants (**Figure 5**A). SEC indicated that these three variants mostly remained in monomeric forms and displayed the same elution volume as scFv S1A0 and scFv S1D4 (**Figure 5**B,C). Likewise, the packing angles of the four scFvs were estimated in an equivalent manner, but with a slight difference from cluster III (**Figure 5**C). When we back-mutated the VH domain of scFv S1D4 to wild-type (WT) VHA, a higher

production yield was observed for cluster II substitutions (+6.1 mg/L) when compared to cluster III (+1.4 mg/L). Again, the combination of both clusters II and III mutations was somewhat encouraging and compatible, as S1D4 exhibited a higher production yield increased by +0.3 mg/L (**Figure 5**C,D). Concerning pH stability, cluster III substitutions seemed useful because aggregation was observed with scFv S1A4 and scFv S1C4 (stable at 68 and 75%, respectively), in contrast to scFv S1B4 (90%) and scFv S1D4 (91%) (**Figure 5**C). Tm values were used to rank stability enhancements provided by each individual or combined mutations. The Tms of scFv S1A4, scFv S1C4, scFv S1B4, and scFv S1D4 were 71.6 °C, 73.3 °C, 78.3 °C, and 80.5 °C, respectively (**Figure 5**C,D). Cluster III substitutions have mainly shown impacted thermal stability by increasing Tm by +6.7 °C compared with scFv S1A4 while cluster II substitutions only increased Tm by +1.7 °C. However, the combination of clusters II and III mutations seemed positive, as S1D4 exhibited an additional higher Tm increased by +0.5 °C (**Figure 5**D).

Chemical scFv denaturation with aqueous guanidinium chloride (GdnHCl) showed slightly different results than those observed for thermal challenge. The following values were obtained in the order of increasing stability: scFv S1A4 (DC_{50} = 3.1 M), scFv S1C4 (DC_{50} = 3.5 M), S1D4 (DC_{50} = 3.8 M), and scFv S1B4 (extrapolated DC_{50} = 4.5 M). Cluster II substitutions led to increased chemical stability as shown by scFv S1C4 (+0.4 M), and cluster III substitutions also led to major stability gain as shown by scFv S1B4 (+1.4 M). As illustrated in **Figure 5**D, cluster II and III substitutions were nonviable (−1.1 M). Unexpectedly, the combination of cluster II and III substitutions (scFv S1D4) did not result in the most stable variant. ScFvs S1C4 and S1D4 broadly showed the same chemical stabilities (DC_{50} = 3.5 M and 3.8 M, respectively) which were definitely lower than those obtained for scFv S1B4 (extrapolated DC_{50} = 4.5 M).

Step no. 5: Back-mutation of residues

In order to introduce back-mutation residues (step 5) in the VL domain, especially at positions 4 and 96 (**Figure 2** and **Figure 3**), three new variants named scFv S1B3 (P96Q), scFv S1B2 (M4V), and scFv S1B1 (P96Q and M4V) were generated from scFv S1B4 and hereby produced (**Figure 6**). Following Protein L purification, all variants were obtained (**Figure 6**A). SEC indicated that these mutants remained mostly comparable to each other and to their parental scFv S1B4 (**Figure 6**B). Independently, M4V or P96Q substitutions on VL did not dramatically change the production yield and thermal stability. Conversely, simultaneous P96Q and M4V substitutions (scFv S1B1) resulted in a decreased production yield by −0.5mg/L and thermal stability by −2.4 °C when compared to the scFv S1B4 (**Figure 6**C).

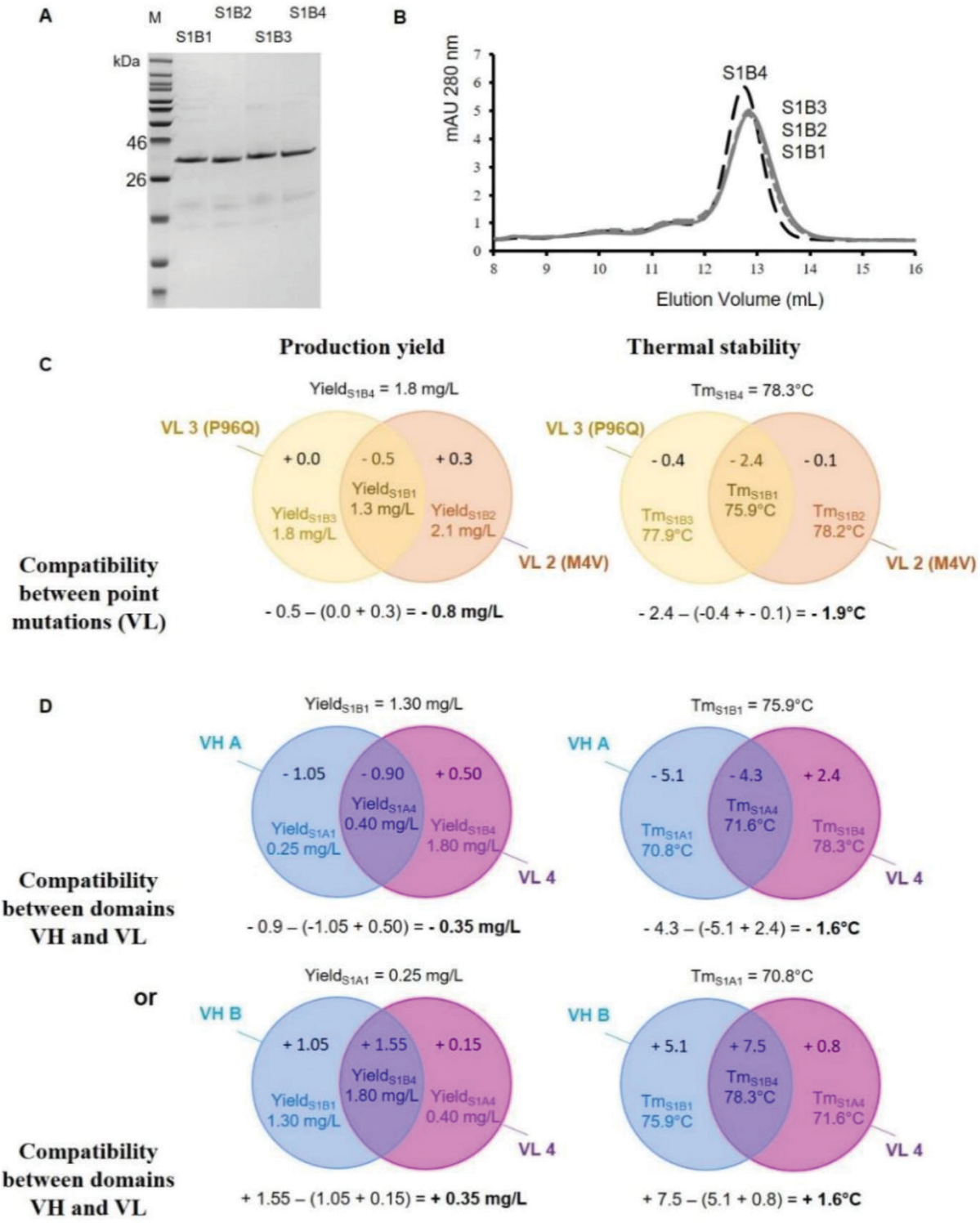

Figure 6. Structural and functional characterization of the scFvs S1B4, S1B3, S1B2, and S1B1. (**A**) SDS-PAGE analysis of purified scFv variants under reducing conditions (M: Molecular marker). (**B**) Analytical Size-exclusion chromatography (SEC) chromatogram on a calibrated SuperdexTM 75 10/300 GL column of the purified scFv variants: scFv S1B4 (long dashed line), scFv S1B3 (solid gray line), scFv S1B2 (short

dashed gray line), and scFv S1B1 (dotted gray line). (**C**) Venn diagram for analysis of production yield and thermal stability following the presence of single amino acid (AA) mutations in the VL (P96Q and M4V). Compatibility has been calculated below the diagrams. (**D**) Venn diagram for analysis of production yield and thermal stability according to the VH (A or B) and VL (1 or 4) domains viewed from two perspectives. Compatibility has been calculated below the diagrams.

When cluster III was additionally back-mutated (scFv S1A1), the production yield returned to a low level (0.25 mg/L) and the thermal stability dropped to 70.8 °C, still well above the values found for scFv S1A0 (**Figure 6**D). Thus, two mutations (VL-T8P and VL-F103Y) allowed for a gain in molecule thermal stability of + 9.9 °C.

The study of scFvs S1A1, S1B1, S1A4, and S1B4 also showed that there might be a positive/negative relationship between certain VH and VL domains, be it in terms of thermal stability or production yield; adverse between VH A and VL 4 or between VH B and VL 1 or beneficial between VH A and VL 1 or between VH B and VL 4 (**Figure 6**D). Indeed, the Tm of scFv S1B1 remained higher than that of scFv S1A1 (+5.1 °C). Importantly, scFv S1B4 presents an even higher thermal stability when compared to scFv S1A4 (+6.7 °C), suggesting enhanced stabilization of VL 4 when combined with VH B (+1.6 °C). Likewise, there is a cumulative effect on its production level (0.35 mg/L).

2.3. Functional Analysis

The full functional analysis of scFvs was assessed by surface plasmon resonance (SPR), which allows measurement of target binding events to immobilized antigen SAG1. All scFv fragments were able to recognize the target with similar affinities, of around 2.10^{-7} M, indicating that substitutions did not have a significant impact on affinity (**Figure 7**). Nevertheless, cluster II substitutions (scFv S1C4) seemed to improve affinity as compared to scFv variants carrying the WT VH A (scFv S1A0 and scFv S1A4). In contrast, affinities were not affected by any cluster III substitutions (scFv S1B4) alone or in combination with those of cluster II (S1D4). As a result, five scFv variants were successfully generated with modified biophysical properties.

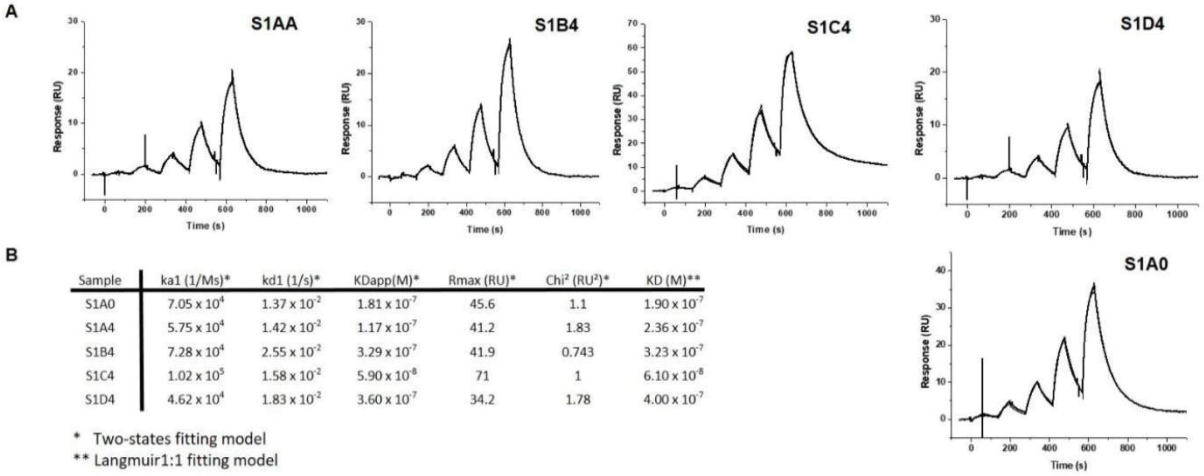

Sample	ka1 (1/Ms)*	kd1 (1/s)*	KDapp(M)*	Rmax (RU)*	Chi² (RU²)*	KD (M)**
S1A0	7.05×10^{4}	1.37×10^{-2}	1.81×10^{-7}	45.6	1.1	1.90×10^{-7}
S1A4	5.75×10^{4}	1.42×10^{-2}	1.17×10^{-7}	41.2	1.83	2.36×10^{-7}
S1B4	7.28×10^{4}	2.55×10^{-2}	3.29×10^{-7}	41.9	0.743	3.23×10^{-7}
S1C4	1.02×10^{5}	1.58×10^{-2}	5.90×10^{-8}	71	1	6.10×10^{-8}
S1D4	4.62×10^{4}	1.83×10^{-2}	3.60×10^{-7}	34.2	1.78	4.00×10^{-7}

* Two-states fitting model
** Langmuir1:1 fitting model

Figure 7. Affinity binding analysis by surface plasmon resonance (SPR) of purified scFvs on immobilized Surface Antigen-1 (SAG1). (A) Single cycle kinetic titrations (600-200-66-22-7.5 nM) of scFvs on immobilized SAG1. The thin-lined curves

represent fitting by two state fitting model. (B) SPR analyses of binding kinetic parameters.

3. Discussion

In the present study, the S1A0 scFv was developed from the variable sequences extracted from the 4F11E12 monoclonal antibody. S1A0 and its variants were all designed in the VH-VL orientation and linked by the peptide (Gly4Ser)3. Globally, S1A0 exhibited poor biophysical qualities. Through a methodology based on replacing the FR sequences, 11 S1A0 variants were designed and exhibited diverse biophysical properties.

For the design of a scFv with new frameworks, the comparison of the amino acid sequence of heavy and light domain frameworks with a V- or J-REGION domain directory is required. There is no wrong choice, since we must not prejudge and anticipate the evolution of fragment properties. The key is to identify FR domains with strong identity to the parental framework to study the evolution of biophysical properties through very few mutations or clusters. Variant IGHV1-63*02 was chosen based on 14 mutations distributed in FR2 and FR3 (including five in the C-C′ loop). To test whether FR4 substitutions impacted scFv properties, the IGHJ2 gene was mutated at three positions to be identical to FR4 of the IGHJ3 gene. The VL framework has been preserved to the maximum to limit the number of variants (only four mutations). Thus, the variable domains of scFv S1Z9 have 89.8% of identity compared with WT scFv (23 mutations out of 226).

When designing antibody fragments, the purification process is one of the main concerns to be addressed. Affinity chromatography with Protein L agarose column is an established method [35,36,37,38]. It has been previously demonstrated that it is possible to confer a PpL recognition site to all kappa chain antibody molecules, which even made the purification of IgA molecules through PpL resins viable [8,39]. Protein L did not naturally recognize the VL domain of scFv S1Z9 (IGKV-10-94). Thus, the VL-T8P and VL-S24R substitutions were introduced into the design of scFvs S1Z8 and S1Z4 respectively, allowing purification by Protein L affinity chromatography [8]. For scFv S1A0 purification, a poly-histidine tag was grafted onto the C-Terminal end. In order to compare changes due to AA mutations inserted in the VH and VL domains, the same poly-histidine tag was conserved for all other variants.

All of the assessed biophysical properties for scFv S1Z4 were improved when compared to scFv A0: (i) Protein L recognition; (ii) increased production yield by 15 fold, reaching 4.6 mg/L; (iii) higher pH stability without aggregation, even at higher concentrations (until 400 µg/mL); (iv) higher thermal stability with an increased Tm by +19 °C. However, conformational tweaking was observed. SEC indicated that scFv S1Z4 showed a lower elution volume than scFv S1A0. Thus, the selected mutations to replace the FR sequences were successfully conducted.

With the purpose of analyzing how cluster I substitutions impacted on scFv properties, residues were back-mutated from scFv S1Z4 to create scFv S1D4. In general, little effect of cluster I substitutions was observed, except for production yields (+3.6 mg/L). As indicated by IMGT®, only one (T82K) of these five mutations was very dissimilar while four were similar (L39M, E69Q, L78M, A80V) according to (i) the volume; (ii) the hydrophobicity; (iii) the type of AA chain [40]. However, the side chain

of residues M39, M78, V80 could change the steric hindrance of the VH domain's core, providing a more compact structure, that slightly increased thermal stability and also improved production yield by a favorable effect on protein folding. Therefore, the cluster I back-mutation was positive, especially in improving scFv production. Moreover, cluster II represents the mutations performed at the C-C′ loop. The RPGHG amino acid sequence has allowed, on its own, a remarkable improvement in the fragment's production (+ 6.1 mg/L) without modifying the molecule's biophysical features. The sequence would certainly lead to a more favorable folding of the VH domain, thanks to the formation of a structural elbow with the "PG" motif. Ultimately, scFv S1D4 displayed the best improvement in terms of production yield (by 27-fold) when compared to the wild-type scFv (S1A0).

Additionally, cluster III mutations seem to have an impact on the pH Stability. The four scFvs (S1A4, S1B4, S1C4, and S1D4) have the same estimated pI (7.83), which indicates that the pH stability might not only be influenced by the shift of charged residues. Studies should be performed with new mutants in order to prove this point. Moreover, additional studies on the influence of the Tag presence could also provide interesting insights [41].

Cluster III substitutions mainly impacted thermal stability by increasing Tm by +6.7 °C compared with scFv S1A4 while cluster II substitutions only increased Tm by +1.7 °C (Figure 4). However, the combination of clusters II and III mutations seemed additional, S1D4 exhibited an additional higher Tm increased by +0.5 °C. This profile could be explained by the spatial proximity and compatibility between VH-RPGHG (positions 45 to 49) and the nearby VH-V101. Thus, creating better complementarity between the Aas of the same domain or at the interface between the variable domains may improve stability of scFv (16). Moreover, the scFv S1D4 exhibited a very high thermal stability [19,41,42] even without additional disulfide bridge [43], which could greatly increase long-term storage stability compared to other scFvs [30]. In terms of chemical stability, clusters II and III substitutions were deleterious. This finding confirms that biophysical properties of an antibody fragment differently vary depending on the applied stress.

In terms of affinity, all variants retained similar binding properties when compared to scFv S1A0. Cluster III substitutions alone had a slight negative impact whereas cluster II substitutions alone showed the best affinity profile, demonstrating improved binding (<10−7 M) compared with scFv S1A0. One possible explanation could lie in the scFvs packing angle, in particular H47 of cluster II (or H42 in Kabat) (44). However, the predictions for cluster II show a very slight decrease of −0.1° in the packing angle valid for the two scFvs S1C4 and S1D4 (−49.2°), as opposed to −49.1° for the scFvs S1A4 and S1B4. Thus, cluster II substitutions could somewhat twist the C-C′ strands and change part of the H-CDRs 1 and 2 conformations, but under the influence of other residues present in cluster III. In addition, binding affinity was not altered by VH-FR4 substitutions (cluster III), and therefore the complementarity of strand G located near A and F strands could be more thoroughly studied. Indeed, as Egan et al. (2017) already showed, substitution of a human Vκ1-FR4 with the corresponding germline sequence of a λ-type VL chain improved the biophysical properties of a scFv without altering its affinity [44].

ScFv S1A1 had a higher Tm than scFv S1A0 (+9.9 °C) with only two mutations, T8P and F103Y, performed on the VL domain. This profile could be explained by new hydrogen bonds created between the alcohol functional group on tyrosine that interacts with the side chain of the glutamine at position 44. As previously described, VH-Q44 and VL-Q44 largely impact scFv stability as tyrosine VH-Y103 and VL-Y103 might also provide stronger VH/VL interaction [23,45]. To better understand the impact of VL 4 substitutions, M4V and P96Q mutations were introduced into the scFv S1B4 based on the better stability and production profiles observed for this molecule, rather than scFv S1A4, the latter having shown poorer features. Favorable effects have been demonstrated when the two residues M4 and P96 were present on the VL domain (VL 4) and when the VL 4 domain was combined with the VH B domain. These results were surprising and not anticipated by three-dimensional structural analysis because the localization of the different mutations (on the VL or on the VH and the VL) was spatially distant. Ultimately, it is important to approach the structures of each V-domain as an ensemble when envisaging the molecule optimization and we believe the use of the methodology for replacing the FR sequences proves interesting for this purpose.

4. Materials and Methods

4.1. Protein Expression and Purification

A scFv fragment resulted from the association of the heavy and light variable domains of an antibody via the (Gly4Ser)3 peptide link and the inclusion of peptide flag Gly3AlaSerHis6 in the C-terminal portion. The pSW1 plasmid was used in the expression of all scFv constructs. Three scFv nucleotide sequences (S1A0, S1Z9, and S1B4) were designed and then synthesized by GeneArt (Thermo Fisher Scientific, Waltham, USA). For the generation of plasmid pSW1-scFv S1A4 or pSW1-scFv S1A1, cDNA-VHA was digested by Pst1/BamH1 restriction enzymes from pSW1-S1A0 and cloned into the vectors pSW1-S1B4 or pSW1-S1B1, restricted in the same manner. Other constructs (S1Z8, S1Z4, S1D4, S1B3, S1B2, S1B1, S1C4) were generated through PCR site-directed mutagenesis. Based on the NEBase Changer™ technology, primers were designed, and site-directed mutagenesis was performed following the manufacturer's instructions (Q5® Site-Directed Mutagenesis Kit). Subsequently, TG1 chemically competent bacteria were transformed with the neo-formed plasmids. All constructs were sequenced and thus confirmed. Escherichia coli strain HB2151 was used for the expression of functional recombinant antibody fragments in the bacterial periplasm, as reported by Aubrey et al. (2003) [46]. ScFv expression was induced with 0.1 M isopropyl β-D-1-thiogalactopyranoside, at 16 °C for 16 h, under gentle agitation (75 rpm). Periplasmic extracts were collected after mild osmotic shock, extensively dialyzed against PBS, pH 7.4, and centrifuged (10,000 g, 4 °C, 30 min).

ScFv S1A0 was purified by loading the periplasmic preparation (35 mL), corresponding to half a liter of culture, onto a HisTrap™ HP column (GE Healthcare Bio-Science, 17-5247-01). For all other constructs, scFvs were purified by loading periplasmic preparations (35 mL) onto a HiScreen™ Capto™ L column (GE Healthcare Bio-Science, 17-5478-14). For all the following purifications, columns were

washed with 16 mL of PBS (pH 7.4), and the recombinant proteins were eluted in 1 mL fractions with Glycine (0.1 M, pH 2.0). Production yield calculations were based on purified scFv quantities and expressed as milligrams per liter of culture (mg/L). These yields are representative of three independent productions. Fractions containing the recombinant proteins were selected at A280 nm, pooled, dialyzed against PBS (pH 7.4) overnight, and centrifuged (10,000 g, 4 °C, 10 min). Subsequently, the pH stability of scFv fragments was calculated. Similar purification and dialysis protocols were carried out for all fragments, and a delay of 30 min between column elution and dialysis was always respected. ScFvs molecular mass, pI, and molar extinction coefficient data were all generated by the Protparam tool from http://web.expasy.org/protparam/. The packing angle was calculated using the "Packing Angle Prediction Server (PAPS)" (http://www.bioinf.org.uk/abs/paps/). The fragments mass was later confirmed using Hclass Chromatography hyphenated to a Vion IMS Qtof mass spectrometer, both from Waters Corporation (Wilmslow, UK).

4.2. Biochemical Characterization and scFv Integrity Analysis

The size and integrity of all purified scFvs were assessed by sodium dodecyl sulfate-polyacrylamide gel electrophoresis (SDS-PAGE) on homogeneous 12% polyacrylamide gel, under reducing conditions. Purified scFv samples were all loaded at 1 µg for Coomassie Blue staining (0.1% Coomassie Brilliant Blue R-250, 30% methanol, and 10% glacial acetic acid).

The purified scFv preparations were resolved by size-exclusion chromatography (SEC) on a Superdex 75 10/300 GL column (molecular mass range 3000–70,000) (GE Healthcare Life Sciences, 17-5174-01) with an Äkta purifier. The column was loaded with 20 µg of each scFv construct. Proteins were eluted with PBS at a rate of 0.5 mL/min, and detected with a UV detector at 280 nm.

4.3. Determination of Thermal and Chemical Stabilities

Each scFv was diluted at a concentration of 0.75 µM in PBS buffer and heated from 25–97 °C. At every 4.0 °C, the emission spectra was recorded from 310 to 410 nm with 1 nm step and 0.5 s dwell time on an FS5 spectrofluorometer (Edinburgh Instruments) for the 275 nm tryptophan excitation wavelength. The spectrofluorometer was equipped with a thermostated cell and a TC 125 temperature control unit (Quantum Northwest). All spectra were measured four times and obtained values were added in order to determine the center of mass of each spectrum. For each construct, the Tm was deduced from the first derivative curve of the center of gravity of each spectrum in function of the temperature. Results are representative of three independent experiments. ScFv solutions (0.75 µM) buffered with 20 mM sodium phosphate (pH 7.4) and in containing increasing concentrations of GdnHCL (0 to 5 M) were prepared from freshly purified fragments. Samples were incubated overnight at 37 °C and the fluorescence emission spectra was then recorded on an FS5 spectrofluorometer. For each construct, the concentration of the GdnHCL required to denature 50% of fragment (DC50) was deduced from the first derivative curve of the center of gravity of each spectrum in function of GdnHCl concentration (21).

4.4. Affinity Analysis by Surface Plasmon Resonance

SPR analyses were performed on a T200 apparatus at 25 °C in HBS-EP + (GE Healthcare). For affinity measurements, SAG1 in acetate buffer, pH 4.5, was covalently immobilized (1000 RU) to a CM5S sensor chip using EDC/NHS activation, following the manufacturer's instructions (GE Healthcare). Five increasing ScFv (600-200-66-22-7.5 nM) concentrations were injected (injection time = 60 s) at 50 µL/min. After a dissociation step of 600 s in running buffer, sensor surfaces were regenerated using 10 µL of Gly-HCl pH 1.7. The Kd values were first calculated using a Langmuir 1:1 fitting model and then by a two-state fitting model in order to achieve better fitting (BiaEvaluation3.2, GE Healthcare). Similar Kd values were obtained in both models. All sensorgrams were corrected by subtracting the low signal from the control reference surface (without any immobilized protein) and blank buffer injections before fitting evaluation.

5. Conclusions

The proposed method to replace the FR sequences has been demonstrated and successfully employed in this study. This method can be applied for fragments of various qualities, since all mutations and therefore all evolutions of the molecule's biophysical properties could provide relevant information. In addition, this method could be used on other recombinant antibody formats, such as Fabs or even IgGs, in which the variable domains are linked to the constant domains.

In the present study, we clearly demonstrated that a set of mutations in the FRs can influence one or more biophysical properties of a scFv (Figure 8). Substitutions on the VH C-C′ loop (cluster II) or on core residues of the VH C″-D loop (cluster I) considerably improved production yields, hence making this the first time that such a large improvement in production yield has been reported for only five mutations (cluster II). Substitutions located in cluster III were remarkable. They provided betterment in all three settings of molecule stability: pH, thermal, and chemical. Certainly, a more thorough study and analysis of cluster III is utterly necessary and would provide interesting insights on the influence of AA residues in antibody molecule's stability.

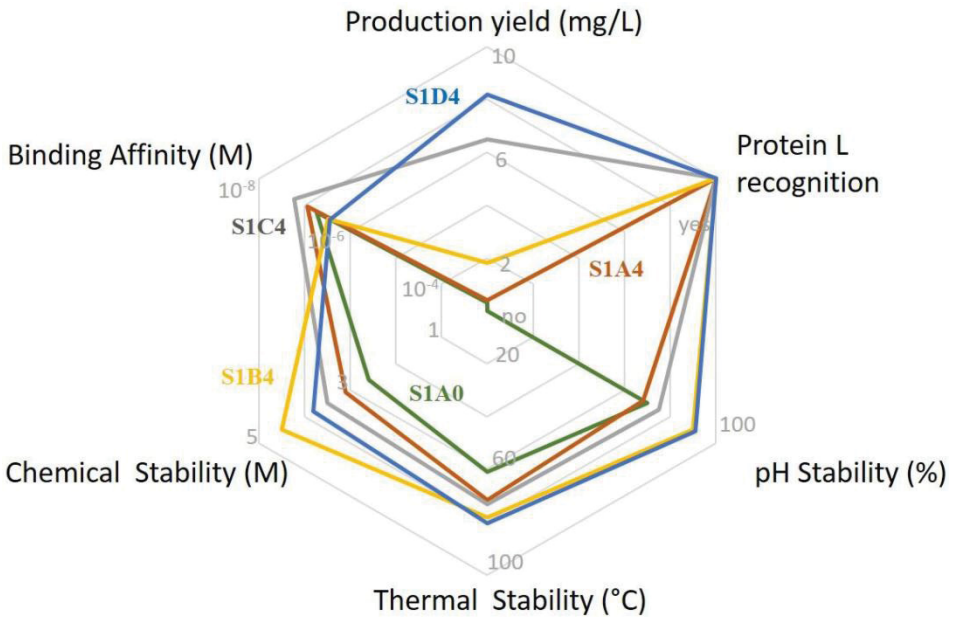

Figure 8. Spider graph representation of all parameters analyzed for wild-type scFv S1A0 and four scFv variants.

Finally, the creation of high identity variants with different biophysical properties sheds a new light into the complexity of antibody fragments, thus providing qualitative items for their optimization.

All studied parameters are outlined in a spider graph for scFv S1A0 (green), scFv S1A4 (brown), scFv S1C4 (grey), scFv S1B4 (orange), and scFv S1D4 (blue): (i) Production yield is expressed in mg/L from 0 to 10; (ii) Protein L recognition (expressed as yes or no); (iii) pH stability in % from 0 to 100; (iv) thermal stability in °C from 0 to 100; (v) chemical stability in molarity (M) from 0 to 5; affinity in molarity (M) from 10−3 to 10−8.

Author Contributions

Conceptualization, N.A.; methodology, N.A.; investigation, T.C., Z.L., J.B., F.B., C.H. (Corinne Henriquet), M.P.; writing—original draft preparation, N.A., T.C., Z.L., M.P.; writing—review and editing, N.A., T.C., Z.L., C.H. (Catherine Horiot), A.d.T., M.O.J., I.G.J., I.D.-P., M.-N.M.; supervision, A.d.T., M.O.J., I.D.-P., M.-N.M.; project administration, N.A.; funding acquisition, N.A. All authors have read and agreed to the published version of the manuscript.

Funding

This research was funded by a grant from the “Région Centre-Val de Loire: APR IR Vab and ARD2020 Biomedicaments BIO-S”.

Acknowledgments

This work has been funded with the support from the French Higher Education and Research Ministry under the program “Investissements d’avenir” Grant Agreement: LabEx MabImprove ANR- 10-LABX-53–01. We thank Eloi Haudebourg (EA 7501 GICC, Université de Tours) for carrying out mass spectrometry characterizations and Professor Igor Chourpa (EA6295 NMNS, Université de Tours) for the technical support (FS5 spectrofluorometer; Edinburgh Instruments).

Conflicts of Interest

The authors declare no conflict of interest.

Abbreviations/Acronyms

AA	**Amino acid**
CDR	complementary-determining regions
FR	Framework
Gly	glycine
GdnHCl	guanidinium chloride
PBS	phosphate-buffered saline
scFv	single-chain antibody variable fragment
SDS-PAGE	sodium dodecyl sulfate-polyacrylamide gel electrophoresis
SEC	size exclusion chromatography
SPR	surface plasmon resonance
Tm	midpoint temperature
VH	heavy-chain variable
VL	light-chain variable
WT	Wild-type

References

[1] Spiess, C.; Zhai, Q.; Carter, P.J. Alternative molecular formats and therapeutic applications for bispecific antibodies. Mol. Immunol. 2015, 67, 95–106. [Google Scholar] [CrossRef]
[2] Brinkmann, U.; Kontermann, R.E. The making of bispecific antibodies. Mabs 2017, 9, 182–212. [Google Scholar] [CrossRef]
[3] Chiu, M.L.; Goulet, D.R.; Teplyakov, A.; Gilliland, G.L. Antibody Structure and Function: The Basis for Engineering Therapeutics. Antibodies 2019, 8, 55. [Google Scholar] [CrossRef]
[4] Holliger, P.; Hudson, P.J. Engineered antibody fragments and the rise of single domains. Nat. Biotechnol. 2005, 23, 1126–1136. [Google Scholar] [CrossRef]
[5] El-Sayed, A.; Bernhard, W.; Barreto, K.; Gonzalez, C.; Hill, W.; Pastushok, L.; Fonge, H.; Geyer, C.R. Evaluation of antibody fragment properties for near-infrared fluorescence imaging of HER3-positive cancer xenografts. Theranostics 2018, 8, 4856–4869. [Google Scholar] [CrossRef]

[6] Wu, S.J.; Luo, J.; O'Neil, K.T.; Kang, J.; Lacy, E.R.; Canziani, G.; Baker, A.; Huang, M.; Tang, Q.M.; Raju, T.S.; et al. Structure-based engineering of a monoclonal antibody for improved solubility. Protein Eng. Des. Sel. 2010, 23, 643–651. [Google Scholar] [CrossRef]
[7] Lee, C.C.; Perchiacca, J.M.; Tessier, P.M. Toward aggregation-resistant antibodies by design. Trends Biotechnol. 2013, 31, 612–620. [Google Scholar] [CrossRef]
[8] Lakhrif, Z.; Pugnière, M.; Henriquet, C.; Di Tommaso, A.; Dimier-Poisson, I.; Billiald, P.; Juste, M.O.; Aubrey, N. A method to confer Protein L binding ability to any antibody fragment. Mabs 2016, 8, 379–388. [Google Scholar] [CrossRef]
[9] Lebozec, K.; Jandrot-Perrus, M.; Avenard, G.; Favre-Bulle, O.; Billiald, P. Quality and cost assessment of a recombinant antibody fragment produced from mammalian, yeast and prokaryotic host cells: A case study prior to pharmaceutical development. New Biotechnol. 2018, 44, 31–40. [Google Scholar] [CrossRef]
[10] Wang, Q.; Chen, Y.; Park, J.; Liu, X.; Hu, Y.; Wang, T.; McFarland, K.; Betenbaugh, M.J. Design and Production of Bispecific Antibodies. Antibodies 2019, 8, 43. [Google Scholar] [CrossRef]
[11] Carter, P.; Presta, L.; Gorman, C.M.; Ridgway, J.B.; Henner, D.; Wong, W.L.; Rowland, A.M.; Kotts, C.; Carver, M.E.; Shepard, H.M. Humanization of an anti-p185HER2 antibody for human cancer therapy. Proc. Natl. Acad. Sci. USA 1992, 89, 4285–4289. [Google Scholar] [CrossRef]
[12] Ducancel, F.; Muller, B.H. Molecular engineering of antibodies for therapeutic and diagnostic purposes. Mabs 2012, 4, 445–457. [Google Scholar] [CrossRef]
[13] Choi, Y.; Hua, C.; Sentman, C.L.; Ackerman, M.E.; Bailey-Kellogg, C. Antibody humanization by structure-based computational protein design. Mabs 2015, 7, 1045–1057. [Google Scholar] [CrossRef]
[14] He, X.; Duan, C.F.; Qi, Y.H.; Dong, J.; Wang, G.N.; Zhao, G.X.; Wang, J.P.; Liu, J. Virtual mutation and directional evolution of anti-amoxicillin ScFv antibody for immunoassay of penicillins in milk. Anal. Biochem. 2017, 523, 44–45. [Google Scholar] [CrossRef]
[15] Lebozec, K.; Jandrot-Perrus, M.; Avenard, G.; Favre-Bulle, O.; Billiald, P. Design, development and characterization of ACT017, a humanized Fab that blocks platelet's glycoprotein VI function without causing bleeding risks. Mabs 2017, 9, 945–958. [Google Scholar] [CrossRef]
[16] Zhang, Y.F.; Ho, M. Humanization of rabbit monoclonal antibodies via grafting combined Kabat/IMGT/Paratome complementarity-determining regions: Rationale and examples. Mabs 2017, 9, 419–429. [Google Scholar] [CrossRef]
[17] Yui, A.; Akiba, H.; Kudo, S.; Nakakido, M.; Nagatoishi, S.; Tsumoto, K. Thermodynamic analyses of amino acid residues at the interface of an antibody B2212A and its antigen roundabout homolog 1. J. Biochem. 2017, 162, 255–258. [Google Scholar] [CrossRef]
[18] Sun, W.; Yang, Z.; Lin, H.; Liu, M.; Zhao, C.; Hou, X.; Hu, Z.; Cui, B. Improvement in affinity and thermostability of a fully human antibody against interleukin-17A by yeast-display technology and CDR grafting. Acta Pharm. Sin. B 2019, 9, 960–972. [Google Scholar] [CrossRef]

[19] Tu, C.; Terraube, V.; Tam, A.S.P.; Stochaj, W.; Fennell, B.J.; Lin, L.; Stahl, M.; LaVallie, E.R.; Somers, W.; Finlay, W.J.J.; et al. A combination of structural and empirical analyses delineates the key contacts mediating stability and affinity increases in an optimized biotherapeutmrtic single-chain Fv (scFv). J. Biol. Chem. 2016, 291, 1267–1276. [Google Scholar] [CrossRef]
[20] Miller, B.R.; Demarest, S.J.; Lugovskoy, A.; Huang, F.; Wu, X.; Snyder, W.B.; Croner, L.J.; Wang, N.; Amatucci, A.; Michaelson, J.S.; et al. Stability engineering of scFvs for the development of bispecific and multivalent antibodies. Protein Eng. Des. Sel. 2010, 23, 549–557. [Google Scholar] [CrossRef]
[21] Unkauf, T.; Hust, M.; Frenzel, A. Antibody Affinity and Stability Maturation by Error-Prone PCR. In Methods in Molecular Biology; Hust, M., Lim, T.S., Eds.; Springer New York: New York, NY, USA, 2018; Volume 1701, pp. 393–407. [Google Scholar]
[22] Hsu, H.J.; Lee, K.H.; Jian, J.W.; Chang, H.J.; Yu, C.M.; Lee, Y.C.; Chen, I.C.; Peng, H.P.; Wu, C.Y.; Huang, Y.F.; et al. Antibody variable domain interface and framework sequence requirements for stability and function by high-throughput experiments. Structure 2014, 22, 22–34. [Google Scholar] [CrossRef] [PubMed]
[23] Rodríguez-Rodríguez, E.R.; Ledezma-Candanoza, L.M.; Contreras-Ferrat, L.G.; Olamendi-Portugal, T.; Possani, L.D.; Becerril, B.; Riaño-Umbarila, L. A single mutation in framework 2 of the heavy variable domain improves the properties of a diabody and a related single-chain antibody. J. Mol. Biol. 2012, 423, 337–350. [Google Scholar] [CrossRef] [PubMed]
[24] Quintero-Hernández, V.; Del Pozo-Yauner, L.; Pedraza-Escalona, M.; Juárez-González, V.R.; Alcántara-Recillas, I.; Possani, L.D.; Becerril, B. Evaluation of three different formats of a neutralizing single chain human antibody against toxin Cn2: Neutralization capacity versus thermodynamic stability. Immunol. Lett. 2012, 143, 152–160. [Google Scholar] [CrossRef] [PubMed]
[25] Proba, K.; Wörn, A.; Honegger, A.; Plückthun, A. Antibody scFv fragments without disulfide bonds made by molecular evolution. J. Mol. Biol. 1998, 275, 245–253. [Google Scholar] [CrossRef] [PubMed]
[26] Montoliu-Gaya, L.; Murciano-Calles, J.; Martinez, J.C.; Villegas, S. Towards the improvement in stability of an anti-Aβ single-chain variable fragment, scFv-h3D6, as a way to enhance its therapeutic potential. Amyloid 2017, 24, 167–175. [Google Scholar] [CrossRef]
[27] Miklos, A.E.; Kluwe, C.; Der, B.S.; Pai, S.; Sircar, A.; Hughes, R.A.; Berrondo, M.; Xu, J.; Codrea, V.; Buckley, P.E.; et al. Brief Communication Structure-Based Design of Supercharged, Highly Thermoresistant Antibodies. Chem. Biol. 2012, 19, 449–455. [Google Scholar] [CrossRef]
[28] Perchiacca, J.M.; Lee, C.C.; Tessier, P.M. Optimal charged mutations in the complementarity-determining regions that prevent domain antibody aggregation are dependent on the antibody scaffold. Protein Eng. Des. Sel. 2014, 27, 29–39. [Google Scholar] [CrossRef]
[29] Austerberry, J.I.; Dajani, R.; Panova, S.; Roberts, D.; Golovanov, A.P.; Pluen, A.; Van der Walle, C.F.; Uddin, S.; Warwicker, J.; Derrick, J.P.; et al. The effect

of charge mutations on the stability and aggregation of a human single chain Fv fragment. Eur. J. Pharm. Biopharm. 2017, 115, 18–30. [Google Scholar] [CrossRef]
[30] Sakhnini, L.I.; Greisen, P.J.; Wiberg, C.; Bozoky, Z.; Lund, S.; Wolf Perez, A.M.; Karkov, H.S.; Huus, K.; Hansen, J.J.; Bülow, L.; et al. Improving the Developability of an Antigen Binding Fragment by Aspartate Substitutions. Biochemistry 2019, 58, 2750–2759. [Google Scholar] [CrossRef]
[31] Seeliger, D.; Schulz, P.; Litzenburger, T.; Spitz, J.; Hoerer, S.; Blech, M.; Enenkel, B.; Studts, J.M.; Garidel, P.; Karow, A.R. Boosting antibody developability through rational sequence optimization. Mabs 2015, 7, 505–515. [Google Scholar] [CrossRef]
[32] Graille, M. ; Stura, E.A. ; Bossus, M. ; Muller, B.H. ; Letourneur, O. ; Battail-Poirot, N. ; Sibaï, G. ; Gauthier, M. ; Rolland, D. ; Le Du, M.-H. ; et al. Crystal Structure of the Complex between the Monomeric Form of Toxoplasma gondii Surface Antigen 1 (SAG1) and a Monoclonal Antibody that Mimics the Human Immune Response. J. Mol. Biol. 2005, 354, 447–458. [Google Scholar] [CrossRef]
[33] Hannachi, E.; Bouratbine, A.; Mousli, M. Enhancing the detection of Toxoplasma gondii via an anti-SAG1 scFv-alkaline phosphatase immunoconjugate. Biotechnol. Rep. 2019, 23, e00360. [Google Scholar] [CrossRef]
[34] Ehrenmann, F.; Kaas, Q.; Lefranc, M.P. IMGT/3dstructure-DB and IMGT/domaingapalign: A database and a tool for immunoglobulins or antibodies, T cell receptors, MHC, IgSF and MHcSF. Nucleic Acids Res. 2009, 38, 301–307. [Google Scholar] [CrossRef]
[35] Muzard, J.; Adi-Bessalem, S.; Juste, M.; Laraba-Djebari, F.; Aubrey, N.; Billiald, P. Grafting of protein L-binding activity onto recombinant antibody fragments. Anal. Biochem. 2009, 388, 331–338. [Google Scholar] [CrossRef]
[36] Zahid, M.; Loyau, S.; Bouabdelli, M.; Aubrey, N.; Jandrot-Perrus, M.; Billiald, P. Design and reshaping of an scFv directed against human platelet glycoprotein VI with diagnostic potential. Anal. Biochem. 2011, 417, 274–282. [Google Scholar] [CrossRef]
[37] Di Tommaso, A.; Juste, M.O.; Martin-Eauclaire, M.-F.; Dimier-Poisson, I.; Billiald, P.; Aubrey, N. Diabody mixture providing full protection against experimental scorpion envenoming with crude Androctonus australis venom. J. Biol. Chem. 2012, 287, 14149–14156. [Google Scholar] [CrossRef]
[38] Rodrigo, G.; Gruvegård, M.; Van Alstine, J. Antibody Fragments and Their Purification by Protein L Affinity Chromatography. Antibodies 2015, 4, 259–277. [Google Scholar] [CrossRef]
[39] Puligedda, R.D.; Vigdorovich, V.; Kouiavskaia, D.; Sather, D.N.; Dessain, S.K. Human IgA Monoclonal Antibodies That Neutralize Poliovirus, Produced by Hybridomas and Recombinant Expression. Antibodies 2020, 9, 5. [Google Scholar] [CrossRef]
[40] Pommié, C.; Levadoux, S.; Sabatier, R.; Lefranc, G.; Lefranc, M.P. IMGT standardized criteria for statistical analysis of immunoglobulin V-Region amino acid properties. J. Mol. Recognit. 2004, 17, 17–32. [Google Scholar] [CrossRef]

[41] Lee, J.; Kim, M.; Seo, Y.; Lee, Y.; Park, H.; Byun, S.J.; Kwon, M.H. The catalytic activity of a recombinant single chain variable fragment nucleic acid-hydrolysing antibody varies with fusion tag and expression host. Arch. Biochem. Biophys. 2017, 633, 110–117. [Google Scholar] [CrossRef]
[42] Zhang, K.; Geddie, M.L.; Kohli, N.; Kornaga, T.; Kirpotin, D.B.; Jiao, Y.; Rennard, R.; Drummond, D.C.; Nielsen, U.B.; Xu, L.; et al. Comprehensive optimization of a single-chain variable domain antibody fragment as a targeting ligand for a cytotoxic nanoparticle. Mabs 2015, 0862, 42–52. [Google Scholar] [CrossRef]
[43] Weatherill, E.E.; Cain, K.L.; Heywood, S.P.; Compson, J.E.; Heads, J.T.; Adams, R.; Humphreys, D.P. Towards a universal disulphide stabilised single chain Fv format: Importance of interchain disulphide bond location and vLvH orientation. Protein Eng. Des. Sel. 2012, 25, 321–329. [Google Scholar] [CrossRef]
[44] Egan, T.J.; Diem, D.; Weldon, R.; Neumann, T.; Meyer, S.; Urech, D.M. Novel multispecific heterodimeric antibody format allowing modular assembly of variable domain fragments. Mabs 2017, 9, 68–84. [Google Scholar] [CrossRef]
[45] Miller, K.D.; Weaver-Feldhaus, J.; Gray, S.A.; Siegel, R.W.; Feldhaus, M.J. Production, purification, and characterization of human scFv antibodies expressed in Saccharomyces cerevisiae, Pichia pastoris, and Escherichia coli. Protein Expr. Purif. 2005, 42, 255–267. [Google Scholar] [CrossRef]
[46] Aubrey, N.; Devaux, C.; Sizaret, P.Y.; Rochat, H.; Goyffon, M.; Billiald, P. Design and evaluation of a diabody to improve protection against a potent scorpion neurotoxin. Cell. Mol. Life Sci. 2003, 60, 617–628. [Google Scholar] [CrossRef]

5.2. Estudo do Mecanismo de Inibição de um Anticorpo Monoclonal Humanizado (Glenzocimab) em relação ao seu antígeno glicoproteico GPVI (Em processo de submissão - confidencial)

Targeting platelet GPVI with glenzocimab: a novel mechanism for inhibition

Abstract:

Platelet glycoprotein VI (GPVI) is attracting interest as a potential target for the development of new antiplatelet molecules with a low bleeding risk. GPVI binding to vascular collagen initiates thrombus formation and GPVI interactions with fibrin(ogen) promote the growth and stability of the thrombus. In the present study we show that glenzocimab, a clinical stage humanized antibody fragment with high affinity for GPVI, blocks binding of both ligands through a combination of steric hindrance and structural change. A co-crystal of glenzocimab with an extracellular domain of monomeric GPVI was obtained and its structure determined to a resolution of 1.9 Å. The data revealed (i) that glenzocimab binds to the D2 domain of GPVI; GPVI dimerisation was not observed in the crystal structure because glenzocimab prevented D2 homotypic interactions and the formation of dimers which have a high affinity for collagen and fibrin(ogen); (ii) the light variable (VL) domain of the GPVI-bound Fab caused steric hindrance that should prevent the collagen-related peptide (CRP)/collagen fibers from extending out of their binding site; (iii) subtle conformational changes resulted in the CRP-binding groove. Glenzocimab did not bind to a truncated GPVI missing loop residues 129-136, thus validating the epitope identified in the crystal structure. Overall, our findings demonstrated that the binding of glenzocimab to the D2 domain of GPVI induces steric hindrance and subtle structural modifications that drive the inhibition of GPVI interactions with its major ligands.

6. CONCLUSÕES:

Os dados compilados nos estudos aqui apresentados permitem de maneira geral concluir que:

- A humanização de anticorpos monoclonais é delicada e deve considerar uma série de variáveis e critérios de *developability*, bem como parâmetros físico-químico após a produção como rendimento, estabilidade térmica e tolerância a variações de pH e manutenção de funcionalidade. A mutação de certos resíduos de aminoácidos das regiões estruturais, bem como certos formatos de fragmentos aventados podem acarretar uma perda da qualidade dos parâmetros supracitados.
- A conservação de bons parâmetros biofísicos e de funcionalidade em relação à molécula parental pode estar atrelada ao ao *design* da sua sequência de aminoácidos. A utilização de diversos critérios para humanização e consequente geração de um maior número de variantes humanizadas também permite estudos mais consistentes e abrangentes.
- O sistema de expressão de escolha para produção de anticorpos recombinantes bem como o formato dessas moléculas (scFv, diabody, Fab, IgG inteira) tem influência importante no seu rendimento de produção e propriedades biofísicas (estabilidade térmica e química, tolerância a baixos pHs, agregação) e funcionalidade.
- Resíduos de aminoácidos presentes nas regiões estruturais dos domínios de cadeia leve e pesada influenciam diretamente em parâmetros biofísicos em moléculas de anticorpos produzidas de maneira recombinante. Isso foi evidenciado pela mutação pontual de resíduos específicos, que resultou em moléculas com alta identidade, mas com propriedades biofísicas bastante distintas.
- A ligação de um Fab humanizado ao seu alvo e análises *in sílico* do cristal dessa interação, compiladas com dados *in vitro*, sugerem que eventos moleculares como impedimento estérico e indução de mudança conformacional são mecanismos pelos quais este anticorpo provoca a

inibição de seu alvo farmacológico, corroborando com os mecanismos de inibição por anticorpos descritos na literatura.

- O entendimento acerca mecanismos de neutralização de anticorpos permite não só conhecimento da molécula em si, mas futura otimização para desenvolvimento farmacêutico de moléculas inéditas e mais adaptadas.

REFERÊNCIAS:

ABHINANDAN, K. R.; MARTIN, A. C. R. Analyzing the “Degree of Humanness” of Antibody Sequences. **Journal of Molecular Biology**, v. 369, n. 3, p. 852–862, 2007. Disponível em: <https://linkinghub.elsevier.com/retrieve/pii/S0022283607003038>. Acesso em: 6/4/2022.

ABHINANDAN, K. R.; MARTIN, A. C. R. Analysis and prediction of VH/VL packing in antibodies. **Protein engineering, design & selection: PEDS**, v. 23, n. 9, p. 689–697, 2010.

ADLER, A. S.; MIZRAHI, R. A.; SPINDLER, M. J.; et al. Rare, high-affinity anti-pathogen antibodies from human repertoires, discovered using microfluidics and molecular genomics. **mAbs**, v. 9, n. 8, p. 1282–1296, 2017

AHMAD, Z. A.; YEAP, S. K.; ALI, A. M.; et al. scFv antibody: principles and clinical application. **Clinical & Developmental Immunology**, v. 2012, p. 980250, 2012.

AHMADZADEH, V.; FARAJNIA, S.; FEIZI, M. A. H.; NEJAD, R. A. K. Antibody Humanization Methods for Development of Therapeutic Applications. **Monoclonal Antibodies in Immunodiagnosis and Immunotherapy**, v. 33, n. 2, p. 67–73, 2014. Disponível em: <https://www.liebertpub.com/doi/abs/10.1089/mab.2013.0080>. Acesso em: 11/4/2022.

ALEWINE, C.; HASSAN, R.; PASTAN, I. Advances in Anticancer Immunotoxin Therapy. **The Oncologist**, v. 20, n. 2, p. 176–185, 2015

ALMAGRO, J. C.; DANIELS-WELLS, T. R.; PEREZ-TAPIA, S. M.; PENICHET, M. L. Progress and Challenges in the Design and Clinical Development of Antibodies for Cancer Therapy. **Frontiers in Immunology**, v. 8, 2018. Disponível em: <https://www.frontiersin.org/article/10.3389/fimmu.2017.01751>. Acesso em: 14/4/2022.

DE ALMEIDA, D. M.; FERNANDES-PEDROSA, M. DE F.; DE ANDRADE, R. M. G.; et al. A new anti-loxoscelic serum produced against recombinant sphingomyelinase D: results of preclinical trials. **The American Journal of Tropical Medicine and Hygiene**, v. 79, n. 3, p. 463–470, 2008.

ALTSCHUL, S. F.; LIPMAN, D. J. Protein database searches for multiple alignments. **Proceedings of the National Academy of Sciences**, v. 87, n. 14, p. 5509–5513, 1990. Disponível em: <https://pnas.org/doi/full/10.1073/pnas.87.14.5509>. Acesso em: 6/4/2022.

ALVARENGA, L. M.; MARTINS, M. S.; MOURA, J. F.; et al. Production of monoclonal antibodies capable of neutralizing dermonecrotic activity of Loxosceles intermedia spider venom and their use in a specific immunometric assay. **Toxicon**, v. 42, n. 7, p. 725–731, 2003. Disponível em: <https://linkinghub.elsevier.com/retrieve/pii/S0041010103002733>. Acesso em: 6/4/2022.

AMBROSETTI, F.; JIMÉNEZ-GARCÍA, B.; ROEL-TOURIS, J.; BONVIN, A. M. J. J. Modeling Antibody-Antigen Complexes by Information-Driven Docking. **Structure**, v. 28, n. 1, p. 119- 129.e2, 2020. Disponível em: <https://www.cell.com/structure/abstract/S0969-2126(19)30352-1>. Acesso em: 14/4/2022.

APPEL, M. H.; DA SILVEIRA, R. B.; CHAIM, O. M.; et al. Identification, cloning and functional characterization of a novel dermonecrotic toxin (phospholipase D) from brown spider (Loxosceles intermedia) venom. **Biochimica Et Biophysica Acta**, v. 1780, n. 2, p. 167–178, 2008.

APPEL, R. D.; BAIROCH, A.; HOCHSTRASSER, D. F. A new generation of information retrieval tools for biologists: the example of the ExPASy WWW server. **Trends in Biochemical Sciences**, v. 19, n. 6, p. 258–260, 1994. Disponível em: <https://linkinghub.elsevier.com/retrieve/pii/0968000494901538>. Acesso em: 6/4/2022.

AUBREY, N.; BILLIALD, P. Antibody Fragments Humanization: Beginning with the End in Mind. In: M. Steinitz (Org.); **Human Monoclonal Antibodies**. v. 1904, p.231–252, 2019. New York, NY: Springer New York. Disponível em: <http://link.springer.com/10.1007/978-1-4939-8958-4_10>. Acesso em: 6/4/2022.

AUBREY, N.; DEVAUX, C.; SIZARET, P.-Y.; et al. Design and evaluation of a diabody to improve protection against a potent scorpion neurotoxin. **Cellular and Molecular Life Sciences (CMLS)**, v. 60, n. 3, p. 617–628, 2003. Disponível em: <http://link.springer.com/10.1007/s000180300053>. Acesso em: 6/4/2022.

AUSTERBERRY, J. I.; DAJANI, R.; PANOVA, S.; et al. The effect of charge mutations on the stability and aggregation of a human single chain Fv fragment. **European Journal of Pharmaceutics and Biopharmaceutics**, v. 115, p. 18–30, 2017. Disponível em: <https://linkinghub.elsevier.com/retrieve/pii/S0939641116304350>. Acesso em: 6/4/2022.

BAILLY, M.; MIECZKOWSKI, C.; JUAN, V.; et al. Predicting Antibody Developability Profiles Through Early Stage Discovery Screening. **mAbs**, v. 12, n. 1, p. 1743053, 2020. Disponível em: <https://www.ncbi.nlm.nih.gov/pmc/articles/PMC7153844/>. Acesso em: 11/4/2022.

BATES, A.; POWER, C. A. David vs. Goliath: The Structure, Function, and Clinical Prospects of Antibody Fragments. **Antibodies**, v. 8, n. 2, p. 28, 2019. Disponível em: <https://www.mdpi.com/2073-4468/8/2/28>. Acesso em: 7/4/2022.

BECK, A.; WURCH, T.; BAILLY, C.; CORVAIA, N. Strategies and challenges for the next generation of therapeutic antibodies. **Nature Reviews Immunology**, v. 10, n. 5, p. 345–352, 2010. Disponível em: <https://www.nature.com/articles/nri2747>. Acesso em: 8/4/2022.

BERTONI DA SILVEIRA, R.; PIGOZZO, R. B.; CHAIM, O. M.; et al. Molecular cloning and functional characterization of two isoforms of dermonecrotic toxin from Loxosceles intermedia (Brown spider) venom gland. **Biochimie**, v. 88, n. 9, p. 1241–1253, 2006.

Disponível em: <https://linkinghub.elsevier.com/retrieve/pii/S0300908406000253>. Acesso em: 6/4/2022.

BHOSKAR, P.; BELONGIA, B.; SMITH, R.; et al. Free light chain content in culture media reflects recombinant monoclonal antibody productivity and quality. **Biotechnology Progress**, v. 29, n. 5, p. 1131–1139, 2013. Disponível em: <https://onlinelibrary.wiley.com/doi/10.1002/btpr.1767>. Acesso em: 6/4/2022.

BRENKE, R.; HALL, D. R.; CHUANG, G.-Y.; et al. Application of asymmetric statistical potentials to antibody–protein docking. **Bioinformatics**, v. 28, n. 20, p. 2608–2614, 2012. Disponível em: <https://academic.oup.com/bioinformatics/article/28/20/2608/203109>. Acesso em: 6/4/2022.

BRINKMANN, U.; KONTERMANN, R. E. The making of bispecific antibodies. **mAbs**, v. 9, n. 2, p. 182–212, 2017. Disponível em: <https://www.tandfonline.com/doi/full/10.1080/19420862.2016.1268307>. Acesso em: 6/4/2022.

CARTER, P. Improving the efficacy of antibody-based cancer therapies. **Nature Reviews Cancer**, v. 1, n. 2, p. 118–129, 2001. Disponível em: <https://www.nature.com/articles/35101072>. Acesso em: 8/4/2022.

CARTER, P.; PRESTA, L.; GORMAN, C. M.; et al. Humanization of an anti-p185HER2 antibody for human cancer therapy. **Proceedings of the National Academy of Sciences**, v. 89, n. 10, p. 4285–4289, 1992. Disponível em: <https://pnas.org/doi/full/10.1073/pnas.89.10.4285>. Acesso em: 6/4/2022.

CASADEVALL, A.; DADACHOVA, E.; PIROFSKI, L. Passive antibody therapy for infectious diseases. **Nature Reviews Microbiology**, v. 2, n. 9, p. 695–703, 2004. Disponível em: <https://www.nature.com/articles/nrmicro974>. Acesso em: 1/5/2022.

CHAMES, P.; VAN REGENMORTEL, M.; WEISS, E.; BATY, D. Therapeutic antibodies: successes, limitations and hopes for the future: Therapeutic antibodies: an update. **British Journal of Pharmacology**, v. 157, n. 2, p. 220–233, 2009. Disponível em: <https://onlinelibrary.wiley.com/doi/10.1111/j.1476-5381.2009.00190.x>. Acesso em: 6/4/2022.

CHAVES-MOREIRA, D.; CHAIM, O. M.; SADE, Y. B.; et al. Identification of a direct hemolytic effect dependent on the catalytic activity induced by phospholipase-D (dermonecrotic toxin) from brown spider venom. **Journal of Cellular Biochemistry**, v. 107, n. 4, p. 655–666, 2009. Disponível em: <https://onlinelibrary.wiley.com/doi/10.1002/jcb.22148>. Acesso em: 6/4/2022.

CHAVES-MOREIRA, D.; SENFF-RIBEIRO, A.; WILLE, A. C. M.; et al. Highlights in the knowledge of brown spider toxins. **Journal of Venomous Animals and Toxins including Tropical Diseases**, v. 23, n. 1, p. 6, 2017. Disponível em: <http://jvat.biomedcentral.com/articles/10.1186/s40409-017-0097-8>. Acesso em: 6/4/2022.

CHIU, M. L.; GOULET, D. R.; TEPLYAKOV, A.; GILLILAND, G. L. Antibody Structure and Function: The Basis for Engineering Therapeutics. **Antibodies**, v. 8, n. 4, p. 55, 2019. Disponível em: <https://www.mdpi.com/2073-4468/8/4/55>. Acesso em: 6/4/2022.

CHOI, Y.; HUA, C.; SENTMAN, C. L.; ACKERMAN, M. E.; BAILEY-KELLOGG, C. Antibody humanization by structure-based computational protein design. **mAbs**, v. 7, n. 6, p. 1045–1057, 2015. Disponível em: <http://www.tandfonline.com/doi/full/10.1080/19420862.2015.1076600>. Acesso em: 6/4/2022.

CNUDDE, T.; LAKHRIF, Z.; BOURGOIN, J.; et al. Exploration and Modulation of Antibody Fragment Biophysical Properties by Replacing the Framework Region Sequences. **Antibodies**, v. 9, n. 2, p. 9, 2020. Disponível em: <https://www.mdpi.com/2073-4468/9/2/9>. Acesso em: 6/4/2022.

CORDEIRO, F. A.; AMORIM, F. G.; ANJOLETTE, F. A. P.; ARANTES, E. C. Arachnids of medical importance in Brazil: main active compounds present in scorpion and spider venoms and tick saliva. **Journal of Venomous Animals and Toxins including Tropical Diseases**, v. 21, n. 1, p. 24, 2015. Disponível em: <http://www.jvat.org/content/21/1/24>. Acesso em: 6/4/2022.

CORONADO, M. A.; ULLAH, A.; DA SILVA, L. S.; et al. Structural Insights into Substrate Binding of Brown Spider Venom Class II Phospholipases D. **Current Protein & Peptide Science**, v. 16, n. 8, p. 768–774, 2015.

CORPET, F.; GOUZY, J.; KAHN, D. Browsing protein families via the “Rich Family Description” format. **Bioinformatics (Oxford, England)**, v. 15, n. 12, p. 1020–1027, 1999.

COURTOIS, F.; AGRAWAL, N. J.; LAUER, T. M.; TROUT, B. L. Rational design of therapeutic mAbs against aggregation through protein engineering and incorporation of glycosylation motifs applied to bevacizumab. **mAbs**, v. 8, n. 1, p. 99–112, 2016. Disponível em: <https://www.tandfonline.com/doi/full/10.1080/19420862.2015.1112477>. Acesso em: 6/4/2022.

DEVAUX, C.; MOREAU, E.; GOYFFON, M.; ROCHAT, H.; BILLIALD, P. Construction and functional evaluation of a single-chain antibody fragment that neutralizes toxin AahI from the venom of the scorpion Androctonus australis hector. **European Journal of Biochemistry**, v. 268, n. 3, p. 694–702, 2001.

DIAS-LOPES, C.; FELICORI, L.; RUBRECHT, L.; et al. Generation and molecular characterization of a monoclonal antibody reactive with conserved epitope in sphingomyelinases D from Loxosceles spider venoms. **Vaccine**, v. 32, n. 18, p. 2086–2092, 2014. Disponível em: <https://linkinghub.elsevier.com/retrieve/pii/S0264410X14001856>. Acesso em: 6/4/2022.

DIAS-LOPES, C.; GUIMARÃES, G.; FELICORI, L.; et al. A protective immune response against lethal, dermonecrotic and hemorrhagic effects of Loxosceles

intermedia venom elicited by a 27-residue peptide. **Toxicon**, v. 55, n. 2–3, p. 481–487, 2010. Disponível em: <https://linkinghub.elsevier.com/retrieve/pii/S004101010900470X>. Acesso em: 6/4/2022.

DIAS-LOPES, C.; NESHICH, I. A. P.; NESHICH, G.; et al. Identification of New Sphingomyelinases D in Pathogenic Fungi and Other Pathogenic Organisms. (E. A. Permyakov, Org.)**PLoS ONE**, v. 8, n. 11, p. e79240, 2013. Disponível em: <https://dx.plos.org/10.1371/journal.pone.0079240>. Acesso em: 6/4/2022.

DOEVENDANS, E.; SCHELLEKENS, H. Immunogenicity of Innovative and Biosimilar Monoclonal Antibodies. **Antibodies**, v. 8, n. 1, p. 21, 2019. Disponível em: <https://www.mdpi.com/2073-4468/8/1/21>. Acesso em: 6/4/2022.

DONDELINGER, M.; FILÉE, P.; SAUVAGE, E.; et al. Understanding the Significance and Implications of Antibody Numbering and Antigen-Binding Surface/Residue Definition. **Frontiers in Immunology**, v. 9, p. 2278, 2018. Disponível em: <https://www.frontiersin.org/article/10.3389/fimmu.2018.02278/full>. Acesso em: 6/4/2022.

Drugs@FDA: FDA-Approved Drugs. .Disponível em: <https://www.accessdata.fda.gov/scripts/cder/daf/>. Acesso em: 7/4/2022.

DUARTE, C. G.; BONILLA, C.; GUIMARÃES, G.; et al. Anti-loxoscelic horse serum produced against a recombinant dermonecrotic protein of Brazilian Loxosceles intermedia spider neutralize lethal effects of Loxosceles laeta venom from Peru. **Toxicon: Official Journal of the International Society on Toxinology**, v. 93, p. 37–40, 2015.

DUCANCEL, F.; MULLER, B. H. Molecular engineering of antibodies for therapeutic and diagnostic purposes. **mAbs**, v. 4, n. 4, p. 445–457, 2012. Disponível em: <http://www.tandfonline.com/doi/abs/10.4161/mabs.20776>. Acesso em: 6/4/2022.

EGAN, T. J.; DIEM, D.; WELDON, R.; et al. Novel multispecific heterodimeric antibody format allowing modular assembly of variable domain fragments. **mAbs**, v. 9, n. 1, p. 68–84, 2017. Disponível em: <https://www.tandfonline.com/doi/full/10.1080/19420862.2016.1248012>. Acesso em: 6/4/2022.

EHRENMANN, F.; KAAS, Q.; LEFRANC, M.-P. IMGT/3Dstructure-DB and IMGT/DomainGapAlign: a database and a tool for immunoglobulins or antibodies, T cell receptors, MHC, IgSF and MhcSF. **Nucleic Acids Research**, v. 38, n. suppl_1, p. D301–D307, 2010. Disponível em: <https://academic.oup.com/nar/article-lookup/doi/10.1093/nar/gkp946>. Acesso em: 6/4/2022.

EHRENMANN, F.; LEFRANC, M.-P. IMGT/DomainGapAlign: IMGT standardized analysis of amino acid sequences of variable, constant, and groove domains (IG, TR, MH, IgSF, MhSF). **Cold Spring Harbor Protocols**, v. 2011, n. 6, p. 737–749, 2011.

EL-SAYED, A.; BERNHARD, W.; BARRETO, K.; et al. Evaluation of antibody fragment properties for near-infrared fluorescence imaging of HER3-positive cancer xenografts.

Theranostics, v. 8, n. 17, p. 4856–4869, 2018. Disponível em: <http://www.thno.org/v08p4856.htm>. Acesso em: 6/4/2022.

ENGMARK, M.; ANDERSEN, M. R.; LAUSTSEN, A. H.; et al. High-throughput immuno-profiling of mamba (Dendroaspis) venom toxin epitopes using high-density peptide microarrays. **Scientific Reports**, v. 6, n. 1, p. 36629, 2016. Disponível em: <http://www.nature.com/articles/srep36629>. Acesso em: 6/4/2022.

FELICORI, L.; ARAUJO, S. C.; DE AVILA, R. A. M.; et al. Functional characterization and epitope analysis of a recombinant dermonecrotic protein from Loxosceles intermedia spider. **Toxicon: Official Journal of the International Society on Toxinology**, v. 48, n. 5, p. 509–519, 2006.

FELICORI, L.; FERNANDES, P. B.; GIUSTA, M. S.; et al. An in vivo protective response against toxic effects of the dermonecrotic protein from Loxosceles intermedia spider venom elicited by synthetic epitopes. **Vaccine**, v. 27, n. 31, p. 4201–4208, 2009.

FERNANDES, C. F. C.; PEREIRA, S. DOS S.; LUIZ, M. B.; et al. Camelid Single-Domain Antibodies As an Alternative to Overcome Challenges Related to the Prevention, Detection, and Control of Neglected Tropical Diseases. **Frontiers in Immunology**, v. 8, 2017a. Disponível em: <https://www.frontiersin.org/article/10.3389/fimmu.2017.00653>. Acesso em: 16/4/2022.

FERNANDES, C. F. C.; PEREIRA, S. DOS S.; LUIZ, M. B.; et al. Camelid Single-Domain Antibodies As an Alternative to Overcome Challenges Related to the Prevention, Detection, and Control of Neglected Tropical Diseases. **Frontiers in Immunology**, v. 8, 2017b. Disponível em: <https://www.frontiersin.org/article/10.3389/fimmu.2017.00653>. Acesso em: 16/4/2022.

FERNANDES PEDROSA, M. DE F.; JUNQUEIRA DE AZEVEDO, I. DE L. M.; GONÇALVES-DE-ANDRADE, R. M.; et al. Molecular cloning and expression of a functional dermonecrotic and haemolytic factor from Loxosceles laeta venom. **Biochemical and Biophysical Research Communications**, v. 298, n. 5, p. 638–645, 2002. Disponível em: <https://linkinghub.elsevier.com/retrieve/pii/S0006291X02025214>. Acesso em: 6/4/2022.

FERNÁNDEZ-MARRERO, Y.; ROQUE-NAVARRO, L.; HERNÁNDEZ, T.; et al. A cytotoxic humanized anti-ganglioside antibody produced in a murine cell line defective of N-glycolylated-glycoconjugates. **Immunobiology**, v. 216, n. 12, p. 1239–1247, 2011. Disponível em: <https://linkinghub.elsevier.com/retrieve/pii/S0171298511001355>. Acesso em: 6/4/2022.

FERNÁNDEZ-QUINTERO, M. L.; HEISS, M. C.; LIEDL, K. R. Antibody humanization—the Influence of the antibody framework on the CDR-H3 loop ensemble in solution. **Protein Engineering, Design and Selection**, v. 32, n. 9, p.

411–422, 2019. Disponível em: <https://academic.oup.com/peds/article/32/9/411/5780185>. Acesso em: 6/4/2022.

FERNÁNDEZ-QUINTERO, M. L.; KROELL, K. B.; HOFER, F.; RICCABONA, J. R.; LIEDL, K. R. Mutation of Framework Residue H71 Results in Different Antibody Paratope States in Solution. **Frontiers in Immunology**, v. 12, p. 630034, 2021. Disponível em: <https://www.frontiersin.org/articles/10.3389/fimmu.2021.630034/full>. Acesso em: 6/4/2022.

FIGUEIREDO, L. F. M.; DIAS-LOPES, C.; ALVARENGA, L. M.; et al. Innovative immunization protocols using chimeric recombinant protein for the production of polyspecific loxoscelic antivenom in horses. **Toxicon**, v. 86, p. 59–67, 2014. Disponível em: <https://linkinghub.elsevier.com/retrieve/pii/S0041010114001330>. Acesso em: 6/4/2022.

FLEMING, A. THE DISCOVERY OF PENICILLIN. **British Medical Bulletin**, v. 2, n. 1, p. 4–5, 1944. Disponível em: <https://academic.oup.com/bmb/article-lookup/doi/10.1093/oxfordjournals.bmb.a071032>. Acesso em: 1/5/2022.

FOGAÇA, R. L.; ALVARENGA, L. M.; WOISKI, T. D.; et al. Biomolecular engineering of antidehydroepiandrosterone antibodies: a new perspective in cancer diagnosis and treatment using single-chain antibody variable fragment. **Nanomedicine**, v. 14, n. 6, p. 689–705, 2019. Disponível em: <https://www.futuremedicine.com/doi/10.2217/nnm-2018-0230>. Acesso em: 6/4/2022.

FORTHAL, D. N. Functions of Antibodies. (J. E. Crowe Jr., D. Boraschi, & R. Rappuoli, Orgs.)**Microbiology Spectrum**, v. 2, n. 4, p. 2.4.21, 2014. Disponível em: <https://journals.asm.org/doi/10.1128/microbiolspec.AID-0019-2014>. Acesso em: 1/5/2022.

FRENZEL, A.; HUST, M.; SCHIRRMANN, T. Expression of Recombinant Antibodies. **Frontiers in Immunology**, v. 4, 2013. Disponível em: <https://www.frontiersin.org/article/10.3389/fimmu.2013.00217>. Acesso em: 6/4/2022.

GAO, S. H.; HUANG, K.; TU, H.; ADLER, A. S. Monoclonal antibody humanness score and its applications. **BMC Biotechnology**, v. 13, n. 1, p. 55, 2013. Disponível em: <https://bmcbiotechnol.biomedcentral.com/articles/10.1186/1472-6750-13-55>. Acesso em: 6/4/2022.

GETTS, D. R.; GETTS, M. T.; MCCARTHY, D. P.; CHASTAIN, E. M.; MILLER, S. D. Have we overestimated the benefit of human(ized) antibodies? **mAbs**, v. 2, n. 6, p. 682–694, 2010. Disponível em: <https://www.ncbi.nlm.nih.gov/pmc/articles/PMC3011222/>. Acesso em: 14/4/2022.

DE GIUSEPPE, P. O.; ULLAH, A.; SILVA, D. T.; et al. Structure of a novel class II phospholipase D: Catalytic cleft is modified by a disulphide bridge. **Biochemical and Biophysical Research Communications**, v. 409, n. 4, p. 622–627, 2011. Disponível

em: <https://linkinghub.elsevier.com/retrieve/pii/S0006291X11008205>. Acesso em: 6/4/2022.

GOULET, D. R.; ATKINS, W. M. Considerations for the Design of Antibody-Based Therapeutics. **Journal of Pharmaceutical Sciences**, v. 109, n. 1, p. 74–103, 2020. Disponível em: <https://jpharmsci.org/article/S0022-3549(19)30364-8/fulltext>. Acesso em: 1/5/2022.

GOULET, D. R.; CHATTERJEE, S.; LEE, W.-P.; et al. Engineering an Enhanced EGFR Engager: Humanization of Cetuximab for Improved Developability. **Antibodies**, v. 11, n. 1, p. 6, 2022. Disponível em: <https://www.mdpi.com/2073-4468/11/1/6>. Acesso em: 14/4/2022.

GRAILLE, M.; STURA, E. A.; BOSSUS, M.; et al. Crystal structure of the complex between the monomeric form of Toxoplasma gondii surface antigen 1 (SAG1) and a monoclonal antibody that mimics the human immune response. **Journal of Molecular Biology**, v. 354, n. 2, p. 447–458, 2005.

GREMSKI, L. H.; DA JUSTA, H. C.; DA SILVA, T. P.; et al. Forty Years of the Description of Brown Spider Venom Phospholipases-D. **Toxins**, v. 12, n. 3, p. E164, 2020.

GREMSKI, L. H.; DA SILVEIRA, R. B.; CHAIM, O. M.; et al. A novel expression profile of the Loxosceles intermedia spider venomous gland revealed by transcriptome analysis. **Molecular bioSystems**, v. 6, n. 12, p. 2403–2416, 2010.

GREMSKI, L. H.; TREVISAN-SILVA, D.; FERRER, V. P.; et al. Recent advances in the understanding of brown spider venoms: From the biology of spiders to the molecular mechanisms of toxins. **Toxicon: Official Journal of the International Society on Toxinology**, v. 83, p. 91–120, 2014.

GRONEMEYER, P.; DITZ, R.; STRUBE, J. Trends in Upstream and Downstream Process Development for Antibody Manufacturing. **Bioengineering**, v. 1, n. 4, p. 188–212, 2014. Disponível em: <http://www.mdpi.com/2306-5354/1/4/188>. Acesso em: 11/4/2022.

GUILHERME, P.; FERNANDES, I.; BARBARO, K. C. Neutralization of dermonecrotic and lethal activities and differences among 32–35 kDa toxins of medically important Loxosceles spider venoms in Brazil revealed by monoclonal antibodies. **Toxicon**, v. 39, n. 9, p. 1333–1342, 2001. Disponível em: <https://linkinghub.elsevier.com/retrieve/pii/S004101010100085X>. Acesso em: 6/4/2022.

HANNACHI, E.; BOURATBINE, A.; MOUSLI, M. Enhancing the detection of Toxoplasma gondii via an anti-SAG1 scFv-alkaline phosphatase immunoconjugate. **Biotechnology Reports**, v. 23, p. e00360, 2019. Disponível em: <https://linkinghub.elsevier.com/retrieve/pii/S2215017X19302474>. Acesso em: 6/4/2022.

HARDING, F. A.; STICKLER, M. M.; RAZO, J.; DUBRIDGE, R. The immunogenicity of humanized and fully human antibodies: Residual immunogenicity resides in the

CDR regions. **mAbs**, v. 2, n. 3, p. 256–265, 2010. Disponível em: <http://www.tandfonline.com/doi/abs/10.4161/mabs.2.3.11641>. Acesso em: 6/4/2022.

HE, X.; DUAN, C. F.; QI, Y. H.; et al. Erratum to “Virtual mutation and directional evolution of anti-amoxicillin ScFv antibody for immunoassay of penicillins in milk” [Anal. Biochem. 517 (2017) 9–17]. **Analytical Biochemistry**, v. 523, p. 44–45, 2017. Disponível em: <https://linkinghub.elsevier.com/retrieve/pii/S0003269717300623>. Acesso em: 6/4/2022.

HEBDITCH, M.; KEAN, R.; WARWICKER, J. Modelling of pH-dependence to develop a strategy for stabilising mAbs at acidic steps in production. **Computational and Structural Biotechnology Journal**, v. 18, p. 897–905, 2020. Disponível em: <https://linkinghub.elsevier.com/retrieve/pii/S2001037019302995>. Acesso em: 6/4/2022.

HOGAN, C. J.; BARBARO, K. C.; WINKEL, K. Loxoscelism: old obstacles, new directions. **Annals of Emergency Medicine**, v. 44, n. 6, p. 608–624, 2004.

HOLLIGER, P.; HUDSON, P. J. Engineered antibody fragments and the rise of single domains. **Nature Biotechnology**, v. 23, n. 9, p. 1126–1136, 2005. Disponível em: <http://www.nature.com/articles/nbt1142>. Acesso em: 6/4/2022.

HONEGGER, A.; MALEBRANCHE, A. D.; RÖTHLISBERGER, D.; PLÜCKTHUN, A. The influence of the framework core residues on the biophysical properties of immunoglobulin heavy chain variable domains. **Protein Engineering, Design and Selection**, v. 22, n. 3, p. 121–134, 2009. Disponível em: <https://academic.oup.com/peds/article-lookup/doi/10.1093/protein/gzn077>. Acesso em: 8/4/2022.

HONEGGER, A.; PLÜCKTHUN, A. Yet Another Numbering Scheme for Immunoglobulin Variable Domains: An Automatic Modeling and Analysis Tool. **Journal of Molecular Biology**, v. 309, n. 3, p. 657–670, 2001. Disponível em: <https://linkinghub.elsevier.com/retrieve/pii/S0022283601946625>. Acesso em: 6/4/2022.

HSU, H.-J.; LEE, K. H.; JIAN, J.-W.; et al. Antibody variable domain interface and framework sequence requirements for stability and function by high-throughput experiments. **Structure (London, England: 1993)**, v. 22, n. 1, p. 22–34, 2014.

IGAWA, T.; MIMOTO, F.; HATTORI, K. pH-dependent antigen-binding antibodies as a novel therapeutic modality. **Biochimica et Biophysica Acta (BBA) - Proteins and Proteomics**, v. 1844, n. 11, p. 1943–1950, 2014. Disponível em: <https://linkinghub.elsevier.com/retrieve/pii/S1570963914002015>. Acesso em: 6/4/2022.

ISBISTER, G. K.; FAN, H. W. Spider bite. **The Lancet**, v. 378, n. 9808, p. 2039–2047, 2011. Disponível em: <https://linkinghub.elsevier.com/retrieve/pii/S0140673610622301>. Acesso em: 6/4/2022.

JAIN, T.; SUN, T.; DURAND, S.; et al. Biophysical properties of the clinical-stage antibody landscape. **Proceedings of the National Academy of Sciences**, v. 114, n. 5, p. 944–949, 2017. Disponível em: <https://pnas.org/doi/full/10.1073/pnas.1616408114>. Acesso em: 6/4/2022.

JARASCH, A.; KOLL, H.; REGULA, J. T.; et al. Developability Assessment During the Selection of Novel Therapeutic Antibodies. **Journal of Pharmaceutical Sciences**, v. 104, n. 6, p. 1885–1898, 2015. Disponível em: <https://www.sciencedirect.com/science/article/pii/S0022354915300848>. Acesso em: 7/4/2022.

JENKINS, T. P.; LAUSTSEN, A. H. Cost of Manufacturing for Recombinant Snakebite Antivenoms. **Frontiers in Bioengineering and Biotechnology**, v. 8, 2020. Disponível em: <https://www.frontiersin.org/article/10.3389/fbioe.2020.00703>. Acesso em: 6/4/2022.

JERABEK-WILLEMSEN, M.; WIENKEN, C. J.; BRAUN, D.; BAASKE, P.; DUHR, S. Molecular interaction studies using microscale thermophoresis. **Assay and Drug Development Technologies**, v. 9, n. 4, p. 342–353, 2011.

JIACOMINI, I.; SILVA, S. K.; AUBREY, N.; et al. Immunodetection of the “brown” spider (Loxosceles intermedia) dermonecrotoxin with an scFv-alkaline phosphatase fusion protein. **Immunology Letters**, v. 173, p. 1–6, 2016. Disponível em: <https://linkinghub.elsevier.com/retrieve/pii/S0165247816300268>. Acesso em: 6/4/2022.

JIANG, X.-R.; SONG, A.; BERGELSON, S.; et al. Advances in the assessment and control of the effector functions of therapeutic antibodies. **Nature Reviews Drug Discovery**, v. 10, n. 2, p. 101–111, 2011. Disponível em: <https://www.nature.com/articles/nrd3365>. Acesso em: 7/4/2022.

KALAPOTHAKIS, E.; ARAUJO, S. C.; DE CASTRO, C. S.; et al. Molecular cloning, expression and immunological properties of LiD1, a protein from the dermonecrotic family of Loxosceles intermedia spider venom. **Toxicon**, v. 40, n. 12, p. 1691–1699, 2002. Disponível em: <https://linkinghub.elsevier.com/retrieve/pii/S0041010102002015>. Acesso em: 6/4/2022.

VAN DER KANT, R.; KAROW-ZWICK, A. R.; VAN DURME, J.; et al. Prediction and Reduction of the Aggregation of Monoclonal Antibodies. **Journal of Molecular Biology**, v. 429, n. 8, p. 1244–1261, 2017. Disponível em: <https://linkinghub.elsevier.com/retrieve/pii/S0022283617301183>. Acesso em: 6/4/2022.

KARIM-SILVA, S.; BECKER-FINCO, A.; JIACOMINI, I. G.; et al. Loxoscelism: Advances and Challenges in the Design of Antibody Fragments with Therapeutic Potential. **Toxins**, v. 12, n. 4, p. 256, 2020. Disponível em: <https://www.mdpi.com/2072-6651/12/4/256>. Acesso em: 6/4/2022.

KARIM-SILVA, S.; MOURA, J. DE; NOIRAY, M.; et al. Generation of recombinant antibody fragments with toxin-neutralizing potential in loxoscelism. **Immunology**

Letters, v. 176, p. 90–96, 2016. Disponível em: <https://linkinghub.elsevier.com/retrieve/pii/S0165247816301043>. Acesso em: 6/4/2022.

KÖHLER, G.; MILSTEIN, C. Continuous cultures of fused cells secreting antibody of predefined specificity. **Nature**, v. 256, n. 5517, p. 495–497, 1975. Disponível em: <https://www.nature.com/articles/256495a0>. Acesso em: 7/4/2022.

KOZAKOV, D.; HALL, D. R.; XIA, B.; et al. The ClusPro web server for protein–protein docking. **Nature Protocols**, v. 12, n. 2, p. 255–278, 2017. Disponível em: <https://www.nature.com/articles/nprot.2016.169>. Acesso em: 6/4/2022.

KRISHNA, M.; NADLER, S. G. Immunogenicity to Biotherapeutics – The Role of Anti-drug Immune Complexes. **Frontiers in Immunology**, v. 7, 2016.

KUMAR, R.; PARRAY, H. A.; SHRIVASTAVA, T.; SINHA, S.; LUTHRA, K. Phage display antibody libraries: A robust approach for generation of recombinant human monoclonal antibodies. **International Journal of Biological Macromolecules**, v. 135, p. 907–918, 2019.

KUNERT, R.; REINHART, D. Advances in recombinant antibody manufacturing. **Applied Microbiology and Biotechnology**, v. 100, n. 8, p. 3451–3461, 2016. Disponível em: <http://link.springer.com/10.1007/s00253-016-7388-9>. Acesso em: 6/4/2022.

LAJOIE, D. M.; ROBERTS, S. A.; ZOBEL-THROPP, P. A.; et al. Variable Substrate Preference among Phospholipase D Toxins from Sicariid Spiders. **Journal of Biological Chemistry**, v. 290, n. 17, p. 10994–11007, 2015. Disponível em: <https://linkinghub.elsevier.com/retrieve/pii/S0021925820426262>. Acesso em: 6/4/2022.

LAKHRIF, Z.; PUGNIÈRE, M.; HENRIQUET, C.; et al. A method to confer Protein L binding ability to any antibody fragment. **mAbs**, v. 8, n. 2, p. 379–388, 2016. Disponível em: <https://www.tandfonline.com/doi/full/10.1080/19420862.2015.1116657>. Acesso em: 6/4/2022.

LASKOWSKI, R. A.; WATSON, J. D.; THORNTON, J. M. Protein function prediction using local 3D templates. **Journal of Molecular Biology**, v. 351, n. 3, p. 614–626, 2005.

LASTRA, J. M. P. DE LA; BACA-GONZÁLEZ, V.; GONZÁLEZ-ACOSTA, S.; et al. Antibodies targeting enzyme inhibition as potential tools for research and drug development. **Biomolecular Concepts**, v. 12, n. 1, p. 215–232, 2021. Disponível em: <https://www.degruyter.com/document/doi/10.1515/bmc-2021-0021/html>. Acesso em: 1/5/2022.

LAUSTSEN, A. H.; KARATT-VELLATT, A.; MASTERS, E. W.; et al. In vivo neutralization of dendrotoxin-mediated neurotoxicity of black mamba venom by oligoclonal human IgG antibodies. **Nature Communications**, v. 9, n. 1, p. 3928, 2018a.

LAUSTSEN, A. H.; MARÍA GUTIÉRREZ, J.; KNUDSEN, C.; et al. Pros and cons of different therapeutic antibody formats for recombinant antivenom development. **Toxicon**, v. 146, p. 151–175, 2018b. Disponível em: <https://linkinghub.elsevier.com/retrieve/pii/S0041010118301144>. Acesso em: 6/4/2022.

LAUSTSEN, A.; SOLÀ, M.; JAPPE, E.; et al. Biotechnological Trends in Spider and Scorpion Antivenom Development. **Toxins**, v. 8, n. 8, p. 226, 2016. Disponível em: <http://www.mdpi.com/2072-6651/8/8/226>. Acesso em: 6/4/2022.

LAWRENCE, P. B.; PRICE, J. L. How PEGylation influences protein conformational stability. **Current Opinion in Chemical Biology**, v. 34, p. 88–94, 2016. Disponível em: <https://linkinghub.elsevier.com/retrieve/pii/S136759311630103X>. Acesso em: 6/4/2022.

LEAVY, O. Therapeutic antibodies: past, present and future. **Nature Reviews Immunology**, v. 10, n. 5, p. 297–297, 2010. Disponível em: <https://www.nature.com/articles/nri2763>. Acesso em: 7/4/2022.

LEBOZEC, K.; JANDROT-PERRUS, M.; AVENARD, G.; FAVRE-BULLE, O.; BILLIALD, P. Design, development and characterization of ACT017, a humanized Fab that blocks platelet's glycoprotein VI function without causing bleeding risks. **mAbs**, v. 9, n. 6, p. 945–958, 2017. Disponível em: <https://www.tandfonline.com/doi/full/10.1080/19420862.2017.1336592>. Acesso em: 6/4/2022.

LEBOZEC, K.; JANDROT-PERRUS, M.; AVENARD, G.; FAVRE-BULLE, O.; BILLIALD, P. Quality and cost assessment of a recombinant antibody fragment produced from mammalian, yeast and prokaryotic host cells: A case study prior to pharmaceutical development. **New Biotechnology**, v. 44, p. 31–40, 2018. Disponível em: <https://linkinghub.elsevier.com/retrieve/pii/S1871678418300529>. Acesso em: 6/4/2022.

LEE, C. C.; PERCHIACCA, J. M.; TESSIER, P. M. Toward aggregation-resistant antibodies by design. **Trends in Biotechnology**, v. 31, n. 11, p. 612–620, 2013. Disponível em: <https://linkinghub.elsevier.com/retrieve/pii/S0167779913001601>. Acesso em: 6/4/2022.

LEE, J.; KIM, M.; SEO, Y.; et al. The catalytic activity of a recombinant single chain variable fragment nucleic acid-hydrolysing antibody varies with fusion tag and expression host. **Archives of Biochemistry and Biophysics**, v. 633, p. 110–117, 2017. Disponível em: <https://linkinghub.elsevier.com/retrieve/pii/S0003986117304150>. Acesso em: 6/4/2022.

LEDSGAARD, L.; KILSTRUP, M.; KARATT-VELLATT, A.; MCCAFFERTY, J.; LAUSTSEN, A. H. Basics of Antibody Phage Display Technology. **Toxins**, v. 10, n. 6, p. 236, 2018

LI, J.; ZHU, Z. Research and development of next generation of antibody-based therapeutics. **Acta Pharmacologica Sinica**, v. 31, n. 9, p. 1198–1207, 2010. Disponível em: <http://www.nature.com/articles/aps2010120>. Acesso em: 6/4/2022.

LIMA, S. DE A.; GUERRA-DUARTE, C.; COSTAL-OLIVEIRA, F.; et al. Recombinant Protein Containing B-Cell Epitopes of Different Loxosceles Spider Toxins Generates Neutralizing Antibodies in Immunized Rabbits. **Frontiers in Immunology**, v. 9, p. 653, 2018. Disponível em: <http://journal.frontiersin.org/article/10.3389/fimmu.2018.00653/full>. Acesso em: 6/4/2022.

LING, W.-L.; LUA, W.-H.; POH, J.-J.; et al. Effect of VH–VL Families in Pertuzumab and Trastuzumab Recombinant Production, Her2 and FcγIIA Binding. **Frontiers in Immunology**, v. 9, p. 469, 2018. Disponível em: <http://journal.frontiersin.org/article/10.3389/fimmu.2018.00469/full>. Acesso em: 6/4/2022.

LOPES, P. H.; MURAKAMI, M. T.; PORTARO, F. C. V.; et al. Targeting *Loxosceles* spider Sphingomyelinase D with small-molecule inhibitors as a potential therapeutic approach for loxoscelism. **Journal of Enzyme Inhibition and Medicinal Chemistry**, v. 34, n. 1, p. 310–321, 2019. Disponível em: <https://www.tandfonline.com/doi/full/10.1080/14756366.2018.1546698>. Acesso em: 6/4/2022.

LU, R.-M.; HWANG, Y.-C.; LIU, I.-J.; et al. Development of therapeutic antibodies for the treatment of diseases. **Journal of Biomedical Science**, v. 27, n. 1, p. 1, 2020. Disponível em: <https://jbiomedsci.biomedcentral.com/articles/10.1186/s12929-019-0592-z>. Acesso em: 6/4/2022.

LUIZ, M.; PEREIRA, S.; PRADO, N.; et al. Camelid Single-Domain Antibodies (VHHs) against Crotoxin: A Basis for Developing Modular Building Blocks for the Enhancement of Treatment or Diagnosis of Crotalic Envenoming. **Toxins**, v. 10, n. 4, p. 142, 2018. Disponível em: <http://www.mdpi.com/2072-6651/10/4/142>. Acesso em: 6/4/2022.

MA, H.; Ó'FÁGÁIN, C.; O'KENNEDY, R. Unravelling enhancement of antibody fragment stability – Role of format structure and cysteine modification. **Journal of Immunological Methods**, v. 464, p. 57–63, 2019. Disponível em: <https://linkinghub.elsevier.com/retrieve/pii/S0022175918302412>. Acesso em: 6/4/2022.

MA, H.; Ó'FÁGÁIN, C.; O'KENNEDY, R. Antibody stability: A key to performance - Analysis, influences and improvement. **Biochimie**, v. 177, p. 213–225, 2020. Disponível em: <https://linkinghub.elsevier.com/retrieve/pii/S0300908420302054>. Acesso em: 6/4/2022.

MADDEN, T. The BLAST Sequence Analysis Tool. 2002 Oct 9 [Updated 2003 Aug 13]. In: McEntyre J, Ostell J, editors. **The NCBI Handbook.** Bethesda (MD): National Center for Biotechnology Information (US); 2002-. Chapter 16. Available from: http://www.ncbi.nlm.nih.gov/books/NBK21097/

MAKABE, K.; NAKANISHI, T.; TSUMOTO, K.; et al. Thermodynamic Consequences of Mutations in Vernier Zone Residues of a Humanized Anti-human Epidermal Growth Factor Receptor Murine Antibody, 528. **Journal of Biological Chemistry**, v. 283, n. 2, p. 1156–1166, 2008. Disponível em: <https://linkinghub.elsevier.com/retrieve/pii/S0021925820690263>. Acesso em: 14/4/2022.

MANZONI-DE-ALMEIDA, D.; SQUAIELLA-BAPTISTÃO, C. C.; LOPES, P. H.; VAN DEN BERG, C. W.; TAMBOURGI, D. V. Loxosceles venom Sphingomyelinase D activates human blood leukocytes: Role of the complement system. **Molecular Immunology**, v. 94, p. 45–53, 2018.

MARGULIES, D.; HAMILTON, A. D. Combinatorial protein recognition as an alternative approach to antibody-mimetics. **Current Opinion in Chemical Biology**, v. 14, n. 6, p. 705–712, 2010. Disponível em: <https://linkinghub.elsevier.com/retrieve/pii/S136759311000102X>. Acesso em: 7/4/2022.

MASUDA, K.; SAKAMOTO, K.; KOJIMA, M.; et al. The role of interface framework residues in determining antibody VH/VL interaction strength and antigen-binding affinity. **FEBS Journal**, v. 273, n. 10, p. 2184–2194, 2006. Disponível em: <https://onlinelibrary.wiley.com/doi/10.1111/j.1742-4658.2006.05232.x>. Acesso em: 6/4/2022.

MAYRHOFER, P.; KUNERT, R. Nomenclature of humanized mAbs: Early concepts, current challenges and future perspectives. **Human Antibodies**, v. 27, n. 1, p. 37–51, 2019. Disponível em: <https://content.iospress.com/articles/human-antibodies/hab180347>. Acesso em: 11/4/2022.

MCCONNELL, A. D.; ZHANG, X.; MACOMBER, J. L.; et al. A general approach to antibody thermostabilization. **mAbs**, v. 6, n. 5, p. 1274–1282, 2014. Disponível em: <http://www.tandfonline.com/doi/full/10.4161/mabs.29680>. Acesso em: 6/4/2022.

MENDES, T. M.; OLIVEIRA, D.; FIGUEIREDO, L. F. M.; et al. Generation and characterization of a recombinant chimeric protein (rCpLi) consisting of B-cell epitopes of a dermonecrotic protein from Loxosceles intermedia spider venom. **Vaccine**, v. 31, n. 25, p. 2749–2755, 2013.

MENZEN, T.; FRIESS, W. High-Throughput Melting-Temperature Analysis of a Monoclonal Antibody by Differential Scanning Fluorimetry in the Presence of Surfactants. **Journal of Pharmaceutical Sciences**, v. 102, n. 2, p. 415–428, 2013. Disponível em: <https://linkinghub.elsevier.com/retrieve/pii/S0022354915312363>. Acesso em: 6/4/2022.

MIKLOS, A. E.; KLUWE, C.; DER, B. S.; et al. Structure-Based Design of Supercharged, Highly Thermoresistant Antibodies. **Chemistry & Biology**, v. 19, n. 4, p. 449–455, 2012. Disponível em: <https://linkinghub.elsevier.com/retrieve/pii/S1074552112000774>. Acesso em: 6/4/2022.

MILLER, B. R.; DEMAREST, S. J.; LUGOVSKOY, A.; et al. Stability engineering of scFvs for the development of bispecific and multivalent antibodies. **Protein Engineering, Design and Selection**, v. 23, n. 7, p. 549–557, 2010. Disponível em: <https://academic.oup.com/peds/article-lookup/doi/10.1093/protein/gzq028>. Acesso em: 6/4/2022.

MILLER, K. D.; WEAVER-FELDHAUS, J.; GRAY, S. A.; SIEGEL, R. W.; FELDHAUS, M. J. Production, purification, and characterization of human scFv antibodies expressed in Saccharomyces cerevisiae, Pichia pastoris, and Escherichia coli. **Protein Expression and Purification**, v. 42, n. 2, p. 255–267, 2005. Disponível em: <https://linkinghub.elsevier.com/retrieve/pii/S104659280500152X>. Acesso em: 6/4/2022.

MOHAMED, H. E.; MOHAMED, A. A.; AL-GHOBASHY, M. A.; FATHALLA, F. A.; ABBAS, S. S. Stability assessment of antibody-drug conjugate Trastuzumab emtansine in comparison to parent monoclonal antibody using orthogonal testing protocol. **Journal of Pharmaceutical and Biomedical Analysis**, v. 150, p. 268–277, 2018. Disponível em: <https://linkinghub.elsevier.com/retrieve/pii/S0731708517327838>. Acesso em: 6/4/2022.

MONTOLIU-GAYA, L.; MURCIANO-CALLES, J.; MARTINEZ, J. C.; VILLEGAS, S. Towards the improvement in stability of an anti-Aβ single-chain variable fragment, scFv-h3D6, as a way to enhance its therapeutic potential. **Amyloid**, v. 24, n. 3, p. 167–175, 2017. Disponível em: <https://www.tandfonline.com/doi/full/10.1080/13506129.2017.1348347>. Acesso em: 6/4/2022.

MORGAN, H.; TSENG, S.-Y.; GALLAIS, Y.; et al. Evaluation of in vitro Assays to Assess the Modulation of Dendritic Cells Functions by Therapeutic Antibodies and Aggregates. **Frontiers in Immunology**, v. 10, p. 601, 2019. Disponível em: <https://www.frontiersin.org/article/10.3389/fimmu.2019.00601/full>. Acesso em: 6/4/2022.

MORRISON, SHERIE L.; JOHNSON, M. J.; HERZENBERG, L. A.; OI, V. T. Chimeric Human Antibody Molecules: Mouse Antigen-Binding Domains with Human Constant Region Domains. **Proceedings of the National Academy of Sciences of the United States of America**, v. 81, n. 21, p. 6851–6855, 1984. Disponível em: <https://www.jstor.org/stable/24845>. Acesso em: 14/4/2022.

MOTLEY, M. P.; BANERJEE, K.; FRIES, B. C. Monoclonal Antibody-Based Therapies for Bacterial Infections. **Current opinion in infectious diseases**, v. 32, n. 3, p. 210–216, 2019. Disponível em: <https://www.ncbi.nlm.nih.gov/pmc/articles/PMC7050834/>. Acesso em: 11/4/2022.

DE MOURA, J.; FELICORI, L.; MOREAU, V.; et al. Protection against the toxic effects of Loxosceles intermedia spider venom elicited by mimotope peptides. **Vaccine**, v. 29, n. 45, p. 7992–8001, 2011.

MOUSSA, E. M.; PANCHAL, J. P.; MOORTHY, B. S.; et al. Immunogenicity of Therapeutic Protein Aggregates. **Journal of Pharmaceutical Sciences**, v. 105, n. 2, p. 417–430, 2016. Disponível em: <https://linkinghub.elsevier.com/retrieve/pii/S0022354915000337>. Acesso em: 6/4/2022.

MULLARD, A. FDA approves 100th monoclonal antibody product. **Nature Reviews Drug Discovery**, v. 20, n. 7, p. 491–495, 2021a. Disponível em: <http://www.nature.com/articles/d41573-021-00079-7>. Acesso em: 13/4/2022.

MURAKAMI, M. T.; FERNANDES-PEDROSA, M. F.; TAMBOURGI, D. V.; ARNI, R. K. Structural Basis for Metal Ion Coordination and the Catalytic Mechanism of Sphingomyelinases D. **Journal of Biological Chemistry**, v. 280, n. 14, p. 13658–13664, 2005. Disponível em: <https://linkinghub.elsevier.com/retrieve/pii/S0021925819604400>. Acesso em: 6/4/2022.

MUZARD, J.; ADI-BESSALEM, S.; JUSTE, M.; et al. Grafting of protein L-binding activity onto recombinant antibody fragments. **Analytical Biochemistry**, v. 388, n. 2, p. 331–338, 2009.

MYUNG, Y.; PIRES, D. E. V.; ASCHER, D. B. mmCSM-AB: guiding rational antibody engineering through multiple point mutations. **Nucleic Acids Research**, v. 48, n. W1, p. W125–W131, 2020b. Disponível em: <https://academic.oup.com/nar/article/48/W1/W125/5841134>. Acesso em: 18/4/2022.

NAKANISHI, T.; TSUMOTO, K.; YOKOTA, A.; KONDO, H.; KUMAGAI, I. Critical contribution of VH-VL interaction to reshaping of an antibody: The case of humanization of anti-lysozyme antibody, HyHEL-10. **Protein Science**, v. 17, n. 2, p. 261–270, 2008. Disponível em: <http://doi.wiley.com/10.1110/ps.073156708>. Acesso em: 6/4/2022.

NARCISO, J. E. T.; UY, I. D. C.; CABANG, A. B.; et al. Analysis of the antibody structure based on high-resolution crystallographic studies. **New Biotechnology**, Antibodies: From Basics to Therapeutics., v. 28, n. 5, p. 435–447, 2011. Disponível em: <https://www.sciencedirect.com/science/article/pii/S1871678411000744>. Acesso em: 14/4/2022.

NAZARI, A.; SAMIANIFARD, M.; RABIE, H.; MIRAKABADI, A. Z. Recombinant antibodies against Iranian cobra venom as a new emerging therapy by phage display technology. **Journal of Venomous Animals and Toxins including Tropical Diseases**, v. 26, p. e20190099, 2020. Disponível em: <http://www.scielo.br/scielo.php?script=sci_arttext&pid=S1678-91992020000100317&tlng=en>. Acesso em: 6/4/2022.

OLAFSEN, T.; WU, A. M. Antibody vectors for imaging. **Seminars in Nuclear Medicine**, v. 40, n. 3, p. 167–181, 2010.

PAULI, I.; MINOZZO, J. C.; HENRIQUE DA SILVA, P.; CHAIM, O. M.; VEIGA, S. S. Analysis of therapeutic benefits of antivenin at different time intervals after

experimental envenomation in rabbits by venom of the brown spider (Loxosceles intermedia). **Toxicon**, v. 53, n. 6, p. 660–671, 2009. Disponível em: <https://linkinghub.elsevier.com/retrieve/pii/S0041010109000828>. Acesso em: 6/4/2022.

PEJCHAL, R.; WALKER, L. M.; STANFIELD, R. L.; et al. Structure and function of broadly reactive antibody PG16 reveal an H3 subdomain that mediates potent neutralization of HIV-1. **Proceedings of the National Academy of Sciences**, v. 107, n. 25, p. 11483–11488, 2010. Disponível em: <https://pnas.org/doi/full/10.1073/pnas.1004600107>. Acesso em: 8/4/2022.

PERCHIACCA, J. M.; LEE, C. C.; TESSIER, P. M. Optimal charged mutations in the complementarity-determining regions that prevent domain antibody aggregation are dependent on the antibody scaffold. **Protein Engineering Design and Selection**, v. 27, n. 2, p. 29–39, 2014. Disponível em: <https://academic.oup.com/peds/article-lookup/doi/10.1093/protein/gzt058>. Acesso em: 6/4/2022.

PETTERSEN, E. F.; GODDARD, T. D.; HUANG, C. C.; et al. UCSF Chimera?A visualization system for exploratory research and analysis. **Journal of Computational Chemistry**, v. 25, n. 13, p. 1605–1612, 2004. Disponível em: <https://onlinelibrary.wiley.com/doi/10.1002/jcc.20084>. Acesso em: 6/4/2022.

PHAM, P. V. Medical Biotechnology. **Omics Technologies and Bio-Engineering**. p.449–469, 2018. Elsevier. Disponível em: <https://linkinghub.elsevier.com/retrieve/pii/B9780128046593000191>. Acesso em: 6/4/2022.

POMMIÉ, C.; LEVADOUX, S.; SABATIER, R.; LEFRANC, G.; LEFRANC, M.-P. IMGT standardized criteria for statistical analysis of immunoglobulin V-REGION amino acid properties. **Journal of Molecular Recognition**, v. 17, n. 1, p. 17–32, 2004. Disponível em: <https://onlinelibrary.wiley.com/doi/10.1002/jmr.647>. Acesso em: 6/4/2022.

PROBA, K.; WÖRN, A.; HONEGGER, A.; PLÜCKTHUN, A. Antibody scFv fragments without disulfide bonds made by molecular evolution. **Journal of Molecular Biology**, v. 275, n. 2, p. 245–253, 1998.

PRZEPIORKA, D.; KERNAN, N. A.; IPPOLITI, C.; et al. Daclizumab, a humanized anti-interleukin-2 receptor alpha chain antibody, for treatment of acute graft-versus-host disease. **Blood**, v. 95, n. 1, p. 83–89, 2000. Disponível em: <https://ashpublications.org/blood/article/95/1/83/180841/Daclizumab-a-humanized-antiinterleukin2-receptor>. Acesso em: 11/4/2022.

PULIGEDDA, R. D.; VIGDOROVICH, V.; KOUIAVSKAIA, D.; et al. Human IgA Monoclonal Antibodies That Neutralize Poliovirus, Produced by Hybridomas and Recombinant Expression. **Antibodies**, v. 9, n. 1, p. 5, 2020. Disponível em: <https://www.mdpi.com/2073-4468/9/1/5>. Acesso em: 6/4/2022.

QUINTERO-HERNÁNDEZ, V.; DEL POZO-YAUNER, L.; PEDRAZA-ESCALONA, M.; et al. Evaluation of three different formats of a neutralizing single chain human antibody against toxin Cn2: neutralization capacity versus thermodynamic stability. **Immunology Letters**, v. 143, n. 2, p. 152–160, 2012.

QUINTERO-HERNÁNDEZ, V.; JUÁREZ-GONZÁLEZ, V. R.; ORTÍZ-LEÓN, M.; et al. The change of the scFv into the Fab format improves the stability and in vivo toxin neutralization capacity of recombinant antibodies. **Molecular Immunology**, v. 44, n. 6, p. 1307–1315, 2007. Disponível em: <https://linkinghub.elsevier.com/retrieve/pii/S0161589006001969>. Acesso em: 6/4/2022.

RABIA, L. A.; DESAI, A. A.; JHAJJ, H. S.; TESSIER, P. M. Understanding and overcoming trade-offs between antibody affinity, specificity, stability and solubility. **Biochemical engineering journal**, v. 137, p. 365–374, 2018. Disponível em: <https://www.ncbi.nlm.nih.gov/pmc/articles/PMC6338232/>. Acesso em: 14/4/2022.

RAMADA, J. S.; BECKER-FINCO, A.; MINOZZO, J. C.; et al. Synthetic peptides for in vitro evaluation of the neutralizing potency of Loxosceles antivenoms. **Toxicon**, v. 73, p. 47–55, 2013. Disponível em: <https://linkinghub.elsevier.com/retrieve/pii/S004101011300250X>. Acesso em: 6/4/2022.

REYNISSON, B.; ALVAREZ, B.; PAUL, S.; PETERS, B.; NIELSEN, M. NetMHCpan-4.1 and NetMHCIIpan-4.0: improved predictions of MHC antigen presentation by concurrent motif deconvolution and integration of MS MHC eluted ligand data. **Nucleic Acids Research**, v. 48, n. W1, p. W449–W454, 2020. Disponível em: <https://academic.oup.com/nar/article/48/W1/W449/5837056>. Acesso em: 6/4/2022.

RICHARD, G.; MEYERS, A. J.; MCLEAN, M. D.; et al. In vivo neutralization of α-cobratoxin with high-affinity llama single-domain antibodies (VHHs) and a VHH-Fc antibody. **PloS One**, v. 8, n. 7, p. e69495, 2013.

RODRIGO, G.; GRUVEGÅRD, M.; VAN ALSTINE, J. Antibody Fragments and Their Purification by Protein L Affinity Chromatography. **Antibodies**, v. 4, n. 3, p. 259–277, 2015. Disponível em: <http://www.mdpi.com/2073-4468/4/3/259>. Acesso em: 6/4/2022.

RODRÍGUEZ-RODRÍGUEZ, E. R.; LEDEZMA-CANDANOZA, L. M.; CONTRERAS-FERRAT, L. G.; et al. A single mutation in framework 2 of the heavy variable domain improves the properties of a diabody and a related single-chain antibody. **Journal of Molecular Biology**, v. 423, n. 3, p. 337–350, 2012.

RÖTHLISBERGER, D.; HONEGGER, A.; PLÜCKTHUN, A. Domain Interactions in the Fab Fragment: A Comparative Evaluation of the Single-chain Fv and Fab Format Engineered with Variable Domains of Different Stability. **Journal of Molecular Biology**, v. 347, n. 4, p. 773–789, 2005. Disponível em: <https://linkinghub.elsevier.com/retrieve/pii/S002228360500094X>. Acesso em: 6/4/2022.

SAEED, A. F. U. H.; WANG, R.; LING, S.; WANG, S. Antibody Engineering for Pursuing a Healthier Future. **Frontiers in Microbiology**, v. 8, 2017. Disponível em: <https://www.frontiersin.org/article/10.3389/fmicb.2017.00495>. Acesso em: 7/4/2022.

SAFDARI, Y.; FARAJNIA, S.; ASGHARZADEH, M.; KHALILI, M. Antibody humanization methods – a review and update. **Biotechnology and Genetic Engineering Reviews**, v. 29, n. 2, p. 175–186, 2013. Disponível em: <http://www.tandfonline.com/doi/abs/10.1080/02648725.2013.801235>. Acesso em: 6/4/2022.

SAKHNINI, L. I.; GREISEN, P. J.; WIBERG, C.; et al. Improving the Developability of an Antigen Binding Fragment by Aspartate Substitutions. **Biochemistry**, v. 58, n. 24, p. 2750–2759, 2019. Disponível em: <https://pubs.acs.org/doi/10.1021/acs.biochem.9b00251>. Acesso em: 6/4/2022.

ŠALI, A.; OVERINGTON, J. P. Derivation of rules for comparative protein modeling from a database of protein structure alignments. **Protein Science**, v. 3, n. 9, p. 1582–1596, 1994. Disponível em: <https://onlinelibrary.wiley.com/doi/10.1002/pro.5560030923>. Acesso em: 6/4/2022.

SANCHEZ-MAZAS, A.; NUNES, J. M.; MIDDLETON, D.; et al. Common and well-documented HLA alleles over all of Europe and within European sub-regions: A catalogue from the European Federation for Immunogenetics. **HLA**, v. 89, n. 2, p. 104–113, 2017. Disponível em: <https://onlinelibrary.wiley.com/doi/10.1111/tan.12956>. Acesso em: 6/4/2022.

SANTOS, M. L. DOS; QUINTILIO, W.; MANIERI, T. M.; TSURUTA, L. R.; MORO, A. M. Advances and challenges in therapeutic monoclonal antibodies drug development. **Brazilian Journal of Pharmaceutical Sciences**, v. 54, n. spe, 2018. Disponível em: <http://www.scielo.br/scielo.php?script=sci_arttext&pid=S1984-82502018000700406&lng=en&tlng=en>. Acesso em: 11/4/2022.

SCHLATTER, S.; STANSFIELD, S. H.; DINNIS, D. M.; et al. On the Optimal Ratio of Heavy to Light Chain Genes for Efficient Recombinant Antibody Production by CHO Cells. **Biotechnology Progress**, v. 21, n. 1, p. 122–133, 2008. Disponível em: <http://doi.wiley.com/10.1021/bp049780w>. Acesso em: 6/4/2022.

SCHROEDER, H. W.; CAVACINI, L. Structure and Function of Immunoglobulins. **The Journal of allergy and clinical immunology**, v. 125, n. 2 0 2, p. S41–S52, 2010. Disponível em: <https://www.ncbi.nlm.nih.gov/pmc/articles/PMC3670108/>. Acesso em: 8/4/2022.

SEELIGER, D.; SCHULZ, P.; LITZENBURGER, T.; et al. Boosting antibody developability through rational sequence optimization. **mAbs**, v. 7, n. 3, p. 505–515, 2015. Disponível em: <http://www.tandfonline.com/doi/full/10.1080/19420862.2015.1017695>. Acesso em: 6/4/2022.

SHUKLA, A. A.; HUBBARD, B.; TRESSEL, T.; GUHAN, S.; LOW, D. Downstream processing of monoclonal antibodies—Application of platform approaches. **Journal of Chromatography B**, Polyclonal and Monoclonal Antibody Production, Purification, Process and Product Analytics., v. 848, n. 1, p. 28–39, 2007. Disponível em: <https://www.sciencedirect.com/science/article/pii/S1570023206007549>. Acesso em: 7/4/2022.

SHUKLA, A. A.; THÖMMES, J. Recent advances in large-scale production of monoclonal antibodies and related proteins. **Trends in Biotechnology**, v. 28, n. 5, p. 253–261, 2010. Disponível em: <https://www.cell.com/trends/biotechnology/abstract/S0167-7799(10)00031-4>. Acesso em: 1/5/2022.

SIEVERS, F.; WILM, A.; DINEEN, D.; et al. Fast, scalable generation of high-quality protein multiple sequence alignments using Clustal Omega. **Molecular Systems Biology**, v. 7, n. 1, p. 539, 2011. Disponível em: <https://onlinelibrary.wiley.com/doi/10.1038/msb.2011.75>. Acesso em: 6/4/2022.

DA SILVEIRA, R. B.; PIGOZZO, R. B.; CHAIM, O. M.; et al. Two novel dermonecrotic toxins LiRecDT4 and LiRecDT5 from Brown spider (Loxosceles intermedia) venom: From cloning to functional characterization. **Biochimie**, v. 89, n. 3, p. 289–300, 2007. Disponível em: <https://linkinghub.elsevier.com/retrieve/pii/S030090840600318X>. Acesso em: 6/4/2022.

SINANWEB - Dados Epidemiológicos Sinan. .Disponível em: <https://portalsinan.saude.gov.br/dados-epidemiologicos-sinan>. Acesso em: 7/4/2022.

SINGH, A.; CHAUDHARY, S.; AGARWAL, A.; VERMA, A. S. Chapter 15 - Antibodies: Monoclonal and Polyclonal. In: Ashish S. Verma; A. Singh (Orgs.); **Animal Biotechnology**. p.265–287, 2014. San Diego: Academic Press. Disponível em: <https://www.sciencedirect.com/science/article/pii/B9780124160026000158>. Acesso em: 7/4/2022.

SINGH, S.; TANK, N. K.; DWIWEDI, P.; et al. Monoclonal Antibodies: A Review. **Current Clinical Pharmacology**, v. 13, n. 2, p. 85–99. Disponível em: <https://www.eurekaselect.com/article/85198>. Acesso em: 6/4/2022.

SOUTHWOOD, S.; SIDNEY, J.; KONDO, A.; et al. Several common HLA-DR types share largely overlapping peptide binding repertoires. **Journal of Immunology (Baltimore, Md.: 1950)**, v. 160, n. 7, p. 3363–3373, 1998.

SPIESS, C.; ZHAI, Q.; CARTER, P. J. Alternative molecular formats and therapeutic applications for bispecific antibodies. **Molecular Immunology**, v. 67, n. 2, p. 95–106, 2015. Disponível em: <https://linkinghub.elsevier.com/retrieve/pii/S016158901500005X>. Acesso em: 6/4/2022.

STEWART, C. S.; MACKENZIE, C. R.; CHRISTOPHER HALL, J. Isolation, characterization and pentamerization of α-cobrotoxin specific single-domain antibodies from a naïve phage display library: Preliminary findings for antivenom development. **Toxicon**, v. 49, n. 5, p. 699–709, 2007.

SQUAIELLA-BAPTISTÃO, C. C.; SANT'ANNA, O. A.; MARCELINO, J. R.; TAMBOURGI, D. V. The history of antivenoms development: Beyond Calmette and Vital Brazil. **Toxicon**, v. 150, p. 86–95, 2018. Disponível em: <https://linkinghub.elsevier.com/retrieve/pii/S0041010118301958>. Acesso em: 7/4/2022.

SU, C. T.-T.; LING, W.-L.; LUA, W.-H.; POH, J.-J.; GAN, S. K.-E. The role of Antibody Vκ Framework 3 region towards Antigen binding: Effects on recombinant production and Protein L binding. **Scientific Reports**, v. 7, n. 1, p. 3766, 2017. Disponível em: <http://www.nature.com/articles/s41598-017-02756-3>. Acesso em: 6/4/2022.

SUN, W.; YANG, Z.; LIN, H.; et al. Improvement in affinity and thermostability of a fully human antibody against interleukin-17A by yeast-display technology and CDR grafting. **Acta Pharmaceutica Sinica B**, v. 9, n. 5, p. 960–972, 2019. Disponível em: <https://linkinghub.elsevier.com/retrieve/pii/S2211383518311729>. Acesso em: 6/4/2022.

SWANSON, D. L.; VETTER, R. S. Loxoscelism. **Clinics in Dermatology**, v. 24, n. 3, p. 213–221, 2006.

TAM, S.; MCCARTHY, S.; ARMSTRONG, A.; et al. Functional, Biophysical, and Structural Characterization of Human IgG1 and IgG4 Fc Variants with Ablated Immune Functionality. **Antibodies**, v. 6, n. 3, p. 12, 2017. Disponível em: <https://www.mdpi.com/2073-4468/6/3/12>. Acesso em: 6/4/2022.

TAMBOURGI, D. V.; GONÇALVES-DE-ANDRADE, R. M.; VAN DEN BERG, C. W. Loxoscelism: From basic research to the proposal of new therapies. **Toxicon: Official Journal of the International Society on Toxinology**, v. 56, n. 7, p. 1113–1119, 2010.

TAMBOURGI, D. V.; PAIXÃO-CAVALCANTE, D.; GONÇALVES DE ANDRADE, R. M.; et al. Loxosceles sphingomyelinase induces complement-dependent dermonecrosis, neutrophil infiltration, and endogenous gelatinase expression. **The Journal of Investigative Dermatology**, v. 124, n. 4, p. 725–731, 2005.

TANG, Y.; CAO, Y. Modeling Pharmacokinetics and Pharmacodynamics of Therapeutic Antibodies: Progress, Challenges, and Future Directions. **Pharmaceutics**, v. 13, n. 3, p. 422, 2021. Disponível em: <https://www.mdpi.com/1999-4923/13/3/422>. Acesso em: 14/4/2022.

DI TOMMASO, A.; JUSTE, M. O.; LAKHRIF, Z.; et al. Engineering and Functional Evaluation of Neutralizing Antibody Fragments Against Congenital Toxoplasmosis. **The Journal of Infectious Diseases**, v. 224, n. 4, p. 705–714, 2021. Disponível em: <https://academic.oup.com/jid/article/224/4/705/6174436>. Acesso em: 13/4/2022.

DI TOMMASO, A.; JUSTE, M. O.; MARTIN-EAUCLAIRE, M.-F.; et al. Diabody Mixture Providing Full Protection against Experimental Scorpion Envenoming with Crude Androctonus australis Venom. **Journal of Biological Chemistry**, v. 287, n. 17, p. 14149–14156, 2012. Disponível em: <https://linkinghub.elsevier.com/retrieve/pii/S0021925820529852>. Acesso em: 6/4/2022.

TORIDE KING, M.; BROOKS, C. L. Epitope Mapping of Antibody-Antigen Interactions with X-Ray Crystallography. **Methods in Molecular Biology (Clifton, N.J.)**, v. 1785, p. 13–27, 2018.

TU, C.; TERRAUBE, V.; TAM, A. S. P.; et al. A Combination of Structural and Empirical Analyses Delineates the Key Contacts Mediating Stability and Affinity Increases in an Optimized Biotherapeutic Single-chain Fv (scFv). **Journal of Biological Chemistry**, v. 291, n. 3, p. 1267–1276, 2016. Disponível em: <https://linkinghub.elsevier.com/retrieve/pii/S0021925820361627>. Acesso em: 6/4/2022.

ULLAH, A.; DE GIUSEPPE, P. O.; MURAKAMI, M. T.; et al. Crystallization and preliminary X-ray diffraction analysis of a class II phospholipase D from Loxosceles intermedia venom. **Acta Crystallographica. Section F, Structural Biology and Crystallization Communications**, v. 67, n. Pt 2, p. 234–236, 2011.

UNKAUF, T.; HUST, M.; FRENZEL, A. Antibody Affinity and Stability Maturation by Error-Prone PCR. In: M. Hust; T. S. Lim (Orgs.); **Phage Display: Methods and Protocols**, Methods in Molecular Biology. p.393–407, 2018. New York, NY: Springer. Disponível em: <https://doi.org/10.1007/978-1-4939-7447-4_22>. Acesso em: 6/4/2022.

URLAUB, G.; CHASIN, L. A. Isolation of Chinese hamster cell mutants deficient in dihydrofolate reductase activity. **Proceedings of the National Academy of Sciences**, v. 77, n. 7, p. 4216–4220, 1980. Disponível em: <https://pnas.org/doi/full/10.1073/pnas.77.7.4216>. Acesso em: 6/4/2022.

VOORS-PETTE, C.; LEBOZEC, K.; DOGTEROM, P.; et al. Safety and Tolerability, Pharmacokinetics, and Pharmacodynamics of ACT017, an Antiplatelet GPVI (Glycoprotein VI) Fab. **Arteriosclerosis, Thrombosis, and Vascular Biology**, v. 39, n. 5, p. 956–964, 2019.

VUITIKA, L.; CHAVES-MOREIRA, D.; CARUSO, I.; et al. Active site mapping of Loxosceles phospholipases D: Biochemical and biological features. **Biochimica et Biophysica Acta (BBA) - Molecular and Cell Biology of Lipids**, v. 1861, n. 9, p. 970–979, 2016. Disponível em: <https://linkinghub.elsevier.com/retrieve/pii/S1388198116301329>. Acesso em: 6/4/2022.

WÄLCHLI, R.; RESSURREIÇÃO, M.; VOGG, S.; et al. Understanding mAb aggregation during low pH viral inactivation and subsequent neutralization. **Biotechnology and Bioengineering**, v. 117, n. 3, p. 687–700, 2020. Disponível em: <https://onlinelibrary.wiley.com/doi/10.1002/bit.27237>. Acesso em: 6/4/2022.

WALDMANN, H. Human Monoclonal Antibodies: The Benefits of Humanization. In: M. Steinitz (Org.); **Human Monoclonal Antibodies: Methods and Protocols**, Methods in Molecular Biology. p.1–10, 2019. New York, NY: Springer. Disponível em: <https://doi.org/10.1007/978-1-4939-8958-4_1>. Acesso em: 6/4/2022.

WANG, Q.; CHEN, Y.; PARK, J.; et al. Design and Production of Bispecific Antibodies. **Antibodies**, v. 8, n. 3, p. 43, 2019. Disponível em: <https://www.mdpi.com/2073-4468/8/3/43>. Acesso em: 6/4/2022.

WARD, E. S.; GÜSSOW, D.; GRIFFITHS, A. D.; JONES, P. T.; WINTER, G. Binding activities of a repertoire of single immunoglobulin variable domains secreted from Escherichia coli. **Nature**, v. 341, n. 6242, p. 544–546, 1989.

WEATHERILL, E. E.; CAIN, K. L.; HEYWOOD, S. P.; et al. Towards a universal disulphide stabilised single chain Fv format: importance of interchain disulphide bond location and vL-vH orientation. **Protein Engineering Design and Selection**, v. 25, n. 7, p. 321–329, 2012. Disponível em: <https://academic.oup.com/peds/article-lookup/doi/10.1093/protein/gzs021>. Acesso em: 6/4/2022.

WEBB, B.; SALI, A. Comparative Protein Structure Modeling Using MODELLER. **Current Protocols in Bioinformatics**, v. 54, n. 1, 2016. Disponível em: <https://onlinelibrary.wiley.com/doi/10.1002/cpbi.3>. Acesso em: 18/4/2022.

WEINER, G. J. Building better monoclonal antibody-based therapeutics. **Nature Reviews Cancer**, v. 15, n. 6, p. 361–370, 2015. Disponível em: <https://www.nature.com/articles/nrc3930>. Acesso em: 8/4/2022.

WILLE, A. C. M.; CHAVES-MOREIRA, D.; TREVISAN-SILVA, D.; et al. Modulation of membrane phospholipids, the cytosolic calcium influx and cell proliferation following treatment of B16-F10 cells with recombinant phospholipase-D from Loxosceles intermedia (brown spider) venom. **Toxicon**, v. 67, p. 17–30, 2013. Disponível em: <https://www.sciencedirect.com/science/article/pii/S0041010113000615>. Acesso em: 6/4/2022.

WINKLER, K.; KRAMER, A.; KÜTTNER, G.; et al. Changing the antigen binding specificity by single point mutations of an anti-p24 (HIV-1) antibody. **Journal of Immunology (Baltimore, Md.: 1950)**, v. 165, n. 8, p. 4505–4514, 2000.

WINTER, G.; MILSTEIN, C. Man-made antibodies. **Nature**, v. 349, n. 6307, p. 293–299, 1991.

WISEMAN, A. C. Immunosuppressive Medications. **Clinical Journal of the American Society of Nephrology**, v. 11, n. 2, p. 332–343, 2016. Disponível em: <https://cjasn.asnjournals.org/content/11/2/332>. Acesso em: 1/5/2022.

WONG, W. K.; LEEM, J.; DEANE, C. M. Comparative Analysis of the CDR Loops of Antigen Receptors. **Frontiers in Immunology**, v. 10, 2019. Disponível em: <https://www.frontiersin.org/article/10.3389/fimmu.2019.02454>. Acesso em: 8/4/2022.

WU, S.-J.; LUO, J.; O'NEIL, K. T.; et al. Structure-based engineering of a monoclonal antibody for improved solubility. **Protein Engineering Design and Selection**, v. 23, n. 8, p. 643–651, 2010. Disponível em: <https://academic.oup.com/peds/article-lookup/doi/10.1093/protein/gzq037>. Acesso em: 6/4/2022.

XENAKI, K. T.; OLIVEIRA, S.; VAN BERGEN EN HENEGOUWEN, P. M. P. Antibody or Antibody Fragments: Implications for Molecular Imaging and Targeted Therapy of Solid Tumors. **Frontiers in Immunology**, v. 8, p. 1287, 2017. Disponível em: <http://journal.frontiersin.org/article/10.3389/fimmu.2017.01287/full>. Acesso em: 6/4/2022.

XU, J. L.; DAVIS, M. M. Diversity in the CDR3 Region of VH Is Sufficient for Most Antibody Specificities. **Immunity**, v. 13, n. 1, p. 37–45, 2000. Disponível em: <https://www.cell.com/immunity/abstract/S1074-7613(00)00006-6>. Acesso em: 8/4/2022.

XU, Y.; WANG, D.; MASON, B.; et al. Structure, heterogeneity and developability assessment of therapeutic antibodies. **mAbs**, v. 11, n. 2, p. 239–264, 2019. Disponível em: <https://doi.org/10.1080/19420862.2018.1553476>. Acesso em: 7/4/2022.

YUI, A.; AKIBA, H.; KUDO, S.; et al. Thermodynamic analyses of amino acid residues at the interface of an antibody B2212A and its antigen roundabout homolog 1. **The Journal of Biochemistry**, 2017. Disponível em: <http://academic.oup.com/jb/article/doi/10.1093/jb/mvx050/4061582/Thermodynamic-analyses-of-amino-acid-residues-at>. Acesso em: 6/4/2022.

ZAHID, M.; LOYAU, S.; BOUABDELLI, M.; et al. Design and reshaping of an scFv directed against human platelet glycoprotein VI with diagnostic potential. **Analytical Biochemistry**, v. 417, n. 2, p. 274–282, 2011. Disponível em: <https://linkinghub.elsevier.com/retrieve/pii/S0003269711004337>. Acesso em: 6/4/2022.

ZHANG, K.; GEDDIE, M. L.; KOHLI, N.; et al. Comprehensive optimization of a single-chain variable domain antibody fragment as a targeting ligand for a cytotoxic nanoparticle. **mAbs**, v. 7, n. 1, p. 42–52, 2015. Disponível em: <https://www.tandfonline.com/doi/full/10.4161/19420862.2014.985933>. Acesso em: 6/4/2022.

ZHANG, Y.-F.; HO, M. Humanization of rabbit monoclonal antibodies via grafting combined Kabat/IMGT/Paratome complementarity-determining regions: Rationale and examples. **mAbs**, v. 9, n. 3, p. 419–429, 2017. Disponível em: <https://www.tandfonline.com/doi/full/10.1080/19420862.2017.1289302>. Acesso em: 6/4/2022.

ZHOU, J. O.; ZAIDI, H. A.; TON, T.; FERA, D. The Effects of Framework Mutations at the Variable Domain Interface on Antibody Affinity Maturation in an HIV-1 Broadly Neutralizing Antibody Lineage. **Frontiers in Immunology**, v. 11, 2020. Disponível em: <https://www.frontiersin.org/article/10.3389/fimmu.2020.01529>. Acesso em: 8/4/2022.

ANEXOS:

ANEXO 1. Avaliação Do Mecanismo De Ação Do Veneno De *L. Intermedia In Vitro* (doi: 10.1016/J.Toxlet.2021.07.014)

Toxicology Letters 350 (2021) 202–212

Contents lists available at ScienceDirect

Toxicology Letters

journal homepage: www.elsevier.com/locate/toxlet

A new insight into the cellular mechanisms of envenomation: Elucidating the role of extracellular vesicles in Loxoscelism

Larissa Magalhães Alvarenga[a,*], Guillermo Andrés Cerquera Cardenas[a], Isabella Gizzi Jiacomini[a], Marcel Ivan Ramírez[b]

[a] Laboratório de Imunoquímica, Departamento de Patologia Básica, Universidade Federal do Paraná, Curitiba, PR, Brazil
[b] EVAHPI – Extracellular Vesicles and Host-Parasite Interactions Research Group Laboratório de Biologia Molecular e Sistemática de Tripanossomatideos, Instituto Carlos Chagas-Fiocruz, Curitiba, PR, Brazil

HIGHLIGHTS

- Venoms of Loxosceles spiders induce extracellular vesicle (EVs) production in different cell lines.
- Phospholipases D (PLDs) present in *L. intermedia* venom have crucial toxic effects on the induction of EV production.
- EVs carrying toxins can contribute to the progression of the envenomation process.

GRAPHICAL ABSTRACT

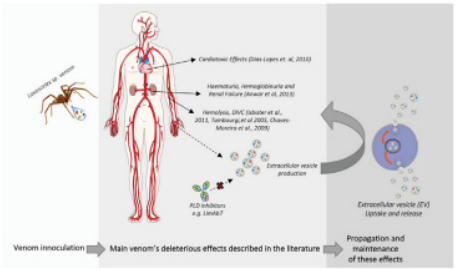

ARTICLE INFO

Article history:
Received 11 May 2021
Received in revised form 8 July 2021
Accepted 21 July 2021
Editor: Dr. Angela Mally
Available online 24 July 2021

Keywords:
Loxosceles
Phospholipases D
Extracellular vesicles
Envenomation

ABSTRACT

Envenomation by the *Loxosceles* genus spiders is a recurring health issue worldwide and specially in the Americas. The physiopathology of the envenomation is tightly associated to the venom's rich toxin composition, able to produce a local dermonecrotic lesion that can evolve systemically and if worsened, might result in multiple organ failure and lethality. The cellular and molecular mechanisms involved with the physiopathology of Loxoscelism are not completely understood, however, the venom's Phospholipases D (PLDs) are known to trigger membrane injury in various cell types. Here, we report for the first time the *Loxosceles* venom's ability to stimulate the production of extracellular vesicles (EVs) in various human cell lineages. Components of the *Loxosceles* venom were also detectable in the cargo of these vesicles, suggesting that they may be implicated in the process of extracellular venom release. EVs from venom treated cells exhibited phospholipase D activity and were able to induce *in vitro* hemolysis in human red blood cells and alter the HEK cell membranes' permeability. Nonetheless, the PLD activity was inhibited when an anti-venom PLDs monoclonal antibody was co-administered with the whole venom. In summary, our findings shed new light on the mechanisms underlying cellular events in the context of loxoscelism and suggest a crucial role of EVs in the process of envenomation.

* Corresponding author. Present address: Coronel Francisco Heráclito dos Santos Avenue, 100 – Curitiba, 81530-000, Brazil.
E-mail address: lmalvarenga@ufpr.br (L.M. Alvarenga).

http://dx.doi.org/10.1016/j.toxlet.2021.07.014
0378-4274/

ANEXO 2. Avaliação Dos Mecanismo De Ação Do Veneno De *L. Intermedia In Vivo* No Modelo De Zebrafish (Em Processo De Submissão)

Evaluation of the effects of *Loxosceles intemedia's* venom in zebrafish

Ollavo Nogueira Tozzi[1#], Isabella Gizzi Jiacomini[1#], Thaís Sibioni Berti Bastos[1], Laura Helena Cherem Netto Nicolazzi[1], Rebeca Bosso dos Santos Luz[1], Laís Cavalieri Paredes[2], Luis Eduardo Goncalves[2], Murilo Henrique Saturnino Lima[3], Waldiceu A. Verri Jr[4], Niels Olsen Saraiva Camara[2], Helena Cristina Silva de Assis[5], Marisa Fernandes de Castilho[6], Larissa Magalhaes Alvarenga[1], Tárcio Teodoro Braga[1,3*].

[1] Department of Basic Pathology, Federal University of Parana, Curitiba, Brazil

[2] Department of Immunology, University of São Paulo, Sao Paulo, Brazil

[3] Graduate Program in Biosciences and Biotechnology, Instituto Carlos Chagas, Fiocruz, Curitiba, Brazil

[4] Department of Pathology, Biological Science Center, Londrina State University, Brazil

[5] Department of Pharmacology, Federal University of Parana, Curitiba, Brazil

[6] Department of Physiology, Federal University of Parana, Curitiba, Brazil

# These authors contributed equally

*Corresponding Author: tarcio.braga@ufpr.br

FUNDING

WAVJ acknowledges PRONEX grant supported by Araucaria Foundation, SETI, MCTI/CNPq and Paraná State Government (agreement 014/2017, protocol 46.843) and CNPq Researcher fellowship (# 309633/2021-4). This study was financed in part by the Coordenação de Aperfeiçoamento de Pessoal de Nível Superior – Brasil (CAPES) – Finance Code 001.

ABSTRACT

Zebrafish is a model of increasing use for studies in several biomedical areas, including toxicology, inflammation and tissue regeneration. We investigated the inflammatory effects that *Loxosceles intermedia's* venom (LIV) on zebrafish. Moreover, the effects of specialized pro-resolving mediators (SPM) Maresin 2 (Mar2) and Resolvin D5 (RvD5) on tissue regeneration after fin fold amputation were also investigated. Different concentrations (250 to 2000 ng) of LIV were tested in its haemolysis capacity *in vitro* and afterwards injected intraperitoneally into the animals. LIV caused haemolysis in human red blood cells, but not in zebrafish's ones. The survival curve was not altered upon LIV injection, regardless the dosage. Histology analysis of renal and hepatic tissues and whole animal revealed no differences among LIV-injected and PBS-control groups. Fin fold regeneration rate was also not altered among groups, even in the presence of MaR2 and RvD5. Ultimately, swimming behavioural analysis did not differ among the groups. *In silico* data pointed to differences in cell membrane composition between human and zebrafish, such as phospholipase and sphingomyelinase substrates, that could lead to fish's protection to LIV. Although it cannot be used as a toxicological model in the context of LIV, the absence of effects may represent a further step towards understanding the role of venom in mammals and the fundamental evolutionary processes involved.

Key words: Zebrafish**,** *Loxosceles intermedia* venom, Maresin 2 and Resolvin D5